

Published in Journals: Fractal and Fractional, Axioms,  
Mathematical and Computational Applications,  
Mathematics and Symmetry

Topic Reprint

---

# Fractional Calculus

Theory and Applications  
Volume I

---

Edited by  
António Lopes, Alireza Alfi, Liping Chen and Sergio Adriani David

[mdpi.com/topics](https://mdpi.com/topics)



# **Fractional Calculus: Theory and Applications—Volume I**

# Fractional Calculus: Theory and Applications—Volume I

Editors

**António Lopes**

**Alireza Alfi**

**Liping Chen**

**Sergio Adriani David**



Basel • Beijing • Wuhan • Barcelona • Belgrade • Novi Sad • Cluj • Manchester

*Editors*

António Lopes  
University of Porto  
Porto  
Portugal

Alireza Alfi  
Shahrood University of  
Technology  
Shahrood  
Iran

Liping Chen  
Hefei University of  
Technology  
Hefei  
China

Sergio Adriani David  
University of São Paulo  
Pirassununga  
Brazil

*Editorial Office*

MDPI  
St. Alban-Anlage 66  
4052 Basel, Switzerland

This is a reprint of articles from the Topic published online in the open access journals *Fractal and Fractional* (ISSN 2504-3110), *Axioms* (ISSN 2075-1680), *Mathematical and Computational Applications* (ISSN 2297-8747), *Mathematics* (ISSN 2227-7390), and *Symmetry* (ISSN 2073-8994) (available at: <https://www.mdpi.com/topics/Fractional.Calculus>).

For citation purposes, cite each article independently as indicated on the article page online and as indicated below:

Lastname, A.A.; Lastname, B.B. Article Title. <i>Journal Name</i> <b>Year</b> , <i>Volume Number</i> , Page Range.
--

**Volume I**

ISBN 978-3-7258-1145-8 (Hbk)

ISBN 978-3-7258-1146-5 (PDF)

[doi.org/10.3390/books978-3-7258-1146-5](https://doi.org/10.3390/books978-3-7258-1146-5)

**Set**

ISBN 978-3-7258-1143-4 (Hbk)

ISBN 978-3-7258-1144-1 (PDF)

© 2024 by the authors. Articles in this book are Open Access and distributed under the Creative Commons Attribution (CC BY) license. The book as a whole is distributed by MDPI under the terms and conditions of the Creative Commons Attribution-NonCommercial-NoDerivs (CC BY-NC-ND) license.

# Contents

<b>Preface</b> . . . . .	<b>vii</b>
<b>Qibing Jin, Bin Wang and Zeyu Wang</b> Recursive Identification for MIMO Fractional-Order Hammerstein Model Based on AIAGS Reprinted from: <i>Mathematics</i> <b>2022</b> , <i>10</i> , 212, doi:10.3390/math10020212 . . . . .	<b>1</b>
<b>Ahmed Salem and Sanaa Abdullah</b> Non-Instantaneous Impulsive BVPs Involving Generalized Liouville–Caputo Derivative Reprinted from: <i>Mathematics</i> <b>2022</b> , <i>10</i> , 291, doi:10.3390/math10030291 . . . . .	<b>22</b>
<b>Bodo Herzog</b> Adopting Feynman–Kac Formula in Stochastic Differential Equations with (Sub-)Fractional Brownian Motion Reprinted from: <i>Mathematics</i> <b>2022</b> , <i>10</i> , 340, doi:10.3390/math10030340 . . . . .	<b>40</b>
<b>Ramsha Shafqat, Azmat Ullah Khan Niazi, Mdi Begum Jeelani and Nadiyah Hussain Alharthi</b> Existence and Uniqueness of Mild Solution Where $\alpha \in \text{InfoNumber}(1, 2)$ for Fuzzy Fractional Evolution Equations with Uncertainty Reprinted from: <i>Fractal Fract.</i> <b>2022</b> , <i>6</i> , 65, doi:10.3390/fractalfract6020065 . . . . .	<b>53</b>
<b>Wang Jun, Cao Lei, Wang Bin, Gong Hongtao and Tang Wei</b> Overview of One-Dimensional Continuous Functions with Fractional Integral and Applications in Reinforcement Learning Reprinted from: <i>Fractal Fract.</i> <b>2022</b> , <i>6</i> , 69, doi:10.3390/fractalfract6020069 . . . . .	<b>71</b>
<b>Dinesh Kumar, Dumitru Baleanu, Frédéric Ayant and Norbert Südland</b> On Transformation Involving Basic Analogue to the Aleph-Function of Two Variables Reprinted from: <i>Fractal Fract.</i> <b>2022</b> , <i>6</i> , 71, doi:10.3390/fractalfract6020071 . . . . .	<b>93</b>
<b>Jiaxin Yuan and Tao Chen</b> Switched Fractional Order Multiagent Systems Containment Control with Event-Triggered Mechanism and Input Quantization Reprinted from: <i>Fractal Fract.</i> <b>2022</b> , <i>6</i> , 77, doi:10.3390/fractalfract6020077 . . . . .	<b>101</b>
<b>Foad Shokrollahi</b> Equity Warrants Pricing Formula for Uncertain Financial Market Reprinted from: <i>Math. Comput. Appl.</i> <b>2022</b> , <i>27</i> , 18, doi:10.3390/mca27020018 . . . . .	<b>130</b>
<b>Wei qiu Pan, Tianzeng Li, Muhammad Sajid, Safdar Ali and Lingping Pu</b> Parameter Identification and the Finite-Time Combination–Combination Synchronization of Fractional-Order Chaotic Systems with Different Structures under Multiple Stochastic Disturbances Reprinted from: <i>Mathematics</i> <b>2022</b> , <i>10</i> , 712, doi:10.3390/math10050712 . . . . .	<b>138</b>
<b>Thongchai Botmart, Zulqurnain Sabir, Muhammad Asif Zahoor Raja, Wajaree Weera, Rahma Sadat and Mohamed R. Ali</b> A Numerical Study of the Fractional Order Dynamical Nonlinear Susceptible Infected and Quarantine Differential Model Using the Stochastic Numerical Approach Reprinted from: <i>Fractal Fract.</i> <b>2022</b> , <i>6</i> , 139, doi:10.3390/fractalfract6030139 . . . . .	<b>164</b>

<b>Jessada Tariboon, Ayub Samadi and Sotiris K. Ntouyas</b> Multi-Point Boundary Value Problems for $(k, \phi)$ -Hilfer Fractional Differential Equations and Inclusions Reprinted from: <i>Axioms</i> <b>2022</b> , <i>11</i> , 110, doi:10.3390/axioms11030110 . . . . .	177
<b>Mian Zhou, Chengfu Li and Yong Zhou</b> Existence of Mild Solutions for Hilfer Fractional Evolution Equations with Almost Sectorial Operators Reprinted from: <i>Axioms</i> <b>2022</b> , <i>11</i> , 144, doi:10.3390/axioms11040144 . . . . .	194
<b>Chen Chen and Qixiang Dong</b> Existence and Hyers–Ulam Stability for a Multi-Term Fractional Differential Equation with Infinite Delay Reprinted from: <i>Mathematics</i> <b>2022</b> , <i>10</i> , 1013, doi:10.3390/math10071013 . . . . .	207
<b>Hanifa Hanif and Sharidan Shafie</b> Impact of $Al_2O_3$ in Electrically Conducting Mineral Oil-Based Maxwell Nanofluid: Application to the Petroleum Industry Reprinted from: <i>Fractal Fract.</i> <b>2022</b> , <i>6</i> , 180, doi:10.3390/fractalfract6040180 . . . . .	222
<b>Wenxing Chen, Shuyang Dai and Baojuan Zhen</b> Continuum Damage Dynamic Model Combined with Transient Elastic Equation and Heat Conduction Equation to Solve RPV Stress Reprinted from: <i>Fractal Fract.</i> <b>2022</b> , <i>6</i> , 215, doi:10.3390/fractalfract6040215 . . . . .	243
<b>Na Liu, Jie Fang, Junwei Sun and Sanyi Li</b> Epidemic Dynamics of a Fractional-Order SIR Weighted Network Model and Its Targeted Immunity Control Reprinted from: <i>Fractal Fract.</i> <b>2022</b> , <i>6</i> , 232, doi:10.3390/fractalfract6050232 . . . . .	280
<b>Basim N. Abood, Saleh S. Redhwan, Omar Bazighifan and Kamsing Nonlaopon</b> Investigating a Generalized Fractional Quadratic Integral Equation Reprinted from: <i>Fractal Fract.</i> <b>2022</b> , <i>6</i> , 251, doi:10.3390/fractalfract6050251 . . . . .	297
<b>Mohammed Shqair, Mohammed Alabedalhadi, Shrideh Al-Omari and Mohammed Al-Smadi</b> Abundant Exact Travelling Wave Solutions for a Fractional Massive Thirring Model Using Extended Jacobi Elliptic Function Method Reprinted from: <i>Fractal Fract.</i> <b>2022</b> , <i>6</i> , 252, doi:10.3390/fractalfract6050252 . . . . .	309
<b>Miran B. M. Amin and Shazad Shawki Ahmad</b> Laplace Transform for Solving System of Integro-Fractional Differential Equations of Volterra Type with Variable Coefficients and Multi-Time Delay Reprinted from: <i>Symmetry</i> <b>2022</b> , <i>14</i> , 984, doi:10.3390/sym14050984 . . . . .	325
<b>Ahmad Mugbil and Nasser-Eddine Tatar</b> Hadamard-Type Fractional Integro-Differential Problem: A Note on Some Asymptotic Behavior of Solutions Reprinted from: <i>Fractal Fract.</i> <b>2022</b> , <i>6</i> , 267, doi:10.3390/fractalfract6050267 . . . . .	336

# Preface

Fractional calculus (FC) generalizes the operations of differentiation and integration to non-integer orders. FC has emerged as an important tool for the study of dynamical systems since fractional order operators are non-local and capture the history of dynamics. Moreover, FC and fractional processes have become one of the most useful approaches to dealing with the particular properties of (long) memory effects in a myriad of applied sciences. Linear, nonlinear, and complex dynamical systems have attracted researchers from many areas of science and technology, involved in systems modelling and control, with applications to real-world problems. Despite the extraordinary advances in FC, addressing both systems' modelling and control, new theoretical developments and applications are still needed in order to accurately describe or control many systems and signals characterized by chaos, bifurcations, criticality, symmetry, memory, scale invariance, fractality, fractionality, and other rich features. This reprint focuses on new and original research results on fractional calculus in science and engineering. Manuscripts address fractional calculus theory, methods for fractional differential and integral equations, nonlinear dynamical systems, advanced control systems, fractals and chaos, complex dynamics, and other topics of interest within FC.

**António Lopes, Alireza Alfi, Liping Chen, and Sergio Adriani David**  
*Editors*

Article

# Recursive Identification for MIMO Fractional-Order Hammerstein Model Based on AIAGS

Qibing Jin, Bin Wang\* and Zeyu Wang

Institute of Automation, Beijing University of Chemical Technology, Beijing 100020, China; jinqb@mail.buct.edu.cn (Q.J.); wangzeyu@buct.edu.cn (Z.W.)

\* Correspondence: 2019210478@buct.edu.cn

**Abstract:** In this paper, adaptive immune algorithm based on a global search strategy (AIAGS) and auxiliary model recursive least square method (AMRLS) are used to identify the multiple-input multiple-output fractional-order Hammerstein model. The model's nonlinear parameters, linear parameters, and fractional order are unknown. The identification step is to use AIAGS to find the initial values of model coefficients and order at first, then bring the initial values into AMRLS to identify the coefficients and order of the model in turn. The expression of the linear block is the transfer function of the differential equation. By changing the stimulation function of the original algorithm, adopting the global search strategy before the local search strategy in the mutation operation, and adopting the parallel mechanism, AIAGS further strengthens the original algorithm's optimization ability. The experimental results show that the proposed method is effective.

**Keywords:** adaptive immune algorithm; multiple-input multiple-output; fractional-order model; Hammerstein model; system identification

**Citation:** Jin, Q.; Wang, B.; Wang, Z. Recursive Identification for MIMO Fractional-Order Hammerstein Model Based on AIAGS. *Mathematics* **2022**, *10*, 212. <https://doi.org/10.3390/math10020212>

Academic Editors: António M. Lopes, Alireza Alf, Liping Chen and Sergio A. David

Received: 30 November 2021

Accepted: 9 January 2022

Published: 11 January 2022

**Publisher's Note:** MDPI stays neutral with regard to jurisdictional claims in published maps and institutional affiliations.



**Copyright:** © 2022 by the authors. Licensee MDPI, Basel, Switzerland. This article is an open access article distributed under the terms and conditions of the Creative Commons Attribution (CC BY) license (<https://creativecommons.org/licenses/by/4.0/>).

## 1. Introduction

In recent years, with the rapid economic and social development, the complexity of industry has been increasing. In order to understand and control these industrial processes more accurately, it is necessary to study system identification. However, in real life, nonlinear processes are inevitable and widespread. Nowadays, there is no definite characterization for nonlinear processes. A block-oriented model is a description of nonlinear model, which is the result of the interaction between the dynamic linear module and static nonlinear module. These model components can be connected in series, parallel, or feedback [1]. Hammerstein model is a typical block-oriented model that consists of a static nonlinear block in cascade with a dynamic linear block [2]. Because the dynamic behavior of the model is only included in the linear block, and the nonlinear block is static, this feature is conducive to identifying and controlling the nonlinear system constructed by the Hammerstein model [3]. Hammerstein model is extensively used to identify nonlinear systems [4–7]. As the model is widely used, the identification methods are also intensively discussed. These methods include neural networks [8,9], piecewise linear model [6], least square method [10], support vector machine [11], combined prior information [12], and so on.

In real life, it is evident that the dynamic linear block based on integer order cannot fully simulate the real model [13]. The fractional-order model extends the order of the model from the integer level to the fractional level. Therefore, the study of the fractional-order nonlinear model is essential [14]. At present, fractional-order models have been discussed in many fields, such as molecular materials [15,16], the voltage and current of the drive end impedance [17], industrial battery [18–20], and so on.

With the wide application of the fractional-order model, the problem of model identification has also been intensively discussed. However, the current methods have some

limitations. The particle swarm optimization algorithm can be used to identify the parameters of the fractional Hammerstein model [21]. This method excessively depends on the optimization ability of the algorithm and does not consider the internal relationship between system parameters. Once the optimization algorithm has problems, it will significantly impact the identification results. The Levenberg–Marquardt algorithm developed by combining the two decomposition principles [22] can only be applied to the theoretical environment. Once the system is affected by noise, the model's parameters will not be identified exactly. Reference [23] also requires an ideal environment. Some scholars pay attention to the fractional-order Hammerstein model with single-input single-output [24–28]. Some pay attention to the fractional-order Hammerstein model with multiple-input multiple-output, but most use the state space equation as the linear block of the model [29,30]. However, fractional-order calculus is a whole concept [31]. Using the transfer function of differential equation to construct the linear block of the Hammerstein model can better integrate the two concepts.

Based on the above background, this paper discusses a new method to identify the nonlinear coefficients, linear coefficients, and fractional order of the MIMO fractional Hammerstein model. In this method, AIAGS greatly improves the optimization ability by improving the immune algorithm's stimulation function and search strategy. Then, the algorithm estimates the initial values of all MIMO fractional Hammerstein model parameters, including fractional order. The estimated result provides relatively accurate initial values for the subsequent algorithm. It solves the problem that the two-step method [28], which identifies coefficient and order, depends on the initial values. Then, using AMRLS, a method for accurate parameter identification of the MIMO fractional-order model is proposed. Finally, the effectiveness of the proposed method is verified by numerical simulation.

The main contribution of this paper is to propose an adaptive immune algorithm with a global search strategy to accurately identify the initial parameters of the fractional Hammerstein system. Secondly, a new recursive identification method for coefficients and fractional order of MIMO fractional-order nonlinear system with differential equation transfer function as linear block model is derived using an auxiliary model. Due to the different ways of selecting the optimal solution, the AIAGS algorithm proposed in this paper has higher reliability than the classical immune algorithm. Based on the auxiliary model, the recursive identification algorithm for the MIMO fractional Hammerstein model is given using the recursive least square method. The method in this paper solves the initial value problem of previous methods and provides more accurate initial values. This initial value cooperates with AMRLS, making the result of parameters identification of multi-input and multi-output fractional Hammerstein model closer to reality.

In this paper, an improved immune algorithm is proposed in Section 2. In Section 3, a new recursive identification method for MIMO fractional-order Hammerstein model with differential equation transfer function as linear block model is derived by using auxiliary model is discussed. In Section 4, numerical simulations show the effectiveness of the proposed method. Finally, Section 5 gives some conclusions.

## 2. Adaptive Immune Algorithm Based on Global Search Strategy

### 2.1. Review of Immune Algorithms

The immune algorithm is an adaptive intelligent system inspired by immunology and simulates the functions and principles of the biological immune system to solve complex problems. It retains several characteristics of the biological immune system, including global search capability, diversity maintenance mechanism, strong robustness, and parallel distributed search mechanism. The immune algorithm automatically generates the initial population by uniform probability distribution. After initialization, the population evolves and improves by the following steps: calculation of stimulation, selection, cloning, mutation, clonal inhibition, etc. [32].

## 2.2. AIAGS

### 2.2.1. Stimulation Improvement

Individual stimulation is the evaluation result of individual quality, which needs to be comprehensively considered individual affinity and concentration. The individual stimulation can usually be obtained by a simple mathematical calculation based on the evaluation results of individual affinity and concentration. In the traditional immune algorithm [33], the stimulation is expressed as

$$f_{sim}(x_i) = a \cdot f_{aff}(x_i) - b \cdot f_{den}(x_i) \tag{1}$$

where  $x_i$  means the  $i$ th individual of the population;  $f_{aff}(x_i)$  is affinity, which represents the Euclidean distance between the current individual and the optimal individual;  $f_{den}(x_i)$  is the concentration, indicating the number of other individuals whose Euclidean distance between the current individual and other individuals is within a certain threshold;  $f_{sim}(x_i)$  is the stimulation;  $a$  and  $b$  is the calculation parameter. The algorithm will sort the individuals according to the stimulation and make the next choice.

This paper made the following changes to the coefficients of affinity and concentration. Firstly, the minus sign of Equation (1) is changed on the plus sign. Because the concentration represents the quality of population diversity, and too high concentration means that there are many very similar individuals in the population, the key point of the immune algorithm is to suppress the individuals with a high concentration to achieve global optimization. However, in both the original algorithm and various improved immune algorithms today, the coefficient  $b$  is non-negative, which leads to a minor incentive for individuals with low affinity and high concentration [34–38]. This improvement conforms to the core concept of the algorithm.

Secondly, this paper designs a parameter  $\beta$  related to the current population’s maximum, minimum, and individual affinity values. In the original algorithm, the  $a$  and  $b$  are constants. In various improved algorithms [34–38], the adaptive coefficients are only related to the number of current iterations. Because the comparison of stimulations between individuals is carried out in the population of the current iteration, these adaptive coefficients are not different from constants. They will not affect the stimulation ranking of the population. In this paper, because  $\beta$  is quadratic when selecting individuals based on stimulations, individuals with low affinity and individuals with high affinity will be considered, increasing the global searchability. The parameter is expressed as

$$\beta = \left( \frac{f_{aff}(x_i) - f_{aff_a}}{f_{aff_{max}} - f_{aff_a}} \right)^2 \tag{2}$$

where  $f_{aff_a}$  is the average of  $f_{aff_{max}}$  and  $f_{aff_{min}}$ .

Finally, after a certain number of iterations, the population will move closer to the optimal global individual. If the concentration problem is also considered, it may give up the found optimal range and select the new random individual when selecting the individuals. Therefore, a monotone decreasing adaptive operator is designed in this paper. In the middle and later iteration stages, the concentration effect is negligible.

To sum up, the stimulation for this paper is expressed as

$$f_{sim}(x_i) = (1 - \beta) \cdot f_{aff}(x_i) + \left[ 1 - \sqrt{\frac{2gen}{G} - \left(\frac{gen}{G}\right)^2} \right] \cdot 0.5\beta \cdot f_{den}(x_i) \tag{3}$$

where  $gen$  means the current number of iterations and  $G$  is the total number of iterations.

After improvement, the approximate trend of individual stimulations is shown in Figure 1a. The approximate trend of the stimulations of the original or other improved immune algorithm is shown in Figure 1b. The  $x$ -axis is 100 individuals sorted from smallest to largest according to affinity, and the  $y$ -axis is individual stimulation. It can be seen from Figure 1 that the original algorithm and other improved algorithms generally only

select individuals with low affinity. In contrast, the algorithm in this paper can consider individuals with high affinity.

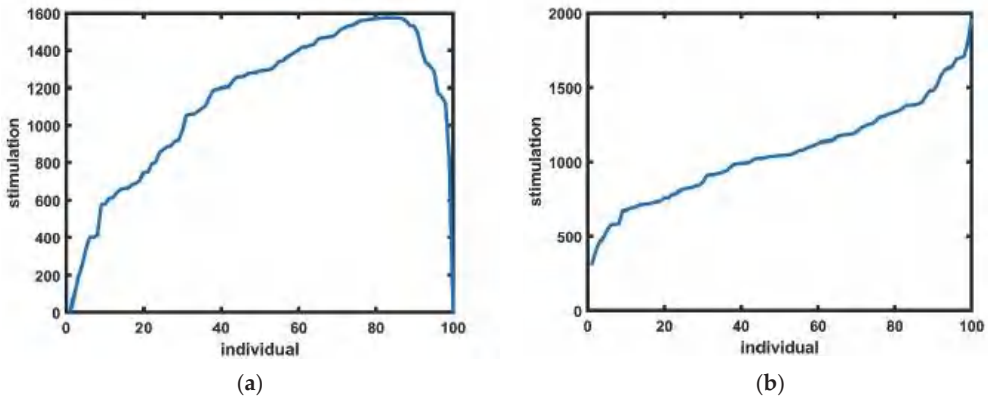


**Figure 1.** Comparison of stimulations. (a) The stimulations of AIAGS. (b) The stimulations of other algorithms.

### 2.2.2. Mutation Strategy Improvement

The original algorithm has a single strategy in the mutation stage. The algorithm improved by others will enrich the mutation strategy and improve the probability of all individuals for mutation. However, the mutation strategy is selected only by random numbers, which makes the algorithm not flexible [38].

The algorithm of this paper has two minor changes in the mutation stage. First, an adaptive operator  $pm$  that changes from algebra is designed, and its value decreases monotonically between 0 and 0.8. The parameter can be expressed as

$$pm = 0.8 \cdot \left(1 - \frac{gen}{G}\right) \tag{4}$$

Secondly, when setting the global optimization step, a variable  $sv$  is added based on adaptation, gradually changing the mutation step. The optimal individual is selected for retention of the individuals after several mutations, which greatly enhances the global search ability.

To sum up, the mutation strategy for this paper can be expressed as

$$x_{i,j} = \begin{cases} x_{best,j} + pm \cdot (x_{r1,j} - x_{r2,j}), & rand > pm \\ x_{r1,j} + (pm + sv) \cdot (x_{r2,j} - x_{r3,j}), & otherwise \end{cases} \tag{5}$$

where  $i$  means the sequence of individuals in the population;  $j$  denotes the sequence of dimensions in the individual;  $x_{r1}$ ,  $x_{r2}$ , and  $x_{r3}$  are different individuals randomly selected from the population except for the  $x_i$ .

Obviously, in the early stage of the iteration, the mutation strategy will mostly choose the second mutation strategy, edge mutation strategy, which will enhance the global optimization ability of the algorithm. In the middle and later stages of the iteration, the first mutation strategy, the optimal individual mutation strategy, will be selected for local search.

### 2.2.3. Simulated Annealing Strategy

The simulated annealing algorithm mimics the annealing process in metallurgy and is classified as a single-based solution method. After comparing the current optimal solution with the previous optimal solution, if the fitness of the current optimal solution is greater than that of the previous one, it may abandon the current result and choose the previous result [39].

At the end of the improved algorithm, simulated annealing is added to avoid the algorithm falling into the local optimum. Some people have done similar work, but both the initial algorithm and others' improved algorithm use stimulus to evaluate the optimal solution [33]. This paper uses affinity to evaluate the optimal solution at the end. However, the stimulation of the optimal individual of the previous generation may be slightly big, resulting in not being selected during mutation selection, so the affinity of the optimal individual of the current generation may be greater than that of the previous generation. At this time, the effect of simulated annealing will likely jump back to the result to optimize further. The replacement for such a case depends on the probability  $p$  as defined as

$$p = e^{-\Delta F} \Delta F = \frac{f_{aff}(x_i')}{f_{aff}(x_i)} - 1 \tag{6}$$

where  $x_i'$  is the current optimal solution;  $x_i$  denotes the previous optimal solution. This part will replace the solution if  $p < rand(0, 1)$ .

#### 2.2.4. Pseudo Code of AIAGS

To sum up, there are some innovations of this paper on the existing immune algorithms. The pseudo code of AIAGS is explained in detail in Algorithm 1. The flowchart of AIAGS is explained in detail in Figure 2.

---

#### Algorithm 1: AIAGS

---

- Step.1** Define the objective function  $F(x)$ ;
  - Step.2** Initialize population  $X$ ;
  - Step.3** Evaluate all the individuals  $x_i$  by the objective function  $F(x)$ ;
  - Step.4** Calculate the affinity  $f_{aff}(x_i)$  and concentration  $f_{den}(x_i)$  of each individual;
  - Step.5** Initialize the number of iteration  $m = 1$ ;
  - Step.6** While  $m < \text{max number of iterations } M$ ;
  - Step.7** Calculate the stimulation  $f_{sim}(x_i)$  of each individual by the Equation (3);
  - Step.8** Select the individuals in the population by stimulation and clone the individuals;
  - Step.9** Mutate the cloned individuals by the Equation (5);
  - Step.10** If the generated mutation vector exceeds the boundary, a new mutation vector is generated randomly until it is within the boundary;
  - Step.11** Inhibit cloning and calculate the affinity of each new individual;
  - Step.12** Generate optimal individual by Simulated Annealing by the Equation (6);
  - Step.13** End;
  - Step.14**  $m = m + 1$ ;
  - Step.15** End while;
  - Step.16** Return the best solution.
- 

#### 2.3. Benchmark Function

Due to the limitations of intelligent optimization algorithms, unlike the traditional algorithm, which has a mathematical theoretical basis, it is not strict. After improving the optimization algorithm, most people use the classical benchmark function to test the algorithm's effectiveness. This article uses eight classical and four CEC2017 benchmark functions to evaluate AIAGS. The  $u()$  of F6 and F7 is expressed as

$$u(x_i, a, k, m) = \begin{cases} K(x_i - a)^m, & \text{if } x_i > a \\ 0, & -a \leq x_i \leq a \\ K(-x_i - a)^m, & -a \leq x_i \end{cases} \tag{7}$$

These classical functions are divided into three groups: unimodal (F1–F4), multimodal (F5–F7), and fixed-dimension multimodal (F8). The unimodal benchmark function has only one optimal solution, which can verify the development and convergence. The multimodal benchmark function has many optimal solutions. However, there is only one global optimal

solution, and the rest are local optimal solutions. The fixed dimensional multimodal functions can define the desired number of design variables and could provide a different search space. Therefore, the multimodal functions are responsible for testing exploration and avoiding the entrapment in the optimal local solution. Hybrid and composition functions can reflect some problems that are closer to reality [40]. In Table 1, the corresponding properties of these functions are listed, where dim represents the dimensions of the functions and range indicates the scope of the search space.

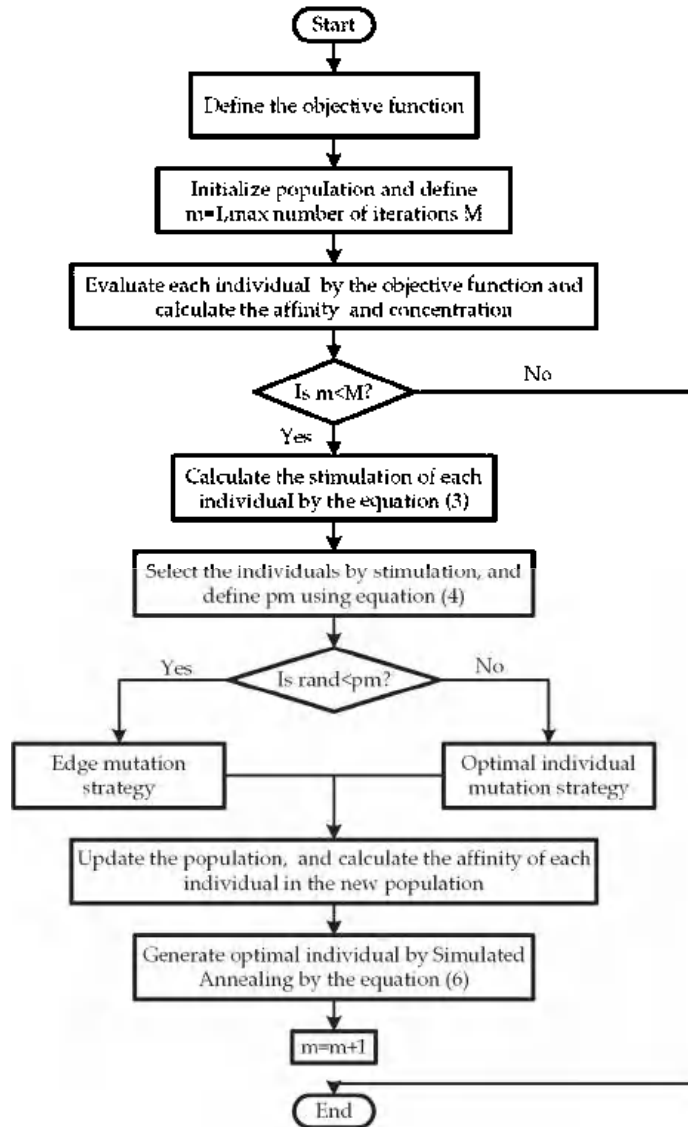


Figure 2. AIAGS.

**Table 1.** Benchmark functions.

Name	Formula	Range	$f_{min}$
Sphere	$F1(x) = \sum_{i=1}^D x_i^2$	$[-20, 20]$	0
Schwefel 1.2	$F2(x) = \sum_{i=1}^D (\sum_{j=1}^i x_j)^2$	$[-100, 100]$	0
Rosenbrock	$F3(x) = \sum_{i=1}^{D-1} [100 \cdot (x_i^2 - x_{i+1})^2 + (x_i - 1)^2]$	$[-30, 30]$	0
Step	$F4(x) = \sum_{i=1}^D (x_i + 0.5)^2$	$[-100, 100]$	0
Ackley	$F5(x) = -20 \exp(-0.2 \sqrt{\frac{1}{D} \sum_{i=1}^D x_i^2}) - \exp[\frac{1}{D} \sum_{i=1}^D \cos(2\pi x_i)] + 20 + e$	$[-40, 40]$	0
Generalized penalized 1	$F6(x) = \frac{\pi}{n} [10 \sin(\pi y_1)] + \sum_{i=1}^{D-1} (y_i - 1)^2 [1 + 10 \sin^2(\pi y_{i+1})] + \sum_{i=1}^D u(x_i, 10, 100, 4), y_i = 1 + \frac{x_i + 1}{4}$	$[-50, 50]$	0
Generalized penalized 2	$F7(x) = 0.1 \{ \sin^2(3\pi x_1) + \sum_{i=1}^D (x_i - 1)^2 [1 + \sin^2(3\pi x_i + 1)] + (x_D - 1)^2 + \sin^2(2\pi x_D) \} + \sum_{i=1}^n u(x_i, 5, 100, 4)$	$[-50, 50]$	0
Shekel's Foxholes	$F8(x) = [\frac{1}{500} + \sum_{j=1}^{25} \frac{1}{j + \sum_{i=1}^n (x_i - a_{ij})}]^{-1}$	$[-70, 70]$	1
Hybrid function 4 ( $N = 4$ )	F9(x)	$[-100, 100]$	1400
Hybrid function 7 ( $N = 5$ )	F10(x)	$[-100, 100]$	1700
Composition function 1 ( $N = 3$ )	F11(x)	$[-100, 100]$	2100
Composition function 4 ( $N = 4$ )	F12(x)	$[-100, 100]$	2400

2.3.1. Comparison of AIAGS with Other Algorithms

In order to reflect the improvement effect of the immune algorithm in this paper, this section compares AIAGS with the original immune algorithm two improved immune algorithms: improved artificial immune algorithm (IAIA) [28] and modified artificial immune algorithm (MAIA) [29], and two new algorithms: Harris hawks optimization (HHO) [41] and Aquila optimizer (AO) [42]. The parameter settings of the counterparts' algorithms are given in Table 2. The comparison results are shown in Table 3. However, intelligent algorithms are highly accidental. After several tests, this paper calculates the average value and standard deviation of each test result to avoid misleading the experimental results and the practical application of the algorithm.

**Table 2.** Parameter settings.

Algorithm	Parameter Settings
AIAGS	$\delta = 0.1, sv = 0.2$
AO	$\alpha = 0.5, \delta = 0.5$
IA	$\alpha = 2, \beta = 1, \delta = 0.2, pm = 0.7$
IAIA	$\alpha = 2, \beta = 1, \delta = 0.613, pm = 0.7$
MAIA	$\delta = 0.8, pm = 0.8, cr = 0.8$
HHO	$\alpha = 0.5, \delta = 0.5$

**Table 3.** Comparison of results obtained for the benchmark functions.

	AIAGS	AO	IA	IAIA	MAIA	HHO
F1						
worst	0	$2.86 \times 10^{-71}$	0.000124	0.000145	0.030882	$1.98 \times 10^{-46}$
best	0	$7.37 \times 10^{-76}$	$7.65 \times 10^{-5}$	$3.54 \times 10^{-5}$	0.001683	$2.62 \times 10^{-58}$
Avg	0	$5.74 \times 10^{-72}$	$9.86 \times 10^{-5}$	$7.71 \times 10^{-5}$	0.012509	$1.99 \times 10^{-47}$
Std	0	$1 \times 10^{-71}$	$1.46 \times 10^{-5}$	$3.28 \times 10^{-5}$	0.009914	$5.95 \times 10^{-47}$
F2						
worst	0	$2.82 \times 10^{-56}$	0.006578	0.022761	16.07011	$1.71 \times 10^{-42}$
best	0	$1.72 \times 10^{-73}$	0.002606	0.013182	0.812125	$1.15 \times 10^{-51}$

Table 3. Cont.

	AIAGS	AO	IA	IAIA	MAIA	HHO
Avg	0	$2.82 \times 10^{-57}$	0.003962	0.017273	4.565824	$3.78 \times 10^{-43}$
Std	0	$8.93 \times 10^{-57}$	0.001401	0.003087	4.947259	$6.69 \times 10^{-43}$
<b>F3</b>						
worst	$6.39 \times 10^{-7}$	0.001305	433.5283	696.2436	83.41411	0.008889
Best	$5.5 \times 10^{-9}$	$5 \times 10^{-6}$	0.99727	0.762353	4.4702	$2.1 \times 10^{-5}$
Avg	$9.99 \times 10^{-8}$	0.000319	80.76008	143.8289	29.75245	0.002238
Std	$1.83 \times 10^{-7}$	0.000424	143.8194	240.8117	30.68641	0.002581
<b>F4</b>						
worst	0	$6.97 \times 10^{-5}$	0.004139	0.00329	0.00329	$9.33 \times 10^{-5}$
Best	0	$2.3 \times 10^{-7}$	0.001612	0.00174	0.00174	$7.93 \times 10^{-10}$
Avg	0	$1.87 \times 10^{-5}$	0.003066	0.002567	0.002567	$2.05 \times 10^{-5}$
Std	0	$2.32 \times 10^{-5}$	0.00077	0.00053	0.00053	$2.64 \times 10^{-5}$
<b>F5</b>						
worst	$8.88 \times 10^{-16}$	$8.88 \times 10^{-16}$	4.663342	3.223428	1.019824	$8.88 \times 10^{-16}$
Best	$8.88 \times 10^{-16}$	$8.88 \times 10^{-16}$	0.017455	0.019081	0.137416	$8.88 \times 10^{-16}$
Avg	$8.88 \times 10^{-16}$	$8.88 \times 10^{-16}$	1.139553	0.342006	0.437464	$8.88 \times 10^{-16}$
Std	0	0	1.617355	1.012431	0.323219	0
<b>F6</b>						
worst	$4.71 \times 10^{-32}$	$3.84 \times 10^{-5}$	4.772913	6.250579	0.005788	$2.07 \times 10^{-5}$
Best	$4.71 \times 10^{-32}$	$7.83 \times 10^{-8}$	$1.16 \times 10^{-5}$	0.335882	0.000107	$1.56 \times 10^{-7}$
Avg	$4.71 \times 10^{-32}$	$7.48 \times 10^{-6}$	1.984778	3.781554	0.001743	$6.34 \times 10^{-6}$
Std	0	$1.16 \times 10^{-5}$	1.830602	2.512286	0.002048	$6.86 \times 10^{-6}$
<b>F7</b>						
worst	$1.35 \times 10^{-32}$	0.000281	0.000101	$8.19 \times 10^{-5}$	0.039677	0.000501
best	$1.35 \times 10^{-32}$	$1.31 \times 10^{-6}$	$5.21 \times 10^{-5}$	$3.87 \times 10^{-5}$	0.002672	$1.18 \times 10^{-7}$
Avg	$1.35 \times 10^{-32}$	$4.25 \times 10^{-5}$	$8.01 \times 10^{-5}$	$5.89 \times 10^{-5}$	0.017996	$8.5 \times 10^{-5}$
Std	$2.88 \times 10^{-48}$	$8.69 \times 10^{-5}$	$1.55 \times 10^{-5}$	$1.58 \times 10^{-5}$	0.01293	0.000143
<b>F8</b>						
worst	0.998004	2.982105	1.992031	0.998004	0.999027	1.992031
best	0.998004	0.998004	0.998004	0.998004	0.998004	0.998004
Avg	0.998004	1.593234	1.166875	0.998004	0.998107	1.196819
Std	$2.34 \times 10^{-16}$	0.958412	0.362935	$2.01 \times 10^{-15}$	0.000323	0.397606
<b>F9</b>						
worst	1528.366	5142.015	2215.496	2302.871	5755.439	4349.2
best	1472.889	1557.776	1443.205	1428.962	1488.148	1450.039
Avg	1503.786	2462.484	1580.193	1655.434	2510.73	1833.8
Std	19.26844	978.4552	223.2629	287.2931	1264.939	843.7423
<b>F10</b>						
worst	1794.68	1838.131	1763.443	1782.14	2200.955	1840.59
Best	1744.138	1731.296	1722.813	1725.397	1766.414	1744.772
Avg	1774.579	1781.842	1738.947	1748.674	1898.936	1781.998
Std	17.10128	32.03933	10.8574	22.15373	122.3724	30.2191
<b>F11</b>						
worst	2260.104	2338.993	2264.487	2288.434	2319.733	2388.341
Best	2209.787	2204.09	2200.005	2200.003	2201.822	2205.34
Avg	2236.802	2272.26	2211.444	2211.249	2265.511	2272.888
Std	18.17673	56.04231	18.0651	25.8142	44.29724	71.44948
<b>F12</b>						
worst	2717.367	2778.692	2772.984	2762.261	2824.593	2857.503
Best	2521.748	2746.416	2500.074	2500.073	2505.906	2770.847
Avg	2626.946	2767.838	2669.676	2629.372	2710.07	2799.953
Std	61.88762	9.524766	114.739	111.2591	104.6337	28.32715

### 2.3.2. Convergence

Convergence is the ability of the algorithm to search and converge to an acceptable solution in a certain time. Convergence is an important index to evaluate the performance of the algorithm. An algorithm has high convergence, which means fast optimization speed and high precision. Generally, the convergence speed can be measured by the number of iterations, and the convergence value can measure the accuracy.

The convergence curves of AIAGS and the other five algorithms in 12 benchmark functions are shown in Figure 3. It can be seen from Table 2 and Figure 3 that the convergence speed and optimization ability of AIAGS are not the strongest in individual benchmark functions. On the whole, AIAGS is far better than other immune algorithms in terms of convergence speed and optimization ability, and it is also better than the other two algorithms.

### 2.4. Summary

In this chapter, the immune algorithm’s stimulation function and mutation strategy are improved, and simulated annealing is added to the final step to select the optimal solution. The core idea of these improvements is to avoid finding the optimal local solution. After improving the algorithm, 12 different types of benchmark functions are used to evaluate the algorithm’s performance. Experiments show that the development and exploration ability of AIAGS is significantly improved compared with the previous immune algorithm. These conclusions provide substantial proof for the following system identification work.

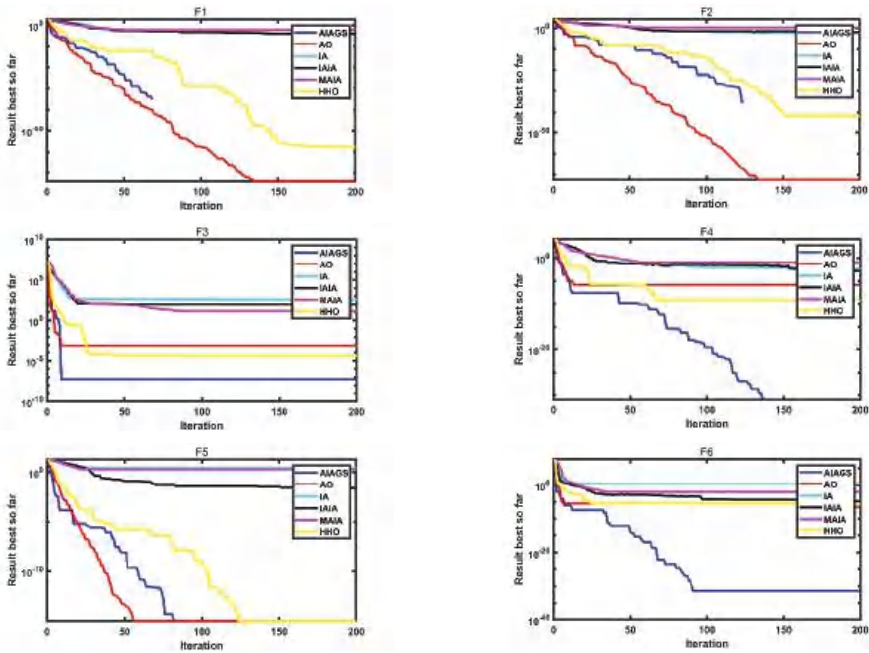


Figure 3. Cont.

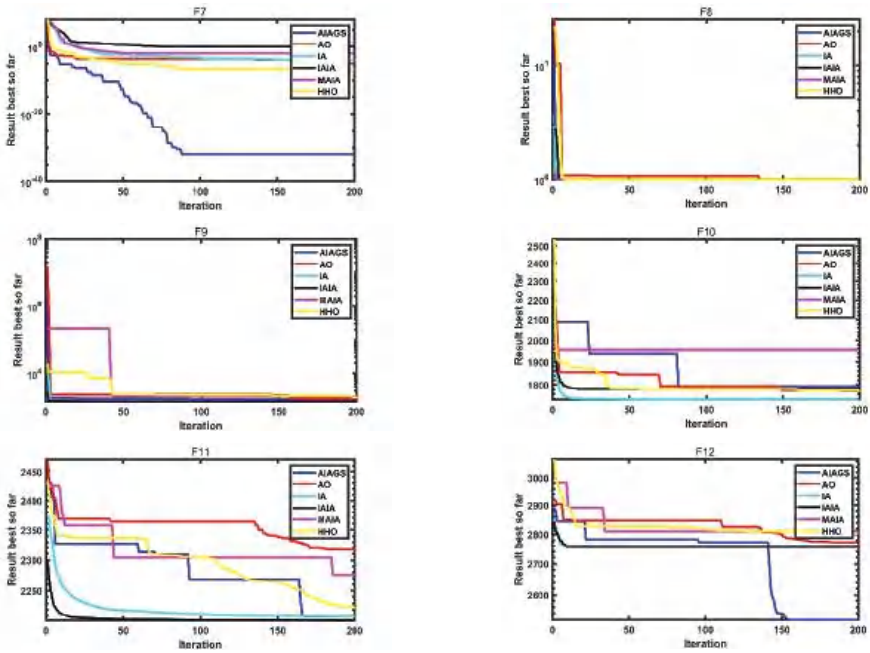


Figure 3. The convergence curves of AIAGS and other six algorithms.

### 3. Identification Method of MIMO Fractional Order Hammerstein Model

#### 3.1. MIMO Fractional Order Hammerstein Model

##### 3.1.1. Fractional Order Differentiation

At present, there are three definitions widely used in the field of fractional calculus: Grünwald–Letnikov (GL), Riemann–Liouville (RL), and Caputo definitions. Because the GL is easy to program [43], this paper considers it the research object. The definition of fractional order calculus can be expressed as

$$D_t^\alpha f(t) = \lim_{h \rightarrow 0} \frac{1}{h^\alpha} \sum_{j=0}^{\lceil \frac{t-t_0}{h} \rceil} (-1)^j \binom{\alpha}{j} f(t - jh) \tag{8}$$

where  $\alpha$  is the fractional order. Because this paper explores differential equations,  $\alpha > 0$ .  $h$  is the sampling time;  $\lceil \cdot \rceil$  means that the integer part is reserved;  $(-1)^j \binom{\alpha}{j}$  is the binomials of  $(1 - z)^\alpha$ . By denoting  $w_j^\alpha$  to replace the binomials, so  $w_j^\alpha$  can be expressed as

$$w_j^\alpha = (-1)^j \binom{\alpha}{j} = \frac{(-1)^j \Gamma(\alpha + 1)}{\Gamma(j + 1) \Gamma(\alpha - j + 1)} \tag{9}$$

Finally, when  $t_0 = 0$ , the definition of fractional order calculus can be expressed as

$$D_t^\alpha f(t) = \frac{1}{h^\alpha} \sum_{j=0}^{\lceil \frac{t-a}{h} \rceil} w_j^\alpha f(t - jh) \tag{10}$$

### 3.1.2. MIMO Fractional-Order Hammerstein System

The MIMO Hammerstein model of this paper can be schematically represented in Figure 4. Hammerstein model is a typical nonlinear model composed of static nonlinear block and dynamic linear block. the dynamic linear block can be expressed as

$$\begin{bmatrix} y_1(t) \\ y_2(t) \\ \vdots \\ y_N(t) \end{bmatrix} = \begin{bmatrix} G_{1,1} & G_{1,2} & \dots & G_{1,M} \\ G_{2,1} & G_{2,2} & \dots & G_{2,M} \\ \vdots & \vdots & \dots & \vdots \\ G_{N,1} & G_{N,2} & \dots & G_{N,M} \end{bmatrix} \begin{bmatrix} u'_1(t) \\ u'_2(t) \\ \vdots \\ u'_M(t) \end{bmatrix} \quad (11)$$

where  $y_k(t)$  is the  $k$ th system output;  $u'_l(t)$  is generated by the  $l$ th system input  $u_l(t)$  through the nonlinear block, which can be expressed as

$$\begin{aligned} u'_l(t) &= c_{l,1} \cdot f_{l,1}(u_l(t)) + c_{l,2} \cdot f_{l,2}(u_l(t)) + \dots + c_{l,n_l} \cdot f_{l,n_l}(u_l(t)) \\ &= \sum_{m=1}^{n_l} c_{l,m} \cdot f_{l,m}(u_l(t)) \end{aligned} \quad (12)$$

where  $c_{l,}$  are coefficients to be identified;  $f_{l,}()$  are a series of basic functions.  $G_{k,l}$  is a fractional-order transfer function, which can reflect the relationship between  $u'_l(t)$  and  $y_k(t)$ ; it is defined as

$$G_{k,l}(s) = \frac{b_{k,l,m} s^{m\alpha} + b_{k,l,m-1} s^{(m-1)\alpha} + \dots + b_{k,l,0}}{a_{k,l,n} s^{n\alpha} + a_{k,l,n-1} s^{(n-1)\alpha} + \dots + a_{k,l,0}} \quad (13)$$

where  $a_{k,l,}$  and  $b_{k,l,}$  are coefficients to be identified;  $\alpha$  is the fractional order to be identified. For the convenience of calculation and programming, in this paper  $a_{k,l,0}$  is assumed to be 1. According to Equations (11) and (13), the  $k$ th system output can be expressed as

$$\begin{aligned} y_k &= G_{k,1}u'_1 + G_{k,2}u'_2 + \dots + G_{k,M}u'_M \\ &= \frac{b_{k,1,m}S^{m\alpha} + b_{k,1,m-1}S^{(m-1)\alpha} + \dots + b_{k,1,0}}{a_{k,1,n}S^{n\alpha} + a_{k,1,n-1}S^{(n-1)\alpha} + \dots + a_{k,1,0}S^0 + 1} u'_1 \\ &\quad + \frac{b_{k,2,m}S^{m\alpha} + b_{k,2,m-1}S^{(m-1)\alpha} + \dots + b_{k,2,0}}{a_{k,2,n}S^{n\alpha} + a_{k,2,n-1}S^{(n-1)\alpha} + \dots + a_{k,2,0}S^0 + 1} u'_2 \\ &\quad + \dots + \frac{b_{k,M,m}S^{m\alpha} + b_{k,M,m-1}S^{(m-1)\alpha} + \dots + b_{k,M,0}}{a_{k,M,n}S^{n\alpha} + a_{k,M,n-1}S^{(n-1)\alpha} + \dots + a_{k,M,0}S^0 + 1} u'_M \end{aligned} \quad (14)$$

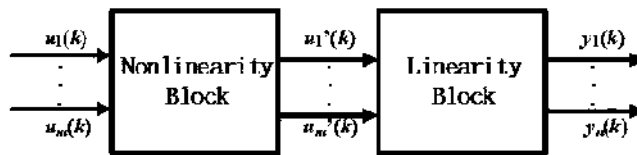


Figure 4. MIMO Hammerstein model.

By reduction of fractions to a common denominator and simplifying Equation (14), we can get an equation described as

$$\begin{aligned} & \left( A_{k,N_A} S^{N_A\alpha} + A_{k,N_A-1} S^{(N_A-1)\alpha} + \dots + A_{k,1} S^0 + 1 \right) y_k \\ &= \left( B_{k,1,N_B} S^{N_B\alpha} + B_{k,1,N_B-1} S^{(N_B-1)\alpha} + \dots + B_{k,1,0} \right) u'_1 + \\ & \left( B_{k,2,N_B} S^{N_B\alpha} + B_{k,2,N_B-1} S^{(N_B-1)\alpha} + \dots + B_{k,2,0} \right) u'_2 + \dots + \\ & \left( B_{k,M,N_B} S^{N_B\alpha} + B_{k,M,N_B-1} S^{(N_B-1)\alpha} + \dots + B_{k,M,0} \right) u'_M \end{aligned} \quad (15)$$

where  $A$  is the polynomial containing  $a$ ;  $B$  is the polynomial containing  $a$  and  $b$ ; the coefficient of fractional order  $N_A = M * n, N_B = (M - 1) * n + m$ . To sum up, the MIMO fractional-order Hammerstein system discussed in this paper can be expressed as

$$\begin{cases} y_k(t) + \sum_{i=1}^{n_A} A_{k,i} D^{i\alpha} y_k(t) = \sum_{l=0}^M \sum_{j=0}^{n_B} B_{k,l,j} D^{j\alpha} u_l'(t) \\ y_k'(t) = y_k(t) + v(t) \end{cases} \tag{16}$$

where  $v(t)$  is the Gaussian white noise;  $y_k'(t)$  is the measured output containing noise. According to Equations (10) and (16), the MIMO fractional-order Hammerstein system can be expressed as

$$y_k'(t) = \frac{1}{(1 + \sum_{i=1}^{n_A} A_i / h^{i\alpha})} \cdot \left[ \sum_{l=0}^M \sum_{i=0}^{n_B} \sum_{m=1}^{n_c} \frac{B_{k,l,i}}{h^{i\alpha}} c_{l,m} \cdot \sum_{j=0}^{[t/h]} w_j^{i\alpha} f_{l,m}(u_l(t - jh)) - \sum_{i=1}^{n_A} \frac{A_i}{h^{i\alpha}} \sum_{j=1}^{[t/h]} w_j^{i\alpha} y_k(t - jh) \right] + v(t) \tag{17}$$

### 3.2. Parameter Identification Based on Auxiliary Model Recursive Least Square Method

In the MIMO fractional-order Hammerstein model, all the coefficients and the fractional order are needed to be identified. Previous articles usually considered only part of coefficients or for the SISO system. The work of this paper is rarely concerned before. The identification work is divided into coefficient identification and order identification. However, the two results affect each other, which cannot identify coefficients precisely without a precise fractional order. This paper will first use a series of input and output data to obtain the initial values of coefficients and the fractional order by the AIAGS algorithm mentioned above. The initial value is a little precise. Then, the initial value will be used to get the parameter identification result of the fractional-order Hammerstein model through the auxiliary model recursive least squares (AMRLS) algorithm.

#### 3.2.1. Coefficient Identification

According to the basic knowledge of system identification, the input–output relations can be expressed as

$$y_k'(t) = y_k(t) + v(t) = \varnothing_k(t) \cdot \theta_k^T + v(t) \tag{18}$$

where  $\varnothing_k(t)$  is the variable vector including input–output data, which is expressed as

$$\begin{aligned} \varnothing_k(t) &= \left[ \varnothing_{k,A}(t), \varnothing_{B_{k,1,0}}(t), \varnothing_{B_{k,1,1}}(t), \dots, \varnothing_{B_{k,1,n_B}}(t), \dots, \varnothing_{B_{k,M,0}}(t), \varnothing_{B_{k,M,1}}(t), \dots, \varnothing_{B_{k,M,n_B}}(t) \right] \\ \varnothing_{k,A}(t) &= \left[ -\sum_{j=1}^{[t/h]} w_j^\alpha y_k(t - jh), \dots, -\sum_{j=1}^{[t/h]} w_j^{n_A \alpha} y_k(t - jh) \right] \\ \varnothing_{B_{k,l,i}}(t) &= \left[ \sum_{j=0}^{[t/h]} w_j^{i\alpha} f_{l,1}(u_l(t - jh)), \dots, \sum_{j=0}^{[t/h]} w_j^{i\alpha} f_{l,M}(u_l(t - jh)) \right] \end{aligned} \tag{19}$$

According to Equations (16) and (17), the vector  $\theta_k$  is found and expressed as

$$\begin{aligned} \theta_k &= \left[ \theta_{k,A}, \theta_{B_{k,1,0}}, \dots, \theta_{B_{k,1,n_B}}, \dots, \theta_{B_{k,M,0}}, \dots, \theta_{B_{k,M,n_B}} \right] \\ \theta_{k,A} &= [Q_{k,1}, Q_{k,2}, \dots, Q_{k,n_A}] \\ \theta_{B_{k,l,i}} &= [W_{k,1,i} c_{1,1}, \dots, W_{k,1,i} c_{1,n_c}, \dots, W_{k,M,i} c_{M,1}, \dots, W_{k,M,i} c_{M,n_c}] \end{aligned} \tag{20}$$

where

$$\begin{aligned} Q_{k,i} &= \frac{\frac{A_{k,i}}{h^{i\alpha}}}{1 + \sum_{i=1}^{n_A} \frac{A_{k,i}}{h^{i\alpha}}} \\ W_{k,l,j} &= \frac{\frac{B_{k,l,j}}{h^{j\alpha}}}{1 + \sum_{i=1}^{n_A} \frac{A_{k,i}}{h^{i\alpha}}} \end{aligned} \tag{21}$$

It can be clearly seen that  $\theta_k$  contains coefficients that need to be identified. It is worth mentioning that  $y_k(t - jh)$  is unknown so that  $\theta_{k,A}$  cannot be identified directly by  $\varphi_{k,A}(t)$ . According to references [44], an auxiliary model is used to estimate the unknown variable  $y_k(t - jh)$ . The auxiliary model of this paper can be schematically represented in Figure 5. The main idea of the auxiliary model is that the real output of the system  $y_k'(t)$  is replaced by the output of the auxiliary model  $y_{amk}(t)$ . Then, the identification problem has changed from the relationship between  $y_k'(t)$  and  $u_1$  to the relationship between  $y_{amk}(t)$  and  $u_1$ .

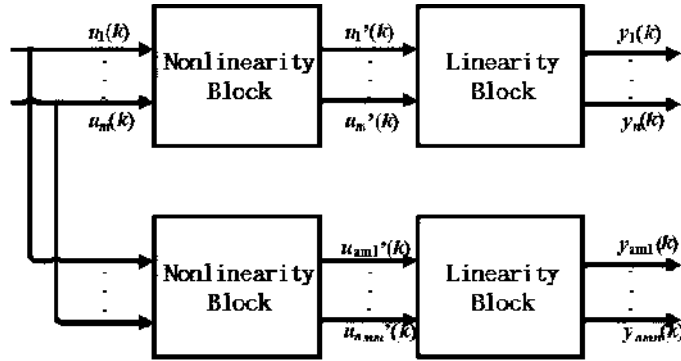


Figure 5. The MIMO Hammerstein model based on the auxiliary model.

According to Figure 5, the input–output relations of the auxiliary model can be written as

$$y_{amk}(t) = \varphi_{amk}(t) \cdot \theta_{amk}^T \tag{22}$$

where

$$\begin{aligned} \varphi_{amk}(t) &= \left[ \varphi_{amk,A}(t), \varphi_{B_{k,1,0}}(t), \varphi_{B_{k,1,2}}(t), \dots, \varphi_{B_{k,1,n_B}}(t), \dots, \varphi_{B_{k,M,0}}(t), \varphi_{B_{k,M,2}}(t), \dots, \varphi_{B_{k,M,n_B}}(t) \right] \\ \varphi_{amk,A}(t) &= \left[ -\sum_{j=1}^{\lfloor t/h \rfloor} w_j^\alpha y_{amk}(t - jh), \dots, -\sum_{j=1}^{\lfloor t/h \rfloor} w_j^{n_{A\alpha}} y_{amk}(t - jh) \right] \theta_{amk} = \hat{\theta}_k \end{aligned} \tag{23}$$

The estimate of  $\varphi_k(t)$  can be used as the value of the auxiliary model information vector  $\varphi_{amk}(t)$  and the parameter identification of  $\theta_k$  can be used as the value of the auxiliary model parameter vector  $\theta_{amk}$ . Define the criterion function as

$$J(\hat{\theta}_k^T) = \frac{1}{2} \sum_{i=1}^t \left[ y_k'(i) - \varphi_{amk}(i) \hat{\theta}_k^T \right]^2 \tag{24}$$

By finding the minimum value of the criterion function, the value of  $\varphi_{amk}(i) \hat{\theta}_k^T$  can approach the value of  $y_k'(i)$  to identify  $\theta_k$ . The minimum value can be obtained by the following equation.

$$\frac{\partial J(\hat{\theta}_k^T)}{\partial \hat{\theta}_k^T} = -\sum_{i=1}^t \varphi_{amk}^T(i) \cdot [y_k'(i) - \varphi_{amk}(i) \hat{\theta}_k^T] = 0 \tag{25}$$

When  $\sum_{i=1}^t \varphi_{amk}^T(i-1) \cdot \varphi_{amk}(i-1)$  can be inverted, the value of  $\hat{\theta}_k$  can be identified by the recursive least squares as follows:

$$\begin{aligned}
 \hat{\theta}_k^T(t) &= [\sum_{i=1}^t \varnothing_{amk}^T(i-1) \cdot \varnothing_{amk}(i-1)]^{-1} \cdot \sum_{i=1}^t \varnothing_{amk}^T(i) y_k'(i) \\
 \hat{\theta}_k^T(t) &= \hat{\theta}_k^T(t-1) + L(t) [y_k'(t) - \varnothing_{amk}(t) \hat{\theta}_k^T(t-1)] \\
 L(t) &= P(t-1) \varnothing_{amk}^T(t) [1 + \varnothing_{amk}(t) P(t-1) \varnothing_{amk}^T(t)]^{-1} \\
 P(t) &= [I - L(t) \varnothing_{amk}(t)] P(t-1)
 \end{aligned}
 \tag{26}$$

where  $P(0)$  is a diagonal matrix in which the main diagonal elements are huge and equal.

According to the above equations, the elements of  $\hat{\theta}_k$  are all identified. Without losing generality, assuming  $c_{l,1}$  as 1 can facilitate calculation and ensure the uniqueness of the final parameters. Then, the unique values of  $W_{k,l,j}$  and  $c_{l,m}$  are calculated; they can be expressed as

$$\begin{aligned}
 W_{k,l,j} &= \theta_{B_{k,l,i}} [(l-1) * n_{lc} + 1] \\
 c_{l,m} &= \sum_{i=0}^{n_{lc}} \frac{\theta_{B_{k,l,i}}(k)}{W_{k,l,j}}
 \end{aligned}
 \tag{27}$$

So far, the estimates of  $A$ ,  $B$ , and  $c$  have been obtained.

### 3.2.2. Order Identification

In the previous section, this paper discusses the identification of coefficients. Substituting the accurate estimated value of the coefficients into Equation (17) can identify the order accurately. Define the criterion function as

$$J(\alpha) = \frac{1}{2} \sum_{i=1}^t [y_k'(i) - \hat{y}_k(i)]^2
 \tag{28}$$

By finding the minimum value of the criterion function, the value of  $\hat{y}_k(i)$  can approach the value of  $y_k'(i)$ . The minimum value can be obtained by the following equation:

$$\frac{\partial J(\alpha)}{\partial \alpha} = - \sum_{i=1}^t \frac{\partial \hat{y}_k(i)}{\partial \alpha} \cdot [y_k'(i) - \hat{y}_k(i)] = 0
 \tag{29}$$

where

$$\begin{aligned}
 \frac{\partial \hat{y}_k(t)}{\partial \alpha} &= - \frac{\partial}{\partial \alpha} (G_{k,1}(s^\alpha) u_1'(t) + G_{k,2}(s^\alpha) u_2'(t) + \dots + G_{k,M}(s^\alpha) u_M'(t)) \\
 &= \sum_{l=0}^M \left[ \left( \frac{B_{k,l,N_B} S^{N_B \alpha} + \dots + B_{k,l,0}}{(A_{k,N_A} S^{N_A \alpha} + \dots + 1)^2} \right) \right. \\
 &\quad \cdot (N_A \cdot A_{k,N_A} S^{N_A \alpha} + \dots + A_{k,1} s^\alpha) - \frac{N_B \cdot B_{k,l,N_B} S^{N_B \alpha} + \dots + B_{k,l,1} s^\alpha}{A_{k,N_A} S^{N_A \alpha} + \dots + 1} \left. \right] \cdot \ln(s) \cdot u_l'(t)
 \end{aligned}
 \tag{30}$$

According to references [24],  $\ln(s) \cdot u_l'(t)$  can be replaced by  $s^\alpha \cdot (\ln(s) / s^\alpha) \cdot u_l'(t)$ . The inverse Laplace transform of  $\ln(s) / s^\alpha$  is a digamma function can be expressed as

$$L^{-1} \left( \frac{\ln(s)}{s^\alpha} \right) = \frac{t^{\alpha-1}}{\Gamma(\alpha)} \left[ \frac{1}{\Gamma(\alpha)} \frac{d\Gamma(\alpha)}{d\alpha} - \ln(t) \right]
 \tag{31}$$

Then,  $\ln(s) \cdot u_l'(t)$  can be expressed as

$$D^\alpha \left[ \frac{1}{\Gamma(\alpha)} \frac{d\Gamma(\alpha)}{d\alpha} D^\alpha u_l'(t) - \frac{1}{\Gamma(\alpha)} \int_0^t (t-\tau)^{\alpha-1} \ln(t-\tau) u_l'(t) d\tau \right]
 \tag{32}$$

It's easy to see that  $\alpha$  can be calculated by Equations (28)–(32).

### 3.3. Summary

So far, the estimates of  $A, B, c,$  and  $\alpha$  have been obtained. Because  $A$  are polynomials about  $a, B$  are polynomials about  $a$  and  $b,$  it is feasible to estimate the value of  $n_A a$  by the value of  $n_A A.$  Then, it is feasible to estimate the value of  $b$  by the value of  $a$  and  $B.$  To sum up, all estimates work has been completed.

## 4. Experimental Results

In this section, two numerical examples will demonstrate the validity of the proposed method.

### 4.1. Example 1

Consider the following model, which is expressed as

$$\begin{bmatrix} y_1(t) \\ y_2(t) \end{bmatrix} = \begin{bmatrix} G_{1,1} & G_{1,2} \\ G_{2,1} & G_{2,2} \end{bmatrix} \begin{bmatrix} u_1'(t) \\ u_2'(t) \end{bmatrix} y'(t) = y(t) + v(t) \tag{33}$$

where

$$\begin{aligned} G_{1,1} &= \frac{4}{5s^{0.3}+1}, & G_{1,2} &= \frac{3}{3s^{0.3}+1}, \\ G_{2,1} &= \frac{4}{6s^{0.3}+1}, & G_{2,2} &= \frac{5}{2s^{0.3}+1}. \end{aligned} \tag{34}$$

$$\begin{aligned} u_1'(t) &= u_1(t) + 0.5u_1^2(t) + 0.3u_1^3(t) + 0.1u_1^4(t) \\ u_2'(t) &= u_2(t) + 0.4u_2^2(t) + 0.2u_2^3(t) + 0.1u_2^4(t) \end{aligned}$$

The inputs  $u_1$  and  $u_2$  are persistent excitation signal sequences with unit variance and zero mean.  $v(t)$  is the stochastic Gaussian noise with zero mean and variance is 0.005. Then, the outputs  $y(t)$  are generated by their respective transfer functions of the MIMO fractional-order Hammerstein model.

According to the model, the  $\theta$  to be identified are

$$\begin{aligned} \theta &= [a_{1,1,1}, a_{1,2,1}, b_{1,1,0}, b_{1,2,0}, a_{2,1,1}, a_{2,2,1}, b_{2,1,0}, b_{2,2,0}, c_{1,1}, c_{1,2}, c_{1,3}, c_{2,1}, c_{2,2}, c_{2,3}, \alpha] \\ &= [5, 3, 4, 3, 6, 2, 4, 5, 0.5, 0.3, 0.1, 0.4, 0.2, 0.1, 0.3] \end{aligned} \tag{35}$$

The identification steps are described in Section 3. At first, the intelligent optimization algorithm identifies the initial value of the model. Then, using AMRLS to identify the model coefficients, and at this time regarding the initial value of fractional order as the model's actual value. When the coefficients are estimated, the estimated values of the coefficients are considered to be the true value to identify the fractional order. Finally, identifying coefficients and order is repeated until the iteration's end or satisfactory results are obtained. The pseudo-code of the identification process is explained in detail in Algorithm 2.

---

**Algorithm 2:** Identification process

---

- Step.1**   Collect the dates of all inputs, outputs;
  - Step.2**   Obtain the initial of unknown parameters by using intelligent optimization algorithm;
  - Step.3**   **While**  $m < \text{max number of iterations } M;$
  - Step.4**    Estimate the value of model coefficients according to Equation (25);
  - Step.5**    Estimate the value of fractional order according to Equation (29);
  - Step.6**    If the two criterion function values  $J$  within the actual accuracy requirements;
  - Step.7**    Break;
  - Step.8**    End;
  - Step.9**     $m = m + 1;$
  - Step.10**   **End while;**
  - Step.11**   Return the best solution.
- 

In order to reflect the importance of the initial value of fractional order, in this section, the initial value is identified by three different optimization algorithms: AIAGS, HHO,

and AO. The next identification work is carried out under four initial values. This section evaluates the final identification results from two aspects: RQE and MSE. They can be expressed as

$$RQE = \sqrt{\frac{(\hat{\theta} - \theta)^2}{\theta^2}} \tag{36}$$

$$MSE = \frac{\sum_{i=1}^n (y_i - \hat{y}_i)^2}{n}$$

where  $\hat{\theta}$  and  $\hat{y}_i$  are estimated values;  $\theta$  and  $y_i$  are true values.

The final identification results obtained by Algorithm 2 are shown in Table 4, and the RQE and MSE of the results are shown in Table 5. The outputs of the real model and the outputs of the model obtained through identification are shown in Figures 6 and 7. Figure 8 shows the estimated fractional-order convergence curve.

**Table 4.** The final identification results.

Method (and AMRLS)	$a_{1,1,1}$	$a_{1,2,1}$	$b_{1,1,0}$	$b_{1,2,0}$	$a_{2,1,1}$	$a_{2,2,1}$	$b_{2,1,0}$	$b_{2,2,0}$	$c_{1,1}$	$c_{1,2}$	$c_{1,3}$	$c_{2,1}$	$c_{2,2}$	$c_{2,3}$	$\alpha$	$\alpha_0$
AIAGS	5.127	3.120	3.976	2.959	6.118	2.017	3.996	4.970	0.501	0.289	0.095	0.400	0.200	0.100	0.299	0.333
AO	4.619	3.325	3.887	3.465	5.377	1.760	4.196	5.272	0.509	0.297	0.098	0.404	0.198	0.098	0.275	0.391
HHO	4.641	3.329	3.882	3.448	5.289	1.757	4.152	5.283	0.508	0.296	0.097	0.404	0.198	0.099	0.278	0.382

**Table 5.** The RQE and MSE of the results.

Method (and AMRLS)	AIAGS	AO	HHO
RQE	0.1360	0.2931	0.2987
MSE	0.0144	0.0944	0.1019

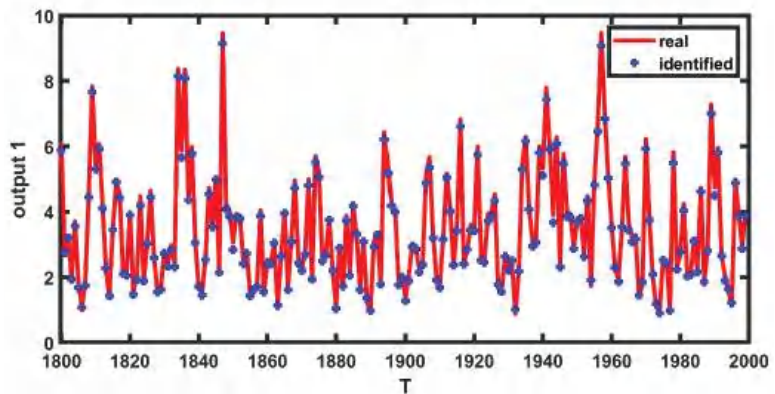


**Figure 6.** The real output 1 and the identified output 1.

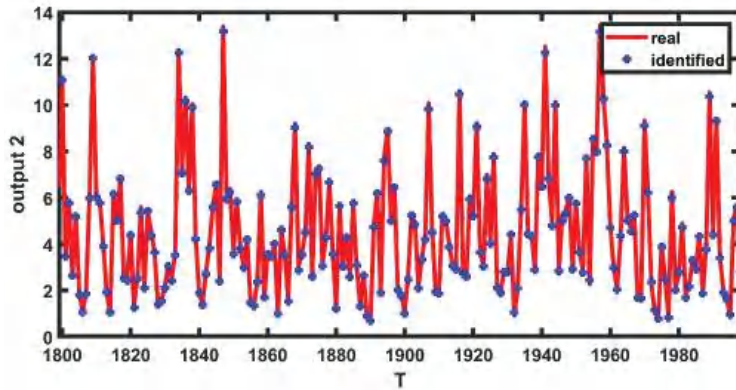


Figure 7. The real output 2 and the identified output 2.

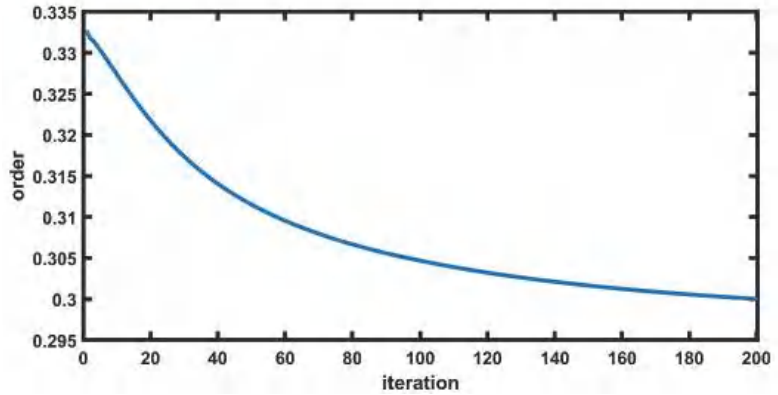


Figure 8. The estimated fractional-order convergence curve.

4.2. Example 2

Consider the following model, which is expressed as

$$\begin{bmatrix} y_1(t) \\ y_2(t) \end{bmatrix} = \begin{bmatrix} G_{1,1} & G_{1,2} \\ G_{2,1} & G_{2,2} \end{bmatrix} \begin{bmatrix} u_1'(t) \\ u_2'(t) \end{bmatrix} \tag{37}$$

$$y'(t) = y(t) + v(t)$$

where

$$\begin{aligned} G_{1,1} &= \frac{5}{2s^{0.7}+1}, & G_{1,2} &= \frac{1.7s^{0.7}+1.9}{1.5s^{1.4}+1.3s^{0.7}+1}, \\ G_{2,1} &= \frac{1.8s^0+1.5}{2.2s^{1.4}+2.1s^{0.7}+1}, & G_{2,2} &= \frac{1}{1.6s^{0.7}+1}. \end{aligned} \tag{38}$$

$$\begin{aligned} u_1'(t) &= u_1(t) + 0.5u_1^2(t) + 0.2u_1^3(t) + 0.1u_1^4(t) \\ u_2'(t) &= u_2(t) + 0.4u_2^2(t) + 0.3u_2^3(t) + 0.1u_2^4(t) \end{aligned}$$

The parameter meanings are similar to that of Example 1, so  $\theta$  can be expressed as

$$\begin{aligned} \theta &= [a_{1,1,1}, a_{1,2,2}, a_{1,2,1}, b_{1,1,0}, b_{1,2,1}, b_{1,2,0}, a_{2,1,2}, a_{2,1,1}, a_{2,2,1}, b_{2,1,1}, b_{2,1,0}, b_{2,2,0}, c_{1,1}, c_{1,2}, c_{1,3}, c_{2,1}, c_{2,2}, c_{2,3}, \alpha] \\ &= [2, 1.5, 1.3, 5, 1.7, 1.9, 2.2, 2.1, 1.6, 1.8, 1.5, 1, 0.5, 0.2, 0.1, 0.4, 0.3, 0.1, 0.7] \end{aligned} \tag{39}$$

By repeating the identification process similar to Example 1, the final identification results are shown in Table 6, and the RQE and MSE of the results are shown in Table 7. The outputs of the real model and the outputs of the model obtained through identification

are shown in Figures 9 and 10. Figure 11 shows the estimated fractional-order convergence curve.

Table 6. The final identification results.

Method (and AMRLS)	$a_{1,1,1}$	$a_{1,2,2}$	$a_{1,2,1}$	$b_{1,1,0}$	$b_{1,2,1}$	$b_{1,2,0}$	$a_{2,1,2}$	$a_{2,1,1}$	$a_{2,2,1}$	$b_{2,1,1}$	$b_{2,1,0}$	$b_{2,2,0}$	$c_{1,1}$	$c_{1,2}$	$c_{1,3}$	$c_{2,1}$	$c_{2,2}$	$c_{2,3}$	$\alpha$
AIAGS	2.002	1.501	1.297	5.033	1.703	1.915	2.164	2.215	1.766	1.675	1.564	1.029	0.504	0.191	0.095	0.385	0.293	0.101	0.700
AO	2.946	1.453	1.174	5.642	1.127	1.832	2.459	2.544	0.733	4.680	1.626	1.122	0.483	0.188	0.100	0.347	0.290	0.106	0.582
HHO	3.182	1.42	1.197	5.697	1.004	1.808	2.463	2.605	0.691	4.962	1.631	1.132	0.482	0.188	0.100	0.344	0.288	0.106	0.570

Table 7. The RQE and MSE of the results.

Method (and AMRLS)	AIAGS	AO	HHO
RQE	0.1819	0.6579	0.6935
MSE	0.0351	0.5133	0.6626

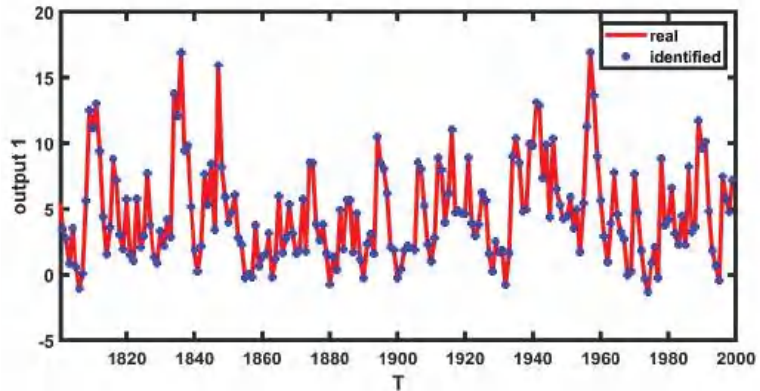


Figure 9. The real output 1 and the identified output 1.

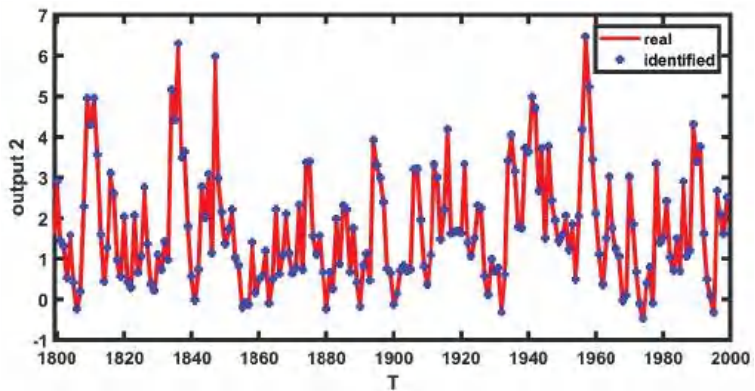
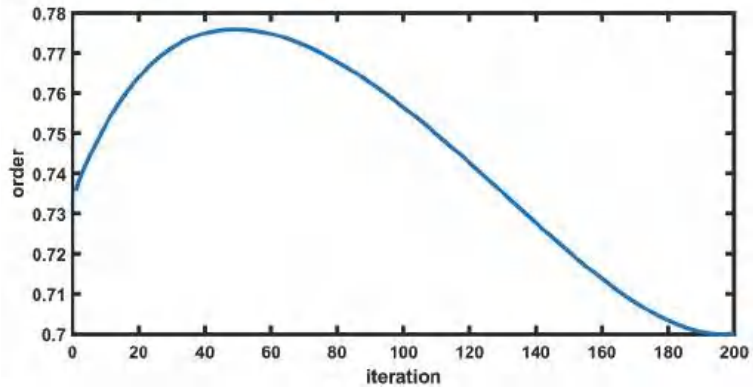


Figure 10. The real output 2 and the identified output 2.



**Figure 11.** The estimated fractional-order convergence curve.

## 5. Conclusions

This paper discusses a new identification method for MIMO fractional-order Hammerstein models. In order to improve the accuracy of identification results, the identification process needs a heuristic algorithm to provide the initial value. Because the immune algorithm is prone to premature convergence, this paper improves the immune algorithm and proposes AIAGS. In AIAGS, the immune algorithm's stimulation function and mutation strategy are improved, and simulated annealing is added to the final step to select the optimal solution. The core idea of these improvements is to avoid finding the optimal local solution. Then, through the obtained initial value, the auxiliary model recursive least squares method is used to accurately identify all the MIMO fractional-order Hammerstein model parameters. The experimental results show the effectiveness of the proposed algorithm. The proposed methods in this paper can be applied to other literature [45–47], such as parameter identification problems of different systems, engineering applications, fault diagnosis, and so on.

**Author Contributions:** Conceptualization, Q.J. and B.W.; methodology, Q.J.; software, B.W.; validation, Q.J., B.W. and Z.W.; formal analysis, B.W.; investigation, B.W.; resources, Q.J.; data curation, Q.J. and B.W.; writing—original draft preparation, B.W.; writing—review and editing, Q.J., B.W. and Z.W.; visualization, Q.J.; supervision, Q.J. All authors have read and agreed to the published version of the manuscript.

**Funding:** This research received no external funding.

**Institutional Review Board Statement:** Not applicable.

**Informed Consent Statement:** Not applicable.

**Data Availability Statement:** In the paper, all the data generation information has been given in detail in the related chapter.

**Conflicts of Interest:** The authors declare no conflict of interest.

## References

1. Billings, S.A.; Fakhouri, S.Y. Identification of systems containing linear dynamic and static nonlinear element. *Automatica* **1982**, *18*, 15–26. [CrossRef]
2. Narendra, K.S.; Gallman, P.G. An Iterative Method for the Identification of Nonlinear Systems using the Hammerstein Model. *IEEE Trans. Autom. Control* **1966**, *AC11*, 546–550. [CrossRef]
3. Moghaddam, M.J.; Mojallali, H.; Teshnehlab, M. Recursive identification of multiple-input single-output fractional-order Hammerstein model with time delay. *Appl. Soft Comput.* **2018**, *70*, 486–500. [CrossRef]
4. Chen, H.F. Strong consistency of recursive identification for Hammerstein systems with discontinuous piecewise-linear memoryless block. *IEEE Trans. Autom. Control* **2005**, *50*, 1612–1617. [CrossRef]

5. Sznaier, M. Computational complexity analysis of set membership identification of Hammerstein and Wiener systems. *Automatica* **2009**, *45*, 701–705. [CrossRef]
6. Kung, M.C.; Womack, B. Discrete time adaptive control of linear dynamic systems with a two-segment piecewise-linear asymmetric nonlinearity. *IEEE Trans. Autom. Control* **2003**, *29*, 170–172. [CrossRef]
7. Mccannon, T.E.; Gallagher, N.C.; Minoo-Hamedani, D.; Wise, J.L. On the design of nonlinear discrete-time predictors. *IEEE Trans. Inf. Theory* **1982**, *28*, 366–371. [CrossRef]
8. Jin, Q.; Wang, H.; Su, Q. A novel optimization algorithm for MIMO Hammerstein model identification under heavy-tailed noise. *ISA Trans.* **2018**, *72*, 77–91. [CrossRef] [PubMed]
9. Jin, Q.; Xu, Z.; Cai, W. An Improved Whale Optimization Algorithm with Random Evolution and Special Reinforcement Dual-Operation Strategy Collaboration. *Symmetry* **2021**, *13*, 238. [CrossRef]
10. Dong, S.; Yu, L.; Zhang, W.A. Robust extended recursive least squares identification algorithm for Hammerstein systems with dynamic disturbances. *Digit. Signal Process.* **2020**, *101*, 102716. [CrossRef]
11. Dhaifallah, M.A.; Westwick, D.T. Support Vector Machine Identification of Output Error Hammerstein Models. *IFAC Proc. Vol.* **2011**, *44*, 13948–13953. [CrossRef]
12. Schlegel, M.; Čech, M. Fractal System Identification for Robust Control—The Moment Approach. In Proceedings of the 5th International Carpathian Control Conference, Zakopane, Poland, 25–28 May 2004.
13. Torvik, P.J.; Bagley, R.L. On the Appearance of the Fractional Derivative in the Behavior of Real Materials. *J. Appl. Mech.* **1984**, *51*, 725–728. [CrossRef]
14. Zhao, C.; Dingy, X. Closed-form solutions to fractional-order linear differential equations. *Front. Electr. Electr. Eng. China* **2008**, *3*, 214–217. [CrossRef]
15. Chen, S.; Liu, F.; Turner, I. Numerical inversion of the fractional derivative index and surface thermal flux for an anomalous heat conduction model in a multi-layer medium. *Appl. Math. Model.* **2018**, *59*, 514–526. [CrossRef]
16. Deng, J. Higher-order stochastic averaging for a SDOF fractional viscoelastic system under bounded noise excitation. *J. Frankl. Inst.* **2017**, *354*, 7917–7945. [CrossRef]
17. Das, S. *Functional Fractional Calculus*; Springer: Berlin/Heidelberg, Germany, 2011; pp. 110–122.
18. Table, M.A.; Béthoux, O.; Godoyb, E. Identification of a PEMFC fractional order model. *Int. J. Hydrogen Energy* **2017**, *42*, 1499–1509.
19. Kumar, S.; Ghosh, A. Identification of fractional order model for a voltammetric E-tongue system. *Measurement* **2019**, *150*, 107064. [CrossRef]
20. Zhang, Q.; Shang, Y.; Li, Y. A novel fractional variable-order equivalent circuit model and parameter identification of electric vehicle Li-ion batteries. *ISA Trans.* **2019**, *97*, 448–457. [CrossRef]
21. Hammar, K.; Djamah, T.; Bettayeb, M. Fractional hammerstein system identification using particle swarm optimization. In Proceedings of the 2015 7th International Conference on Modelling, Identification and Control (ICMIC) 2015, Sousse, Tunisia, 18–20 December 2015; pp. 1–6.
22. Hammar, K.; Djamah, T.; Bettayeb, M. Fractional Hammerstein system identification based on two decomposition principles. *IFAC-PapersOnLine* **2019**, *52*, 206–210. [CrossRef]
23. Chetoui, M.; Aoun, m. Instrumental variables based methods for linear systems identification with fractional models in the EIV context. In Proceedings of the 2019 16th International Multi-Conference on Systems, Signals & Devices (SSD) 2019, Istanbul, Turkey, 21–24 March 2019; pp. 90–95.
24. Wang, J.; Wei, Y.; Liu, T. Fully parametric identification for continuous time fractional order Hammerstein systems. *J. Frankl. Inst.* **2020**, *357*, 651–666. [CrossRef]
25. Cui, R.; Wei, Y.; Chen, Y. An innovative parameter estimation for fractional-order systems in the presence of outliers. *Nonlinear Dyn.* **2017**, *89*, 453–463. [CrossRef]
26. Tang, Y.; Liu, H.; Wang, W. Parameter identification of fractional order systems using block pulse functions. *Signal Process.* **2015**, *107*, 272–281. [CrossRef]
27. Cui, R.; Wei, Y.; Cheng, S. An innovative parameter estimation for fractional order systems with impulse noise. *Isa Trans.* **2017**, *120*–129. [CrossRef] [PubMed]
28. Zhao, Y.; Yan, L.; Chen, Y. Complete parametric identification of fractional order Hammerstein systems. In Proceedings of the ICFDA'14 International Conference on Fractional Differentiation and Its Applications 2014, Catania, Italy, 23–25 June 2014; pp. 1–6.
29. Zeng, L.; Zhu, Z.; Shu, L. Subspace identification for fractional order Hammerstein systems based on instrumental variables. *Int. J. Control Autom. Syst.* **2012**, *10*, 947–953.
30. Khanra, M.; Pal, J. Reduced Order Approximation of MIMO Fractional Order Systems. *IEEE J. Emerg. Sel. Top. Circuits Syst.* **2013**, *3*, 451–458. [CrossRef]
31. Lakshmikantham, V.; Vatsala, A.S. Basic theory of fractional differential equations. *Nonlinear Anal. Theory Methods Appl.* **2008**, *69*, 2677–2682. [CrossRef]
32. Chun, J.S.; Jung, H.K.; Hahn, S.Y. A study on comparison of optimization performances between immune algorithm and other heuristic algorithms. *IEEE Trans Magn.* **1998**, *34*, 297222975.
33. Castro, L.N.; Castro, D.L.; Timmis, J. *Artificial Immune Systems: A New Computational Intelligence Approach*; Springer Science & Business Media: London, UK, 2002.

34. Chen, X.L.; Li, J.Q.; Han, Y.Y. Improved artificial immune algorithm for the flexible job shop problem with transportation time. *Meas. Control* **2020**, *53*, 2111–2128. [CrossRef]
35. Lu, L.; Guo, Z.; Wang, Z. Parameter Estimation for a Capacitive Coupling Communication Channel Within a Metal Cabinet Based on a Modified Artificial Immune Algorithm. *IEEE Access* **2021**, 75683–75698. [CrossRef]
36. Samigulina, G.; Samigulina, Z. Diagnostics of industrial equipment and faults prediction based on modified algorithms of artificial immune systems. *J. Intell. Manuf.* **2021**. [CrossRef]
37. Yu, T.; Xie, M.; Li, X. Quantitative method of damage degree of power system network attack based on improved artificial immune algorithm. In Proceedings of the ICAIIS 2021: 2021 2nd International Conference on Artificial Intelligence and Information Systems, Chongqing, China, 28–30 May 2021.
38. Xu, Y.; Zhang, J. Regional Integrated Energy Site Layout Optimization Based on Improved Artificial Immune Algorithm. *Energies* **2020**, *13*, 4381. [CrossRef]
39. Eker, E.; Kayri, M.; Ekinçi, S. A New Fusion of ASO with SA Algorithm and Its Applications to MLP Training and DC Motor Speed Control. *Arab. J. Sci. Eng.* **2021**, *46*, 3889–3911. [CrossRef]
40. Wu, G.; Mallipeddi, R.; Suganthan, P.N. *Problem Definitions and Evaluation Criteria for the CEC 2017 Competition and Special Session on Constrained Single Objective Real-Parameter Optimization*; Technical Report; Nanyang Technological University: Singapore, 2016.
41. Heidari, A.A.; Mirjalili, S.; Faris, H.; Aljarah, H. Harris hawks optimization: Algorithm and applications. *Future Gener. Comput. Syst.* **2019**, *97*, 849–872. [CrossRef]
42. Abualigah, L.; Yousri, D.; Elaziz, M.A. Matlab Code of Aquila Optimizer: A novel meta-heuristic optimization algorithm. *Comput. Ind. Eng.* **2021**, *157*, 107250. [CrossRef]
43. Dzieliński, A.; Sierociuk, D. Stability of discrete fractional order state-space systems. *IFAC Proc. Vol.* **2006**, *39*, 505–510. [CrossRef]
44. Ding, F.; Chen, H.; Li, M. Multi-innovation least squares identification methods based on the auxiliary model for MISO systems. *Appl. Math. Comput.* **2007**, *187*, 658–668. [CrossRef]
45. Zhao, X.; Lin, Z.; Bo, F. Research on Automatic Generation Control with Wind Power Participation Based on Predictive Optimal 2-Degree-of-Freedom PID Strategy for Multi-area Interconnected Power System. *Energies* **2018**, *11*, 3325. [CrossRef]
46. Ding, J.; Chen, J.; Lin, J. Particle filtering based parameter estimation for systems with output-error type model structures. *J. Frankl. Inst.* **2019**, *356*, 5521–5540. [CrossRef]
47. Wang, L.; Liu, H.; Dai, L. Novel Method for Identifying Fault Location of Mixed Lines. *Energies* **2018**, *11*, 1529. [CrossRef]

Article

# Non-Instantaneous Impulsive BVPs Involving Generalized Liouville–Caputo Derivative

Ahmed Salem \* and Sanaa Abdullah

Department of Mathematics, Faculty of Science, King Abdulaziz University, P.O. Box 80203, Jeddah 21589, Saudi Arabia; samalotebi@kau.edu.sa

\* Correspondence: asaalsheef@kau.edu.sa

**Abstract:** This manuscript investigates the existence, uniqueness and Ulam–Hyers stability (UH) of solution to fractional differential equations with non-instantaneous impulses on an arbitrary domain. Using the modern tools of functional analysis, we achieve the required conditions. Finally, we provide an example of how our results can be applied.

**Keywords:** non-instantaneous impulses; Generalized Liouville–Caputo derivative; Leray–Schauder alternative theorem

**MSC:** 34A08; 34A12; 47H08; 47H10; 46B45

**Citation:** Salem, A.; Abdullah, S. Non-Instantaneous Impulsive BVPs Involving Generalized Liouville–Caputo Derivative. *Mathematics* **2022**, *10*, 291. <https://doi.org/10.3390/math10030291>

Academic Editors: António M. Lopes, Alireza Alfi, Liping Chen and Sergio A. David

Received: 13 December 2021

Accepted: 13 January 2022

Published: 18 January 2022

**Publisher’s Note:** MDPI stays neutral with regard to jurisdictional claims in published maps and institutional affiliations.



**Copyright:** © 2022 by the authors. Licensee MDPI, Basel, Switzerland. This article is an open access article distributed under the terms and conditions of the Creative Commons Attribution (CC BY) license (<https://creativecommons.org/licenses/by/4.0/>).

## 1. Introduction

The study of differential equations with fractional order has become increasingly popular in recent decades. The reasons behind it are fractional order derivatives provide powerful tools for describing inherited or defined properties in a wide range of science and engineering fields [1–8].

There are several approaches of fractional derivatives, Riemann–Liouville, Caputo, Hadamard, Hilfer, etc. It is important to cite that the Caputo derivative is useful to affront problems where initial conditions are done in the function and in the respective derivatives of integer order. Due to the importance of the Caputo version, there are many versions established as generalization of it, such as Caputo–Katugampola, Caputo–Hadamard, Caputo–Fabrizio, etc. Furthermore, it is drawn attention of huge number of contributors to study physical and mathematical modelings contain it and its related versions, see [9–13] and references cited therein.

Finding exact solutions to the differential equations, whether they are ordinary, partial, or fractional, is a extremely difficult and complex issue, and that is why mathematicians have resorted to studying the properties of solutions such as existence, uniqueness, stability, invariant, controllability and others. The most important of these properties are existence and uniqueness which attracted the attention of many contributors to their study [14–20]. Furthermore, Ulam–Hyers stability analysis that is necessary for nonlinear problems in terms of optimization and numerical solutions and plays a key role in numerical solutions where exact solutions are difficult to get.

The fractional differential equations (FDEs) with instantaneous impulses are increasingly being used to analyze abrupt shifts in the evolution pace of dynamical systems, such as those brought about by shocks, disturbances, and natural disasters [21,22]. The duration of instantaneous impulses is relatively short in comparison to the duration of the overall process. However, certain dynamics of evolution processes have been observed to be inexplicable by instantaneous impulsive dynamic systems. As an instance, the injection and absorption of drugs in the blood is a gradual and continuous process. Here, each spontaneous, the action begins in an arbitrary fixed position and lasts for a finite amount of time. This type of system is known as a non-instantaneous impulsive system, which

are more suitable for investigating the dynamics of evolutionary processes [23–25] and the references cited therein. Hernandez and O’Regan [26] discussed the evolution equations involving non-instantaneous impulses of the form:

$$\begin{cases} x' = Ax(t) + f(t, x(t)), & t \in (s_k, t_{k+1}], k = 0, 1, \dots, m, \\ y(t) = g_k(t, x(t)), & t \in (t_k, s_k], k = 1, 2, \dots, m, \\ x(0) = x_0. \end{cases}$$

Liu et al. [27] explored generalized Ulam–Hyers–Rassias stability for the following fractional differential equation:

$$\begin{cases} {}^c D_{0,w}^v z(w) = f(w, z(w)), & w \in (w_k, s_k], k = 0, 1, \dots, m, 0 < v < 1, \\ z(w) = g_k(w, z(w)), & w \in (s_{k-1}, w_k], k = 1, \dots, m \end{cases}$$

where  ${}^c D_{0,w}^v$  is a Caputo derivative of fractional order  $0 < v < 1$  with the lower limit 0. Ho and Ngo [28] analyzed generalized Ulam–Hyers–Rassias stability for the following fractional differential equation:

$$\begin{cases} {}^c D_{a^+}^{\alpha,\rho} x(t) = f(t, x(t)), & t \in (t_k, s_k], k = 0, 1, \dots, m, 0 < \alpha < 1, \\ x(t) = I_k(t, x(t)), & t \in (s_{k-1}, t_k], k = 1, \dots, m, \\ x(a^+) = x_0 \end{cases}$$

where  ${}^c D_{a^+}^{\alpha,\rho}$  is a Caputo–Katugampola derivative of fractional order  $0 < \alpha < 1$ . Recently, Abbas [29] has studied non-instantaneous impulsive fractional integro-differential equations with proportional fractional derivatives with respect to another function by using the nonlinear alternative Leray–Schauder type and the Banach contraction mapping principle

$$\begin{cases} {}_a D^{\alpha,\rho,\delta} y(t) = f(t, y(t), {}_a I^{\beta,\rho,\delta} y(t)), & t \in (s_k, t_{k+1}], k = 0, 1, \dots, m, \\ y(t) = \Psi_k(t, y(t_k^+)), & t \in (t_k, s_k], k = 1, 2, \dots, m, \\ {}_a I^{\beta,\rho,\delta} y(a) = y_0, & y_0 \in \mathbb{R} \end{cases}$$

where  $0 < \alpha \leq 1, \beta, \rho > 0, {}_a D^{\alpha,\rho,\delta}$  is the proportional fractional derivative of order  $\alpha$  with respect to another function  $g$ .

It is remarkable that the most of contributions focus on the case when the order of fractional derivative lies in the unit interval  $(0, 1)$ . This observation encourages us to study these equations when the order of fractional derivative lies in the unit interval  $(1, 2)$ . Furthermore, although the Generalized Liouville–Caputo fractional derivative is considered a generalization of Caputo and Hadamard fractional derivatives, there is a rareness of the studies with this approach.

Inspire of the above, we investigate the existence of solutions for non-instantaneous impulsive fractional boundary value problems in this paper. Specifically, we consider the following problem:

$$\begin{cases} {}^c D_{0^+}^{\beta,\rho} y(\tau) = h(\tau, y(\tau), \tau^{1-\rho} y'(\tau)), & \tau \in (s_r, \tau_{r+1}], r = 0, 1, \dots, k, \\ y(\tau) = \Phi_r(\tau, y(\tau), y(\tau_r - 0)), & \tau \in (\tau_r, s_r], r = 1, 2, \dots, k, \\ y'(\tau) = \tau^{\rho-1} \Psi_r(\tau, y(\tau), y(\tau_r - 0)), & \tau \in (\tau_r, s_r], r = 1, 2, \dots, k, \\ y(0) = y_0, \quad \lim_{\tau \rightarrow 0} \tau^{1-\rho} y'(\tau) = y_1, \quad y_0, y_1 \in \mathbb{R} \end{cases} \tag{1}$$

where all intervals are subset of  $J = [0, T]$ ,  ${}^c D^{\beta,\rho}$  is a generalized Caputo–Liouville (Katugampola) derivative of order  $1 < \beta \leq 2$  and type  $0 < \rho \leq 1$  and  $h : J \times \mathbb{R} \times \mathbb{R} \rightarrow \mathbb{R}$  is a given continuous function. Here,  $0 = s_0 < \tau_1 < s_1 < \dots < \tau_k < s_k < \tau_{k+1} = T, k \in \mathbb{N}$  are fixed real numbers and  $\Phi_r$  and  $\Psi_r : (\tau_r, s_r) \rightarrow \mathbb{R}, r = 1, \dots, k$  are non-instantaneous impulses.

The main objectives of our work are to develop the existence theory and Ulam–Hyers stability of non-instantaneous impulsive BVPs involving Generalized Liouville–Caputo derivatives. This work is based on modern functional analysis techniques. Three basic results introduce: the first two deal with the existence and uniqueness of solutions by applying a nonlinear Leray–Schauder alternative theorem and the Banach fixed point theorem, respectively. While the third concerns the Ulam–Hyers stability analysis of solutions for the given problem by establishing a criterion for ensuring various types of Ulam–Hyers stability.

For the rest of the paper, it is arranged as follows: Section 2 provides some preliminary concepts about our work and a key lemma that deals with the linear variant of the given problem, along with giving a formula for converting the given problem into a fixed point problem. Using the Banach contraction mapping principle and the Leray–Schauder nonlinear alternative, the existence and uniqueness of problem (1) are presented in Section 3.

**Remark 1.** For fractional differential equation for non-instantaneous impulsive (1). The intervals  $(\tau_r, s_r], r = 1, \dots, k$  are known as non-instantaneous impulse intervals, and the functions  $\Phi_r(\tau, y(\tau), y(\tau_r - 0)), r = 1, \dots, k$  are known as non-instantaneous impulsive functions. The fractional differential equation with non-instantaneous impulses (1) is reduced to a fractional differential equation with instantaneous impulses if  $\tau_r = s_{r-1}, r = 1, \dots, k$ .

**2. Preliminaries**

Let the space of continuous real-valued functions on  $J$  be denoted by  $C(J, \mathbb{R})$ . Consider the space

$$PC(J, \mathbb{R}) = \{y : J \rightarrow \mathbb{R} : y \in C((\tau_k, \tau_{k+1}], \mathbb{R})\}$$

and there exist  $y(\tau_k^-)$  and  $y(\tau_k^+), k = 1, \dots, r$  with  $y(\tau_k^-) = y(\tau_k)$ .

Furthermore, consider the space:

$$PC_\delta^1(J, \mathbb{R}) = \{y : J \rightarrow \mathbb{R} : \delta y \in PC(J, \mathbb{R})\}$$

such that  $\delta y(\tau_k^+)$  and  $\delta y(\tau_k^-)$  exist and  $\delta y$  is left continuous at  $\tau_k$  for  $k = 1, \dots, r$  and  $\delta = \tau^{1-\rho} d/d\tau$ . The space  $PC_\delta^1(J, \mathbb{R})$  equipped with the norm:

$$\|y\| = \sup_{\tau \in J} \{|y(\tau)|_{PC} + |\delta y(\tau)|_{PC_\delta^1}\} = \|y(\tau)\|_{PC} + \|\delta y(\tau)\|_{PC_\delta^1}.$$

Furthermore, we recall that:

$$AC^n(J, \mathbb{R}) = \{h : J \rightarrow \mathbb{R} : h, h', \dots, h^{n-1} \in C(J, \mathbb{R})\}$$

and  $h^{(n-1)}$  is absolutely continuous.

For  $0 \leq \varepsilon < 1$ , we define the space:

$$C_{\varepsilon, \rho}(J, \mathbb{R}) = \{f : J \rightarrow \mathbb{R} : (\tau^\rho - a^\rho)^\varepsilon f(\tau) \in C(J, \mathbb{R})\}$$

endowed with the norm

$$\|f\|_{C_{\varepsilon, \rho}} = \|(\tau^\rho - a^\rho)^\varepsilon f(\tau)\|_C.$$

Furthermore, we define a class of functions  $f$  that is absolutely continuous  $\delta^{n-1}, n \in \mathbb{N}$  derivative, denoted by  $AC_\delta^n(J, \mathbb{R})$  as follows:

$$AC_\delta^n(J, \mathbb{R}) = \left\{ f : J \rightarrow \mathbb{R} : \delta^k f \in AC(J, \mathbb{R}), \delta = \tau^{1-\rho} \frac{d}{d\tau}, k = 0, 1, \dots, n-1 \right\}$$

Equipped with the norm

$$\|f\|_{C_\delta^n} = \sum_{k=0}^{n-1} \|\delta^k f\|_C.$$

Generally, a space of functions that is endowed with the norm

$$\|f\|_{C_{\delta,\varepsilon}^n} = \sum_{k=0}^{n-1} \|\delta^k f\|_C + \|\delta^n f\|_{C_{\varepsilon,\rho}}$$

is defined by

$$C_{\delta,\varepsilon}^n(J, \mathbb{R}) = \{f : J \rightarrow \mathbb{R} : f \in \mathcal{AC}_{\delta}^n(J, \mathbb{R}), \delta^n f \in C_{\varepsilon,\rho}(J, \mathbb{R})\}.$$

Note that  $C_{\delta,0}^n = C_{\delta}^n$ .

**Definition 1** ([30]). *The left-sided and right-sided generalized fractional integrals of order  $\alpha > 0$  and type  $0 < \rho \leq 1$  are defined, respectively, by:*

$$I_{a^+}^{\alpha,\rho} f(x) = \frac{\rho^{1-\alpha}}{\Gamma(\alpha)} \int_a^x (x^\rho - t^\rho)^{\alpha-1} t^{\rho-1} f(t) dt,$$

$$I_{b^-}^{\alpha,\rho} f(x) = \frac{\rho^{1-\alpha}}{\Gamma(\alpha)} \int_x^b (x^\rho - t^\rho)^{\alpha-1} t^{\rho-1} f(t) dt.$$

**Definition 2** ([31]). *Let  $n = [\alpha] + 1$ ,  $n \in \mathbb{N}$ ,  $0 \leq a < b < \infty$  and  $f \in \mathcal{AC}_{\delta}^n[a, b]$ . The left-sided and right-sided Generalized Liouville–Caputo-type (Katugampola) fractional derivatives of order  $\alpha > 0$  and type  $0 < \rho \leq 1$  are defined via the above generalized integrals, respectively, as*

$$({}^c D_{a^+}^{\alpha,\rho} f)(x) = \left( I_{a^+}^{n-\alpha,\rho} \left( x^{1-\rho} \frac{d}{dx} \right)^n f \right)(x) = \frac{\rho^{1-n+\alpha}}{\Gamma(n-\alpha)} \int_a^x \frac{t^{\rho-1}}{(x^\rho - t^\rho)^{1-n+\alpha}} \left( t^{1-\rho} \frac{d}{dt} \right)^n f(t) dt,$$

$$({}^c D_{b^-}^{\alpha,\rho} f)(x) = \left( I_{b^-}^{n-\alpha,\rho} \left( -x^{1-\rho} \frac{d}{dx} \right)^n f \right)(x) = \frac{\rho^{1-n+\alpha}}{\Gamma(n-\alpha)} \int_x^b \frac{t^{\rho-1}}{(x^\rho - t^\rho)^{1-n+\alpha}} \left( -t^{1-\rho} \frac{d}{dt} \right)^n f(t) dt.$$

**Lemma 1** ([31]). *Let  $n - 1 < \alpha \leq n$ ;  $n \in \mathbb{N}$  and  $f \in \mathcal{AC}_{\delta}^n[a, b]$  or  $f \in C_{\delta}^n[a, b]$ . Then,*

$$I_{a^+}^{\alpha,\rho} {}^c D_{a^+}^{\alpha,\rho} f(x) = f(x) - \sum_{k=0}^{n-1} \frac{\delta^k f(a)}{k!} \left( \frac{t^\rho - a^\rho}{\rho} \right)^k,$$

$$I_{b^-}^{\alpha,\rho} {}^c D_{b^-}^{\alpha,\rho} f(x) = f(x) - \sum_{k=0}^{n-1} \frac{(-1)^k \delta^k f(b)}{k!} \left( \frac{b^\rho - t^\rho}{\rho} \right)^k.$$

In particular, for  $1 < \alpha \leq 2$ , we have:

$$I_{a^+}^{\alpha,\rho} {}^c D_{a^+}^{\alpha,\rho} f(x) = f(x) - f(a) - \frac{t^\rho - a^\rho}{\rho} \delta f(a),$$

$$I_{b^-}^{\alpha,\rho} {}^c D_{b^-}^{\alpha,\rho} f(x) = f(x) - f(b) + \frac{b^\rho - t^\rho}{\rho} \delta f(b).$$

**Lemma 2.** *Let  $1 < \beta < 2$  and  $v : J \rightarrow \mathbb{R}$  be an integrable function. Then, there is a solution to the linear problem:*

$$\begin{aligned} {}^c D_{s_r}^{\beta,\rho} y(\tau) &= v(\tau) & \tau \in (s_r, \tau_{r+1}], r = 0, 1, \dots, k \\ y(\tau) &= \Phi_r(\tau, y(\tau), y(\tau_r - 0)), & \tau \in (\tau_r, s_r], r = 1, 2, \dots, k \\ \tau^{1-\rho} y'(\tau) &= \Psi_r(\tau, y(\tau), y(\tau_r - 0)), & \tau \in (\tau_r, s_r], r = 1, 2, \dots, k \\ y(0) &= y_0, \quad \lim_{\tau \rightarrow 0} \tau^{1-\rho} y'(\tau) = y_1, & y_0, y_1 \in \mathbb{R} \end{aligned} \tag{2}$$

given by:

$$y(\tau) = \begin{cases} \frac{\rho^{1-\beta}}{\Gamma(\beta)} \int_0^\tau t^{\rho-1} (\tau - t^\rho)^{\beta-1} v(t) dt + y_0 + \frac{y_1}{\rho} \tau^\rho, & \tau \in [0, \tau_1], \\ \Phi_r(\tau, y(\tau), y(\tau_r - 0)), & \tau \in (\tau_r, s_r], \\ \frac{\rho^{1-\beta}}{\Gamma(\beta)} \int_{s_r}^\tau t^{\rho-1} (\tau - t^\rho)^{\beta-1} h(t) dt + \Phi_r(s_r, y(s_r), y(\tau_r - 0)) \\ + \frac{\tau^\rho - s_r^\rho}{\rho} \Psi_r(s_r, y(s_r), y(\tau_r - 0)), & \tau \in (s_r, \tau_{r+1}]. \end{cases} \quad (3)$$

**Proof.** Applying the operator  $I_{s_r}^{\beta, \rho}$  to fractional differential equation in (2) and using Lemma 1, we have:

$$y(\tau) = I_{s_r}^{\beta, \rho} v(\tau) + c_{1,r} + c_{2,r} \frac{\tau^\rho - s_r^\rho}{\rho} \quad \text{and} \quad \tau^{1-\rho} y'(\tau) = I_{s_r}^{\beta-1, \rho} v(\tau) + c_{2,r}$$

where  $c_{1,r}, c_{2,r} \in \mathbb{R}$ ,  $r = 0, 1, \dots, k$  are constants to be determined.

- For  $\tau \in [0, \tau_1]$ , we obtain:

$$y(\tau) = I_0^{\beta, \rho} v(\tau) + c_{1,0} + c_{2,0} \frac{\tau^\rho}{\rho} \quad \text{and} \quad \tau^{1-\rho} y'(\tau) = I_0^{\beta-1, \rho} v(\tau) + c_{2,0}.$$

Applying the initial conditions  $y(0) = y_0$  and  $\lim_{\tau \rightarrow 0} \tau^{\rho-1} y'(\tau) = y_1$  give  $c_{1,0} = y_0$  and  $c_{2,0} = y_1$  which imply that:

$$y(\tau) = I_0^{\beta, \rho} v(\tau) + y_0 + y_1 \frac{\tau^\rho}{\rho} \quad \text{and} \quad \tau^{1-\rho} y'(\tau) = I_0^{\beta-1, \rho} v(\tau) + y_1.$$

- For  $\tau \in (\tau_1, s_1]$ . Then,

$$y(\tau) = \Phi_1(\tau, y(\tau), y(\tau_1 - 0)) \quad \text{and} \quad y'(\tau) = \tau^{\rho-1} \Psi_1(\tau, y(\tau), y(\tau_1 - 0)).$$

- For  $\tau \in (s_1, \tau_2]$ . Then,

$$y(\tau) = I_{s_1}^{\beta, \rho} v(\tau) + c_{1,1} + c_{2,1} \frac{\tau^\rho - s_1^\rho}{\rho} \quad \text{and} \quad \tau^{1-\rho} y'(\tau) = I_{s_1}^{\beta-1, \rho} v(\tau) + c_{2,1}.$$

Due to the previous impulsive conditions, we get

$$c_{1,1} = \Phi_1(s_1, y(s_1), y(\tau_1 - 0)) \quad \text{and} \quad c_{2,1} = \Psi_1(s_1, y(s_1), y(\tau_1 - 0))$$

which imply that

$$y(\tau) = I_{s_1}^{\beta, \rho} v(\tau) + \Phi_1(s_1, y(s_1), y(\tau_1 - 0)) + \Psi_1(s_1, y(s_1), y(\tau_1 - 0)) \frac{\tau^\rho - s_1^\rho}{\rho},$$

$$\tau^{1-\rho} y'(\tau) = I_{s_1}^{\beta-1, \rho} v(\tau) + \Psi_1(s_1, y(s_1), y(\tau_1 - 0)).$$

- By similar process. For  $\tau \in (s_r, \tau_{r+1}]$ . Then,

$$y(\tau) = I_{s_r}^{\beta, \rho} v(\tau) + \Phi_r(s_r, y(s_r), y(\tau_r - 0)) + \frac{\tau^\rho - s_r^\rho}{\rho} \Psi_r(s_r, y(s_r), y(\tau_r - 0)).$$

Hence, from the previous, we obtain the solution (3). By direct computation, the converse follows. The proof is complete.  $\square$

Next, we present the concept of Ulam stability for problem (1). First, consider  $\mathcal{E} = \mathcal{PC}_\delta^1(J, \mathbb{R}) \cap \mathcal{AC}_\delta^2(J, \mathbb{R})$  with  $y \in \mathcal{E}$  and  $\epsilon > 0$ . Let us introduce the following inequality

$$\begin{cases} \| {}^c D_{s_r}^{\beta, \rho} y(\tau) - h(\tau) \| \leq \epsilon, & \tau \in (s_r, \tau_{r+1}], r = 0, 1, \dots, k \\ \| y(\tau) - \Phi_r \| \leq \epsilon, & \tau \in (\tau_r, s_r], r = 1, \dots, k \\ \| \tau^{1-\rho} y'(\tau) - \Psi_r \| \leq \epsilon, & \tau \in (\tau_r, s_r], r = 1, \dots, k \end{cases} \quad (4)$$

**Definition 3** ([32]). *If there is a constant  $\Lambda > 0$  and  $\epsilon > 0$  such that for any solution  $\tilde{y} \in \mathcal{E}$  of the inequality (4), there is a unique solution  $y \in \mathcal{E}$  to the problem (1) fulfilling*

$$\| \tilde{y}(\tau) - y(\tau) \| \leq \Lambda \epsilon.$$

Then the problem (1) is said to be UH stable.

**Definition 4** ([32]). *If there is a function  $\mu \in (\mathbb{R}^+, \mathbb{R}^+)$ ,  $\mu(0) = 0$ , for  $\epsilon > 0$  such that for any solution  $\tilde{y} \in \mathcal{E}$  of the inequality (4), there is a unique solution  $y \in \mathcal{E}$  to the problem (1) fulfilling*

$$\| \tilde{y}(\tau) - y(\tau) \| \leq \mu(\epsilon).$$

Then the problem (1) is said to be GUIH stable.

**Remark 2.** *If one has a function  $\varrho \in \mathcal{E}$  together with a sequences  $\varrho_r, r = 0, \dots, r$  dependent on  $y$ . Then  $y \in \mathcal{E}$  is called a solution of the inequality (4) such that:*

- (a)  $|\varrho(\tau)| \leq \epsilon, |\varrho_r| \leq \epsilon, \quad \tau \in J, r = 0, \dots, k$
- (b)  ${}^c D_{s_r}^{\beta, \rho} \tilde{y}(\tau) = \tilde{h}(\tau) + \varrho(\tau), \quad \tau \in (s_r, \tau_{r+1}], r = 0, 1, \dots, k$
- (c)  $\tilde{y}(\tau) = \Phi_r(\tau, \tilde{y}(\tau), \tilde{y}(\tau_r - 0)) + \varrho_r, \quad \tau \in (\tau_r, s_r], r = 1, 2, \dots, k$
- (d)  $\tau^{1-\rho} \tilde{y}'(\tau) = \Psi_r(\tau, \tilde{y}(\tau), \tilde{y}(\tau_r - 0)) + \varrho_r, \quad \tau \in (\tau_r, s_r], r = 1, 2, \dots, k.$

### 3. Existence and Uniqueness Results

Our results for uniqueness and existence for problem (1) are presented in this section. By using Lemma 2, we convert the non-instantaneous fractional differential Equation (1) into a fixed point problem. define the operator  $\mathcal{G} : \mathcal{E} \rightarrow \mathcal{E}$  by:

$$\mathcal{G}y(\tau) = \begin{cases} \frac{\rho^{1-\beta}}{\Gamma(\beta)} \int_0^\tau t^{\rho-1} (\tau^\rho - t^\rho)^{\beta-1} h(t) dt + y_0 + \frac{y_1}{\rho} \tau^\rho, & \tau \in [0, \tau_1], \\ \Phi_r(\tau, y(\tau), y(\tau_r - 0)), & \tau \in (\tau_r, s_r], \\ \frac{\rho^{1-\beta}}{\Gamma(\beta)} \int_{s_r}^\tau t^{\rho-1} (\tau^\rho - t^\rho)^{\beta-1} h(t) dt + \Phi_r(s_r, y(s_r), y(\tau_r - 0)) \\ + \frac{\tau^\rho - s_r^\rho}{\rho} \Psi_r(s_r, y(s_r), y(\tau_r - 0)), & \tau \in (s_r, \tau_{r+1}]. \end{cases} \quad (5)$$

where  $h(\tau) = h(\tau, y(\tau), \tau^{1-\rho} y'(\tau))$ .

To explain and prove our main results, we first introduce these hypotheses. Consider the following

(H1) The function  $h : [0, T] \times \mathbb{R} \times \mathbb{R} \rightarrow \mathbb{R}$  is continuous and  $\Phi_r, \Psi_r : [\tau_r, s_r] \times \mathbb{R} \times \mathbb{R} \rightarrow \mathbb{R}$  are continuous functions  $\forall r = 1, \dots, k$  and  $k \in \mathbb{N}$ .

(H2)  $|\hat{h}(\tau)| = |h(\tau, y, \tau^{1-\rho} y')| \leq q(\tau)v(|y|)$ , where  $q \in C([0, T], \mathbb{R}^+)$  and  $v : \mathbb{R}^+ \rightarrow \mathbb{R}^+$  is a nondecreasing function.

(H3) There exist constants  $\theta_r > 0, \theta_r^* > 0, r = 1, \dots, k; k \in \mathbb{N}$  such that

$$|\Phi_r(\tau, y, v)| \leq \theta_r, \quad \text{and} \quad |\Psi_r(\tau, y, v)| \leq \theta_r^*$$

$$\forall \tau \in [\tau_r, s_r], \quad y, v \in \mathbb{R}.$$

( $\mathfrak{H}_4$ ) There exist  $\mathcal{A} > 0$  satisfies  $\|y\|_{\mathcal{E}} \neq \mathcal{A}$  for some  $y \in \mathcal{E}$ .

( $\mathfrak{H}_5$ ) There exist positive constants  $\kappa_{1r}, \kappa_{2r}, \kappa_{1r}^*$  and  $\kappa_{2r}^*, r = 1, \dots, k; k \in \mathbb{N}$  such that:

$$\begin{aligned} |\Phi_r(\tau, y_1, v_1) - \Phi_r(\tau, y_2, v_2)| &\leq \kappa_{1r}|y_1 - y_2| + \kappa_{2r}|v_1 - v_2|, \\ |\Psi_r(\tau, y_1, v_1) - \Psi_r(\tau, y_2, v_2)| &\leq \kappa_{1r}^*|y_1 - y_2| + \kappa_{2r}^*|v_1 - v_2| \end{aligned}$$

for each  $\tau \in [\tau_r, s_r]$  and  $y_1, y_2, v_1, v_2 \in \mathbb{R}$ .

( $\mathfrak{H}_6$ ) There exists  $\mathcal{L} > 0$  satisfies

$$|h(\tau, y, \delta y) - h(\tau, u, \delta u)| \leq \mathcal{L}(|y - u| + \delta|y - u|)$$

$\forall \tau \in [0, T]$  and  $y, u \in \mathbb{R}$ .

Below are the short constants that we will use later to simplify handling:

$$\Omega = \Omega(\beta) + \Omega(\beta - 1) \tag{6}$$

$$\Omega_r = \Omega_r(\beta) + \Omega_r(\beta - 1), \tag{7}$$

$$\mathcal{Q} = \frac{\mathcal{A}}{\Omega\|q\|v(\mathcal{A}) + |y_0| + \frac{|y_1|}{\rho}(\rho + \tau_1^\rho)}, \tag{8}$$

$$\mathcal{Q}_{1r} = \frac{\mathcal{A}}{\vartheta_r + \vartheta_r^*}, \tag{9}$$

$$\mathcal{Q}_{2r} = \frac{\mathcal{A}}{\Omega_r\|q\|v(\mathcal{A}) + \vartheta_r + \frac{\vartheta_r^*}{\rho}(\rho + T^\rho - s_r^\rho)} \tag{10}$$

where  $r = 1, 2, \dots, k; k \in \mathbb{N}$ ,

$$\Omega(\beta) = \frac{\tau_1^{\rho\beta}}{\rho^\beta\Gamma(\beta + 1)} \quad \text{and} \quad \Omega_r(\beta) = \frac{(T^\rho - s_r^\rho)^\beta}{\rho^\beta\Gamma(\beta + 1)}.$$

**Lemma 3** ([33,34]). (*Leray–Schauder nonlinear alternative*) Assume that  $\mathbb{E}$  is a Banach space,  $B$  is a convex closed subset of  $\mathbb{E}$ , and  $Y \subset B$  is an open subset and  $0 \in Y$ . If  $\mathcal{F} : \bar{Y} \rightarrow B$  is continuous and compact, then either

- In  $\bar{Y}$ ,  $\mathcal{F}$  has a fixed point; or
- For some  $\lambda \in (0, 1)$ , there exists  $y \in \partial Y$  and  $y = \lambda\mathcal{F}y$ .

**Theorem 1.** Consider Hypotheses ( $\mathfrak{H}_1$ )–( $\mathfrak{H}_4$ ) satisfied. If

$$\max\{\mathcal{Q}, \mathcal{Q}_{1r}, \mathcal{Q}_{2r}\} > 1$$

where  $\mathcal{Q}, \mathcal{Q}_{1r}$  and  $\mathcal{Q}_{2r}$  are given by Equations (8), (9) and (10), respectively. Then, the problem in Equation (1) has at least one solution in  $[0, T]$ .

**Proof.** Verifying the hypotheses of Leray–Schauder nonlinear alternative involves a number of steps. The first step is to demonstrate that the operator  $\mathcal{G} : \mathcal{E} \rightarrow \mathcal{E}$  defined by Equation (5) maps bounded sets into bounded sets in  $\mathcal{E}$ . In other word, we show that for a positive number  $\omega$ , there exists a positive constant  $\mathcal{I}$  such that  $\|\mathcal{G}y\|_{\mathcal{E}} \leq \mathcal{I}$  for any  $y \in B_\omega$  where  $B_\omega$  is a closed bounded set defined as

$$B_\omega = \left\{ (y, \delta y) : y \in \mathcal{E} \wedge \|y\|_{\mathcal{E}} = \|y\|_{\mathcal{PC}} + \|\delta y\|_{\mathcal{PC}_s^1} \leq \omega \right\}$$

with the radius:

$$\omega \geq \max\left\{ \Omega\|q\|v(\omega) + |y_0| + \frac{|y_1|}{\rho}(\rho + \tau_1^\rho), \vartheta_r + \vartheta_r^*, \Omega_r\|q\|v(\omega) + \vartheta_r + \frac{\vartheta_r^*}{\rho}(\rho + T^\rho - s_r^\rho) \right\}.$$

Then, in light of  $(\mathfrak{h}_2)$  and  $(\mathfrak{h}_3)$ , we have

- **Case I.** For each  $\tau \in [0, \tau_1]$  and  $(y, \delta y) \in B_\omega$ . Using (6), we have

$$\|\mathcal{G}y\|_{\mathcal{P}\mathcal{C}} \leq \sup_{\tau \in [0, \tau_1]} I_{0^+}^{\beta, \rho} |\widehat{h}(t)| + |y_0| + \left| \frac{y_1}{\rho} \tau^\rho \right| \leq \Omega(\beta) \|q\| v(\omega) + |y_0| + \frac{|y_1|}{\rho} \tau_1^\rho.$$

Similarly, one can establish that

$$\|\delta \mathcal{G}y\|_{\mathcal{P}\mathcal{C}_\delta^1} \leq \sup_{\tau \in [0, \tau_1]} I_{0^+}^{\beta-1, \rho} |\widehat{h}(t)| + |y_1| \leq \Omega(\beta - 1) \|q\| v(\omega) + |y_1|.$$

Consequently, we have

$$\|\mathcal{G}y\|_{\mathcal{E}} \leq \Omega \|q\| v(\omega) + |y_0| + \frac{|y_1|}{\rho} (\rho + \tau_1^\rho) := \mathcal{I}_1.$$

- **Case II.** For each  $\tau \in (\tau_r, s_r]$ ,  $r = 1, 2, \dots, k$  and  $(y, \delta y) \in B_\omega$ , we get

$$\|\mathcal{G}y\|_{\mathcal{E}} = \|\mathcal{G}y\|_{\mathcal{P}\mathcal{C}} + \|\delta \mathcal{G}\|_{\mathcal{P}\mathcal{C}_\delta^1} \leq \vartheta_r + \vartheta_r^* := \mathcal{I}_{2r}.$$

- **Case III.** For each  $\tau \in (s_r, \tau_{r+1}]$ ,  $r = 1, 2, \dots, k$  and  $(y, \delta y) \in B_\omega$ . Using (7), we have

$$\begin{aligned} \|\mathcal{G}y\|_{\mathcal{P}\mathcal{C}} &\leq \sup_{\tau \in (s_r, \tau_{r+1}]} I_{s_r^+}^{\beta, \rho} |\widehat{h}(t)| + |\Phi_r(s_r, y(s_r), y(\tau_r - 0))| + \left| \frac{\tau^\rho - s_r^\rho}{\rho} \Psi_r(s_r, y(s_r), y(\tau_r - 0)) \right| \\ &\leq \Omega_r(\beta) \|q\| v(\omega) + \vartheta_r + \frac{\vartheta_r^*}{\rho} (T^\rho - s_r^\rho). \end{aligned}$$

In a similar manner, one can obtain:

$$\|\delta \mathcal{G}y\|_{\mathcal{P}\mathcal{C}_\delta^1} \leq \Omega_r(\beta - 1) \|q\| v(\omega) + \vartheta_r^*.$$

Hence, we deduce that:

$$\|\mathcal{G}y\|_{\mathcal{E}} \leq \Omega_r \|q\| v(\omega) + \vartheta_r + \frac{\vartheta_r^*}{\rho} (\rho + T^\rho - s_r^\rho) := \mathcal{I}_{3r}.$$

From the above three inequalities, we can conclude that  $\|\mathcal{G}y\|_{\mathcal{E}} \leq \mathcal{I}$  where  $\mathcal{I} = \max_r \{\mathcal{I}_1, \mathcal{I}_{2r}, \mathcal{I}_{3r}\}$ . Thus, the operator  $\mathcal{G}$  maps bounded sets into bounded sets of the space  $\mathcal{E}$ .

In the next step, we check that the operator  $\mathcal{G}$  maps bounded sets into equicontinuous sets in  $\mathcal{E}$ . Considering the condition  $(\mathfrak{h}_1)$ ,  $\mathcal{G}$  is continuous.

- **Case I.** For each  $0 \leq \zeta_1 < \zeta_2 \leq \tau_1$  and  $(y, \delta y) \in B_\omega$ , we obtain that

$$\begin{aligned} |(\mathcal{G}y)(\zeta_2) - (\mathcal{G}y)(\zeta_1)| &\leq \frac{\rho^{1-\beta}}{\Gamma(\beta)} \int_0^{\zeta_1} t^{\rho-1} [(\zeta_2^\rho - t^\rho)^{\beta-1} - (\zeta_1^\rho - t^\rho)^{\beta-1}] |\widehat{h}(t)| dt \\ &\quad + \frac{\rho^{1-\beta}}{\Gamma(\beta)} \int_{\zeta_1}^{\zeta_2} t^{\rho-1} (\zeta_2^\rho - t^\rho)^{\beta-1} |\widehat{h}(t)| dt + \frac{|y_1|}{\rho} (\zeta_2^\rho - \zeta_1^\rho) \\ &\leq \|q\| v(|y|) \frac{1}{\rho^\beta \Gamma(\beta + 1)} (\zeta_2^{\rho\beta} - \zeta_1^{\rho\beta}) + \frac{|y_1|}{\rho} (\zeta_2^\rho - \zeta_1^\rho) \\ &\Rightarrow 0 \quad \text{as } \zeta_2 \rightarrow \zeta_1. \end{aligned}$$

Similarly, one can establish that:

$$\begin{aligned}
 & |(\delta \mathcal{G}y)(\zeta_2) - (\delta \mathcal{G}y)(\zeta_1)| \\
 & \leq \|q\|v(|y|) \frac{\rho^{2-\beta}}{\Gamma(\beta-1)} \left( \int_0^{\zeta_1} t^{\rho-1} [(\zeta_1^\rho - t^\rho)^{\beta-2} - (\zeta_2^\rho - t^\rho)^{\beta-2}] dt + \int_{\zeta_1}^{\zeta_2} t^{\rho-1} (\zeta_2^\rho - t^\rho)^{\beta-2} dt \right) \\
 & \leq 2\|q\|v(|y|) \frac{1}{\rho^{\beta-1}\Gamma(\beta)} (\zeta_2^\rho - \zeta_1^\rho)^{\beta-1} \\
 & \Rightarrow 0 \text{ as } \zeta_2 \rightarrow \zeta_1.
 \end{aligned}$$

- **Case II.** For each  $\tau_r \leq \zeta_1 < \zeta_2 < s_r, r = 1, 2, \dots, k$  and  $(y, \delta y) \in B_\omega$ , we have

$$\begin{aligned}
 & |(\mathcal{G}y)(\zeta_2) - (\mathcal{G}y)(\zeta_1)| \leq |\Phi_r(\zeta_2, y(\zeta_2), y(\tau_r - 0))| - |\Phi_r(\zeta_1, y(\zeta_1), y(\tau_r - 0))| \\
 & |(\delta \mathcal{G}y)(\zeta_2) - (\delta \mathcal{G}y)(\zeta_1)| \leq |\Psi_r(\zeta_2, y(\zeta_2), y(\tau_r - 0))| - |\Psi_r(\zeta_1, y(\zeta_1), y(\tau_r - 0))|.
 \end{aligned}$$

Due to the continuity of both functions. It is clear that the above inequality approaches zero when letting  $\zeta_2 \rightarrow \zeta_1$ .

- **Case III.** For each  $s_r \leq \zeta_1 < \zeta_2 < \tau_{r+1}, r = 1, 2, \dots, k$ , and  $(y, \delta y) \in B_\omega$ , we get

$$\begin{aligned}
 & |(\mathcal{G}y)(\zeta_2) - (\mathcal{G}y)(\zeta_1)| \leq \frac{\rho^{1-\beta}}{\Gamma(\beta)} \int_{s_r}^{\zeta_1} t^{\rho-1} [(\zeta_2^\rho - t^\rho)^{\beta-1} - (\zeta_1^\rho - t^\rho)^{\beta-1}] |\widehat{h}(t)| dt \\
 & + \frac{\rho^{1-\beta}}{\Gamma(\beta)} \int_{\zeta_1}^{\zeta_2} t^{\rho-1} (\zeta_2^\rho - t^\rho)^{\beta-1} |\widehat{h}(t)| dt + \frac{\zeta_2^\rho - \zeta_1^\rho}{\rho} |\Psi_r(s_r, y(s_r), y(\tau_r - 0))| \\
 & \leq \|q\|v(|y|) \frac{1}{\rho^\beta \Gamma(\beta+1)} \left[ (\zeta_2^\rho - s_r^\rho)^\beta - (\zeta_1^\rho - s_r^\rho)^\beta \right] + \frac{\zeta_2^\rho - \zeta_1^\rho}{\rho} |\Psi_r(s_r, y(s_r), y(\tau_r - 0))| \\
 & \Rightarrow 0 \text{ as } \zeta_2 \rightarrow \zeta_1.
 \end{aligned}$$

Moreover, we have:

$$\begin{aligned}
 & |(\delta \mathcal{G}y)(\zeta_2) - (\delta \mathcal{G}y)(\zeta_1)| \\
 & \leq \|q\|v(|y|) \frac{\rho^{2-\beta}}{\Gamma(\beta-1)} \left( \int_{s_r}^{\zeta_1} t^{\rho-1} [(\zeta_1^\rho - t^\rho)^{\beta-2} - (\zeta_2^\rho - t^\rho)^{\beta-2}] dt + \int_{\zeta_1}^{\zeta_2} t^{\rho-1} (\zeta_2^\rho - t^\rho)^{\beta-2} dt \right) \\
 & \leq \|q\|v(|y|) \frac{1}{\rho^{\beta-1}\Gamma(\beta)} \left[ 2(\zeta_2^\rho - \zeta_1^\rho)^{\beta-1} + (\zeta_1^\rho - s_r^\rho)^{\beta-1} - (\zeta_2^\rho - s_r^\rho)^{\beta-1} \right] \\
 & \Rightarrow 0 \text{ as } \zeta_2 \rightarrow \zeta_1.
 \end{aligned}$$

As a result of the three inequalities above, we conclude that  $\|(\mathcal{G}y)(\zeta_2) - (\mathcal{G}y)(\zeta_1)\|_\mathcal{E} \rightarrow 0$  independently of  $(y, \delta y) \in B_\omega$  as  $\zeta_2 \rightarrow \zeta_1$ . Using the preceding arguments and the Arzela-Ascoli theorem, the operator  $\mathcal{G} : \mathcal{E} \rightarrow \mathcal{E}$  is completely continuous.

Finally, we show that there exist an open set  $Y \subset \mathcal{E}$  with  $y \neq \lambda \mathcal{G}y$  for  $\lambda \in (0, 1)$  and  $y \in \partial Y$ . Consider the equation  $y = \lambda \mathcal{G}y$  for  $\lambda \in (0, 1)$ . Then based on **Step 1**, we have the following cases:

- **Case I.** For each  $\tau \in [0, \tau_1]$ , one has

$$\|y(\tau)\| = \|\lambda(\mathcal{G}y)(\tau)\| \leq \Omega \|q\|v(\|y\|) + |y_0| + \frac{|y_1|}{\rho} (\rho + \tau_1^\rho)$$

which implies that:

$$\frac{\|y\|_\mathcal{E}}{\Omega \|q\|v(\|y\|_\mathcal{E}) + |y_0| + \frac{|y_1|}{\rho} (\rho + \tau_1^\rho)} \leq 1. \tag{11}$$

- **Case II.** For each  $\tau \in (\tau_r, s_r], r = 1, 2, \dots, k$ , one has

$$\|y(\tau)\| = \|\lambda(\mathcal{G}y)(\tau)\| \leq \vartheta_r + \vartheta_r^*$$

which implies that:

$$\frac{\|y\|_{\mathcal{E}}}{\vartheta_r + \vartheta_r^*} \leq 1. \tag{12}$$

- **Case III.** For each  $\tau \in (s_r, \tau_{r+1}], r = 1, \dots, k$ , we obtain:

$$\|y(\tau)\| = \|\lambda(\mathcal{G}y)(\tau)\| \leq \Omega_r \|q\| v(\|y\|) + \vartheta_r + \frac{\vartheta_r^*}{\rho} (\rho + T^\rho - s_r^\rho)$$

which implies that:

$$\frac{\|y\|_{\mathcal{E}}}{\Omega_r \|q\| v(\|y\|_{\mathcal{E}}) + \vartheta_r + \frac{\vartheta_r^*}{\rho} (\rho + T^\rho - s_r^\rho)} \leq 1. \tag{13}$$

If (11)–(13) are combined with  $(\mathfrak{H}_4)$  and given condition  $\max_r \{Q, Q_{1r}, Q_{2r}\} > 1$ . A positive number  $\mathcal{A}$  such that  $\|y\|_{\mathcal{E}} \neq \mathcal{A}$  can be found. Create a set  $Y = \{y \in \mathcal{E} : \|y\|_{\mathcal{E}} < \mathcal{A}\}$  with the operator  $\mathcal{G} : \bar{Y} \rightarrow \mathcal{E}$  being continuous and completely continuous. In light of the choice of  $Y$ , there is no  $y \in \partial Y$  satisfying  $y = \lambda \mathcal{G}y$  for  $\lambda \in (0, 1)$ . Thus, it follows from the nonlinear alternative of Leray–Schauder, the operator  $\mathcal{G}$  has a fixed point  $y \in \bar{Y}$  that corresponds to a solution to Equation (1).  $\square$

Using the contraction mapping principle, we ensure the uniqueness of solution to problem (1).

**Theorem 2.** Suppose that Hypotheses  $(\mathfrak{H}_1, \mathfrak{H}_3, \mathfrak{H}_5$  and  $\mathfrak{H}_6)$  are satisfied. If

$$\Delta = \max_r \{ \mathcal{L}\Omega, \mathcal{K}_r + \mathcal{K}_r^*, \mathcal{L}\Omega_r + \mathcal{K}_r + \frac{\mathcal{K}_r^*}{\rho} (\rho + T^\rho - s_r^\rho) \} < 1 \tag{14}$$

where  $\mathcal{K}_r = \kappa_{1r} + \kappa_{2r}$  and  $\mathcal{K}_r^* = \kappa_{1r}^* + \kappa_{2r}^*$ . Thus, the non-instantaneous impulsive fractional differential Equation (1) has a unique solution on  $J$ .

**Proof.** Let us consider a set:

$$B_r = \left\{ (y, \delta y) : y \in \mathcal{E} \wedge \|y\|_{\mathcal{E}} = \|y(\tau)\|_{\mathcal{PC}} + \|\delta y(\tau)\|_{\mathcal{PC}_\delta^1} \leq r \right\}$$

with radius

$$r \geq \max_r \left\{ \frac{\Omega N + |y_0| + \frac{|y_1|}{\rho} (\rho + \tau_1^\rho)}{1 - \mathcal{L}\Omega}, \vartheta_r + \vartheta_r^*, \frac{\Omega_r N + \vartheta_r + \frac{\vartheta_r^*}{\rho} (\rho + T^\rho - s_r^\rho)}{1 - \mathcal{L}\Omega_r} \right\}$$

where  $\sup_{\tau \in [0, T]} |h(\tau, 0, 0)| = N$ . Clearly,  $\mathcal{G}$  is well defined and  $\mathcal{G}y \in \mathcal{E}$  for all  $y \in \mathcal{E}$ . All that remains is to demonstrate that  $\mathcal{G}$  is a contraction mapping. Thus, three cases are considered:

- **Case I.** For each  $\tau \in [0, \tau_1]$  and  $(y, \delta y), (v, \delta v) \in \mathcal{E}$ . Using (6), we get

$$\begin{aligned} \|\mathcal{G}y - \mathcal{G}v\|_{\mathcal{PC}} &\leq \sup_{\tau \in [0, \tau_1]} \frac{\rho^{1-\beta}}{\Gamma(\beta)} \int_0^\tau t^{\beta-1} (\tau^\rho - t^\rho)^{\beta-1} \left| h(t, y, t^{1-\rho}y') - h(t, v, t^{1-\rho}v') \right| dt \\ &\leq \mathcal{L}\Omega(\beta) \|y - v\|. \end{aligned}$$

Similarly, we can obtain:

$$\|\delta\mathcal{G}y - \delta\mathcal{G}v\|_{\mathcal{PC}_\delta^1} \leq \mathcal{L}\Omega(\beta - 1)\|y - v\|$$

which implies that:

$$\|\mathcal{G}y - \mathcal{G}v\|_{\mathcal{E}} \leq \mathcal{L}\Omega\|y - v\|.$$

- **Case II.** For each  $\tau \in (\tau_r, s_r], r = 1, 2, \dots, k$  and  $(y, \delta y), (v, \delta v) \in \mathcal{E}$ , we have:

$$\|\mathcal{G}y - \mathcal{G}v\|_{\mathcal{PC}} \leq (\kappa_{1r} + \kappa_{2r})\|y - v\|.$$

In addition:

$$\|\delta\mathcal{G}y - \delta\mathcal{G}v\|_{\mathcal{PC}_\delta^1} \leq (\kappa_{1r}^* + \kappa_{2r}^*)\|y - v\|.$$

Consequently, we have:

$$\|\mathcal{G}y - \mathcal{G}v\|_{\mathcal{E}} \leq (\mathcal{K}_r + \mathcal{K}_r^*)\|y - v\|.$$

- **Case III.** For each  $\tau \in (s_r, \tau_{r+1}], r = 1, 2, \dots, k$  and  $(y, \delta y), (v, \delta v) \in \mathcal{E}$ . Using (7), we obtain:

$$\begin{aligned} & \|\mathcal{G}y - \mathcal{G}v\|_{\mathcal{PC}} \\ & \leq \sup_{\tau \in (s_r, \tau_{r+1}]} \frac{\rho^{1-\beta}}{\Gamma(\beta)} \int_{s_r}^{\tau} t^{\rho-1} (\tau^\rho - t^\rho)^{\beta-1} \left| h(t, y, t^{1-\rho}y') - h(t, v, t^{1-\rho}v') \right| dt \\ & \quad + |\Phi_r(s_r, y(s_r), y(\tau_r - 0)) - \Phi_r(s_r, v(s_r), v(\tau_r - 0))| \\ & \quad + \left| \frac{\tau^\rho - s_r^\rho}{\rho} (\Psi_r(s_r, y(s_r), y(\tau_r - 0)) - \Psi_r(s_r, v(s_r), v(\tau_r - 0))) \right| \\ & \leq \left[ \mathcal{L}\Omega_r(\beta) + \mathcal{K}_r + \frac{\mathcal{K}_r^*}{\rho} (T^\rho - s_r^\rho) \right] \|y - v\|. \end{aligned}$$

In a similar manner, it can be shown that:

$$\|\delta\mathcal{G}y - \delta\mathcal{G}v\|_{\mathcal{PC}_\delta^1} \leq [\mathcal{L}\Omega_r(\beta - 1) + \mathcal{K}_r^*]\|y - v\|$$

which leads to:

$$\|\mathcal{G}y - \mathcal{G}v\|_{\mathcal{E}} \leq \left[ \mathcal{L}\Omega_r + \mathcal{K}_r + \frac{\mathcal{K}_r^*}{\rho} (\rho + T^\rho - s_r^\rho) \right] \|y - v\|.$$

From the above, we obtain:  $\|\mathcal{G}y - \mathcal{G}v\|_{\mathcal{E}} \leq \Delta\|y - v\|$  which, in view of the given condition  $\Delta < 1$ , shows that the operator  $\mathcal{G}$  is a contraction. This implies that the problem in Equation (1) has a unique solution on  $[0, T]$ , according to the Banach contraction mapping principle.  $\square$

#### 4. Stability Analysis

We present results regarding the Ulam–Hyers stability of our problem (1) in this section.

**Theorem 3.** *Suppose that Hypotheses  $(\mathfrak{H}_1)$ ,  $(\mathfrak{H}_5)$  and  $(\mathfrak{H}_6)$  are satisfied. Then, the non-instantaneous impulsive fractional differential Equation (1) is Ulam–Hyers stable and Generalized Ulam–Hyers stable if  $\Delta < 1$  where  $\Delta$  is defined as (14).*

**Proof.** Assuming a unique solution  $y \in \mathcal{E}$  to the problem (1) corresponds to any solution  $\tilde{y} \in \mathcal{E}$  of the inequality (4). Then, in light of Lemma 2, we have:

$$y(\tau) = \begin{cases} \frac{\rho^{1-\beta}}{\Gamma(\beta)} \int_0^\tau t^{\rho-1} (\tau^\rho - t^\rho)^{\beta-1} v(t) dt + y_0 + \frac{v_1}{\rho} \tau^\rho, & \tau \in [0, \tau_1], \\ \Phi_r(\tau, y(\tau), y(\tau_r - 0)), & \tau \in (\tau_r, s_r], \\ \frac{\rho^{1-\beta}}{\Gamma(\beta)} \int_{s_r}^\tau t^{\rho-1} (\tau^\rho - t^\rho)^{\beta-1} h(t) dt + \Phi_r(s_r, y(s_r), y(\tau_r - 0)) \\ + \frac{\tau^\rho - s_r^\rho}{\rho} \Psi_r(s_r, y(s_r), y(\tau_r - 0)), & \tau \in (s_r, \tau_{r+1}]. \end{cases}$$

Further, if  $\tilde{y}$  is the solution of inequality (4) and using Remark 2, we get:

$$\begin{aligned} {}^c D_{s_r}^{\beta, \rho} \tilde{y}(\tau) &= \tilde{h}(\tau) + \varrho(\tau) & \tau \in (s_r, \tau_{r+1}], r = 0, 1, \dots, k \\ \tilde{y}(\tau) &= \Phi_r(\tau, \tilde{y}(\tau), \tilde{y}(\tau_r - 0)) + \varrho_r, & r = 1, 2, \dots, k \\ \tau^{1-\rho} \tilde{y}'(\tau) &= \Psi_r(\tau, \tilde{y}(\tau), \tilde{y}(\tau_r - 0)) + \varrho_r, & r = 1, 2, \dots, k \end{aligned}$$

where  $\tilde{h}(\tau) = h(\tau, \tilde{y}(\tau), \tau^{1-\rho} \tilde{y}'(\tau))$  and

$$\tilde{y}(\tau) = \begin{cases} I_0^{\beta, \rho} \tilde{h}(\tau) + I_0^{\beta, \rho} \varrho(\tau) + y_0 + \frac{v_1}{\rho} \tau^\rho, & \tau \in [0, \tau_1], \\ \Phi_r(\tau, \tilde{y}(\tau), \tilde{y}(\tau_r - 0)) + \varrho_r, & \tau \in (\tau_r, s_r], \\ I_{s_r}^{\beta, \rho} \tilde{h}(\tau) + I_{s_r}^{\beta, \rho} \varrho(\tau) + \Phi_r(s_r, \tilde{y}(s_r), \tilde{y}(\tau_r - 0)) \\ + \frac{\tau^\rho - s_r^\rho}{\rho} \Psi_r(s_r, \tilde{y}(s_r), \tilde{y}(\tau_r - 0)) + \frac{\varrho_r}{\rho} (\rho + \tau^\rho - s_r^\rho), & \tau \in (s_r, \tau_{r+1}]. \end{cases}$$

For each  $\tau \in [0, \tau_1]$ , we consider:

$$\begin{aligned} \|\tilde{y}(\tau) - y(\tau)\|_{\mathcal{PC}} &\leq \frac{\rho^{1-\beta}}{\Gamma(\beta)} \int_0^\tau t^{\rho-1} (\tau^\rho - t^\rho)^{\beta-1} |\tilde{h}(t) - h(t)| dt + \frac{\rho^{1-\beta}}{\Gamma(\beta)} \int_0^\tau t^{\rho-1} (\tau^\rho - t^\rho)^{\beta-1} |\varrho(t)| dt \\ &\leq \mathcal{L}\Omega(\beta) \|\tilde{y} - y\|_{\mathcal{E}} + \epsilon \Omega(\beta). \end{aligned}$$

Similarly, we can obtain:

$$\|\delta \tilde{y}(\tau) - \delta y(\tau)\|_{\mathcal{PC}_s^1} \leq \mathcal{L}\Omega(\beta - 1) \|\tilde{y} - y\|_{\mathcal{E}} + \epsilon \Omega(\beta - 1)$$

which implies that:

$$\|\tilde{y}(\tau) - y(\tau)\|_{\mathcal{E}} \leq \mathcal{L}\Omega \|\tilde{y} - y\|_{\mathcal{E}} + \epsilon \Omega.$$

Or, equivalently,

$$\|\tilde{y} - y\|_{\mathcal{E}} \leq \frac{\epsilon \Omega}{1 - \mathcal{L}\Omega}, \quad \mathcal{L}\Omega < 1.$$

For each  $\tau \in (\tau_r, s_r], r = 1, 2, \dots, k$ , we consider:

$$\begin{aligned} \|\tilde{y}(\tau) - y(\tau)\|_{\mathcal{PC}} &\leq |\Phi_r(\tau, \tilde{y}(\tau), \tilde{y}(\tau_r - 0)) - \Phi_r(\tau, y(\tau), y(\tau_r - 0))| + |\varrho_r| \\ &\leq (\kappa_{1r} + \kappa_{2r}) \|\tilde{y} - y\| + \epsilon. \end{aligned}$$

In addition:

$$\|\delta \tilde{y}(\tau) - \delta y(\tau)\|_{\mathcal{PC}_s^1} \leq (\kappa_{1r}^* + \kappa_{2r}^*) \|\tilde{y} - y\|_{\mathcal{E}} + \epsilon.$$

Consequently, we have:

$$\|\tilde{y} - y\|_{\mathcal{E}} \leq (\mathcal{K}_r + \mathcal{K}_r^*)\|\tilde{y} - y\|_{\mathcal{E}} + 2\epsilon.$$

Or, equivalently:

$$\|\tilde{y} - y\|_{\mathcal{E}} \leq \frac{2\epsilon}{1 - (\mathcal{K}_r + \mathcal{K}_r^*)}, \quad \mathcal{K}_r + \mathcal{K}_r^* < 1.$$

For each  $\tau \in (s_r, \tau_{r+1}]$ ,  $r = 1, 2, \dots, k$ , we consider:

$$\begin{aligned} \|\tilde{y}(\tau) - y(\tau)\|_{\mathcal{PC}} &\leq \frac{\rho^{1-\beta}}{\Gamma(\beta)} \int_{s_r}^{\tau} t^{\rho-1} (\tau^{\rho} - t^{\rho})^{\beta-1} |h(t) - h(t)| dt + \frac{\rho^{1-\beta}}{\Gamma(\beta)} \int_{s_r}^{\tau} t^{\rho-1} (\tau^{\rho} - t^{\rho})^{\beta-1} |q(t)| dt \\ &+ |\Phi_r(\tau, \tilde{y}(\tau), \tilde{y}(\tau_r - 0)) - \Phi_r(\tau, y(\tau), y(\tau_r - 0))| + |q_r| \\ &+ \left| \frac{\tau^{\rho} - s_r^{\rho}}{\rho} \left| \Psi_r(\tau, \tilde{y}(\tau), \tilde{y}(\tau_r - 0)) - \Psi_r(\tau, y(\tau), y(\tau_r - 0)) \right| \right| + \left| \frac{\tau^{\rho} - s_r^{\rho}}{\rho} q_r \right| \\ &\leq \left[ \mathcal{L}\Omega_r(\beta) + \mathcal{K}_r + \frac{\mathcal{K}_r^*}{\rho} (T^{\rho} - s_r^{\rho}) \right] \|\tilde{y} - y\|_{\mathcal{E}} + \epsilon \left( 1 + \frac{T^{\rho} - s_r^{\rho}}{\rho} \right). \end{aligned}$$

In a similar manner, it can be shown that:

$$\|\delta\tilde{y}(\tau) - \delta y(\tau)\|_{\mathcal{PC}_3^1} \leq [\mathcal{L}\Omega_r(\beta - 1) + \mathcal{K}_r^*] \|\tilde{y} - y\|_{\mathcal{E}} + \epsilon$$

which leads to:

$$\|\tilde{y}(\tau) - y(\tau)\|_{\mathcal{E}} \leq \frac{(2\rho + T^{\rho} - s_r^{\rho})\epsilon}{\rho \left( 1 - \mathcal{L}\Omega_r - \mathcal{K}_r - \frac{\mathcal{K}_r^*}{\rho} (\rho + T^{\rho} - s_r^{\rho}) \right)}, \quad \mathcal{L}\Omega_r + \mathcal{K}_r + \frac{\mathcal{K}_r^*}{\rho} (\rho + T^{\rho} - s_r^{\rho}) < 1.$$

Then, for each  $\tau \in J$ , we obtain:

$$\|\tilde{y}(\tau) - y(\tau)\|_{\mathcal{E}} \leq \Lambda \epsilon.$$

where  $\Lambda = \max \left\{ \frac{\Omega}{1 - \mathcal{L}\Omega}, \frac{2}{1 - (\mathcal{K}_r + \mathcal{K}_r^*)}, \frac{2\rho + T^{\rho} - s_r^{\rho}}{\rho(1 - \mathcal{L}\Omega_r - \mathcal{K}_r - \frac{\mathcal{K}_r^*}{\rho} (\rho + T^{\rho} - s_r^{\rho}))} \right\}$ .  $\square$

Thus, the solution of (1) is UH stable if  $\Delta < 1$ . Additionally, by setting  $\mu(\epsilon) = \Lambda$  and  $\mu(0) = 0$ . Then, the solution of (1) becomes GUH stable.

### 5. Applications

In this section, we describe an application of our main results to demonstrate how they can be applied.

**Example 1.** Consider the following non-instantaneous impulsive fractional differential equations:

$$\begin{aligned} {}^c D_{s_r}^{\beta, \rho} y(\tau) &= h(\tau, y(\tau), \delta y(\tau)) & \tau \in (0, \frac{1}{3}] \cup (\frac{2}{3}, 1], \\ y(\tau) &= \frac{3}{4}\tau^2 + \frac{1}{12} \sin y(\tau) + \frac{1}{8} \cos y(\tau_r - 0), & \tau \in (\frac{1}{3}, \frac{2}{3}], \\ \delta y(\tau) &= \frac{3}{2}\tau + \frac{1}{14} \cos y(\tau) + \frac{1}{10} \sin y(\tau_r - 0), & \tau \in (\frac{1}{3}, \frac{2}{3}], \\ y(0) &= 0, & \lim_{\tau \rightarrow 0} \delta y(\tau) = 1 \end{aligned} \tag{15}$$

where  $J = [0, 1], 0 = s_0 < \tau_1 = \frac{1}{3} < s_1 = \frac{2}{3} < \tau_2 = 1, \rho = \frac{1}{2}, \beta = \frac{5}{4}$  and  $h(\tau, y(\tau), \delta y(\tau))$  will be determined later. Using the given data, we can find that

$$\begin{aligned} \Omega(\beta) &\approx 1.05646621, & \Omega(\beta - 1) &\approx 1.14365822, & \Omega &\approx 2.20012444, \\ \Omega_r(\beta) &\approx 0.25212249, & \Omega_r(\beta - 1) &\approx 0.85871184, & \Omega_r &\approx 1.11083434. \end{aligned}$$

In our example, we take

$$\begin{aligned} \Phi_1(\tau, y, v) &= \frac{3}{4}\tau^2 + \frac{1}{12}\sin y + \frac{1}{8}\cos v, \\ \Psi_1(\tau, y, v) &= \frac{3}{2}\tau + \frac{1}{14}\cos y + \frac{1}{10}\sin v. \end{aligned}$$

It is clear that they are continuous on the interval  $(\frac{1}{3}, \frac{2}{3}]$  which meets the first assumption and satisfy

$$\begin{aligned} |\Phi_1(\tau, y, v)| &\leq \left| \frac{3}{4}\tau^2 \right| + \left| \frac{1}{12}\sin y \right| + \left| \frac{1}{8}\cos v \right| \leq \frac{3}{4}\left(\frac{2}{3}\right)^2 + \frac{1}{12} + \frac{1}{8} = \frac{13}{24}, \\ |\Psi_1(\tau, y, v)| &\leq \left| \frac{3}{2}\tau \right| + \left| \frac{1}{14}\cos y \right| + \left| \frac{1}{10}\sin v \right| \leq 1 + \frac{1}{14} + \frac{1}{10} = \frac{82}{70} \end{aligned}$$

for all  $\tau \in (\frac{1}{3}, \frac{2}{3}]$  and  $y, v \in \mathbb{R}$ . These lead to the third assumption is verified with  $\vartheta_1 = 13/24$  and  $\vartheta_1^* = 82/70$ .

**Theorem 4** (Application to Theorem 1). *The Leray–Schauder nonlinear alternative theorem has been applied in Theorem 1 with the assumptions  $(\mathfrak{H}_1)$ – $(\mathfrak{H}_3)$ . To illustrate our investigation, let us take*

$$h(\tau, y(\tau), \delta y(\tau)) = \frac{1}{2\sqrt{5-\tau}} \left[ \frac{1}{15\pi}\sin(5\pi y) + \frac{3|\delta y(\tau)|}{4(|\delta y(\tau)| + 1)} \right].$$

It is obvious that the function  $h$  is continuous which meets the first assumption and satisfies

$$|\widehat{h}(\tau)| = |h(\tau, y, \delta y)| \leq \frac{1}{2\sqrt{5-\tau}} \left( \frac{1}{3}\|y\| + \frac{3}{4} \right) := q(\tau)v(\|y\|)$$

where

$$q(\tau) = \frac{1}{2\sqrt{5-\tau}} \quad \text{and} \quad v(\|y\|) = \frac{1}{3}\|y\| + \frac{3}{4}.$$

for all  $\tau \in (0, \frac{1}{3}) \cup (\frac{2}{3}, 1]$ . It is obvious that the function  $q(\tau)$  is nondecreasing function which admits the hypothesis  $(\mathfrak{H}_2)$  with  $\|q\| \leq q(1) = 1/4$ . The condition  $(\mathfrak{H}_4)$  and (11)–(13) imply that

$$\mathcal{A} > \max_r \left\{ \frac{\frac{3\|q\|}{4}\Omega + \frac{1}{\rho}(\rho + \tau_1^\rho)}{1 - \frac{\|q\|}{3}\Omega}, \vartheta_r + \vartheta_r^*, \frac{\frac{3\|q\|}{4}\Omega_r + \vartheta_r + \frac{\vartheta_r^*}{\rho}(\rho + T^\rho - s_r^\rho)}{1 - \frac{\|q\|}{3}\Omega_r} \right\}$$

$$\mathcal{A} > \max\{3.018702359, 1.713095238, 2.539578874\}$$

$$\mathcal{A} > 3.018702359.$$

Therefore, the conditions of Theorem (1) are satisfied, and consequently, on  $[0, 1]$  there exists at least one solution to the boundary value problem (15).

**Theorem 5** (Application to Theorem 2). *To demonstrate Theorem 2, which is based on the Banach fixed point theorem, we take*

$$h(\tau, y(\tau), \delta y(\tau)) = \frac{e^{-2\tau}(|y(\tau)| + |\delta y(\tau)|)}{(1 + 9e^\tau)(1 + |y(\tau)| + |\delta y(\tau)|)}$$

*It is clear that the function  $h : [0, 1] \times \mathbb{R} \times \mathbb{R} \rightarrow \mathbb{R}$  is continuous and that it fulfills the hypothesis  $(\mathfrak{H}_2)$*

$$\begin{aligned} |h(\tau, y, \delta y) - h(\tau, u, \delta u)| &\leq \frac{e^{-2\tau}(|y| + |\delta y|) - (|u| + |\delta u|)}{(1 + 9e^\tau)(1 + |y| + |\delta y|)(1 + |u| + |\delta u|)} \\ &\leq \frac{1}{10} \left( |y - u| + |\delta y - \delta u| \right) \\ &\leq \frac{1}{10} (|y - u| + |\delta y - \delta u|). \end{aligned}$$

with  $\mathcal{L} = 1/10$ . For all  $\tau \in (\frac{1}{3}, \frac{2}{3}]$  and  $y_1, y_2, v_1, v_2 \in \mathbb{R}$ , we get

$$\begin{aligned} |\Phi_1(\tau, y_1, v_1) - \Phi_1(\tau, y_2, v_2)| &\leq \frac{1}{12}|y_1 - y_2| + \frac{1}{8}|v_1 - v_2|, \\ |\Psi_1(\tau, y_1, v_1) - \Psi_1(\tau, y_2, v_2)| &\leq \frac{1}{14}|y_1 - y_2| + \frac{1}{10}|v_1 - v_2|. \end{aligned}$$

Thus, the condition  $(\mathfrak{H}_5)$  of Theorem 2 is satisfied with

$$\begin{aligned} \kappa_{11} &= \frac{1}{12}, & \kappa_{21} &= \frac{1}{8}, & \mathcal{K}_1 &\approx 0.20833333, \\ \kappa_{11}^* &= \frac{1}{14}, & \kappa_{22}^* &= \frac{1}{10}, & \mathcal{K}_1^* &\approx 0.17142857. \end{aligned}$$

In conclusion, we have

$$\begin{aligned} \Delta &= \max_r \{ \mathcal{L}\Omega, \mathcal{K}_r + \mathcal{K}_r^*, \mathcal{L}\Omega_r + \mathcal{K}_r + \frac{\mathcal{K}_r^*}{\rho} (\rho + T^\rho - s_r^\rho) \} \\ &= \max\{0.22001244, 0.37976190, 0.55376046\} = 0.55376046 < 1. \end{aligned}$$

Hence, the problem in Equations (15) has a unique solution on  $[0, 1]$  by Theorem 2.

**Theorem 6** (Application to Theorem 3). *To demonstrate Theorem 3, we take*

$$h(\tau, y(\tau), \delta y(\tau)) = \frac{|y(\tau)|}{2(\tau + 8)(1 + |y(\tau)|)} + \frac{|\delta y(\tau)|}{(\tau + 16)}$$

*It is clear that the function  $h : [0, 1] \times \mathbb{R} \times \mathbb{R} \rightarrow \mathbb{R}$  is continuous and that it fulfills the hypothesis  $(\mathfrak{H}_6)$*

$$\begin{aligned} |h(\tau, y, \delta y) - h(\tau, u, \delta u)| &\leq \frac{(|y| - |u|)}{2(\tau + 8)(1 + |y|)(1 + |u|)} + \frac{(|\delta y| - |\delta u|)}{(\tau + 16)} \\ &\leq \frac{1}{16} \left( |y - u| + |\delta y - \delta u| \right) \\ &\leq \frac{1}{16} (|y - u| + |\delta y - \delta u|). \end{aligned}$$

Clearly the assumptions of Theorem 3 are fulfilled with

$$\mathcal{L} = \frac{1}{16}, \quad \mathcal{K}_1 \approx 0.20833333, \quad \mathcal{K}_1^* \approx 0.17142857.$$

$$\Delta = \max\{0.137507777, 0.37976190, 0.55376046\} = 0.51210450 < 1.$$

In conclusion, we have:

$$\|\tilde{y} - y\| \leq \Lambda \epsilon, \quad \tau \in J,$$

where  $\epsilon$  is any positive real constant, and

$$\Lambda = \max \left\{ \frac{\Omega}{1 - \mathcal{L}\Omega'}, \frac{2}{1 - (\mathcal{K}_r + \mathcal{K}_r^*)'}, \frac{2\rho + T^\rho - s_r^\rho}{\rho \left( 1 - \mathcal{L}\Omega_r - \mathcal{K}_r - \frac{\mathcal{K}_r^*}{\rho} (\rho + T^\rho - s_r^\rho) \right)} \right\},$$

$$\Lambda = \max\{2.55089191, 3.22456811, 0.24394774\},$$

$$\Lambda = 3.22456811 > 0.$$

Consequently,

$$\|\tilde{y} - y\| \leq (3.22456811)\epsilon,$$

Thus, problem (15) is UH stable.

Moreover, by putting  $\mu(\epsilon) = (3.22456811)\epsilon$  with  $\mu(0) = 0$ , problem (15) becomes GUH stable.

## 6. Conclusions

Our work involved the development of the existence theory and Ulam–Hyers stability of non-instantaneous impulsive BVPs involving Generalized Liouville–Caputo derivatives. This work is based on modern functional analysis techniques. Three conclusions have been obtained: the first two deal with the existence and uniqueness of solutions, while the third concerns the stability analysis of solutions for the given problem. The first existence result is based on a nonlinear Leray–Schauder alternative, while the second is based on the Banach fixed point theorem. The third conclusion establishes a criterion for ensuring various types of Ulam–Hyers stability, that is necessary for nonlinear problems in terms of optimization and numerical solutions and plays a key role in numerical solutions where exact solutions are difficult to get.

**Author Contributions:** Formal analysis, A.S. and S.A.; Investigation, A.S. and S.A.; Methodology, S.A.; Resources, A.S.; Software, S.A.; Supervision, A.S.; Writing—original draft, S.A. All authors have read and agreed to the published version of the manuscript.

**Funding:** This project was funded by the Deanship of Scientific Research (DSR), King Abdulaziz University, Jeddah, under grant No. (D-310-130-1443). The authors, therefore, gratefully acknowledge DSR technical and financial support.

**Institutional Review Board Statement:** Not applicable.

**Informed Consent Statement:** Not applicable.

**Data Availability Statement:** Not applicable.

**Acknowledgments:** Our deep appreciation goes out to anonymous referees for their helpful suggestions and valuable advice.

**Conflicts of Interest:** The authors declare that they do not have any competing interests.

## References

1. Podlubny, I. *Fractional Differential Equations*; Academic Press: San Diego, CA, USA, 1999.
2. Kilbas, A.; Srivastava, H.; Trujillo, J. *Theory and Applications of Fractional Differential Equations*; Elsevier: Amsterdam, The Netherlands, 2006.
3. Lakshmikantham, V.; Vatsala, A. Basic theory of fractional differential equations. *Nonlinear Anal. TMA* **2008**, *69*, 2677–2682. [CrossRef]
4. Fallahgoul, H.; Focardi, S.; Fabozzi, F. *Fractional Calculus and Fractional Processes with Applications to Financial Economics: Theory and Application*; Elsevier: London, UK; Academic Press: London, UK, 2017.
5. Salem, A.; Mshary, N. On the Existence and Uniqueness of Solution to Fractional-Order Langevin Equation. *Adv. Math. Phys.* **2020**, *2020*, 8890575. [CrossRef]
6. Salem, A.; Al-Dosari, A. Positive Solvability for Conjugate Fractional Differential Inclusion of  $(k, n - k)$  Type without Continuity and Compactness. *Axioms* **2021**, *10*, 170. [CrossRef]
7. Salem, A.; Alnegga, M. Measure of Noncompactness for Hybrid Langevin Fractional Differential Equations. *Axioms* **2020**, *9*, 59. [CrossRef]
8. Salem, A.; Alghamdi, B. Multi-Strip and Multi-Point Boundary Conditions for Fractional Langevin Equation. *Fractal Fract.* **2020**, *4*, 18. [CrossRef]
9. Ganesh, A.; Deepa, S.; Baleanu, D.; Santra, S.S.; Moaaz, O.; Govindan, V.; Ali, R. Hyers-Ulam-Mittag-Leffler stability of fractional differential equations with two caputo derivative using fractional fourier transform. *AIMS Math.* **2022**, *7*, 1791–1810. [CrossRef]
10. He, B.-B.; Zhou, H.-C. Caputo-Hadamard fractional Halanay inequality. *Appl. Math. Lett.* **2022**, *125*, 107723. [CrossRef]
11. Dehestani, H.; Ordokhani, Y. An efficient approach based on Legendre–Gauss–Lobatto quadrature and discrete shifted Hahn polynomials for solving Caputo–Fabrizio fractional Volterra partial integro-differential equations. *J. Comput. Appl. Math.* **2022**, *403*, 113851. [CrossRef]
12. Salem, A.; Mshary, N.; El-Shahed, M.; Alzahrán, F. Compact and Noncompact Solutions to Generalized Sturm–Liouville and Langevin Equation with Caputo-Hadamard Fractional Derivative. *Math. Probl. Eng.* **2021**, *2021*, 9995969. [CrossRef]
13. Salem, A.; Almaghami, L. Existence Solution for Coupled System of Langevin Fractional Differential Equations of Caputo Type with Riemann–Stieltjes Integral Boundary Conditions. *Symmetry* **2021**, *13*, 2123. [CrossRef]
14. Adjabi, Y.; Samei, M.E.; Matar, M.M.; Alzabut, J. Langevin differential equation in frame of ordinary and Hadamard fractional derivatives under three point boundary conditions. *AIMS Math.* **2021**, *6*, 2796–2843. [CrossRef]
15. Boutiara, A.; Abdo, M.S.; Alqudah, M.A.; Abdeljawad, T. On a class of Langevin equations in the frame of Caputo function-dependent-kernel fractional derivatives with antiperiodic boundary conditions. *AIMS Math.* **2021**, *6*, 5518–5534. [CrossRef]
16. Hilal, K.; Ibelazel, L.; Guida, K.; Melliani, S. Fractional Langevin Equations with Nonseparated Integral Boundary Conditions. *Adv. Math. Phys.* **2020**, *2020*, 3173764. [CrossRef]
17. Salem, A.; Al-Dosari, A. Existence results of solution for fractional Sturm–Liouville inclusion involving composition with multi-maps. *J. Taibah Univ. Sci.* **2020**, *14*, 721–733. [CrossRef]
18. Salem, A.; Alghamdi, B. Multi-Point and Anti-Periodic Conditions for Generalized Langevin Equation with Two Fractional Orders. *Fractal Fract.* **2019**, *3*, 51. [CrossRef]
19. Salem, A. Existence results of solutions for ant-periodic fractional Langevin equation. *J. Appl. Anal. Comput.* **2020**, *10*, 2557–2574. [CrossRef]
20. Salem, A.; Alshehri, H.M.; Almaghami, L. Measure of noncompactness for an infinite system of fractional Langevin equation in a sequence space. *Adv. Differ. Equ.* **2021**, *2021*, 132. [CrossRef]
21. Benchohra, M.; Henderson, J.; Ntouyas, S.K. *Impulsive Differential Equations and Inclusions*; Hindawi: New York, NY, USA, 2006.
22. Agarwal, R.; Hristova, S.; O'Regan, D. Iterative techniques for the initial value problem for Caputo fractional differential equations with non-instantaneous impulses. *Appl. Math. Comput.* **2018**, *334*, 407–421. [CrossRef]
23. Luo, D.; Luo, Z. Existence of solutions for fractional differential inclusions with initial value condition and non-instantaneous impulses. *Filomat* **2019**, *33*, 5499–5510. [CrossRef]
24. Wang, J.; Feckan, M.; Zhou, Y. A survey on impulsive fractional differential equations. *Fract. Calc. Appl. Anal.* **2016**, *19*, 806–831. [CrossRef]
25. Liu, S.; Wang, J.; Zhou, Y. Optimal control of non-instantaneous impulsive differential equations. *J. Frankl. Inst.* **2017**, *354*, 7668–7698. [CrossRef]
26. Hernandez, E.; O'Regan, D. On a new class of abstract impulsive differential equation. *Proc. Am. Math. Soc.* **2013**, *141*, 1641–1649. [CrossRef]
27. Wang, J.; Zhou, Y.; Lin, Z. On a new class of impulsive fractional differential equations. *Appl. Math. Comput.* **2014**, *242*, 649–657. [CrossRef]
28. Ho, V.; Ngo, V.H. Non-instantaneous impulses interval-valued fractional differential equations with Caputo-Katugampola fractional derivative concept. *Fuzzy Sets Syst.* **2021**, *404*, 111–141. [CrossRef]
29. Abbas, M.I. Non-instantaneous impulsive fractional integro-differential equations with proportional fractional derivatives with respect to another function. *Math. Methods Appl. Sci.* **2021**, *44*, 10432–10447. [CrossRef]
30. Katugampola, U.N. New approach to a generalized fractional integral. *Appl. Math. Comput.* **2011**, *218*, 860–865. [CrossRef]

31. Jarad, F.; Abdeljawad, T.; Baleanu, D. On the generalized fractional derivatives and their Caputo modification. *J. Nonlinear Sci. Appl.* **2017**, *10*, 2607–2619. [CrossRef]
32. Rus, I.A. Ulam stabilities of ordinary differential equations in a Banach space. *Carpath. J. Math.* **2010**, *26*, 103–107.
33. Kiryakova, V. *Generalized Fractional Calculus and Applications*; Longman Scientific & Technical; Wiley: New York, NY, USA, 1994.
34. Granas, A.; Dugundji, J. *Fixed Point Theory*; Springer: New York, NY, USA, 2003.

Article

# Adopting Feynman–Kac Formula in Stochastic Differential Equations with (Sub-)Fractional Brownian Motion

Bodo Herzog <sup>1,2,3</sup>

<sup>1</sup> Economics Department, ESB Business School, Reutlingen University, 72762 Reutlingen, Germany; Bodo.Herzog@Reutlingen-University.de

<sup>2</sup> Reutlingen Research Institute (RRI), 72762 Reutlingen, Germany

<sup>3</sup> Institute of Finance and Economics (IFE), Reutlingen University, 72762 Reutlingen, Germany

**Abstract:** The aim of this work is to establish and generalize a relationship between fractional partial differential equations (fPDEs) and stochastic differential equations (SDEs) to a wider class of stochastic processes, including fractional Brownian motions  $\{B_t^H, t \geq 0\}$  and sub-fractional Brownian motions  $\{\xi_t^H, t \geq 0\}$  with Hurst parameter  $H \in (\frac{1}{2}, 1)$ . We start by establishing the connection between a fPDE and SDE via the Feynman–Kac Theorem, which provides a stochastic representation of a general Cauchy problem. In hindsight, we extend this connection by assuming SDEs with fractional- and sub-fractional Brownian motions and prove the generalized Feynman–Kac formulas under a (sub-)fractional Brownian motion. An application of the theorem demonstrates, as a by-product, the solution of a fractional integral, which has relevance in probability theory.

**Keywords:** Cauchy problem; fractional-PDE; SDE; fractional Brownian motion; sub-fractional processes; Feynman–Kac formula; fractional calculus

**Citation:** Herzog, B. Adopting Feynman–Kac Formula in Stochastic Differential Equations with (Sub-)Fractional Brownian Motion. *Mathematics* **2022**, *10*, 340. <https://doi.org/10.3390/math10030340>

Academic Editors: António M. Lopes, Alireza Alfi, Liping Chen and Sergio A. David

Received: 28 December 2021

Accepted: 21 January 2022

Published: 23 January 2022

**Publisher’s Note:** MDPI stays neutral with regard to jurisdictional claims in published maps and institutional affiliations.



**Copyright:** © 2022 by the author. Licensee MDPI, Basel, Switzerland. This article is an open access article distributed under the terms and conditions of the Creative Commons Attribution (CC BY) license (<https://creativecommons.org/licenses/by/4.0/>).

## 1. Introduction

Consider the Cauchy problem [1] of the following parabolic partial differential equation (PDE) on  $\mathbb{R}^d$

$$\begin{aligned} \frac{\partial}{\partial t} u(x, t) &= \kappa \frac{\partial^2}{\partial x^2} u(x, t) + \eta B^H(t), & t \geq 0, x \in \mathbb{R}^d, \\ u(x, 0) &= u_0(x), \end{aligned} \quad (1)$$

where  $u(x, t) \in C^{2,1}$ ,  $u_0(x)$  is a bounded measurable function and  $B^H(t)$  is a fractional Brownian motion (cf. Section 2). Without loss of generality, we assume that the parameter  $\kappa$  is constant. This second-order PDE has a stochastic representation for  $\eta = 0$ , according to the Feynman–Kac formula [2,3]. Indeed, we obtain

$$u(x_t, t) = \mathbb{E}_{x,t}[u_T(x)], \quad (2)$$

if  $x_t$  satisfies Equation (3) and the function  $\sigma(x_t, t)$  is sufficiently integrable

$$dx_t = \mu(x_t, t)dt + \sigma(x_t, t)dB_t^H, \quad (3)$$

where  $B_t^H$  is a Brownian motion (BM) if the Hurst parameter is of  $H = \frac{1}{2}$  [4–6]. Additionally, the problem of (1) has an intimate relationship to the fractional partial differential equation (fPDE) [7]:

$$\frac{\partial^{1/2}}{\partial t^{1/2}} u(x, t) = -\frac{\partial}{\partial x} u(x, t). \quad (4)$$

Note that this equation contains a fractional derivative in general or a semi-derivative in respect of time in special [8–13].

There is a large amount of the literature devoted to each issue of the Cauchy problem [6,14]. This research closes a gap by considering the linking relationships of (sub-)fractional Brownian motions as well as fPDEs. The Feynman–Kac formula (2) provides a unique weak solution to Equation (1). Different versions of the Feynman–Kac formula have been discovered for a variety of problems [15,16]. Some generalizations of the Feynman–Kac formula are discovered by Querdiane and Silva [17] and Hu et al. [18,19]. A Feynman–Kac formula also exists for Lévy processes by Nualart and Schoutens [20].

Advancements in stochastic differential equations and fractional partial differential equations to analyse complex systems are related to our research [21–24]. Furthermore, recent developments in fractional calculus contributed to a better understanding and further studies of the relationships between fractional PDEs and stochastic calculus [25–31]. However, we are concerned about the linkage of the Cauchy problem and the representation by a fPDE, as well as the Feynman–Kac formula. For the Cauchy problem, we generalize the stochastic representation of Feynman–Kac by utilizing fractional Brownian motion (fBM) with Hurst parameter  $H > 1/2$ .

In addition, the more recent literature looks at the idea of sub-fractional Brownian motion (sub-fBM). A sub-fBM is an intermediate between a Brownian motion and fractional Brownian motion. The existence and properties, such as long-range dependence, self-similarity and non-stationarity were introduced by Bojdecki et al. [32] and Tudor et al. [33,34]. Since the sub-fractional Brownian motion is not a martingale, methods of stochastic analysis are more sophisticated. However, several authors developed stochastic calculus and integration concepts for an fBM [25] and sub-fBM [35–37]. Recently, for a sub-fractional Brownian motion with Hurst parameters  $H > \frac{1}{2}$ , a maximal inequality was established according to the Burkholder–Davis–Gundy inequality for fractional Brownian motion [38]. It turns out that fBM and sub-fBM are adequate stochastic processes in scientific applications [13,39].

In this paper, our purpose is to construct and prove a general link of the Cauchy problem with the Feynman–Kac equation via Itô’s formula for fBM and sub-fBM. Consequently, this paper links the solution of  $u(x, t)$  defined by Equation (1) with the stochastic Feynman–Kac representation to a fractional Brownian motion  $\{B_t^H\}$  and sub-fBM  $\{\zeta_t^H\}$ . We prove the result and show the properties of (sub-)fractional processes in stochastic analysis. Note that, throughout this paper, we frequently assume  $\frac{1}{2} < H < 1$ .

The paper is organized as follows. Section 2 contains preliminaries on fractional calculus, particularly fractional Brownian motion. Thereafter, we examine sub-fractional stochastic processes and integration rules in Section 3. Here, we list the definitions and assumptions for the remainder of the article. In Section 4, we link the Cauchy problem to the Feynman–Kac formula with stochastic differential equations driven by fractional and sub-fractional Brownian motions. We state our theorems and prove our statements. In Section 5, we examine the Cauchy problem and the relationship to fractional partial differential equations (fPDE). Furthermore, we find a new fractional derivative and integral with relevance in probability theory. The conclusion is in Section 6.

## 2. Preliminaries

In the following section, we define preliminary concepts on fractional stochastic processes and fractional calculus.

### 2.1. Fractional Calculus

Since we deal with the Hurst parameter  $H$ , we need to know fractional calculus. Let  $a, b \in \mathbb{R}, a < b$ . Let  $f \in L^1(a, b)$  and  $\alpha > 0$ . The left- and right-sided fractional integral of  $f$  of order  $\alpha$  are defined for  $x \in (a, b)$ , respectively, as

$${}_a D_x^{-\alpha} f(x) = {}_a I_x^\alpha f(x) = \frac{1}{\Gamma(\alpha)} \int_a^x (x - u)^{\alpha-1} f(u) du \quad -\infty \leq a \leq x,$$

and

$${}_x D_b^{-\alpha} f(x) = {}_x I_b^\alpha f(x) = \frac{1}{\Gamma(\alpha)} \int_x^b (u-x)^{\alpha-1} f(u) du \quad -\infty \leq x \leq b.$$

This is the fractional integral of Riemann–Liouville type. Similarly, the fractional left- and right-sided derivative, for  $f \in I_a^\alpha(L^p)$  and  $0 < \alpha < 1$ , are defined by

$${}_a I_x^{-\alpha} f(x) = {}_a D_x^\alpha f(x) = \frac{1}{\Gamma(1-\alpha)} \left(\frac{d}{dx}\right) \int_a^x (x-u)^{-\alpha} f(u) du \tag{5}$$

and

$${}_x I_b^{-\alpha} f(x) = {}_x D_b^\alpha f(x) = \frac{-1}{\Gamma(1-\alpha)} \left(\frac{d}{dx}\right) \int_x^b (u-x)^{-\alpha} f(u) du, \tag{6}$$

for all  $x \in (a, b)$  and  $I_a^\alpha(L^p)$  is the image of  $L^p(a, b)$ . It is easy to see that if  $f \in I_a^1(L^1)$ ,

$${}_a D_{xa}^\alpha D_x^{1-\alpha} f(x) = Df(x), \quad {}_b D_{xb}^\alpha D_x^{1-\alpha} f(x) = Df(x). \tag{7}$$

Note  $D^\alpha f(x)$  exists for all  $f \in C^\beta([a, b])$  if  $\alpha < \beta$ .

### 2.2. Fractional Stochastic Process

Mandelbrot and van Ness defined a fractional Brownian Motion (fBM),  $B_t^H$ , as a Brownian motion,  $B(t)$ , together with a Hurst parameter (or Hurst index)  $H \in (0, 1)$  in 1968 [8]. The new feature of fBM’s is that the increments are interdependent. The latter property is defined as self-similarity. A self-similar process has invariance with respect to changes in timescale (scaling-invariance). Almost all other stochastic processes, such as the standard Brownian Motion or Lévy processes, likely have independent increments. They create the famous class of Markov processes. Empirically, there is ubiquitous evidence in science that fractional stochastic processes, for instance, spectral densities with a sharp peak, are related to the phenomena of long-range interdependence over time. Indeed, the observable presence of interdependence in many real-world applications calls for fractional stochastic processes.

**Definition 1.** Let  $H$  be  $0 < H < 1$  and  $B_0$  an arbitrary real number. We call  $B^H(t, \omega)$  a fractional Brownian Motion (fBM) with Hurst parameter  $H$  and starting value  $B_0$  at time 0, such as

- (1)  $B^H(0, \omega) = B_0$ , and;
- (2)  $B^H(t, \omega) - B^H(0, \omega) = \frac{1}{\Gamma(H+\frac{1}{2})} \left[ \int_{-\infty}^0 [(t-s)^{H-\frac{1}{2}} - (-s)^{H-\frac{1}{2}}] dB(s, \omega) + \int_0^t (t-s)^{H-\frac{1}{2}} dB(s, \omega) \right]$  [Wyle fractional integral];
- (3) [Or equivalently by the Riemann–Liouville fractional integral:  $B^H(t, \omega) - B^H(0, \omega) = \frac{1}{\Gamma(H+\frac{1}{2})} \int_0^t (t-s)^{H-\frac{1}{2}} dB(s, \omega)$ ].

We immediately obtain the corollary.

**Corollary 1.** For  $H = \frac{1}{2}$  and  $B_0 = 0$ , we obtain a Brownian Motion  $B(t, \omega) = B^{\frac{1}{2}}(t, \omega)$ .

**Proof.** If  $H = \frac{1}{2}$ , we obtain  $B^{\frac{1}{2}}(t, \omega) - B^{\frac{1}{2}}(0, \omega) = \frac{1}{\Gamma(1)} \int_0^t dB(s, \omega) = B(t, \omega)$ . □

For values of  $H$ , such as  $0 < H < \frac{1}{2}$  or  $\frac{1}{2} < H < 1$  the fBM  $B^H(t, \omega)$  has different properties. If  $0 < H < \frac{1}{2}$ , we say that it has the property of short memory. Indeed, Mandelbrot and van Ness [8] shows that this range is associated with negative correlation. If  $\frac{1}{2} < H < 1$ , then the fBM has the property of long-memory or long-range dependence with time-persistence (Mandelbrot and van Ness [8]). Alternatively, we define a fractional Brownian motion by

**Definition 2.** A fractional Brownian Motion (fBM) is a centered Gaussian process  $B^H(t)$  for  $t \geq 0$  with the covariance function

$$R^{fBM}(t, s) = \mathbb{E}[B^H(t)B^H(s)] = \frac{1}{2} [|t|^{2H} + |s|^{2H} - |t - s|^{2H}], \tag{8}$$

where  $H \in (0, 1)$  denotes the Hurst parameter.

**Remark 1.** The covariance is trivially derived by starting with a standard Brownian motion and extending it with the Hurst index  $H$ , such as

$$\begin{aligned} \text{Var}[B(t) - B(s)] &= \mathbb{E}[(B(t) - B(s))^2] = |t - s| \\ \Leftrightarrow \text{Var}[B^H(t) - B^H(s)] &= \mathbb{E}[(B^H(t) - B^H(s))^2] = |t - s|^{2H}, \end{aligned}$$

where, for  $H = \frac{1}{2}$ , we obtain the Brownian motion. The covariance is derived by the following steps

$$\begin{aligned} \text{Cov}[B^H(t)B^H(s)] &= \mathbb{E}[(B^H(t) - \mathbb{E}[B^H(t)])(B^H(s) - \mathbb{E}[B^H(s)])] = \mathbb{E}[B^H(t)B^H(s)] \\ &= \frac{1}{2} \left[ \mathbb{E}[B^H(t)^2] + \mathbb{E}[B^H(s)^2] - \mathbb{E}[(B^H(t) - B^H(s))^2] \right] \\ &= \frac{1}{2} [|t|^{2H} + |s|^{2H} - |t - s|^{2H}]. \end{aligned}$$

**Corollary 2.** The expectation of non-overlapping increments of an fBM is  $\mathbb{E}[B^H(t) - B^H(s)] \neq 0$  and the variance is of  $\mathbb{E}[(B^H(t) - B^H(s))^2] = |t - s|^{2H}$  for all  $t, s \in \mathbb{R}$

**Proof.** Let  $t > s > 0$ . The first part is

$$\begin{aligned} \mathbb{E}[(B^H(t) - B^H(s))(B^H(s) - B^H(0))] &= \mathbb{E}[B^H(t)B^H(s)] - \mathbb{E}[B^H(t)B^H(0)] - \\ &\quad - \mathbb{E}[(B^H(s))^2] + \mathbb{E}[B^H(s)B^H(0)] \\ &= \frac{1}{2} [t^{2H} + s^{2H} - (t - s)^{2H}] - s^{2H} \\ &= \frac{1}{2} [t^{2H} - s^{2H} - (t - s)^{2H}] \neq 0. \end{aligned}$$

Thus, we can see that the expected increments are non-zero. Indeed, the increments are interdependent, contrary to Markov processes. The second part of the variance is

$$\begin{aligned} \mathbb{E}[(B^H(t) - B^H(s))^2] &= \mathbb{E}[(B^H(t) - B^H(s))(B^H(t) - B^H(s))] \\ &= \mathbb{E}[(B^H(t))^2] + \mathbb{E}[(B^H(s))^2] - 2\mathbb{E}[B^H(t)B^H(s)] \\ &= t^{2H} + s^{2H} - 2 \left[ \frac{1}{2} [|t|^{2H} + |s|^{2H} - |t - s|^{2H}] \right] \\ &= |t - s|^{2H} \quad \forall t, s \in \mathbb{R} \end{aligned}$$

□

**Proposition 1.** A fractional Brownian Motion (fBM) has the following properties:

- (1) The fBM has stationary increments:  $B_t^H - B_s^H \stackrel{dis.}{=} B_t^H - B_s^H$ ;
- (2) The fBM is  $H$ -self-similar, such as  $B^H(at) = a^H B^H(t)$ ;
- (3) The fBM has dependence of increments for  $H \neq \frac{1}{2}$ .

**Proof.** Part (1): For  $t_1 < t_2 < t_3 < t_4$ , the equality of the covariance function implies that  $Y := B^H(t_2) - B^H(t_1)$  has the same distribution as  $X := B^H(t_4) - B^H(t_3)$ . From above, we know

$$\begin{aligned} \mathbb{E}[(B^H(t_2) - B^H(t_1))^2] &= (t_2 - t_1)^{2H} = (\Delta t)^{2H} \\ \mathbb{E}[(B^H(t_4) - B^H(t_3))^2] &= (t_4 - t_3)^{2H} = (\Delta t)^{2H}, \end{aligned}$$

where  $t_1 < t_2$  and  $t_3 < t_4$  with  $\Delta t = t_2 - t_1 = t_4 - t_3$ . Hence, the incremental behavior at any point in the future is the same. Thus, we say that it has stationary increments.

Part (2): We show that  $B^H(at) = a^H B^H(t)$ . We utilize the definition,

$$\begin{aligned} \mathbb{E}[(B^H(at))^2] &= \frac{1}{2} [(at)^{2H} + (at)^{2H} - (at - at)^{2H}] = (at)^{2H} = a^{2H} t^{2H} \\ &= a^{2H} \mathbb{E}[(B^H(t))^2], \end{aligned}$$

hence, we obtain  $(B^H(at))^2 = a^{2H} (B^H(t))^2$  and this equal to  $B^H(at) = a^H B^H(t)$ . The proof of part (3) is already in Corollary 2.  $\square$

### 2.3. Itô's Formula for Fractional Brownian Motion

A fractional Brownian motion is continuous but almost certainly not differentiable [8]. Hence, it is inconvenient that an fBM does not have a derivative or integral. Furthermore, the fBM is neither a martingale nor a semi-martingale. Therefore, Itô calculus is not applicable to fractional Brownian Motions if  $H \neq \frac{1}{2}$ .

However, stochastic calculus was developed with respect to fractional Brownian motion by [40] and the stochastic integral was introduced by [25]. The theory is a fractional extension of Itô-calculus, but limited to a Hurst index  $H \in (1/2, 1)$ . If  $H > 1/2$  the fBM exhibits long-range dependence, which is a fundamental property in physics or finance.

By utilizing Wick calculus that has zero mean and explicit expressions for the second moment, we define the stochastic fractional integral, satisfying the property  $\mathbb{E}[\int_0^t f(s) dB^H(s)] = 0$ .

Suppose a filtered probability space  $(\Omega, \mathcal{F}, \mathbb{P}^H)$ , where the probability measure depends on  $H$ . Note that  $H$  is fixed by  $H \in (1/2, 1)$ . Let us define a kernel function  $\phi(s, t) : \mathbb{R}_+ \times \mathbb{R}_+ \rightarrow \mathbb{R}_+$  by

$$\phi^{fBM}(s, t) := \phi(s, t) = H(2H - 1)|s - t|^{2H-2}. \tag{9}$$

Further, the functions  $f$  and  $g$  belong to the Hilbert space  $L^2_\phi$  if

$$|f|_\phi^2 = \int_0^\infty \int_0^\infty f(s)f(t)\phi(s, t)dsdt < \infty, \tag{10}$$

with the inner product defined by

$$\langle f, g \rangle_\phi := \mathbb{E} \left[ \int_0^\infty f(s)dB^H(s) \int_0^\infty g(t)dB^H(t) \right] = \int_0^\infty \int_0^\infty f(s)g(t)\phi(s, t)dsdt \tag{11}$$

This machinery leads to an analogue Itô formula for a fractional Brownian process. Already, Alòs et al. [41] proved this result under certain conditions for Itô's formula.

**Theorem 1.** (Alòs et al., 2001). Let  $f$  be a function of class  $C^2(\mathbb{R})$ , satisfying the growth condition

$$\max[|f(x)|, |f'(x)|, |f''(x)|] \leq ce^{\lambda|x|^2},$$

where  $c$  and  $\lambda$  are positive constants and  $\lambda < \frac{1}{4}T^{-2H}$ . Suppose that  $B^H = \{B_t^H, t \in [0, T]\}$  is a zero mean continuous Gaussian process whose covariance function  $R^{fBM}(t, s)$  is of the form

in Equation (8). Then, the process  $F'(B_t^H)$  belongs to a Hilbert space and, for each  $t \in [0, T]$ , the following Itô's formula holds:

$$f(B_T^H) = f(0) + \int_0^T f'(B_s^H) \delta B_s^H + \frac{1}{H} \int_0^T f''(B_s^H) s^{2H-1} ds. \tag{12}$$

However, we utilize a result by Duncan et al. [25], which is more convenient in our case. Here, is the Itô-Duncan theorem for a fractional Brownian motion:

**Theorem 2.** (Duncan et al., 2000, Thm 4.1, p. 596). *If  $f : \mathbb{R} \rightarrow \mathbb{R}$  is a twice continuously differentiable function with bounded derivatives to order two, i.e.,  $f \in C^2$ , then*

$$f(B_T^H) - f(B_0^H) = \int_0^T f'(B_s^H) dB_s^H + H \int_0^T s^{2H-1} f''(B_s^H) ds \quad a.s.$$

**Remark 2.** *If  $H = \frac{1}{2}$ , we obtain, from Theorem 2, the usual Itô formula for a Brownian motion*

$$\begin{aligned} f(B^{\frac{1}{2}}(T)) &= f(B_T) = \int_0^T f'(B^{\frac{1}{2}}(s)) dB^{\frac{1}{2}}(s) + \frac{1}{2} \int_0^T s^0 f''(B^{\frac{1}{2}}(s)) ds \\ &= \int_0^T f'(B_s) dB_s + \frac{1}{2} \int_0^T f''(B_s) ds \end{aligned}$$

or in differential form

$$df(B_T) = f'(B_s) dB_s + \frac{1}{2} f''(B_s) ds. \tag{13}$$

Similarly, for a function with two parameters  $f(t, B_t^H)$ , a generalized rule exists according to Duncan et al. [25].

**Theorem 3.** (Duncan et al., 2000, Thm 4.3, p. 596). *Let  $\eta_t = \int_0^t F_u dB_u^H$  for  $t \in [0, T]$  and  $(F_u, 0 \leq u \leq T)$  is a stochastic process in  $\mathcal{L}(0, T)$ . Let  $f : \mathbb{R}_+ \times \mathbb{R} \rightarrow \mathbb{R}$  be a function having the first continuous derivative in its first variable and the second continuous derivative in its second variable. Assume that these derivatives are bounded. Moreover, it is assumed that  $\mathbb{E} \int_0^T |F_s D_s^\phi \eta_s| ds < \infty$  and  $(f'(s, \eta_s) F_s, s \in [0, T])$  is in  $\mathcal{L}(0, T)$ . Then, for  $0 \leq t \leq T$ ,*

$$\begin{aligned} f(t, \eta_t) &= f(0, 0) + \int_0^t \frac{\partial f(s, \eta_s)}{\partial s} ds + \int_0^t \frac{\partial f(s, \eta_s)}{\partial x} F_s dB_s^H \\ &\quad + \int_0^t \frac{\partial^2 f(s, \eta_s)}{\partial x^2} F_s D_s^\phi \eta_s ds \quad a.s. \end{aligned}$$

this is equal to

$$df(t, \eta_t) = \frac{\partial f(t, \eta_t)}{\partial t} dt + \frac{\partial f(t, \eta_t)}{\partial x} F_t dB_t^H + \frac{\partial^2 f(t, \eta_t)}{\partial x^2} F_t D_t^\phi \eta_t dt,$$

where  $D_s^\phi \eta_t = \int_0^t D_s^\phi F_u dB_u^H + \int_0^t F_u \phi(s, u) du$  a.s.

For the proof, we refer to Duncan et al. [25]. If  $F(s) = a(s)$  is a deterministic function; then, the rule simplifies. Let  $\eta_t = \int_0^t a_u dB_u^H$ , where  $a \in L^2_\phi$ ; then, we obtain

$$\begin{aligned} f(t, \eta_t) &= f(0, 0) + \int_0^t \frac{\partial f(s, \eta_s)}{\partial s} ds + \int_0^t \frac{\partial f(s, \eta_s)}{\partial x} a(s) dB_s^H \\ &\quad + \int_0^t \frac{\partial^2 f(s, \eta_s)}{\partial x^2} \int_0^s \phi(s, v) a(v) dv ds \quad a.s. \end{aligned} \tag{14}$$

If  $a_s \equiv 1$ , then we obtain Itô's formula, such as in Theorem 2 and in Equation (13).

### 3. Sub-Fractional Stochastic Process

A sub-fractional Brownian motion (sub-fBM) is an intermediate between a Brownian motion and fractional Brownian motion. It is a more general, self-similar Gaussian process or a generalization of a fBM. The sub-fBM has the property of H-self-similarity and long-range dependence, such as the fBM, yet it does not have stationary increments [32].

It is well-established that a stochastic process is uniquely determined by its covariance function  $\text{Cov}(\zeta_t^H, \zeta_s^H)$ . Thus, we define:

**Definition 3.** A sub-fractional Brownian motion of Hurst parameter  $H$  is a centered mean zero Gaussian process  $\zeta_t^H = \{\zeta_t^H, t \geq 0\}$  with covariance function

$$R^{sfBM}(t, s) := \mathbb{E}[\zeta_t^H \zeta_s^H] = s^{2H} + t^{2H} - \frac{1}{2}[(s + t)^{2H} + |s - t|^{2H}], \tag{15}$$

where  $\zeta_0^H = 0$  and  $\mathbb{E}[\zeta_t^H] = 0$ .

If  $H = \frac{1}{2}$ , it coincides with a Brownian motion on  $\mathbb{R}_+$  with covariance  $\text{Cov}(\zeta_t^H, \zeta_s^H) = s \wedge t := \min[s, t]$ . The process  $\zeta_t^H$  has the following integral representation for  $H > \frac{1}{2}$  (see [41]):

$$\zeta_t^H = \int_0^t K^H(t, s) dW_s, \tag{16}$$

$$K^H(t, s) = c_H \left( H - \frac{1}{2} \right) s^{1/2-H} \int_s^t (u - s)^{H-3/2} u^{H-1/2} du. \tag{17}$$

Hence, the sub-fractional Brownian motion has a kernel of

$$\phi^{sfBM}(s, t) = \frac{\partial^2 \text{Cov}(\zeta_t^H, \zeta_s^H)}{\partial s \partial t} = H(2H - 1) \left[ |s - t|^{2H-2} - (s + t)^{2H-2} \right]. \tag{18}$$

Note that the kernel has similarities to the fBM, as in Equation (9). Next, we discuss the main properties of a sub-fBM:

**Lemma 1.** Let  $\zeta_t^H$  be a sub-fBM for all  $t$ . It has the following properties:

- (1)  $\mathbb{E}[(\zeta_t^H)^2] = (2 - 2^{2H-1})t^{2H}$ .
- (2)  $\mathbb{E}[(\zeta_t^H - \zeta_s^H)^2] = -2^{2H-1}(t^{2H} + s^{2H}) + (t + s)^{2H} + (t - s)^{2H}$ .
- (3) If  $H \neq \frac{1}{2}$ , then  $\zeta_t^H - \zeta_s^H \stackrel{dis.}{\neq} \zeta_u^H - \zeta_s^H$ , i.e., the increments are non-stationary.

**Proof.** Part 1. Let  $t = s$  in the covariance function  $\text{Cov}(\zeta_t^H, \zeta_s^H)$ . We obtain  $\text{Cov}(\zeta_t^H, \zeta_t^H) = \mathbb{E}[\zeta_t^{2H}] - (\mathbb{E}[\zeta_t^H])^2 = \text{Var}(\zeta_t^H)$  and further we have  $\text{Var}(\zeta_t^H) = \mathbb{E}[(\zeta_t^H)^2]$  because  $\zeta_t^H$  is Gaussian with mean zero. Thus, using the covariance function in Definition 3, we obtain

$$\mathbb{E}[(\zeta_t^H)^2] = 2t^{2H} - \frac{1}{2}(2t)^{2H} = 2t^{2H} - \frac{1}{2}(2t)^{2H} = (2 - 2^{2H-1})t^{2H}.$$

Part 2. Given property 1, one immediately obtains

$$\begin{aligned} \mathbb{E}[(\zeta_t^H - \zeta_s^H)^2] &= (2 - 2^{2H-1})t^{2H} + (2 - 2^{2H-1})s^{2H} \\ &= -2^{2H-1}(t^{2H} + s^{2H}) + (t + s)^{2H} + (t - s)^{2H}. \end{aligned}$$

Part 3. Let  $s = 0$  and  $t = h > 0$ , then  $\mathbb{E}[(\zeta_h^H - \zeta_0^H)^2] = \mathbb{E}[(\zeta_h^H)^2] = (2 - 2^{2H-1})h^{2H}$  and we obtain

$$\begin{aligned} \mathbb{E}[(\zeta_{t+h}^H - \zeta_{s+h}^H)^2] &= \mathbb{E}[(\zeta_{2h}^H - \zeta_h^H)^2] \\ &= \mathbb{E}[\zeta_{2h}^{2H}] - 2\mathbb{E}[\zeta_{2h}^H]\mathbb{E}[\zeta_h^H] + \mathbb{E}[\zeta_h^{2H}] \\ &= (2 - 2^{2H-1})(2h)^{2H} + (2 - 2^{2H-1})h^{2H} = \\ &= [2 - 2^{2H-1}](2^{2H} + 1)h^{2H}. \end{aligned}$$

The difference in both increments is

$$\Delta(H) = [2 - 2^{2H-1}] - [2 - 2^{2H-1}](2^{2H} + 1) = -2^{2H}[2 - 2^{2H-1}],$$

where  $\Delta(H) := \mathbb{E}[(\zeta_h^H)^2] - \mathbb{E}[(\zeta_{t+h}^H - \zeta_{s+h}^H)^2]$ . For  $\Delta(0) = -\frac{3}{2}$  and  $\Delta(\frac{1}{2}) = -2$  and  $\Delta(1) = 0$ . This implies that  $\mathbb{E}[(\zeta_{2h}^H - \zeta_h^H)^2] > \mathbb{E}[(\zeta_t^H)^2]$  for all  $H \in (0, 1)$ . Thus, the increments are non-stationary, such as  $\zeta_t^H - \zeta_s^H \stackrel{\text{dis.}}{\neq} \zeta_u^H - \zeta_s^H$ .  $\square$

Finally, we prove two differences of fBM and sub-fBM.

**Proposition 2.** Let  $B_t^H$  be a fractional Brownian motion and  $\zeta_t^H$  be a sub-fractional Brownian motion. For  $H \in (\frac{1}{2}, 1)$  the following holds:

- (1)  $\mathbb{E}[(\zeta_t^H)^2] < \mathbb{E}[(B_t^H)^2]$ ;
- (2)  $R_{\zeta_t^H}(s, t) \leq R_{B_t^H}(s, t)$ .

**Proof.** Part 1. For an fBM, we have  $\text{Var}[B_t^H] = |t|^{2H}$ , and for the sub-fBM, we have  $\text{Var}[\zeta_t^H] = (2 - 2^{2H-1})|t|^{2H}$ . Hence, we obtain  $0 < (2H - 1) \ln 2$  for  $H > \frac{1}{2}$ . For part 2, we show, under  $s, t > 0$ , that

$$\begin{aligned} s^{2H} + t^{2H} - \frac{1}{2}[(s+t)^{2H} + |t-s|^{2H}] &\leq \frac{1}{2}[|t|^{2H} + |s|^{2H} - |t-s|^{2H}] \\ &= s^{2H} + t^{2H} \leq (s+t)^{2H}, \end{aligned}$$

where, only for  $s = t = 0$  or  $s = 0, t \neq 0$ , we obtain equality.  $\square$

*Itô's Formula for Sub-Fractional Brownian Motion*

For a Hurst parameter  $H > \frac{1}{2}$ , the stochastic integral of a sub-fBM  $\int_0^T f(t)d\zeta_t^H$  exists. The following theorem holds and is proven by [42]:

**Theorem 4.** Let  $\zeta_t^H$  be a sub-fBM defined in Definition 3 with  $H > \frac{1}{2}$  and a function  $f \in L([0, T]^2, \phi^{sfBM}d\lambda_2)$ , where  $\lambda_2$  is a Lebesgue measure on  $[0, T]^2$ , where  $\phi^{sfBM}(s, t)$  and  $(s, t) \in [0, T]^2$ . Then, there exists a constant  $C_H > 0$  such that

$$\mathbb{E} \left[ \int_0^T f(t)d\zeta_t^H \right]^2 \leq C_H \|f\|_{L^{1/H}([0,T],\lambda_1)}^2. \tag{19}$$

According to Yan et al. ([36], Theorem 3.2 on p. 139) Itô's formula under a sub-fBM can be computed as follows:

**Theorem 5.** (Yan et al., 2011) Let  $f \in C^2(\mathbb{R})$  and  $H \in (\frac{1}{2}, 1)$ . Then, we have

$$f(\zeta_t^H) = f(0) + \int_0^T f'(\zeta_s^H)d\zeta_s^H + H(2 - 2^{2H-1}) \int_0^T f''(\zeta_s^H)s^{2H-1}ds. \tag{20}$$

Details of the proof are given in ([36], pp. 139–140). The authors even extend Itô's formula to  $d$ -dimensional sub-fBM and convex functions  $f : \zeta_t^H \rightarrow \mathbb{R}$ .

#### 4. Linking Cauchy via Feynman–Kac to SDEs with fBM and Sub-fBM

Next, we derive the link between the Cauchy problem (1) and the stochastic representation according to Feynman–Kac by Equation (2). Consider a stochastic process  $x_s$  on the time interval  $[t, T]$  as the solution to the SDE in Equation (3). Next, use the Dynkin operator or Fokker-Planck operator  $\mathcal{A}$  defined by

$$\mathcal{A} = \mu(x, s) \frac{\partial}{\partial x} + \frac{1}{2} \sigma(x, s) \frac{\partial^2}{\partial x^2}. \tag{21}$$

We may write the Cauchy problem (1) as

$$\begin{aligned} \frac{\partial u(x, s)}{\partial s} + \mathcal{A}u(x, s) &= 0, \\ u(x, T) &= u_T(x). \end{aligned} \tag{22}$$

*Cauchy Problem and Feynman–Kac*

Applying Itô’s lemma to  $u(x, s)$ . We obtain

$$\int_t^T du(x_s, s) ds = \int_t^T \left[ \frac{\partial u(x_s, s)}{\partial s} + \mathcal{A}u(x_s, s) \right] ds + \int_t^T \sigma(x_s, s) \frac{\partial u(x_s, s)}{\partial x_s} dB_s. \tag{23}$$

After integration, we obtain

$$u(x_T, T) - u(x_t, t) = \int_t^T \left[ \frac{\partial u(x_s, s)}{\partial s} + \mathcal{A}u(x_s, s) \right] ds + \int_t^T \sigma(x_s, s) \frac{\partial u(x_s, s)}{\partial x_s} dB_s. \tag{24}$$

Since, by assumption  $u(x, t)$  satisfies Equation (22), the time integral  $ds$  in the last line of Equation (23) will vanish. Furthermore, if the process  $\sigma(x_s, s) \frac{\partial u(x_s, s)}{\partial x_s}$  is sufficiently integrable, and after taking the expectation, the stochastic integral will vanish. Finally, considering the initial and boundary condition, such as  $u(x, T) = u_T(x)$ , we obtain the stochastic representation of the Cauchy problem (1) using the Feynman–Kac Formula (2) [2,3]:

$$u(x_t, t) = \mathbb{E}_{x,t}[u_T(x)]. \tag{25}$$

**Theorem 6.** *The stochastic representation of the Cauchy problem (1) under a generalized fractional Brownian Motion,  $B_t^H$ , with  $H \in (\frac{1}{2}, 1)$ , under the assumptions above, follows*

$$u(x_t, t) = \mathbb{E}_{x,t} \left[ u_T(x) - \int_t^T \frac{\partial^2 u(x_t, t)}{\partial x_t^2} \left[ \int_0^t H f''(B_v^H) v^{2H-1} dv \right] ds \right], \tag{26}$$

and this simplifies under the conditions in Equation (14) to

$$u(x_t, t) = \mathbb{E}_{x,t} \left[ u_T(x) - \int_t^T \frac{\partial^2 u(x_t, t)}{\partial x_t^2} \left[ \int_0^t H(2H - 1) |t - v|^{2H-2} a(v) dv \right] ds \right], \tag{27}$$

if  $x_t \in C^2$  and  $\sigma(x_t, s)$  is independent of  $x_t$ . Note, for  $H = \frac{1}{2}$ , we obtain (2).

**Proof.** Consider  $u(x_t, t)$  as solution of the Cauchy problem (1) under a generalized fractional Brownian Motion,  $B_t^H$ , with  $H \in (\frac{1}{2}, 1)$ . Applying Theorem 2 on  $u(x, s)$ , we obtain

$$\begin{aligned} \int_t^T du(x_s, s) ds &= \int_t^T \left[ \frac{\partial u(x_s, s)}{\partial s} + \mathcal{A}u(x_s, s) \right] ds + \int_t^T \sigma(x_s, s) \frac{\partial u(x_s, s)}{\partial x_s} dB_s + \\ &+ \int_t^T \frac{\partial^2 f(x_s, s)}{\partial x_s^2} \left[ \int_0^t H(2H - 1) |t - v|^{2H-2} a(v) dv \right] ds \end{aligned}$$

After integration and under the assumption that  $u(x, t)$  satisfies Equation (22). The time integrals will vanish. Given  $x_t \in C^2$  and a deterministic  $\sigma$ , we obtain, after taking the expectation and the property that the stochastic integral vanishes, the stochastic representation as follows:

$$u(x_t, t) = \mathbb{E}_{x,t} \left[ u_T(x) - \int_t^T \frac{\partial^2 u(x_t, t)}{\partial x_t^2} \left[ \int_0^t H(2H - 1) |t - v|^{2H-2} a(v) dv \right] ds \right]. \tag{28}$$

If  $H = \frac{1}{2}$ , the stochastic representation simplifies to the well-known Feynman–Kac formula  $u(x_t, t) = \mathbb{E}_{x,t} [u_T(x)]$ .  $\square$

Next, we state the Feynman–Kac formula for our Cauchy problem (1), given a sub-fractional Brownian motion.

**Theorem 7.** *The stochastic representation of the Cauchy problem (1) under a sub-fractional Brownian Motion,  $\mathfrak{z}_t^H$ , with  $H \in (\frac{1}{2}, 1)$  is*

$$u(x_t, t) = \mathbb{E}_{x,t} \left[ u_T(x) - \int_t^T \frac{\partial^2 u(x_t, t)}{\partial x_t^2} \left[ \int_0^t H(2 - 2^{2H-1}) f''(\xi_v^H) v^{2H-1} dv \right] ds \right], \tag{29}$$

if  $x_t \in C^2$ . Note, for  $H = \frac{1}{2}$ , we obtain the same as in Theorem 6.

The proof follows an equal argument as above in the proof of Theorem 6.

### 5. Cauchy Problem and Fractional-PDE

Next, we demonstrate the direct linkage for the Cauchy-problem (1) to the fPDE in Equation (4). In step one, we compute the Laplace transform of the right-hand side of the heat equation:

$$\begin{aligned} \mathfrak{L}[u_t(x, t)] &= \mathfrak{L} \left[ \frac{\partial u(x, t)}{\partial t} \right] = \int_0^\infty e^{-st} \frac{\partial u(x, t)}{\partial t} dt \\ &= -u_0(x) + s\bar{u}(x, t) \\ &= s\bar{u}(x, t), \end{aligned}$$

where  $\bar{u}(x, t) := \mathfrak{L}[u(x, t)]$ . Thus, we obtain

$$\begin{aligned} \mathfrak{L} \left[ \frac{\partial}{\partial x^2} u(x, t) \right] &= s\bar{u}(x, t) \\ \frac{\partial}{\partial x^2} \mathfrak{L}[u(x, t)] &= s\bar{u}(x, t) \\ \frac{\partial}{\partial x^2} \bar{u}(x, t) &= s\bar{u}(x, t). \end{aligned}$$

This is a second-order ordinary differential equation in the  $x$ -variable. The solution is  $\bar{u}(x, t) = c * e^{-\sqrt{sx}}$  for some constant  $c$ . Determining the constant by the second-derivative  $\bar{u}_{xx} = c * se^{-\sqrt{sx}}$  shows that  $c = 1$ . In step two, we compute the first-derivative of the solution

$$\begin{aligned} \frac{\partial}{\partial x} \bar{u}(x, t) &= -\sqrt{s} e^{-\sqrt{sx}} \\ \frac{\partial}{\partial x} \bar{u}(x, t) &= -\sqrt{s} \bar{u}(x, t). \end{aligned}$$

This is a first-order partial differential equation of the Laplace-transform  $\bar{u}(x, t)$ . Finally, compute the inverse Laplace transform and obtain the fPDE in Equation (4) by

$$\frac{\partial}{\partial x} u(x, t) = -\frac{\partial^{\frac{1}{2}}}{\partial t^{\frac{1}{2}}} u(x, t). \tag{30}$$

Indeed, the inverse Laplace transform of the semi-derivative on the right-hand side is as follows:

$$-\mathcal{L}^{-1} \left[ \frac{\partial^{\frac{1}{2}}}{\partial t^{\frac{1}{2}}} u(x, t) \right] = u_0(x) - s^{\frac{1}{2}} \bar{u}(x, t) = -s^{\frac{1}{2}} \bar{u}(x, t) = -\sqrt{s} \bar{u}(x, t).$$

From the fractional representation of the Cauchy problem (1), we find the following fractional derivatives and integrals in relation to the normal distribution:

**Proposition 3.** Consider that the solution of the Cauchy problem (1) is of  $u(x, t) = \frac{1}{\sqrt{2\pi t}} e^{-\frac{x^2}{2t}}$ , which represents the normal probability density function  $N'(x)$  for a constant  $t$ . Thus, the solution of the fPDE (4) implies the following fractional derivative and integral:

- (a)  $\frac{\partial^{\frac{1}{2}}}{\partial t^{\frac{1}{2}}} u(x, t) = D_t^{\frac{1}{2}} u(x, t) = \frac{1}{\sqrt{2\pi t}} \frac{x}{t} e^{-\frac{x^2}{2t}}$ .
- (b) For  $\alpha = \frac{1}{2}$ , we find  $I_t^\alpha u(x, t) = \frac{1}{\Gamma(\alpha)} \int_{-\infty}^x (x-t)^{\alpha-1} u(x, t) dt = N'(x)$ , where  $N'(x)$  is the density of the normal probability distribution in regard to  $x$ , or  $N'(x) = n(x) = \frac{1}{\sqrt{2\pi t}} e^{-\frac{x^2}{2t}}$ .

**Proof.** Part (a): given  $u(x, t)$ , it follows from Equation (30) that the semi-derivative with respect to time  $t$  is equal to  $\frac{\partial}{\partial x} u(x, t)$ . Computing the partial derivative of  $u(x, t)$  with respect to  $x$  is  $u_x(x, t) = \frac{\partial u(x, t)}{\partial x} = \frac{1}{\sqrt{2\pi t}} \frac{x}{t} e^{-\frac{x^2}{2t}}$ .

Part (b): In order to explicitly evaluate the fractional derivative, we utilize the linearity of both operators. Using operator calculus, we see that

$$D_t^{\frac{1}{2}} u(x, t) = D_t^1 D_t^{-\frac{1}{2}} u(x, t) = D_t^1 I_t^{\frac{1}{2}} u(x, t).$$

Thus, the first-derivative of the semi-integral of  $I_t^{\frac{1}{2}} u(x, t)$  with respect to  $t$  must be equal to  $u_x(x, t)$ . Hence, the semi-integral

$$I_t^{\frac{1}{2}} u(x, t) = \frac{1}{\Gamma(\frac{1}{2})} \int_{-\infty}^x (x-t)^{\alpha-1} u(x, t) dt = N'(x) = \frac{1}{\sqrt{2\pi t}} e^{-\frac{x^2}{2t}},$$

consequently, the first-derivative of  $N'(x)$  is of  $\frac{dN'(x)}{dx} = N''(x) = \frac{1}{\sqrt{2\pi t}} \frac{x}{t} e^{-\frac{x^2}{2t}}$ . The final term solves the fPDE in Equation (30). Thus, the fractional integral for  $\alpha = \frac{1}{2}$  must be equal to the probability density function  $N'(x)$  in order to satisfy the fPDE in Equation (30).  $\square$

### 6. Conclusions

This article studies the relationships of the Cauchy problem (1) and relates them to fractional partial-differential equations, as well as to the stochastic representations by the Feynman–Kac formula with a generalized fractional and sub-fractional Brownian motion with Hurst parameter  $H > 1/2$ . In addition, we find fractional derivatives and integrals in relation to the Gaussian probability function by utilizing the novel insight into the linkage of the Cauchy problem and fPDE. This vantage point is of importance in probability theory, fractional calculus and stochastic theory. In future research, we intend to extend our theorems to Hurst parameters  $H < 1/2$  and the stochastic Cauchy problem under a sub-fBM.

**Funding:** This research received funding from RRI-Reutlingen Research Institute.

**Institutional Review Board Statement:** Not applicable.

**Informed Consent Statement:** Not applicable.

**Data Availability Statement:** Not applicable.

**Acknowledgments:** The research of this paper was mainly finalized during my research semester 2021 at ESB Business School, Reutlingen University. I would like to express my thanks for the regular research semester and opportunity to advance scientific research for the good of the society in future.

**Conflicts of Interest:** The author declares no conflict of interest.

## References

- Kolodner, I. Free boundary problem for the heat equation with applications to problems of change of phase. *Commun. Pure Appl. Math.* **1956**, *9*, 1–31. [CrossRef]
- Feynman, R.P. Space-time approach to nonrelativistic quantum mechanics. *Rev. Mod. Phys.* **1948**, *20*, 367–387. [CrossRef]
- Kac, M. On distributions of certain Wiener functionals. *Trans. Am. Math. Soc.* **1949**, *65*, 1–13. [CrossRef]
- Brown, R. A brief description of microscopical observations made in the months of June, July and August 1827, on the particles contained in the pollen of plants. *Ann. Phys.* **1828**, *14*, 294–313. [CrossRef]
- Wiener, N. The average of an analytic functional and the Brownian movement. *Proc. Natl. Acad. Sci. USA* **1921**, *7*, 249–299. [CrossRef]
- Karatzas, I.; Shreve, S. *Brownian Motion and Stochastic Calculus*; Springer: Berlin/Heidelberg, Germany, 1991.
- Babenko, Y. *Teplomassoobmen. Metod Rascheta Teplovykh i Diffuzionnykh Potokov. (Heat and Mass Transfer: Calculating Heat and Diffusion Fluxes)*; Leningrad: Union City, NJ, USA, 1986.
- Mandelbrot, B.; van Ness, J. Fractional Brownian Motions, Fractional Noises and Applications. *SIAM Rev.* **1968**, *10*, 422–437. [CrossRef]
- Oldham, K.; Spanier, J. *The Fractional Calculus*; Academic Press: New York, NY, USA, 1974.
- Podlubny, I. *Fractional Differential Equations*; Elsevier: Amsterdam, The Netherlands, 1998; Volume 1.
- Kilbas, A.; Srivastava, H.; Trujillo, J. *Theory and Applications of Fractional Differential Equations*; Elsevier: Amsterdam, The Netherlands, 2006; Volume 1.
- Uchaikin, V. *Fractional Derivatives for Physicists and Engineers*; Springer: Berlin/Heidelberg, Germany, 2013.
- Povstenko, Y. *Fractional Thermoelasticity*; Springer: Berlin/Heidelberg, Germany, 2015.
- Walsh, J. *An Introduction to Stochastic Partial Differential Equations*; Springer: Berlin/Heidelberg, Germany, 1986; Volume XIV.
- Ocone, D.; Pardoux, E. A stochastic Feynman-Kac formula for anticipating SPDEs, and application to nonlinear smoothing. *Stoch. Rep.* **1993**, *45*, 79–126. [CrossRef]
- Mocioalca, O.; Viens, F. Skorohod integration and stochastic calculus beyond the fractional Brownian scale. *J. Funct. Anal.* **2005**, *222*, 385–434. [CrossRef]
- Querdiane, H.; Silva, J.L. Generalized Feynman-Kac formula with stochastic potentials. *Infin. Dimens. Anal. Quantum Probab. Relat. Top.* **2002**, *5*, 243–255. [CrossRef]
- Hu, Y.; Nualart, D.; Song, J. Feynman-Kac Formula for Heat Equation Driven by Fractional White Noise. *Ann. Probab.* **2011**, *39*, 291–326. [CrossRef]
- Hu, Y.; Lei, F.; Nualart, D. Feynman-Kac Formula for Heat Equation Driven by Fractional White Noise with Hurst Parameter  $H < 1/2$ . *Ann. Probab.* **2012**, *40*, 1041–1068.
- Nualart, D.; Schoutens, W. Backward stochastic differential equations and Feynman-Kac formula for Lévy processes, with applications in finance. *Bernoulli* **2001**, *7*, 761–776. [CrossRef]
- Biagini, F.; Hu, Y.; Oksendal, B.; Zhang, T. *Stochastic Calculus for Fractional Brownian Motion and Applications*; Springer: Berlin/Heidelberg, Germany, 2008.
- Embrechts, P. *Selfsimilar Processes*; Princeton University Press: Princeton, NJ, USA, 2002.
- Nourdin, I. *Selected Aspects of Fractional Brownian Motion*; Springer: Berlin/Heidelberg, Germany, 2012.
- Ruiz, W. Dynamical system method for investigating existence and dynamical property of solution of nonlinear time-fractional PDEs. *Nonlinear Dyn.* **2019**, *99*, 2421–2440.
- Duncan, T.; Hu, Y.; Pasik-Duncan, B. Stochastic Calculus for Fractional Brownian Motion. *SIAM J. Control. Optim.* **2000**, *38*, 582–612. [CrossRef]
- Marinov, T.M.; Ramirez, N.; Santamaria, F. Fractional Integration Toolbox. *Fract. Calc. Appl.* **2013**, *16*, 670–681. [CrossRef] [PubMed]
- Fulinski, A. Fractional Brownian motions: Memory, diffusion velocity, and correlation functions. *J. Phys. A Math. Theor.* **2017**, *50*, 054002. [CrossRef]
- Padhi, S.; Graef, J.; Pati, S. Multiple Positive Solutions for a boundary value problem with nonlinear nonlocal Riemann-Stieltjes Integral Boundary Conditions. *Fract. Calc. Appl. Anal.* **2018**, *21*, 716–745. [CrossRef]

29. Kamran, J.W.; Jamal, A.; Li, X. Numerical Solution of Fractal-Order Fredholm Integro-differential Equation in the Sense of Atangana-Baleanu Derivative. *Math. Probl. Eng.* **2020**, *2021*, 6662803.
30. Guariglia, E. Fractional calculus, zeta functions and Shannon entropy. *Open Math.* **2021**, *19*, 87–100. [CrossRef]
31. Sadhu, T.; Wiese, K. Functionals of fractional Brownian motion and three arcsine laws. *arXiv* **2021**, arXiv:2103.09032.
32. Bojdecki, T.; Gorostiza, L.; Talarczyk, A. Sub-fractional Brownian motion and its relation to occupation times. *Stat. Probab. Lett.* **2004**, *69*, 405–419. [CrossRef]
33. Tudor, C. On the Wiener integral with respect to sub-fractional Brownian motion on an interval. *J. Math. Anal. Appl.* **2009**, *351*, 456–468. [CrossRef]
34. Tudor, C.; Zili, M. Covariance measure and stochastic heat equation with fractional noise. *Fract. Calc.* **2014**, *17*, 807–826. [CrossRef]
35. Shen, G.; Yan, L. The stochastic integral with respect to the sub-fractional Brownian motion with  $H > \frac{1}{2}$ . *J. Math. Sci.* **2010**, *6*, 219–239.
36. Yan, L.; Shen, G.; He, K. Itô's formula for a sub-fractional Brownian motion. *Commun. Stoch. Anal.* **2011**, *5*, 135–159. [CrossRef]
37. Liu, J.; Yan, L. Remarks on asymptotic behavior of weighted quadratic variation of subfractional Brownian motion. *J. Korean Stat. Soc.* **2012**, *41*, 177–187. [CrossRef]
38. Prakasa, R. On some maximal and integral inequalities for sub-fractional Brownian motion. *Stoch. Anal. Appl.* **2017**, *35*, 2017.
39. Monin, A.; Yaglom, A. *Statistical Fluid Mechanics: Mechanics of Turbulence*; Dover Publication: Mineola, NY, USA, 2007; Volume II.
40. Decreusefond, L.; Üstünel, A. Stochastic analysis of the fractional Brownian motion. *Potential Anal.* **1998**, *10*, 177–214. [CrossRef]
41. Alòs, E.; Mazet, O.; Nualart, D. Stochastic Calculus with Respect to Gaussian processes. *Ann. Probab.* **2001**, *29*, 766–801. [CrossRef]
42. Mishura, Y.; Zili, M. *Stochastic Analysis of Mixed Fractional Gaussian Processes*; Mathematics and Statistics; Elsevier: Amsterdam, The Netherlands, 2018.



Article

# Existence and Uniqueness of Mild Solution Where $\alpha \in (1, 2)$ for Fuzzy Fractional Evolution Equations with Uncertainty

Ramsha Shafqat <sup>1,\*</sup>, Azmat Ullah Khan Niazi <sup>1</sup>, Mdi Begum Jeelani <sup>2</sup> and Nadiyah Hussain Alharthi <sup>2</sup>

<sup>1</sup> Department of Mathematics and Statistics, The University of Lahore, Sargodha 40100, Pakistan; azmatullah.khan@math.uol.edu.pk

<sup>2</sup> Department of Mathematics and Statistics, College of Science, Imam Mohammad Ibn Saud Islamic University, Riyadh 13314, Saudi Arabia; mbshaikh@imamu.edu.sa or write2mohammadi@gmail.com (M.B.J.); nhalharthi@imamu.edu.sa (N.H.A.)

\* Correspondence: ramshawarriach@gmail.com

**Abstract:** This paper concerns with the existence and uniqueness of fuzzy fractional evolution equation with uncertainty involves function of form  ${}^c D^\alpha x(t) = f(t, x(t), D^\beta x(t))$ ,  $I^\alpha x(0) = x_0$ ,  $x'(0) = x_1$ , where  $1 < \alpha < 2$ ,  $0 < \beta < 1$ . After determining the equivalent integral form of solution we establish existence and uniqueness by using Rogers conditions, Kooi type conditions and Krasnoselskii-Krein type conditions. In addition, various numerical solutions have been presented to ensure that the main result is true and effective. Finally, a few examples which express fuzzy fractional evolution equations are shown.

**Keywords:** fractional evolution equations; existence; uniqueness; fixed point theorem; Caputo derivative

**MSC:** 26A33; 34K37

**Citation:** Shafqat, R.; Niazi, A.U.K.; Jeelani, M.B.; Alharthi, N.H.

Existence and Uniqueness of Mild Solution Where  $\alpha \in (1, 2)$  for Fuzzy Fractional Evolution Equations with Uncertainty. *Fractal Fract.* **2022**, *6*, 65. <https://doi.org/10.3390/fractalfract6020065>

Academic Editors: António M. Lopes, Alireza Alfi, Liping Chen and Sergio A. David

Received: 28 December 2021

Accepted: 21 January 2022

Published: 26 January 2022

**Publisher's Note:** MDPI stays neutral with regard to jurisdictional claims in published maps and institutional affiliations.



**Copyright:** © 2022 by the authors. Licensee MDPI, Basel, Switzerland. This article is an open access article distributed under the terms and conditions of the Creative Commons Attribution (CC BY) license (<https://creativecommons.org/licenses/by/4.0/>).

## 1. Introduction

A wide variety of physical processes in real-world events exhibit fractional-order behaviour that can change across time and space. Fractional calculus authorises operations of differentiation and integration of fractional order. On both imaginary and real numbers, the fractional-order can be used. The theory of fuzzy sets continues to grab researchers' attention due to its wide range of applications in a variety of domains including mechanics, electrical, engineering, processing signals, thermal system, robotics and control, signal processing and many other fields [1–6]. As a result, it has piqued the curiosity of researchers over the last few years.

In the context of mathematical modeling, developing a suitable fractional differential equation is a difficult task. It requires an investigation into the underlying physical phenomena. Real physical phenomena, on the other hand, are always wrapped in uncertainty. This is true especially when working with “living” resources like soil, water, and microbial communities.

Fuzzy set theory is a fantastic technique for modelling uncertain problems. As a result, a wide range of natural events has been modelled using fuzzy notions. The fuzzy fractional differential equation is a common model in a variety of scientific domains, including population models, weapon system evaluation, civil engineering, and electro-hydraulic modelling. As a result, in fuzzy calculus, the concept of the fractional derivative is crucial. As a result, fuzzy fractional differential equations have received a lot of interest in domains of mathematics and engineering.

The concept of the fractional differential equation was presented in 2010 by Agarwal et al. [7]. However, this concept of Hukuhara differentiability could not provide the large and varied behaviour of crisp solutions at the time. Allahviranloo and Salahshourcite [8]

defined Riemann–Liouville H-derivative based on highly generalised Hukuhara differentiability [9,10] later in 2012. They also defined Riemann–Liouville fractional derivative.

Riemann–Liouville for elaboration appears in a natural method for problems such as transport difficulties from continuum random walks plan or generalises Chapman–Kohmogorov models [11]. Under the external influences and continuum and statistical mechanics for elaborating the behaviour of viscoplastic and viscoelastic, it was also applied.

There are some other papers which were related to existence and uniqueness of solution under Nagumo like conditions [12–16] for fuzzy fractional differential equation. The uniqueness of the solution under condition  $0 < q < 1$  for problem  $D^q x(t) = f(t, x(t))$  was elaborated by Leela and Lakshmikantham [14,15]. With the help of Rogers, Krasnoselskoo–Krein and Kooi conditions the uniqueness of solution was proved by Yoruk et al. [16], for  $1 < q < 2$ .

On the other way, by the use of uncertainty in order to obtained more realistic modeling of phenomena are taken; (see [17–19]). In aspect not fuzzy and fractional differential equations many other scholars have been worked in numerical and theoretical [20–24].

The fuzzy Laplace transform was introduced by Ahmadi and Allahviranloo, which was used to generalized differentiability. Now, further ElJaoui et al. [25] worked on it. The fuzzy initial and boundary value problems and fuzzy fractional differential equations are solved by fuzzy Laplace transform method [26].

Hallaci et al. [27] worked on the existence and uniqueness for delay fractional differential equations in 2020 by using the Krasnoselskii's fixed point theorem and the contraction mapping principle.

In 2021, Niazi et al. [28] worked on the existence, uniqueness, and  $E_q$ -Ulam type stability of Cauchy problem for system of fuzzy fractional differential equation with Caputo derivative of order  $q \in (1, 2]$ ,  ${}^c_0 D_{0+}^q u(t) = \lambda u(t) \oplus f(t, u(t)) \oplus B(t)C(t)$ ,  $t \in [0, T]$  with initial conditions  $u(0) = u_0$ ,  $u'(0) = u_1$ .

In 2021, Iqbal et al. [29] worked on the uniqueness and existence of mild solution for fractional order controlled fuzzy evolution equation with Caputo-derivative of the controlled fuzzy nonlinear evolution equation which is given below

$$\begin{cases} {}^c_0 D_t^\gamma x(t) = \alpha x(t) + p(t, x(t)), B(t)C(t), t \in [0, T] \\ x(t_0) = x_0. \end{cases}$$

Baleanu et al. [30] worked on the existence results for solutions of a coupled system of hybrid boundary value problems with hybrid econditions.

The existence and uniqueness of the Laplace transform was proved by Assia Guezane-Lakoud [31] for below initial value problems of fuzzy fractional differential equation for arbitrary order  $q > 1$ .

$$\begin{cases} D^q x(t) = f(t, x(t), D^{q-1}x(t)), \\ x(0) = y_0, \\ D^{(q-i)}x(0) = \tilde{0}, i = 1, \dots, [q]. \end{cases}$$

By the inspire of above work, we adopted Caputo derivative to prove existence and uniqueness for below initial value problem of fuzzy fractional evolution equation with uncertainty for order  $\alpha \in (1, 2)$ .

$$\begin{cases} {}^c D^\alpha x(t) = f(t, x(t), D^\beta x(t)), \\ I^\alpha x(0) = x_0, \\ x'(0) = x_1, \end{cases} \quad (1)$$

where

$$1 < \alpha < 2, 0 < \beta < 1,$$

and  $x_0 \in \mathbb{E}$  and  $f : \mathbb{E}_0 \rightarrow \mathbb{E}$  is continuous fuzzy-valued function with

$$\mathbb{E}_0 = \{(t, x) : 1 \leq t \leq 2, d(x(t), \tilde{0}) \leq a\}, \quad (2)$$

where  $d$  is Hausdroff distance.

Our goal is to extend and generalise [16] previous uniqueness results.

This study focuses on proving that consecutive approximations converge to a unique solutions using the Rogers type uniqueness theorem, Krasnoselskoo–Krein type uniqueness theory, and Kooi type uniqueness theorem. By using fuzzy Caputo derivative we determine the equivalent integral problem.

The following is a breakdown of the paper’s structure. Basic definitions of fuzzy set theory, Riemann–Liouville and Caputo derivative extended H-differentiability can be found in Section 2. The corresponding integral problem is determined in Section 3 using the fuzzy Laplace transform. The key findings are discussed in Section 4. Section 5, we prove that consecutive approximations converge to a unique solutions using the Krasnoselskii–Krein type of uniqueness theorem, a Kooi type uniqueness theorem, and a Rogers type uniqueness theory.

## 2. Preliminaries

Let us throw the light on some basic definitions of fuzzy numbers and fuzzy sets. The Gamma function is denoted by  $\gamma$  in this and the rest of the paper, while the integral part of  $\alpha$  is denoted by  $[\alpha]$ .

As expressed in [32]  $\mathbb{E} = \{u : \mathbb{R} \rightarrow [0, 1]; u \text{ satisfies } (A_1) - (A_4)\}$  is space of a fuzzy numbers:

(A<sub>1</sub>)  $u$  is a normal; that is, there exist  $x_0 \in \mathbb{R}$  such that  $u(x_0) = 2$ .

(A<sub>2</sub>)  $u$  is a fuzzy convex; that is,  $u(\lambda y + (1 - \lambda)z) \geq \min\{u(x), u(z)\}$  whenever  $x, z \in \mathbb{R}$  and  $\lambda \in [1, 2]$ .

(A<sub>3</sub>)  $u$  is a upper semi-continuous; that is, for any  $x_0 \in \mathbb{R}$  and  $\varepsilon > 1$  there exists  $\xi(x_0, \varepsilon) > 1$  such that  $u(y) < u(y_0) + \varepsilon$  whenever  $|x - x_0| < \xi, x \in \mathbb{R}$ .

(A<sub>4</sub>) The closure of  $\{x \in \mathbb{R}; u(x) > 1\}$  is compact.

The set  $[u]^\gamma = \{u \in \mathbb{R}; u(x) > \gamma\}$  is called  $\gamma$ -level set of  $u$ . It follows from (A<sub>1</sub>) – (A<sub>4</sub>) that  $\alpha \in (1, 2]$ . The fuzzy zero is defined by

$$\bar{0} = \begin{cases} 1 & \text{if } x \neq 1, \\ 2 & \text{if } x = 1. \end{cases} \quad (3)$$

**Definition 1** ([32]). A fuzzy number  $u$  in parametric form is pair of functions  $(\underline{u}(r), \bar{u}(r))$ ,  $1 \leq r \leq 2$ , that meet following conditions:

- (1)  $\underline{u}(r)$  is bounded non-decreasing left continuous function in  $(1, 2]$  and right continuous at 1;
- (2)  $\bar{u}(r)$  is bounded non-decreasing left continuous function in  $(1, 2]$  and right continuous at 1;
- (3)  $\underline{u}(r) \leq \bar{u}(r), 1 \leq r \leq 2$ .

Furthermore,  $r$ -cut representation of fuzzy numbers can be shown as

$$[u]^r = [\underline{u}(r), \bar{u}(r)] \text{ for all } 1 \leq r \leq 2.$$

The features of fuzzy addition and multiplication by scaler on  $\mathbb{E}$  are as follows, according to Zadeh’s extension principle:

$$(u \oplus v)(x) = \sup_{y \in \mathbb{R}} \min\{u(x), v(w - x)\}, w \in \mathbb{R},$$

$$(k \ominus u)(x) = \begin{cases} u(\frac{x}{k}) & \text{if } k \geq 1, \\ \bar{0} & \text{if } k = 1. \end{cases} \quad (4)$$

To keep things simple, we write  $\oplus, \ominus$  with the standard  $P +, \dots$ . The Hausdorff distance between the fuzzy numbers is denoted by  $\mathbb{E} \times \mathbb{E} \rightarrow [0, +\infty[$ , such that

$$D(u, v) = \sup_{r \in [1,2]} \max\{|\underline{u}(r) - \underline{v}(r)|, |\bar{u}(r) - \bar{v}(r)|\}.$$

And  $(d, \mathbb{E})$  is a complete metric space.

**Definition 2.** Let  $x, y \in \mathbb{E}$  be the variables. If  $z \in \mathbb{E}$  exists such that  $x = y + z$ , then  $z$  is known as  $H$ -difference of  $x$  and  $y$  and is symbolised as  $x \ominus y$ .

**Remark 1.** The sign  $\ominus$  denotes the  $H$ -difference and  $x \ominus y \neq x + (-1)y$ .

$C^{\mathbb{F}}[1, a]$  denotes space of all continuous fuzzy-valued functions on  $[1, a]$ , and  $L^{\mathbb{F}}[1, a]$  denotes space of all Lebesgue integrable fuzzy valued functions on  $[1, a]$ , when  $a > 1$ .

$AC^{(n-1)\mathbb{F}}[1, a]$  also denotes space of fuzzy-valued functions  $f$  with continuous  $H$ -derivatives up to  $n - 1$  on  $[1, a]$  such that  $f^{(n-1)}$  in  $AC^{\mathbb{F}}[1, a]$ .

**Definition 3** ([33]). The Riemann–Liouville fractional derivative is defined as

$${}_a D_t^p f(t) = \left(\frac{d}{dt}\right)^{n+1} \int_a^t (t - \tau)^{n-p} f(\tau) d\tau, \quad n \leq p \leq n + 1.$$

**Definition 4** ([33]). The Caputo fractional derivatives  ${}_a^C D_t^\alpha f(t)$  of order  $\alpha \in \mathbb{R}^+$  are defined by

$${}_a^C D_t^\alpha f(t) = {}_a D_t^\alpha (f(t) - \sum_{k=0}^{n-1} \frac{f^{(k)}(a)}{k!} (t - a)^k),$$

respectively, where  $n = [\alpha] + 1$  for  $\alpha \notin \mathbb{N}_0; n = \alpha$  for  $\alpha \in \mathbb{N}_0$ .

In this paper, we consider Caputo fractional derivative of order  $1 < \alpha \leq 2$ , e.g.,

$${}_a^C D_t^{3/2} f(t) = {}_a D_t^{3/2} (f(t) - \sum_{k=0}^{n-1} \frac{f^{(k)}(a)}{k!} (t - a)^k).$$

**Definition 5** ([34]). The Wright function  $\psi_\alpha$  is defined by

$$\begin{aligned} \psi_\alpha(\theta) &= \sum_{n=0}^{\infty} \frac{(-\theta)^n}{n! \Gamma(-\alpha n + 1 - \alpha)} \\ &= \frac{1}{\pi} \sum_{n=1}^{\infty} \frac{(-\theta)^n}{(n-1)!} \Gamma(n\alpha) \sin(n\pi\alpha), \end{aligned}$$

where  $\theta \in \mathbb{C}$  with  $0 < \alpha < 1$ .

**Lemma 1** ([35]). Let  $\{C(t)\}_{t \in \mathbb{R}}$  be a strongly continuous cosine family in  $X$  satisfying  $\|C(t)\|_{L_b(X)} \leq M e^{\omega|t|}, t \in \mathbb{R}$ , and let  $A$  be the infinitesimal generator of  $\{C(t)\}_{t \in \mathbb{R}}$ , then for  $\text{Re} \lambda > \omega, \lambda^2 \in \rho(A)$  and

$$\lambda R(\lambda^2; A)x = \int_0^\infty e^{-\lambda t} C(t) t dt, \quad R(\lambda^2; A)x = \int_0^\infty e^{-\lambda t} S(t) x dt, \quad \text{for } x \in X.$$

Let  $\gamma > 1$  be a real number, we have following results:

**Lemma 2** ([3]). The unique solution of linear fractional differential equation

$${}^c D^\alpha u(t) = 0,$$

is given by

$$u(t) = c_1 + c_2 t + \dots + c_n t^{n-1}, c_i \in \mathbb{R}, i = 1, 2, \dots, n,$$

where

$$n = [\alpha] + 1.$$

**Lemma 3.** Equation (1) is equal to integral equation below:

$$x(t) = \frac{1}{\Gamma k} \int_0^t (t-s)^{k-1} f(s, x(s), D^\beta x(s)) ds + \frac{1}{\Gamma k - 1} \int_0^t (t-s)^{k-2} f(s, x(s), D^\beta x(s)) ds + \sigma(0). \quad (5)$$

**Proof.** Using Lemma 2, Equation (1) can be written as

$${}^c D^\alpha x(t) = I^f(t, u(t), D^\beta(t)) + c_0 t^{\alpha-1}.$$

Using the condition

$$\lim_{t \rightarrow 0} t^{1-kc} D^\beta u(t) = 0,$$

we get  $c_0 = 0$ . On the other hand, from Lemma 2, one gets

$$x(t) = I^k f(t, x(t), D^\beta x(t)) + I^{k-1} g(t, x(t), D^\beta x(t)) + c_1 + c_2 t.$$

Clearly  $x(0) = \sigma(0)$ , so we obtain  $c_1 = \sigma(0)$  and because  $u'(0) = 0$ , we find  $c_2 = 0$ , then we get the integral equation

$$x(t) = \frac{1}{\Gamma k} \int_0^t (t-s)^{k-1} f(s, x(s), D^\beta x(s)) ds + \frac{1}{\Gamma k - 1} \int_0^t (t-s)^{k-2} f(s, x(s), D^\beta x(s)) ds + \sigma(0). \quad \square$$

The Krasnoselskii fixed point theorem and contraction mapping concept are used to achieve our results.

**Theorem 1.** (Krasnoselskii fixed point theorem [36,37]) If  $M$  is nonempty bounded, closed, and convex subset of  $E$ , and  $A$  and  $B$  are two operators defined on  $M$  with values in  $E$ , then

- (i)  $Au + Bv \in G$ , for all  $u, v \in G$ ,
- (ii)  $A$  is continuous and compact,
- (iii) Then there exists  $w \in G$  such that  $h = Aw + Bw$ .

**Theorem 2.** (Contraction mapping principle [36,37]) If  $E$  is Banach space, then it is a Banach space. When  $H : \mathbb{E} \rightarrow \mathbb{E}$  is a contraction,  $H$  has a single fixed point in  $\mathbb{E}$ .

**Definition 6** ([38]). Let  $f \in C^{\mathbb{F}}[1, 2] \cap L^{\mathbb{F}}[1, 2]$ . The fuzzy fractional integral of fuzzy-valued function  $f$  is defined as

$$I^\gamma f(\mathbf{x}; r) = [I^\gamma \underline{f}(\mathbf{x}; r), I^\gamma \bar{f}(\mathbf{x}; r)], 1 \leq r \leq 2, \quad (6)$$

where

$$\begin{aligned} I^\gamma \underline{f}(\mathbf{x}; r) &= \frac{1}{\Gamma(\gamma)} \int_0^x (x-s)^{\gamma-1} \underline{f}(s; r) ds, \\ I^\gamma \bar{f}(\mathbf{x}; r) &= \frac{1}{\Gamma(\gamma)} \int_0^x (x-s)^{\gamma-1} \bar{f}(s; r) ds. \end{aligned} \quad (7)$$

**Definition 7** ([38]). Let  $f \in C^{(n)F}[1, 2] \cap L^{\mathbb{F}}[1, 2]$ ,  $x_0 \in (1, 2)$ , and

$$\varphi(x) = \left( \frac{1}{\Gamma(n-\gamma)} \right) \int_0^t \frac{(f(t)dt)}{(x-t)^{\gamma-n+1}},$$

where

$$n = |\gamma| + 1.$$

One says that  $f$  is a fuzzy Caputo fractional differentiable of order  $\gamma$  at  $x_0$ , if there exists an element  $(D_0^\gamma f)(x_0) \in \mathbb{E}$ , such that, for all  $h > 1$  sufficiently small, one has

$$(D_0^\gamma f)(x_0) = \frac{\lim_{h \rightarrow 0} \frac{\varphi^{(n-1)}(x_0+h) \ominus \varphi^{(n-1)}(x_0)}{h}}{\lim_{h \rightarrow 0} \frac{\varphi^{(n-1)}(x_0) \ominus \varphi^{(n-1)}(x_0-h)}{h}}. \tag{8}$$

or

$$(D_0^\gamma f)(x_0) = \frac{\lim_{h \rightarrow 0} \frac{\varphi^{(n-1)}(x_0) \ominus \varphi^{(n-1)}(x_0+h)}{h}}{\lim_{h \rightarrow 0} \frac{\varphi^{(n-1)}(x_0-h) \ominus \varphi^{(n-1)}(x_0)}{h}}. \tag{9}$$

Denote by  $C^{(n-1)\mathbb{F}}([1, a])$  space of fuzzy-valued functions  $f$  on bounded interval  $[1, a]$  which have continuous Caputo-derivative up to order  $n - 2$  such that  $f^{(n-1)} \in C^\mathbb{F}[1, a]$ .  $C^{(n-1)\mathbb{F}}([1, a])$  is a complete metric space endowed by metric  $D$  such that for every  $g, h \in C^{(n-1)\mathbb{F}}([1, a])$

$$D(g, h) = \sum_{i=0}^{n-1} \sup_{t \in [1, a]} d(g^{(i)}(t), h^{(i)}(t)). \tag{10}$$

We say fuzzy-valued function  $f$  is  ${}^c[(i)-\gamma]$ -differentiable if it is differentiable as in definition case (i) and  ${}^c[(ii)-\gamma]$ -differentiable if it is differentiable as in definition case (ii) in the rest of the article.

**Definition 8** ([38]). Let  $f \in C^{(n)\mathbb{F}} \cap L^\mathbb{F}[1, 2]$ ,  $x_0 \in (1, 2)$ , and

$$\varphi(x) = \left( \frac{1}{\Gamma(\beta - n)} \right) \int_0^x \left( f(t) \frac{dt}{(x - t)^{\beta - n + 1}} \right),$$

where  $n = \gamma + 2$  such that  $1 \leq r \leq 2$ ; then

(i) if  $f$  is  ${}^c[(i)-\gamma]$ -differentiable fuzzy-valued function, then

$$(D_0^\gamma f)(x_0; r) = [(D_0^\gamma \underline{f})(x_0; r), (D_0^\gamma \overline{f})(x_0; r)], \tag{11}$$

or

(ii) if  $f$  is  ${}^c[(ii)-\gamma]$ -differentiable fuzzy-valued function, then

$$(D_0^\gamma f)(x_0; r) = [(D_0^\gamma \overline{f})(x_0; r), (D_0^\gamma \underline{f})(x_0; r)], \tag{12}$$

where

$$\begin{aligned} (D_0^\gamma \underline{f})(x_0; r) &= \left[ \frac{1}{\Gamma(n-\gamma)} \int_0^t (x-t)^{n-\gamma-1} \underline{f}(t; r) dt \right]_{x=x_0} \\ (D_0^\gamma \overline{f})(x_0; r) &= \left[ \frac{1}{\Gamma(n-\gamma)} \int_0^t (x-t)^{n-\gamma-1} \overline{f}(t; r) dt \right]_{x=x_0} \end{aligned} \tag{13}$$

The fuzzy Laplace transforms  $L$  of Caputo-derivative for fuzzy-valued functions is proved by the following theorem.

**Theorem 3.** Let  $f \in C^{(n)\mathbb{F}}[1, \infty) \cap L^\mathbb{F}[1, \infty)$ ; has the below:

(i) if  $f$  is  ${}^c[(i)-\gamma]$ -differentiable fuzzy-valued function,

$$L \left[ (D_0^\gamma f)(x_0) \right] = p^\gamma L[f(t)] \ominus \left( \sum_{k=0}^{n-1} p^{\gamma-k-1} D^k \right) (1), \tag{14}$$

or

(ii) if  $f$  is  ${}^c[(i)-\gamma]$ -differentiable fuzzy-valued function,

$$L\left[(D_0^\gamma f)(x_0)\right] = -\left(\sum_{k=0}^{n-1} p^{\gamma-k-1} D^k\right)(1) \ominus \left(-p^\gamma L[f(t)]\right) \tag{15}$$

### 3. Fuzzy Fractional Integral Equation

Using well-known fuzzy Laplace transform, we investigate the relationship between Equation (1) and fuzzy integral form in this section.

In fact, by applying the Laplace transform to both sides of the equation, get a better result.

$$D^\alpha x(t) = f\left(t, x(t), D^\beta x(t)\right) \triangleq g(t, x), \tag{16}$$

we obtain

$$L[D^\alpha x(t)] = L\left[f\left(t, x(t), D^\beta x(t)\right)\right]. \tag{17}$$

We get two situations depending on the nature of Caputo-differentiability.

Case 1.

If  $D^\alpha x$  is fuzzy-valued function that is  ${}^c[(i)-\alpha]$ -differentiable,

$$Lr(t, x) = -\left(\sum_{k=0}^{n-1} p^{\beta-k-1} D^k\right)(1) \ominus p^\alpha L[x(t)], \tag{18}$$

and the above equation becomes dependent on the lower and higher functions of  $D^\alpha x$ ,

$$\begin{cases} L[\underline{x}(t, x, r)] = p^\alpha L[\underline{x}(t; r)] - \sum_{k=0}^{n-1} p^{\gamma-k-1} D^k \underline{x}(1; r), \\ L[\bar{x}(t, x, r)] = p^\alpha L[\bar{x}(t; r)] - \sum_{k=0}^{n-1} p^{\gamma-k-1} D^k \bar{x}(1; r), \end{cases} \tag{19}$$

where

$$\begin{cases} L[\underline{x}(t, x, r)] = \min\{r(t, u) | u \in [\underline{x}(t; r), \bar{x}(t; r)]\}, 1 \leq r \leq 2, \\ L[\bar{x}(t, x, r)] = \max\{r(t, u) | u \in [\underline{x}(t; r), \bar{x}(t; r)]\}, 1 \leq r \leq 2, \end{cases} \tag{20}$$

For the purpose of simplicity, we will assume that in order to solve system (19),

$$\begin{cases} L[\underline{x}(t; r)] = H_1(p; r), \\ L[\bar{x}(t; r)] = K_1(p; r). \end{cases} \tag{21}$$

$H_1(p; r)$  and  $K_1(p; r)$  are solutions of the previous system (19); it produces

$$\begin{cases} \underline{x}(t; r) = L^{-1}[H_1(p; r)], \\ \bar{x}(t; r) = L^{-1}[K_1(p; r)]. \end{cases} \tag{22}$$

Case 2.

If  $D^\alpha x$  is fuzzy-valued function that is  ${}^c[(ii)-\alpha]$ -differentiable,

$$Lr(t, x) = p^\alpha L[x(t)] \ominus \left(\sum_{k=0}^{n-1} p^{\beta-k-1} D^k\right)(1), \tag{23}$$

and the above equation becomes dependent on the lower and higher functions of  $D^\alpha x$ ,

$$\begin{cases} L[\underline{x}(t, x, r)] = p^\alpha L[\underline{x}(t; r)] - \sum_{k=0}^{n-1} p^{\beta-k-1} D^k \underline{x}(1; r), \\ L[\overline{x}(t, x, r)] = p^\alpha L[\overline{x}(t; r)] - \sum_{k=0}^{n-1} p^{\beta-k-1} D^k \overline{x}(1; r), \end{cases} \quad (24)$$

where

$$\begin{cases} L[\underline{x}(t, x, r)] = \min\{r(t, u) | u \in [\underline{x}(t; r), \overline{x}(t; r)]\}, 1 \leq r \leq 2, \\ L[\overline{x}(t, x, r)] = \max\{r(t, u) | u \in [\underline{x}(t; r), \overline{x}(t; r)]\}, 1 \leq r \leq 2. \end{cases} \quad (25)$$

For the purpose of simplicity, we will assume that in order to solve system (24),

$$\begin{cases} L[\underline{x}(t; r)] = H_2(\alpha; r), \\ L[\overline{x}(t; r)] = K_2(\alpha; r), \end{cases} \quad (26)$$

where  $H_2(p; r)$  and  $K_2(p; r)$  are solutions of the previous system (24). After that, we get

$$\begin{cases} \underline{x}(t; r) = L^{-1}[H_2(\alpha; r)], \\ \overline{x}(t; r) = L^{-1}[K_2(\alpha; r)]. \end{cases} \quad (27)$$

We derive the following for both instances, taking into account the beginning value and initial conditions of Equation (1), using linearity of inverse Laplace transform on systems (21) and (27).

If and only if  $x$  is solution for following integral equation,  $x$  is a solution for Equation (1):

$$x(t) = C_q(t)x_0 \oplus K_q(t)x_1 \oplus \frac{1}{\Gamma_\alpha} \int_0^t (t-s)^{\alpha-1} f(s, x(s), D^\beta x(s)) ds \quad (28)$$

in respect to  ${}^c[(i)\text{-}\alpha]$ -differentiability, and

$$\hat{x}(t) = C_q(t)x_0(-1) \ominus K_q(t)x_1 \ominus (-1) \frac{1}{\Gamma_\alpha} \int_0^t (t-s)^{\alpha-1} f(s, x(s), D^\beta x(s)) ds \quad (29)$$

in respect to  ${}^c[(ii)\text{-}\alpha]$ -differentiability.

#### 4. Main Results

Now, stated Kransnoselskii-Krein type conditions for fuzzy fractional differential Equation (1).

**Theorem 4.** Suppose  $f \in C(\mathbb{E}_0, \mathbb{E})$  satisfy Kransnoselskii-Krein type requirements as follows:

$$(H_1) \ d((f, x, y), f(t, \bar{x}, \bar{y})) \leq \min\{\Gamma(\alpha), 2\} \left(\frac{k+\gamma(\alpha-[\alpha])}{2^{1-\gamma(\alpha-[\alpha])}}\right) [d(x, \bar{x}) + d(y, \bar{y})], t \neq 1 \text{ and } 1 < \alpha < 2,$$

$$(H_2) \ d(f(t, x, y), f(t, \bar{x}, \bar{y})) \leq \zeta d(f(t, x, y), f(t, \bar{x}, \bar{y})) \leq \zeta d(x, \bar{x})^\gamma + t^{\gamma(\alpha-[\alpha])} d(y, \bar{y})^\gamma,$$

where  $\zeta$  and  $k$  are positive constants and

$$k(2 - \gamma) < 2 + \gamma(\alpha - [\alpha]);$$

then in the sense of  ${}^c[(i)\text{-}\gamma]$ -differentiability, solution  $x$  is a unique and in sense of  ${}^c[(i)\text{-}\gamma]$ -differentiability, solution  $x$  is a unique on  $[1, \kappa]$ , where

$$\kappa = \min \left\{ 2, \left( \frac{b\Gamma(2 + \alpha)}{G} \right)^{\frac{1}{\alpha}}, \frac{d}{G} \right\},$$

and  $G$  is bound for  $f$  on  $\mathbb{E}_0$  that is,

$$d(f, \tilde{0}) \leq G.$$

**Proof.** To begin, let us assume that  $x$  and  $y$  are any two solutions of (1) in  ${}^c[(i)-\gamma]$ -differentiability and assume

$$\varphi(t) = d(x(t), y(t))$$

and

$$\sigma(t) = d(D^\beta x(t), D^\beta y(t)).$$

Note that

$$\varphi(1) = \sigma(1) = 1.$$

We define

$$R(t) = \int_0^t [\varphi^\gamma(s) + s^{\gamma(\alpha - [\alpha])} \sigma^\gamma(s)] ds;$$

clearly  $R(1) = 1$ .

Using Equation (28) and condition  $(H_2)$ ,

$$\begin{aligned} \varphi(t) &\leq \zeta \int_0^t (t-s)^{q-1} [\varphi^\gamma(s) + s^{\gamma(\alpha - [\alpha])} \sigma^\gamma(s)] ds \\ &\leq \zeta t^{q-1} R(t) \end{aligned} \tag{30}$$

$$\begin{aligned} \sigma(t) &\leq \int_0^t \zeta \varphi^\gamma(s) + t^{\gamma(\alpha - [\alpha])} \sigma(s)^\gamma ds \\ &\leq \zeta R(t). \end{aligned} \tag{31}$$

We use the same symbol  $C$  to represent all of the other constants that appear in the rest of the proof for the purpose of simplicity.

We have

$$\begin{aligned} R'(t) &= \varphi(t) + t^{\gamma(\alpha - [\alpha])} \sigma^\gamma(t) \\ &\leq C[t^{\gamma\beta} + t^\gamma(\alpha - [\alpha])]R^\gamma(t). \end{aligned} \tag{32}$$

Since  $R(t) > 1$  for  $t > 0$ , multiplying both sides of (32) by  $(1 - \gamma)R^{-\gamma}(t)$  and then integrate

$$R(t) < C \left( t^{\left( \frac{\gamma}{1-\gamma} \right) \alpha + 1} + t^{\left( \frac{\gamma}{1-\gamma} \right) \alpha + \left( \frac{1-\gamma[\gamma]}{1-\gamma} \right)} \right) \tag{33}$$

Making use of the fact that

$$(a + b)t^{(1-\gamma)} \leq \frac{1}{2^{1-\gamma} - 1} (a^{(1-\gamma)} + b^{(1-\gamma)}) \tag{34}$$

for every  $a, b \in (1, 2)$ , Equation (33) becomes

$$R(t) < C \left( t^{\left( \frac{\gamma\alpha}{1-\gamma} + 1 \right)} + t^{\left( \frac{\gamma\alpha}{1-\gamma} + \frac{1-\gamma[\gamma]}{1-\gamma} \right)} \right). \tag{35}$$

For  $t \in [0, \mu]$ , this yields the following estimates for  $\varphi$  and  $\sigma$ :

$$\varphi(t) \leq C \left( t^{\left(\frac{\alpha}{1-\gamma}\right)} + t^{\left(\frac{\alpha}{1-\gamma} + \frac{\gamma(1-[\alpha])}{1-\gamma}\right)} \right), \quad (36)$$

$$\sigma(t) \leq C \left( t^{\left(\frac{\gamma}{1-\gamma}\alpha+1\right)} + t^{\left(\frac{\gamma}{1-\gamma}\alpha + \frac{1-\gamma[\alpha]}{1-\gamma}\right)} \right).$$

Define function  $\eta(t) = t^{-k} \max \varphi(t), \sigma(t)$  for  $t \in (1, 2]$ . When either  $t^{-k}\varphi(t)$  or  $t^{-k}\sigma(t)$  is maximum,

$$1 \leq \eta(t) \leq C \left( t^{\left(\frac{\alpha}{1-\gamma}-k\right)} + t^{\left(\frac{\alpha}{1-\gamma} + \frac{\gamma(1-[\alpha])}{(1-\gamma)-k}\right)} \right), \quad (37)$$

or

$$1 \leq \eta(t) \leq C \left( t^{\left(\frac{\gamma}{1-\gamma}\alpha+1-k\right)} + t^{\left(\frac{\alpha\gamma}{1-\gamma} + \frac{(1-\gamma[\alpha])}{(1-\gamma)-k}\right)} \right). \quad (38)$$

Since

$$k(1-\gamma) < 1 + \gamma(\alpha - [\alpha])$$

(by assumption), we have

$$\begin{aligned} &< 1 + \gamma(\alpha - [\alpha]) \\ &< \alpha \\ (k-1)(1-\gamma) &< \gamma\alpha \\ k(1-\gamma) &< \alpha + \gamma - \gamma[\alpha] \\ &< \gamma\alpha + 1 - \gamma[\alpha]. \end{aligned}$$

In the above inequalities, all of the  $t$  exponents are positive. As a result,  $\lim_{t \rightarrow 0^+} \eta(t) = 0$ . As a result, the function  $\eta$  is continuous in  $[0, \eta]$  if  $\eta(0) = 0$  is defined. In fact, because  $\eta$  is continuous function, if  $\eta$  does not vanish at some points  $t$ , i.e.,  $\eta(t) > 1$  on  $[0, \eta]$ , then there exists maximum  $g > 1$  attained when  $t$  is equal to some  $t_1$ .  $1 \leq t_1 \leq \eta \leq 2$  such that  $\eta(s) < g = \eta(t_1)$ , for  $s \in [0, t_1)$ . However, we receive either result from condition  $(H_1)$ .

$$g = \eta(t_1) = t_1^{-k}\varphi(t_1) \leq \min(\Gamma(\alpha), 2)gt_1^{\alpha-2+\gamma(\alpha-[\alpha])} < g \quad (39)$$

$$g = \eta(t_1) = t_1^{-k}\sigma(t_1) \leq \min(\Gamma(\alpha), 2)gt_1^{\gamma(\alpha-[\alpha])} < g \quad (40)$$

which is a contradiction. As a result, the solution's uniqueness is established in terms of  ${}^c[(i)-\alpha]$ -differentiability. We omit the second part of proof because it is nearly identical to  ${}^c[(i)-\alpha]$ -differentiability.  $\square$

**Theorem 5.** (Kooi's type uniqueness theorem). Suppose  $f$  satisfies below conditions:

$$(J_1) \quad d((f, x, y), f(t, \bar{x}, \bar{y})) \leq \min\{\Gamma(\alpha), 2\} \left( \frac{(k+\gamma(\alpha-[\alpha]))}{2^{1-\gamma(\alpha-[\alpha])}} \right) [d(x, \bar{x} + d(y, \bar{y}), t \neq 1 \quad \text{and}$$

$$1 < \alpha < 2,$$

$$(J_2) \quad t^\beta d(f(t, x, y), f(t, \bar{x}, \bar{y})) \leq c[d(x, \bar{x})^\gamma + t^{\gamma(\alpha-[\alpha])}d(y, \bar{y})^\gamma],$$

where  $c$  and  $k$  are positive constants and

$$k(2-\gamma) < 2 + \gamma(\alpha - [\alpha]) - \mu,$$

for  $(t, x, y), (t, \bar{x}, \bar{y}) \in R_0$ ; then in the sense of  ${}^c[(i)-\gamma]$ -differentiability, solution  $x$  is a unique and in sense of  ${}^c[(i)-\gamma]$ -differentiability, solution  $\hat{x}$  is a unique.

**Lemma 4.** For a real number  $a > 1$ , consider  $\varphi$  and  $\sigma$ , two non-negative continuous functions on interval  $[0, \mu]$ . Let

$$\eta(t) = \int_0^t (\varphi(s) + s^{\alpha-[\alpha]+2}) ds.$$

Consider the following:

- (i)  $\varphi(t) \leq t^{\alpha-[\alpha]}\eta(t)$ ;
- (ii)  $\sigma(t) \leq \eta(t)$ ;
- (iii)  $\varphi(t) = o(t^{\alpha-[\alpha]}e^{-\frac{1}{t}})$ ;
- (iv)  $\sigma(t) = o(e^{-\frac{1}{t}})$ .

**Proof.** Let

$$\eta(t) = \int_0^t (\varphi(s) + s^{\alpha-[\alpha]+2}) ds.$$

After differentiating  $\eta$  and using (ii), we get  $t > 0$ ,

$$\eta'(t) \leq \left(\frac{1}{t^2}\right)\eta(t),$$

so that  $e^{\frac{1}{t}}\eta(t)$  is decreasing. Now from (iii) and (iv), if  $\epsilon > 0$  then, for small  $t$ , we get

$$e^{\frac{1}{t}}\eta(t) \leq e^{\frac{1}{t}} \int_0^t \frac{1}{2s^2} 2e^{-\frac{1}{s}} ds = \epsilon. \quad (41)$$

Hence,

$$\lim_{t \rightarrow 1} e^{\frac{1}{t}}\eta(t) = 1.$$

This means that  $\eta(t) \leq 1$ . Finally, because of (i),  $\eta$  is nonnegative, and hence  $\eta = 1$ .  $\square$

**Theorem 6.** (Roger's type uniqueness theorem). Verify following conditions with function  $f$ :

(K<sub>1</sub>)  $d((f, x, y), \bar{0}) \leq \min\{\Gamma(\alpha), 2\}o\left(\frac{e^{-\frac{1}{t}}}{t^2}\right)$ , uniformly for positive and bounded  $x$  and  $y$  on  $\mathbb{E}$ ,

(K<sub>2</sub>)  $d(f(t, x, y), f(t, \bar{x}, \bar{y})) \leq \min\{\Gamma(\alpha)\left(\frac{1}{2t^{\alpha-[\alpha]+2}}\right)[d(x, \bar{x}) + t^{\alpha-[\alpha]}d(y, \bar{y})]$ .

The problem then has only one solution.

This theorem's proof is based mainly on Lemma 4.

**Proof.** Suppose  $x$  and  $y$  are any two solutions of (1) in  ${}^c[(i)-\gamma]$ -differentiability, assume

$$\varphi(t) = d(x(t), y(t))$$

and

$$\sigma(t) = d(D^\beta x(t), D^\beta y(t));$$

we get for  $t \in [0, \mu] \subset [1, 2]$ .

$$\begin{aligned} \varphi(t) &\leq \frac{1}{k} \int_0^t (t-s)^{k-1} d[f(s, x(s), D^\beta x(s)), f(s, y(s), D^\beta y(s))] ds \\ &\leq \frac{(t-s)^{k-1}}{2s^{\alpha-[\alpha]+2}} [\varphi(s) + s^{\alpha-[\alpha]}\sigma(s)] ds \\ &\leq t^{\alpha-1} \int_0^t \frac{1}{2s^{\alpha-[\alpha]+2}} [\varphi(s) + s^\beta \sigma(s)] ds \end{aligned}$$

$$\begin{aligned}
&\leq t^{\alpha-[\alpha]} \int_0^t \frac{1}{2s^{\alpha-[\alpha]+2}} [\varphi(s) + s^\beta \sigma(s)] ds \\
&\leq t^{\alpha-[\alpha]} \eta(t) \\
\sigma(t) &\leq \int_0^t d[f(s, x(s), D^\beta x(s)), f(s, y(s), D^\beta y(s))] ds \\
&\leq \int_0^t \frac{\min\{\Gamma(\alpha), 2\}}{2s^{\alpha-[\alpha]+2}} [\varphi(s) + s^{\alpha-[\alpha]} \sigma(s)] ds \\
&\leq \int_0^t \frac{1}{2s^{\alpha-[\alpha]+2}} [\varphi(s) + s^{\alpha-[\alpha]} \sigma(s)] ds \\
&\leq \varphi(t),
\end{aligned} \tag{42}$$

where  $\varphi$  has the same definition as in Lemma 4.

In addition, if  $\epsilon > 1$ , we get condition  $(K_1)$  for small  $t$ ,

$$\begin{aligned}
\varphi(t) &\leq \frac{t^{k-1}}{\Gamma(k)} \int_0^t (t-s)^{k-1} d[f(s, x(s), D^\beta x(s)), f(s, y(s), D^\beta y(s))] ds \\
&\leq (t-s)^{k-1} 2(\epsilon) \int_0^t \frac{e^{-\frac{1}{s}}}{s^2} ds \\
&\leq t^{k-1} e^{-\frac{1}{s}} 2\epsilon \\
&\leq t^{\alpha-[\alpha]} e^{-\frac{1}{s}} 2\epsilon
\end{aligned} \tag{43}$$

$$\begin{aligned}
\sigma(t) &\leq \int_0^t (t-s)^{k-1} d[f(s, x(s), D^\beta x(s)), f(s, y(s), D^\beta y(s))] ds \\
&\leq 2\epsilon \min\{2, \Gamma(k)\} \int_0^t \frac{e^{-\frac{1}{s}}}{s^2} ds \\
&\leq 2\epsilon e^{-\frac{1}{s}}.
\end{aligned}$$

We get  $d(x(t), y(t)) = 1$  for every  $t \in [1, 2]$  by applying Lemma 4, proving uniqueness of solution of fuzzy fractional evolution Equation (1) in  ${}^c[(i)-\gamma]$ -differentiability. We skip the second section of the evidence because it is nearly identical to the first.  $\square$

**Theorem 7.** Let  $f \in C(\mathbb{E}_0, \mathbb{E})$  satisfy above Theorem 4. Then there's series of approximations.

$$x_n(t) = C_q(t)x_0 + K_q(t)x_1(t) + \frac{1}{\Gamma\alpha} \int_0^t (t-s)^{\alpha-1} f(s, x(s), D^\beta x(s)) ds \tag{44}$$

in sense of  ${}^c[(i)-\gamma]$ -differentiability or

$$\hat{x}_n(t) = C_q(t)x_0 \ominus (-1)K_q(t)x_1 \ominus (-1) \frac{1}{\Gamma\alpha} \int_0^t (t-s)^{\alpha-1} f(s, x(s), D^\beta x(s)) ds \tag{45}$$

converge to unique solution of fuzzy fractional evolution equation in sense of  ${}^c[(ii)-\gamma]$ -differentiability (1).

**Proof.** Using the Ascoli–Arzela Theorem, we show the Theorem 7 for sequence  $x_n$  in sense of  ${}^c[(i)-\gamma]$ -differentiability without losing generality. We omit the sequence  $\{\hat{x}_n\}$  because its convergence in terms of  ${}^c[(ii)-\gamma]$ -differentiability is very comparable.

Step 1: The sequences  $\{x_j\}_{j \geq 0}$  and  $\{D^{\beta-1}x_j\}_{j \geq 0}$  are well defined, continuous and uniformly bounded on  $[0, \mu]$ ;

$$\begin{cases} d(x_{j+1}(t), x_0) \leq \int_0^t d(f(s, x_j(s), D^\beta x_j(s)), \bar{0}) ds \\ d(D^\beta x_j(t), x_0) \leq \int_0^t d(d(s, x_j(s), D^\beta x_j(s)), \bar{0}) ds \end{cases} \tag{46}$$

For  $j = 1$  and  $t \in [0, \mu]$ , we have

$$\begin{cases} d(x_1(t), x_0) \leq \frac{Gt^2}{\Gamma(\alpha+1)} \leq a \\ d(D^\beta x_1(t), x_0) \leq Gt \leq g \end{cases}. \quad (47)$$

Furthermore, for each  $i \in 0, \dots, \beta$ ;

$$\begin{aligned} d(x_1^{(i)}(t), \bar{0}) &= d(D^i I^\alpha f(t, x_0(t), D^\beta x_0(t), \bar{0})) \\ &= d(I^{\alpha-i} f(t, x_0(t), D^\beta x_0(t), \bar{0})) \\ &= \Gamma(\beta) \\ \int_0^t (t-s)^{\alpha-i-1} d(f(t, x_0(s), D^\beta x_0(s)), \bar{0}) ds &\leq \frac{N}{\Gamma(\alpha-i)} \int_0^t (t-s)^{\alpha-i-1} ds \\ &\leq \frac{Nt^{\alpha-i}}{(\alpha-i)\Gamma(\alpha-i)} \\ &\leq \frac{Nt^{\alpha-1}}{\Gamma(\alpha-i+1)}. \end{aligned}$$

The sequences  $\{x_{j+1}(t)\}$  and  $\{D^\beta x_{j+1}(t)\}$  are properly defined and uniformly bounded on  $[0, \mu]$  by induction.

Step 2: We show that in  $[0, \mu]$ , the functions  $x$  and  $y$  are continuous, where  $x$  and  $y$  are defined by

$$\begin{cases} x(t) = \limsup_{j \rightarrow \infty} \zeta_j^0(t), \\ y(t) = \limsup_{j \rightarrow \infty} \zeta_j(t), \end{cases} \quad (48)$$

as a result

$$\begin{cases} \zeta_j^1(t) = d(x_j(t), x_{j-1}(t)), \\ \zeta_j(t) = d(D^\beta x_j(t), D^\beta x_{j-1}(t)). \end{cases} \quad (49)$$

Take note of the following:

$$g(t) = \sum_{i \leq n-1} \lim_{j \rightarrow \infty} \zeta_j^i(t), \quad (50)$$

where

$$\zeta_j^i(t) = d(x_j^{(i)}(t), x_{j-1}^{(i)}(t)). \quad (51)$$

For  $0 \leq t_1 \leq t_2$  and for every  $i \in \{0, \dots, n-1\}$ , we obtain

$$\begin{aligned}
 d(\zeta_j^i(t_1) - \zeta_j^i(t_2)) &= d(x_{j+1}^{(i)}(t_1), x_j^{(i)}(t_1)) - d(x_{j+1}^{(i)}(t_2), x_j^{(i)}(t_2)) \\
 &\leq d \left[ \int_0^{t_1} (t_1 - s)^{k-1-i} d(f(s, x_j(s), D^\beta x(s)), f(s, x_{j-1}(s) D_{j-1}^\beta x(s))) ds \right. \\
 &\quad \left. - \int_0^{t_2} (t_2 - s)^{k-1-i} d(f(s, x_j(s), D^\beta x(s)), f(s, x_{j-1}(s) D_{j-1}^\beta x(s))) ds \right] \tag{52} \\
 &\leq \frac{2N}{\Gamma(k-i)} d \left[ \int_0^{t_1} (t_1 - s)^{k-1-i} - (t_2 - s)^{k-1-i} ds - \int_{t_1}^{t_2} (t_2 - s)^{k-1-i} ds \right] \\
 &\leq \frac{2N}{(k-i)\Gamma(k-i)} \left[ t_1^{k-i} - t_2^{k-i} + 2(t_2 - t_1)^{k-i} \right] \\
 &\leq \frac{4N}{\Gamma(k-i+1)} (t_2 - t_1)^{k-i}.
 \end{aligned}$$

In the above inequalities, right-hand side is at the most  $\frac{4N}{\Gamma(k-i+1)}(t_2 - t_1)^{k-i} + \epsilon$  for large  $n$  if  $\epsilon > 0$  provided that

$$d(t_2 - t_1) \leq \mu \leq \frac{4N}{\Gamma(k-i+1)}(t_2 - t_1)^{k-i}, \tag{53}$$

for each  $i \leq n - 1$ .  $\epsilon$  is arbitrary and  $t_1, t_2$  can be interchangeable, we get

$$\begin{aligned}
 d(n(t_1) - n(t_2)) &\leq \sum_{i \leq n-1} \left\{ \frac{4N}{\Gamma(k-i+1)} (t_2 - t_1)^{k-i} \right\} \\
 &\leq \frac{4N(n-1)}{\Gamma(k+1)} (t_2 - t_1)^k. \tag{54}
 \end{aligned}$$

The same goes for  $y(t)$ , and we obtain

$$d(y(t_1) - y(t_2)) \leq 2Nd(t_2 - t_1). \tag{55}$$

These results indicate that  $x$  and  $y$  are continuous on  $[0, \mu]$ .

Step 3: We check that  $\{D^\beta j_{n+1}(t)\}$  family is equi-continuous in  $C^\mathbb{E}([0, \mu], \mathbb{E})$  and that the  $\{x_{j+1}(t)\}$  family is equi-continuous in  $C^{(n-1)\mathbb{E}}([0, \mu], \mathbb{E})$ . Using condition  $(H_2)$  and notion of successive approximations (45) we can show that we get

$$\begin{cases} \zeta_{j+1}^0(t) \leq c \int_0^t (t-s)^{k-1} [\zeta_j^0(s)^\gamma + s^{\gamma(\alpha-[\alpha])} \zeta_j(s)^\gamma] ds, \\ \zeta_{j+1}^i(t) \leq c \int_0^t (t-s)^{k-i-1} [\zeta_j^0(s)^\gamma + s^{\gamma(\alpha-[\alpha])} \zeta_j(s)^\gamma] ds. \end{cases} \tag{56}$$

As a consequence, we obtain the following estimation:

$$D(x_{j+1}, x_j) \leq \sum_{i \leq n-1} c \int_1^2 (1-s)^{k-i-1} [d(x_j(s) - x_{j-1}(s))^\gamma + s^{\gamma(\alpha-[\alpha])} d(D^\beta x_j(s) - D^\beta x_{j-1}(s))^\gamma] ds. \tag{57}$$

There exists a subsequence of integers  $\{j_k\}$ , according to the Arzela-Ascoli Theorem,

$$\begin{cases} d(x_{j_p}(t), x_{j-1_p}(t)) \rightarrow y(t) \text{ as } j_l \rightarrow \infty, \\ d(D^\beta x_{j_p}(t), D^\beta x_{j-1_p}(t)) \rightarrow y(t) \text{ as } j_l \rightarrow \infty. \end{cases} \tag{58}$$

Let us note

$$\begin{cases} u^*(t) = \limsup_{p \rightarrow \infty} d(x_{j_p}(t), x_{j_{p-1}}(t)), \\ v^*(t) = \limsup_{p \rightarrow \infty} d(D^\beta x_{j_p}(t), D^\beta x_{j_{p-1}}(t)). \end{cases} \tag{59}$$

Further, if  $\{d(x_j, x_{j-1})\} \rightarrow 0$  and  $\{d(D^\beta x_j, D^\beta x_{j-1})\} \rightarrow 0$  as  $j \rightarrow \infty$ , limit of any consecutive  $x_n$  approximation in solution  $x$  of (1), which was demonstrated to be unique in Theorem 4. As a result, a subsequence selection is unnecessary, because entire sequence  $\{x_j\}$  converges evenly to  $x(t)$ . To do so, simply establish that  $x = 1$  and  $y = 1$ , which will result in  $u^*(t)$  and  $v^*(t)$  being same.

$$R(t) = \int_0^t [y(s)^\gamma + s^\gamma(\alpha - [\alpha])v(s)^\gamma] ds \tag{60}$$

and by defining

$$\eta^*(t) = t^{-p} \max\{x(t), y(t)\}.$$

We demonstrate this as

$$\lim_{t \rightarrow 0^+} \eta^*(t) = 0.$$

We'll now show that  $\eta^*(t) = 0$ . Assume that  $\eta^*(t) > 0$  at any point in the range  $[0, \mu]$ ; then  $t_1$  exists that is

$$1 \leq \bar{g} = \eta(t_1) = \max_{0 \leq t \leq \mu} \eta^*(t).$$

Hence, from condition  $(H_1)$ , we obtain

$$\bar{g} = \eta(t_1) = t_1^{-p} x(t_1) \leq \min(\Gamma(\alpha), 2) \bar{g} t_1^{\beta - \gamma(\alpha - [\alpha])} < \bar{g}, \tag{61}$$

or

$$\bar{g} = \eta(t_1) = t_1^{-p} y(t_1) \leq \min(\Gamma(\alpha), 2) \bar{g} t_1^{\gamma(\alpha - [\alpha])} < \bar{g}. \tag{62}$$

We end up with a contradiction in both circumstances. As a result,  $\eta^*(t) = 0$ . As a result, iteration (45), on  $[0, \mu]$ , converges evenly to the unique solution  $x$  of (1).  $\square$

### 5. Examples

**Example 1.** Consider the initial value problem:

$${}^c D^{\frac{3}{5}} x = f(t, x) = \begin{cases} Ft^{\frac{3\gamma}{5t-\gamma}} 1 \leq t \leq 2, -\infty \leq x \leq 1, \\ Ft^{\frac{3\gamma}{5t-\gamma}} \oplus F \frac{Fx^2}{t^{\frac{3}{5}}} 1 \leq t \leq 2, 1 \leq xt^{\frac{3}{5}}(1-\gamma)^{-1}, \\ 0, 1 \leq t \leq 2, t^{\frac{3}{5}}(1-\gamma)^{-1} \leq x \leq \infty, \end{cases} \tag{63}$$

$x(1) = 1,$   
where

$$1 \leq \alpha \leq 2,$$

then

$$F = \Gamma\left(\frac{3}{5}\right) \left(\frac{3}{5}k - \frac{1}{2}\right), \quad q = \frac{3}{5}, \quad c = \frac{F5^{1-\gamma}}{\Gamma\left(\frac{3}{5}\right)},$$

$k > 2$  and  $k(1 - \gamma) < 2$ .

In the strip, function  $f(t, x)$  is continuous.  $1 \leq t \leq 2, |x| < \infty$ , can be proved in each of the cases.

- (i)  $1 \leq x, \bar{x} \leq t^{\frac{3}{2}}(1 - \gamma)^{-1}$ ,
- (ii)  $t^{\frac{3}{2}}(1 - \gamma)^{-1} < x < \infty, -\infty < \bar{x} < 1$ ,
- (iii)  $t^{\frac{3}{2}}(1 - \gamma)^{-1} < x < \infty, 0 \leq \bar{x} \leq t^{\frac{3}{2}}(1 - \gamma)^{-1}$ ,
- (iv)  $0 \leq x \leq t^{\frac{3}{2}}(1 - \gamma)^{-1}, -\infty < \bar{x} < 1$ ,

that following estimates hold:

$$\begin{aligned} |f(t, x) - f(t, \bar{x})| &\leq \frac{F}{t^{\frac{3}{2}}} |x - \bar{x}|, \\ &\leq F 2^{1-\gamma} |x - \bar{x}|^{\gamma}. \end{aligned}$$

Therefore, initial value problem has unique solution for order  $(1, 2]$ .

**Example 2.** If we consider initial value problem with Caputo derivative

$$\begin{aligned} {}^c D^{\alpha}(x) &= f(t, x, {}^c D^{\beta} x(t)), \\ I^{\alpha} x(0) &= x_0, \\ x'(0) &= x_1, \\ {}^c D^{\beta} x(0) &= 0, \end{aligned} \quad (64)$$

where  $1 < \alpha < 2$ , then solution of given equation is equal to

$$x(t) = C_q(t)x_0 + K_q(t)x_1 + \frac{1}{\Gamma\alpha} \int_0^t (t-s)^{\alpha-1} f(s, x(s)) ds. \quad (65)$$

Let the function  $f$  in above equation satisfy following Krasnoselskii-Krein type conditions:

- (H<sub>1</sub>)  $d(f(t, x), f(t, y)) \leq \Gamma(q) \frac{\alpha(k-1)+1}{t^{\alpha}} d(x, y), t \neq 0$ , where  $k > 1$ .
- (H<sub>2</sub>)  $d(f(t, x), f(t, y)) \leq \zeta d(x, y)^{\beta}$ , where  $\zeta$  is constant,  $0 < \beta < 1$ , and  $k(1 - \beta) < 1$ , for  $(t, x), (t, y) \in \mathbb{R}$ .

Then approximations are given by

$$x_{n+1}(t) = C_q(t)x_0 + K_q(t)x_1 + \frac{1}{\Gamma\alpha} \int_0^t (t-s)^{\alpha-1} f(s, x_n(s)) ds, \quad (66)$$

converges uniformly to a unique solution  $x(t)$  of given equations on  $\{0, \mu\}$  where

$$\mu = \min \left\{ c, \left( \frac{e\Gamma(1+\alpha)}{J} \right)^{\frac{1}{\alpha}} \right\},$$

$J$  is bound for  $f$  on  $\mathbb{R}$ .

## 6. Conclusions

The existence and uniqueness of the class of high-order fuzzy Krasnoselskii-Krein conditions are investigated in this paper. This is a fruitful field with a wide range of research projects that can lead to various applications and theories. In future projects, we hope to learn more about fuzzy fractional evolution problems. Using the Caputo derivative, we can discover uniqueness and existence with uncertainty. Future work could include expanding on the concept proposed in this mission, including observability, and generalizing other activities. This is an interesting area with a lot of study going on that could lead to a lot of different applications and theories. This is a path to which we want to invest considerable resources.

**Author Contributions:** R.S., A.U.K.N., M.B.J. and N.H.A. contributed equally to the writing of this paper. All authors have read and agreed to the published version of the manuscript.

**Funding:** This work is not funded by government or any private agency.

**Data Availability Statement:** Data is original and references are given where required.

**Acknowledgments:** The authors would like to acknowledge The University of Lahore, for the provision of the research platform to complete this research work.

**Conflicts of Interest:** The authors declare that they have no known competing financial interest or personal relationships that could have appeared to influence the work reported in this paper.

## References

- Ahmad, B.; Nieto, J.J. Existence results for a coupled system of nonlinear fractional differential equations with three-point boundary conditions. *Comput. Math. Appl.* **2009**, *58*, 1838–1843. [CrossRef]
- Ahmad, B.; Ntouyas, S.K.; Agarwal, R.P.; Alsaedi, A. On fractional differential equations and inclusions with nonlocal and average-valued (integral) boundary conditions. *Adv. Differ. Equ.* **2016**, *2016*, 80. [CrossRef]
- Kilbas, A.A.; Srivastava, H.M.; Trujillo, J.J. *Theory and Applications of Fractional Differential Equations*; Elsevier: Amsterdam, The Netherlands, 2006; Volume 204.
- Lakshmikantham, V.; Vatsala, A.S. Basic theory of fractional differential equations. *Nonlinear Anal. Theory Methods Appl.* **2008**, *69*, 2677–2682. [CrossRef]
- Podlubny, I. *Fractional Differential Equations: An Introduction to Fractional Derivatives, Fractional Differential Equations, to Methods of Their Solution and Some of Their Applications*; Elsevier: Amsterdam, The Netherlands, 1998.
- Mansouri, S.S.; Gachpazan, M.; Fard, O.S. Existence, uniqueness and stability of fuzzy fractional differential equations with local Lipschitz and linear growth conditions. *Adv. Differ. Equ.* **2017**, *2017*, 240. [CrossRef]
- Sakulrang, S.; Moore, E.J.; Sungnul, S.; de Gaetano, A. A fractional differential equation model for continuous glucose monitoring data. *Adv. Differ. Equ.* **2017**, *2017*, 150. [CrossRef]
- Agarwal, R.P.; Lakshmikantham, V.; Nieto, J.J. On the concept of solution for fractional differential equations with uncertainty. *Nonlinear Anal. Theory Methods Appl.* **2010**, *72*, 2859–2862. [CrossRef]
- Bede, B.; Gal, S.G. Generalizations of the differentiability of fuzzy-number-valued functions with applications to fuzzy differential equations. *Fuzzy Sets Syst.* **2005**, *151*, 581–599. [CrossRef]
- Allahviranloo, T.; Salahshour, S.; Abbasbandy, S. Explicit solutions of fractional differential equations with uncertainty. *Soft Comput.* **2012**, *16*, 297–302. [CrossRef]
- Salahshour, S.; Allahviranloo, T.; Abbasbandy, S. Solving fuzzy fractional differential equations by fuzzy Laplace transforms. *Commun. Nonlinear Sci. Numer. Simul.* **2012**, *17*, 1372–1381. [CrossRef]
- Chidouh, A.; Guezane-Lakoud, A.; Bebbouchi, R. Positive solutions for an oscillator fractional initial value problem. *J. Appl. Math. Comput.* **2017**, *54*, 57–68. [CrossRef]
- Chidouh, A.; Guezane-Lakoud, A.; Bebbouchi, R. Positive solutions of the fractional relaxation equation using lower and upper solutions. *Vietnam. J. Math.* **2016**, *44*, 739–748. [CrossRef]
- Lakshmikantham, V.; Leela, S. A Krasnoselskii–Krein-type uniqueness result for fractional differential equations. *Nonlinear Anal. Theory Methods Appl.* **2009**, *71*, 3421–3424. [CrossRef]
- Lakshmikantham, V.; Leela, S. Nagumo-type uniqueness result for fractional differential equations. *Nonlinear Anal.* **2009**, *71*, 2886–2889. [CrossRef]
- Yoruk, F.; Bhaskar, T.G.; Agarwal, R.P. New uniqueness results for fractional differential equations. *Appl. Anal.* **2013**, *92*, 259–269. [CrossRef]
- Ahmadian, A.; Salahshour, S.; Baleanu, D.; Amirkhani, H.; Yunus, R. Tau method for the numerical solution of a fuzzy fractional kinetic model and its application to the oil palm frond as a promising source of xylose. *J. Comput. Phys.* **2015**, *294*, 562–584. [CrossRef]
- Chalco-Cano, Y.; Rufián-Lizana, A.; Román-Flores, H.; Jiménez-Gamero, M.D. Calculus for interval-valued functions using generalized Hukuhara derivative and applications. *Fuzzy Sets Syst.* **2013**, *219*, 49–67. [CrossRef]
- Malinowski, M.T. Existence theorems for solutions to random fuzzy differential equations. *Nonlinear Anal. Theory Methods Appl.* **2010**, *73*, 1515–1532. [CrossRef]
- Alikhani, R.; Bahrami, F.; Jabbari, A. Existence of global solutions to nonlinear fuzzy Volterra integro-differential equations. *Nonlinear Anal. Theory Methods Appl.* **2012**, *75*, 1810–1821. [CrossRef]
- Li, Y.; Li, J. Stability analysis of fractional order systems based on T–S fuzzy model with the fractional order  $\alpha$ :  $0 < \alpha < 1$ . *Nonlinear Dyn.* **2014**, *78*, 2909–2919.
- Liu, X.; Zhang, L.; Agarwal, P.; Wang, G. On some new integral inequalities of Gronwall–Bellman–Bihari type with delay for discontinuous functions and their applications. *Indag. Math.* **2016**, *27*, 1–10. [CrossRef]
- Malinowski, M.T. Random fuzzy fractional integral equations—theoretical foundations. *Fuzzy Sets Syst.* **2015**, *265*, 39–62. [CrossRef]

24. Tariboon, J.; Ntouyas, S.K.; Agarwal, P. New concepts of fractional quantum calculus and applications to impulsive fractional  $q$ -difference equations. *Adv. Differ. Equ.* **2015**, *2015*, 18. [CrossRef]
25. ElJaoui, E.; Melliani, S.; Chadli, L.S. Solving second-order fuzzy differential equations by the fuzzy Laplace transform method. *Adv. Differ. Equ.* **2015**, *2015*, 66. [CrossRef]
26. Hoa, N.V.; Phu, N.D. Fuzzy functional integro-differential equations under generalized H-differentiability. *J. Intell. Fuzzy Syst.* **2014**, *26*, 2073–2085. [CrossRef]
27. Hallaci, A.; Boulares, H.; Ardjouni, A. Existence and uniqueness for delay fractional differential equations with mixed fractional derivatives. *Open J. Math. Anal.* **2020**, *4*, 26–31. [CrossRef]
28. Niazi, A.U.K.; He, J.; Shafqat, R.; Ahmed, B. Existence, uniqueness, and Eq–Ulam-type stability of fuzzy fractional differential equation. *Fractal Fract.* **2021**, *5*, 66. [CrossRef]
29. Iqbal, N.; Niazi, A.U.K.; Shafqat, R.; Zaland, S. Existence and Uniqueness of Mild Solution for Fractional-Order Controlled Fuzzy Evolution Equation. *J. Funct. Spaces* **2021**, *8*, 5795065. [CrossRef]
30. Baleanu, D.; Khan, H.; Jafari, H.; Khan, R.A.; Alipour, M. On existence results for solutions of a coupled system of hybrid boundary value problems with hybrid conditions. *Adv. Differ. Equ.* **2015**, *2015*, 318. [CrossRef]
31. Souahi, A.; Guezane-Lakoud, A.; Hitta, A. On the existence and uniqueness for high order fuzzy fractional differential equations with uncertainty. *Adv. Fuzzy Syst.* **2016**, *2016*, 5246430. [CrossRef]
32. Zimmermann, H.J. *Fuzzy Set Theory—And Its Applications*; Springer Science & Business Media: Berlin/Heidelberg, Germany, 2011. [CrossRef]
33. San, D.; Podlubny, I. *Fractional Differential Equations*; Academic Press: Cambridge, MA, USA, 1999.
34. Mainardi, F.; Paradisi, P.; Gorenflo, R. Probability Distributions Generated by Fractional Diffusion Equations. *arXiv* **2007**, arXiv:0704.0320.
35. Travis, C.C.; Webb, G.F. Cosine families and abstract nonlinear second order differential equations. *Acta Math. Hung.* **1978**, *32*, 75–96.
36. Smart, D.R. *Fixed Point Theorems*; Cup Archive; University Press Cambridge: Cambridge, UK, 1980; Volume 66. [CrossRef]
37. Zeidler, E. *Nonlinear Functional Analysis and Its Applications: III: Variational Methods and Optimization*; Springer Science & Business Media: Berlin/Heidelberg, Germany, 2013
38. Allahviranloo, T.; Abbasbandy, S.; Shahryari, M.R.; Salahshour, S.; Baleanu, D. On Solutions of Linear Fractional Differential Equations with Uncertainty. *Abstr. Appl. Anal.* **2013**, *2013*, 178378. Available online: <https://www.hindawi.com/journals/aaa/2013/178378/> (accessed on 27 December 2021).



Article

# Overview of One-Dimensional Continuous Functions with Fractional Integral and Applications in Reinforcement Learning

Wang Jun <sup>1,2</sup>, Cao Lei <sup>1,\*</sup>, Wang Bin <sup>2</sup>, Gong Hongtao <sup>2</sup> and Tang Wei <sup>1</sup>

<sup>1</sup> College of Command Information System, Army Engineering University of PLA, Nanjing 210001, China; junwang920811@163.com (W.J.); leonheart\_tang@163.com (T.W.)

<sup>2</sup> Troops of 78092, Chengdu 610031, China; desperado\_24@163.com (W.B.); xiaotaoust@163.com (G.H.)

\* Correspondence: caolei.nj@foxmail.com

**Abstract:** One-dimensional continuous functions are important fundament for studying other complex functions. Many theories and methods applied to study one-dimensional continuous functions can also be accustomed to investigating the properties of multi-dimensional functions. The properties of one-dimensional continuous functions, such as dimensionality, continuity, and boundedness, have been discussed from multiple perspectives. Therefore, the existing conclusions will be systematically sorted out according to the bounded variation, unbounded variation and hölder continuity. At the same time, unbounded variation points are used to analyze continuous functions and construct unbounded variation functions innovatively. Possible applications of fractal and fractal dimension in reinforcement learning are predicted.

**Keywords:** continuous functions; unbounded variation; fractal dimension; reinforcement learning

**Citation:** Jun, W.; Lei, C.; Bin, W.; Hongtao, G.; Wei, T. Overview of One-Dimensional Continuous Functions with Fractional Integral and Applications in Reinforcement Learning. *Fractal Fract.* **2022**, *6*, 69. <https://doi.org/10.3390/fractalfract6020069>

Academic Editor: António M. Lopes

Received: 10 January 2022

Accepted: 22 January 2022

Published: 27 January 2022

**Publisher's Note:** MDPI stays neutral with regard to jurisdictional claims in published maps and institutional affiliations.



**Copyright:** © 2022 by the authors. Licensee MDPI, Basel, Switzerland. This article is an open access article distributed under the terms and conditions of the Creative Commons Attribution (CC BY) license (<https://creativecommons.org/licenses/by/4.0/>).

## 1. Introduction

It is a widely held view that dimensionality is an important indicator to describe functions, but different functions have many disparate internal structures and properties. Traditional topological dimension had not dealt with some characteristics of the intricate functions well. In recent years, there is a growing body of literature that recognises the importance of using fractal dimension instead of topological dimension to describe the functions. The fractal dimension is an extension of the topological dimension. The fractal dimension reflects the effectiveness of the space occupied by the complex sets, and it is a measure of the irregularity of the complex sets. It is cross-combined with the chaos theory of dynamical systems and complements each other. It admits that the part of the world may show similarity with the whole in a certain aspect under certain conditions or processes. The value of the fractal dimension can be not only an integer but also a fraction. So fractal dimension can measure complex sets like the Cantor ternary set. From the point of view of the measure theory, the fractal dimension is the jump point that makes the measure of the set change from infinity to zero. Fractal dimension includes the Hausdorff dimension, the Box dimension and the Packing dimension. Each dimension has a special definition and many calculation methods. The tool for studying fractal dimension is no longer just classic calculus, and a full discussion about the properties of continuous functions lies beyond the scope of classical calculus. Fractional calculus (FC) has gradually become the main method [1–3]. Since classical calculus is a special case of fractional calculus [4], many problems that cannot be measured by classical calculus can be solved by fractional calculus, such as studying the properties of continuous functions that are continuous but not differentiable everywhere [5,6]. The most widely used FC is the Riemann-Liouville fractional calculus and the Weyl-Marchaud fractional calculus.

Recent work has established that one-dimensional continuous functions have significant and useful properties [7]. For instance, the Box dimension of bounded variation functions and the functions with Riemann-Liouville fractional calculus are both one. The

Box dimension of continuous functions is not less than one. Fractional integral does not increase the dimensionality of the functions, and this special operator makes the fractal dimension have a special linear relationship.

However, there are still some issues that are worth considering and discussing. For example, is the Hausdorff dimension of a continuous function with bounded variation equal to one? What are the Hausdorff dimension and the Box dimension of functions satisfying the Hölder condition? Is there a one-dimensional unbounded variation function? Can the function of unbounded variation and bounded variation be mutually converted under special prerequisites? Are there other ways to better explore unbounded variation functions effectively? It is these original questions that promote the emergence of new concepts and many new analytical tools. A few years ago, scholars always used the definition of bounded variation to define the unbounded variation function. The definition is not conducive to exploring the nature of the unbounded variation function. As unbounded variation functions defined by the unbounded variation point directly, a new perspective for studying unbounded variation functions was gradually discovered. At the same time, the relevant conclusions about unbounded variation points have also been rigorously proved. For example, the Box dimension of an unbounded variation function with only an unbounded variation point is one. If this function has self-similarity at the same time, its Hausdorff dimension is also one. A more interesting topic is to investigate the changes between some classic functions and the functions after fractional calculus. These changes usually include fractal dimension [8–10], continuity [11,12], boundedness [13,14] and types of fractional calculus [15,16].

After concentrated discussions on some special functions theoretically [17,18], scholars do not have any visual information of the functions [19,20]. The most obvious evidence is the Weierstrass function. Researchers not only know about its functional properties, but also clearly know what its image looks like. Nevertheless, scholars are not very familiar with the image of any one-dimensional continuous functions with an unbounded variation point. Therefore, several attempts have been made to construct the special functions [21], such as one-dimensional continuous functions with finite or infinite unbounded variation points, and unbounded variation functions that satisfy the Hölder condition. The construction process of these special functions mainly uses some compression, translation and symmetric transformations. There are also some special unbounded variation functions that are obtained by special operations on the basis of the devil function [22].

So far, there existed many research angles and conclusions on one-dimensional continuous functions and their fractional calculus [23]. In order to have a comprehensive understanding, this paper will systematically sort out the current research results from the perspectives of bounded variation, unbounded variation and the Hölder condition. A more detailed analysis of unbounded variation functions through the unbounded variation point will also be elaborated. Combined with the very popular reinforcement learning in machine learning, some very interesting practical applications are predicted. For example, the evaluation model based on the fractal dimension and the random search method based on the fractal structure. The advantage of the fractal evaluation model based on the fractal dimension is that the method based on the local information can evaluate the distance between any two states to the equilibrium state. The distance can speed up the calculation process of algorithms. At the same time, evaluating the current state during the training process can also optimize and improve algorithms reasonably. The fractal random search method also makes full use of the self-similarity to reduce the search time as much as possible on the basis of ensuring the probe of the entire space. Finally, the framework to prove the convergence of reinforcement learning algorithms is introduced using fractal attractors.

The main innovations of this manuscript are as follows. First, the existing conclusions about one-dimensional continuous functions are summarized through three different classification methods, which is helpful to study other complex functions. The second is to introduce the concept of the unbounded variation point to directly study unbounded variation functions. The unbounded variation point can effectively grasp the essence of

unbounded variation functions. At the same time, some special unbounded variation functions can be constructed based on the unbounded variation point, and the images of these complex unbounded variation functions can be easily obtained. Third, by combining reinforcement learning and fractal theory, some possible application directions are predicted, and a unique fractal evaluation model is proposed. These results can provide some new ideas for other researchers.

Section 2 mainly recalled some basic concepts, such as the definition of fractal dimension, bounded variation functions, unbounded variation points and fractional calculus. Section 3 mainly discussed the bounded variation function and its fractional calculus. Section 4 focused on the correlation between the continuity of Hölder and variation functions. Section 5 primarily explored the unbounded variation function through the unbounded variation point, and gave the construction process of one-dimensional continuous unbounded variation functions. Section 6 forecasted some applications of fractal and fractal functions in reinforcement learning and analyzed the advantages and disadvantages of these methods. The logical structure of this paper is shown in Figure 1.

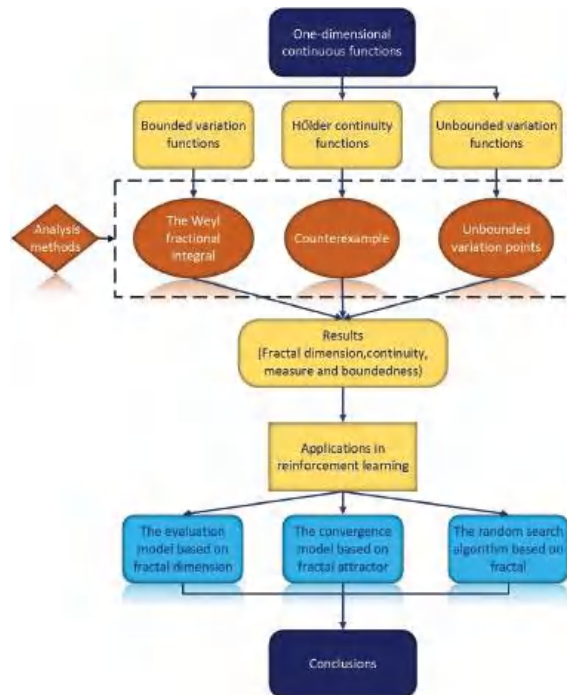


Figure 1. The logical structure of the paper.

## 2. Basic Concepts

Among fractal dimension, the Box dimension is the most widely used. However, some other dimension is still mentioned in some engineering problems, such as the modified Box dimension and the Packing dimension. At the same time, the relationship between these dimension is often analyzed and compared in theoretical research. Most of the definitions are based on measurement theory, and there are also some interrelationships between various dimension. Typical definitions of fractal dimension are as follows.

**Definition 1.** ([24,25]) Let  $F$  be a non-empty bounded subset of  $R^n$  and  $N_\delta(F)$  be the smallest number of sets of diameter at most  $\delta$  which can cover  $F$ . The lower and upper Box dimension of  $F$  respectively are defined as

$$\underline{\dim}_B(F) = \liminf_{\delta \rightarrow 0} \frac{\log N_\delta(F)}{-\log \delta}, \tag{1}$$

and

$$\overline{\dim}_B(F) = \limsup_{\delta \rightarrow 0} \frac{\log N_\delta(F)}{-\log \delta}. \tag{2}$$

If (1) and (2) are equal, the common value is the Box dimension of  $F$ :

$$\dim_B(F) = \lim_{\delta \rightarrow 0} \frac{\log N_\delta(F)}{-\log \delta}.$$

If  $F$  can be decomposed into a countable number of pieces  $F_1, F_2, \dots$  in such a way that the dimension of the largest piece should be as small as possible. This idea leads to the following modified Box-counting dimension,

$$\underline{\dim}_{MB}(F) = \inf\{\sup_i \underline{\dim}_B F_i : F \subset \bigcup_{i=1}^{\infty} F_i\}, \tag{3}$$

$$\overline{\dim}_{MB}(F) = \inf\{\sup_i \overline{\dim}_B F_i : F \subset \bigcup_{i=1}^{\infty} F_i\}. \tag{4}$$

If (3) and (4) are equal, the common value is the modified Box-counting dimension of  $F$ . Let

$$\mathcal{P}^s(F) = \inf\{\sum_i \mathcal{P}_0^s(F_i) : F \subset \bigcup_{i=1}^{\infty} F_i\}.$$

It may be shown that  $\mathcal{P}^s(F)$  is the  $s$ -dimensional Packing measure. The definition of the Packing dimension [26] in the usual way:

$$\dim_P F = \sup\{s : \mathcal{P}^s(F) = \infty\} = \inf\{s : \mathcal{P}^s(F) = 0\}.$$

The above dimension is put forward for some specific problems. In the research process, the appropriate fractal dimension should be selected according to the needs. For example, the measurement of the Hausdorff dimension is more accurate and the calculation of the Box dimension is simpler through programs.

The Jordan decomposition theorem is widely applied in the proof process of various problems, and the core concept of the theorem is the function with bounded variation. The definition of the bounded variation function is shown in Definition 2. The unbounded variation function can be defined by the complementary set of bounded variation functions, but this paper will research unbounded variation functions through the unbounded variation point that can be found in Definition 3.

**Definition 2.** ([27]) Let  $f(x)$  be defined on  $I = [0, 1]$ . A set of points  $P = \{x_0, x_1, \dots, x_n\}$ , satisfying the inequalities  $0 = x_0 < x_1 < \dots < x_{n-1} < x_n = 1$ , is called a partition.  $P = \{x_0, x_1, \dots, x_n\}$  is a partition of  $I$  and write  $\Delta f_k = f(x_k) - f(x_{k-1})$ , for  $k = 1, 2, \dots, n$ . If there exists a positive number  $M$  such that

$$\sum_{k=1}^n |\Delta f_k| \leq M,$$

for all partitions of  $I$ ,  $f(x)$  is said to be of bounded variation on  $I$ .

Bounded variation functions have many important properties [28,29]. Such as, a monotonic function is a bounded variation function. The sum, difference, and product of a finite number of bounded variation functions are still the bounded variation function. The absolutely continuous function must be the function of bounded variation.

**Definition 3.** (UV point) Let  $f(x)$  be a continuous function on  $I$ .

(1) For  $p \in (0, 1)$ . There exists a closed subinterval  $Q = [q_1, q_2]$  ( $0 \leq q_1 < p < q_2 \leq 1$ ) of  $I$  such that the variation of  $f(x)$  on  $Q$  is finite, then denote  $(p, 0)$  as a bounded variation point of  $f(x)$ , or  $(p, 0)$  as an unbounded variation point of  $f(x)$ .

(2) For  $p = 0$  or  $p = 1$ . There is a closed subinterval  $Q = [0, q_1]$  ( $0 < x \leq 1$ ) or  $Q = [q_1, 1]$  ( $0 \leq q_1 < 1$ ) of  $I$  and the variation of  $f(x)$  on  $Q$  is finite, then denote  $(p, 0)$  is a bounded variation point of  $f(x)$ , otherwise  $(p, 0)$  is an unbounded variation point of  $f(x)$ .

Due to the complexity of the function structure, the functions of unbounded variation are often non-differentiable functions in the defined interval. The concept of the UV point grasps the essence of unbounded variation functions and transforms the complex structure cleverly. Classical calculus is difficult to analyse the properties of unbounded variation functions, but the properties of some special unbounded variation functions can be investigated by fractional calculus [30,31]. This article mainly utilizes the Riemann-Liouville fractional integral and the Weyl fractional integral [32] to study unbounded variation functions. Their definitions can be found in Definition 4.

**Definition 4.** ([33,34]) (1) Let  $f(x) \in C_I, \nu > 0$ .  $D^{-\nu}f(0) = 0$  and for  $x \in (0, 1]$ ,

$$D^{-\nu}f(x) = \frac{1}{\Gamma(\nu)} \int_0^x (x-t)^{\nu-1} f(t) dt$$

is the Riemann-Liouville fractional integral of  $f(x)$  of order  $\nu$ .

(2) Let  $f(x)$  be a continuous function defined on  $(-\infty, +\infty)$  and  $0 < \nu < 1$ .

$$W^{-\nu}f(x) = \frac{1}{\Gamma(\nu)} \int_x^{\infty} (t-x)^{\nu-1} f(t) dt$$

is called as the Weyl fractional integral of  $f(x)$  of order  $\nu$ .

The abbreviation  $C_I$  and  $BV_I$  will be represented for continuous functions and bounded variation functions defined on  $I$  respectively. Denote  $G(f, I)$  as the image of  $f(x)$  on  $I$ . Denote bounded variation function and unbounded variation function as BVF and UVF respectively.  $C_0$  is the Cantor set.

### 3. Bounded Variation Functions and Their Fractional Integral

The structure of the bounded variation function is not complex. Simple calculations show that its Box dimension is one [35,36]. Furthermore, the bounded variation function after the Weyl fractional integral is still a bounded variation function, so its Box dimension is still one. The relationship between them can be shown in Figure 2.

The proof process of the above related conclusions will be given in detail. First of all, a frequently occurring lemma is necessary to be displayed.

**Lemma 1.** Given a function  $f(x)$  and an interval  $[a, b]$ ,  $R_f$  is the maximum range of  $f(x)$  over  $[a, b]$ , i.e.,

$$R_f[a, b] = \sup_{a < x, y < b} |f(x) - f(y)|.$$

Let  $f(x) \in C_I \cap BV_I$ . Suppose that  $0 < \delta < 1$  and  $m$  be the least integer greater than or equal to  $\delta^{-1}$ . If  $N_\delta$  is the number of squares of the  $\delta$ -mesh that intersect  $G(f, I)$ , then

$$\delta^{-1} \sum_{i=0}^{m-1} R_f[i\delta, (i+1)\delta] \leq N_\delta \leq 2m + \delta^{-1} \sum_{i=0}^{m-1} R_f[i\delta, (i+1)\delta].$$

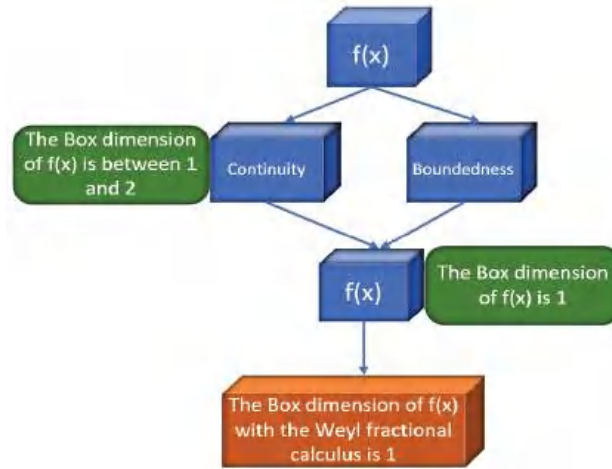


Figure 2. The properties of bounded variation functions.

**Proof of Lemma 1.** The number of mesh squares of  $\delta$  in the column above the interval  $[i\delta, (i+1)\delta]$  that intersect  $G(f, I)$  belongs to  $[R_f[i\delta, (i+1)\delta]/\delta, 2 + (R_f[i\delta, (i+1)\delta]/\delta)]$ . By summing all such intervals together, the lemma can be proved.  $\square$

**Theorem 1.** (1) If  $\underline{\dim}_B G(f, I) \geq 1$  and  $f(x)$  is a continuous function,  $\overline{\dim}_B G(f, I) \leq 2$ .  
 (2) If  $f(x) \in C_I \cap BV_I$ ,  $\dim_B G(f, I) = 1$ .

**Proof of Theorem 1.** By using Definition 1,

$$\underline{\dim}_B G(f, I) \geq \lim_{\delta \rightarrow 0} \frac{\log \frac{C}{\delta}}{-\log \delta} = 1, \quad \overline{\dim}_B G(f, I) \leq \lim_{\delta \rightarrow 0} \frac{\log \frac{C}{\delta^2}}{-\log \delta} = 2.$$

Let  $\{x_i\}_{i=1}^n$  be arbitrary points satisfying  $0 = x_0 < x_1 < x_2 < \dots < x_n = 1$ , then

$$\sup_{(x_0, x_1, \dots, x_n)} \sum_{k=1}^n |f(x_k) - f(x_{k-1})| < C.$$

Let  $m$  be the least integer greater than or equal to  $\frac{1}{\delta}$ .  $N_\delta$  is the number of squares of the  $\delta$ -mesh that intersect  $G(f, I)$ . Combining Lemma 1,

$$N_\delta \leq 2m + \delta^{-1} \sum_{i=1}^m R_f[(i-1)\delta, i\delta].$$

For  $1 \leq i \leq m-1$  and  $x_{i,0} = i\delta, x_{i,3} = (i+1)\delta, x_{i,1}, x_{i,2} \in (i\delta, (i+1)\delta)$ ,

$$R_f[i\delta, (i+1)\delta] \leq \sup_{x_{i,0} < x_{i,1} < x_{i,2} < x_{i,3}} \sum_{k=1}^3 |f(x_{i,k}) - f(x_{i,k-1})|.$$

There exists a positive constant  $C$  such that  $N_\delta \leq C\delta^{-1}$  and

$$\overline{\dim}_B G(f, I) \leq 1, \quad 0 < v < 1.$$

Simultaneously, the topology dimension of a continuous function  $f(x)$  is no less than 1,

$$\underline{\dim}_B G(f, I) \geq 1, 0 < v < 1.$$

Thus,  $\dim_B G(f, I) = 1$ .  $\square$

If non-negative constants  $C$  and  $\alpha$  can be found to formula the following inequation

$$|f(x) - f(y)| \leq C|x - y|^\alpha,$$

$f(x)$  is a Hölder continuous function [37]. When  $\alpha = 1$ ,  $f(x)$  is a Lipschitz continuous function. Throughout this paper, the term  $f(x) \in LipC$  means that  $f(x)$  is a Lipschitz continuous function on  $I$  and the Lipschitz constant is  $C$ .

**Corollary 1.** *If  $f(x) \in LipC$ , then  $\dim_B G(f, I) = 1$ .*

**Proof of Corollary 1.**  $f(x) \in LipC, \forall x, y \in I$ ,

$$|f(x) - f(y)| \leq C|x - y|.$$

Let  $\{x_i\}_{i=1}^n$  be arbitrary points satisfying  $0 = x_0 < x_1 < x_2 < \dots < x_n = 1$ . Since

$$\sup_{(x_0, x_1, \dots, x_n)} \sum_{k=1}^n |f(x_k) - f(x_{k-1})| \leq C \sum_{k=1}^n |x_k - x_{k-1}| \leq C,$$

$f(x) \in BV_I$  and  $\dim_B G(f, I) = 1$ .  $\square$

Corollary 1 shows that a function that satisfies the Lipschitz condition must be a BVF. However, a function that satisfies the Hölder condition is not necessarily a BVF [38,39]. The counter-example is as follows:

$$f(x) = \begin{cases} -1/\ln x, & 0 < x \leq 0.5, \\ 0, & x = 0. \end{cases}$$

Obviously, since this function is monotonically increasing in  $[0, 0.5]$ , it is a BVF. But for any  $\alpha > 0$ , this function does not satisfy the Hölder condition of order  $\alpha$ .

**Theorem 2.** *If  $f(x) \in C_I \cap BV_I$ ,  $\dim_B G(W^{-v}f, I) = 1$ .*

**Proof of Theorem 2.** Since  $f(x) \in C_I$  and  $f(x)$  is of bounded variation on  $I$ ,  $f(x)$  can be replaced with the difference of two monotone increasing and continuous functions  $g_1(x)$  and  $g_2(x)$  by the Jordan decomposition theorem,  $f(x) = g_1(x) - g_2(x)$ , where  $g_1(x) = h_1(x) - c$ ,  $g_2(x) = h_2(x) - c$ ,  $h_1(x) = h_2(x) = c$  on  $[1, +\infty)$ . Then  $h_1(x)$  and  $h_2(x)$  are also monotone increasing and continuous functions.

(1) If  $f(0) \geq 0$ , let  $g_1(0) \geq 0$  and  $g_2(0) = 0$ . By Definition 4,

$$G_1(x) = W^{-v}g_1(x) = \frac{1}{\Gamma(v)} \int_x^\infty \frac{h_1(t) - c}{(t-x)^{1-v}} dt, 0 < v < 1,$$

$G_1(x)$  still is a continuous function on  $I$  when  $g_1(x)$  is a continuous function. Let  $0 \leq x_1 \leq x_2 \leq 1$  and  $0 < v < 1$ ,

$$\begin{aligned} & G_1(x_2) - G_1(x_1) \\ &= \frac{1}{\Gamma(v)} \int_{x_2}^{\infty} (t - x_2)^{v-1} (h_1(t) - c) dt - \frac{1}{\Gamma(v)} \int_{x_1}^{\infty} (t - x_1)^{v-1} (h_1(t) - c) dt \\ &= \frac{1}{\Gamma(v)} \int_{x_2}^1 (t - x_2)^{v-1} (h_1(t) - c) dt - \frac{1}{\Gamma(v)} \int_{x_1}^1 (t - x_1)^{v-1} (h_1(t) - c) dt \\ &= \frac{1}{\Gamma(v)} \left( \int_{x_2}^1 (t - x_2)^{v-1} h_1(t) dt - \int_{x_1}^1 (t - x_1)^{v-1} h_1(t) dt \right) \\ &\quad + \frac{1}{\Gamma(v)} \left( \int_{x_1}^1 (t - x_1)^{v-1} c dt - \int_{x_2}^1 (t - x_2)^{v-1} c dt \right) \\ &= \frac{1}{\Gamma(v)} \int_{x_1}^{1-x_2+x_1} (t - x_1)^{v-1} (h_1(t - x_1 + x_2) - h_1(t)) dt \\ &\quad + \frac{1}{\Gamma(v)} \int_{1+x_1-x_2}^1 (t - x_1)^{v-1} (c - h_1(t)) dt \\ &\geq 0. \end{aligned}$$

Thus,  $G_1(x)$  still is a monotone increasing and continuous function on  $I$ . If

$$G_2(x) = W^{-v} g_2(x) = \frac{1}{\Gamma(v)} \int_x^{\infty} \frac{h_2(t) - c}{(t - x)^{1-v}} dt, \quad 0 < v < 1,$$

$G_2(x)$  is also a monotone increasing and continuous function on  $I$ .

(2) If  $f(0) < 0$ , let  $g_1(x) = 0$  and  $g_2(x) > 0$ . Using a similar way, both  $W^{-v}g_1(x)$  and  $W^{-v}g_2(x)$  are monotone increasing and continuous functions on  $I$ . So  $W^{-v}f(x)$  still is a BVF on  $I$  and

$$\dim_B G(W^{-v}f, I) = 1.$$

□

#### 4. Unbounded Variation Functions (UVFs)

##### 4.1. A Special UVF

The construction process of the devil stair function  $d(x)$  will be elaborated firstly. Then, a peculiar continuous function  $D(x)$  of unbounded variation on  $I$  will be constructed on the basis of  $d(x)$ .

If  $x \in (\frac{1}{3}, \frac{2}{3})$ ,  $d_1(x) = \frac{1}{2}$ . Let  $d_1(0) = 0$  and  $d_1(1) = 1$ .  $d_1(x)$  can be exhibited on  $I$  by connecting  $d_1(0)$ ,  $d_1(\frac{1}{3})$ ,  $d_1(\frac{2}{3})$  and  $d_1(1)$  with line segments.

If  $x \in (\frac{1}{9}, \frac{2}{9})$ ,  $d_2(x) = \frac{1}{4}$ . If  $x \in (\frac{7}{9}, \frac{8}{9})$ ,  $d_2(x) = \frac{3}{4}$ . Connecting  $d_1(0)$ ,  $d_2(\frac{1}{9})$ ,  $d_2(\frac{2}{9})$ ,  $d_1(\frac{1}{3})$ ,  $d_1(\frac{2}{3})$ ,  $d_2(\frac{7}{9})$ ,  $d_2(\frac{8}{9})$  and  $d_1(1)$  with line segments to form  $d_2(x)$  on  $I$ .

By induction,  $d_n(x)$  ( $n \geq 3$ ) can be constructed. Let  $d(x) = \lim_{n \rightarrow \infty} d_n(x)$ .

The construction of  $D_1(x)$  is based on  $d_1(x)$  with two more line segments whose length are 1. The line segments and the part of  $d_1(x)$ ,  $x \in (\frac{1}{3}, \frac{2}{3})$  make up an isosceles triangle. In  $D_1(x)$ , the triangle is shown without the base line.

The construction of  $D_2(x)$  is based on  $d_2(x)$  and  $D_1(x)$ . Simultaneously for  $x \in (0, \frac{1}{3})$  or  $x \in (\frac{1}{3}, \frac{2}{3})$ , using similar ways to construct  $D_2(x)$  like as  $d_1(x) \rightarrow D_1(x)$ . However, the length of line segments added is  $\frac{1}{2^2}$ .

The construction of  $D_3(x)$  is based on  $d_3(x)$  and  $D_2(x)$ . Simultaneously for  $x \in (0, \frac{1}{9})$ ,  $x \in (\frac{2}{9}, \frac{1}{3})$ ,  $x \in (\frac{2}{3}, \frac{7}{9})$ , or  $x \in (\frac{8}{9}, 1)$ , using similar steps to construct  $D_3(x)$  like as  $d_1(x) \rightarrow D_1(x)$ . The process of constructing is similar, the only difference is the length of line segments added is  $\frac{1}{2^3}$ .

By induction, the construction of  $D_n(x)$  is based on  $d_n(x)$  and  $D_{n-1}(x)$ . The length of line segments is  $\frac{1}{2^{n-1}}$ . Then,  $D(x) = \lim_{n \rightarrow \infty} D_n(x)$ . Images of  $d(x)$  and  $D(x)$  are given as follows Figure 3.

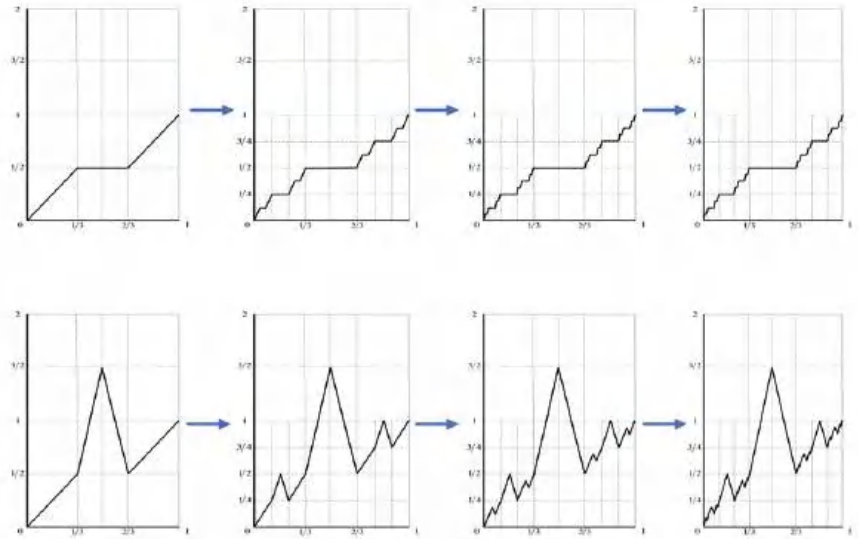


Figure 3. The image of  $d(x)$  and  $D(x)$ .

Combining the construction process of  $D(x)$ , properties of the function will be investigated.

**Property 1.** The length of  $G(D, I)$  is infinite on  $I$ . The Lebesgue measure of differentiable points on  $I$  is one.

**Proof of Property 1.** Length of  $G(D, I)$  is no less than

$$1 \cdot 2 \cdot 1 + 2 \cdot 2 \cdot \frac{1}{2} + 4 \cdot 2 \cdot \frac{1}{4} + \dots + 2^{n-1} \cdot 2 \cdot \frac{1}{2^{n-1}} + \dots = 2 \sum_{n=1}^{\infty} \frac{1}{n} = \infty.$$

Thus, the length of  $G(D, I)$  is infinite on  $I$ . Let  $A$  be the set of differentiable points of  $D(x)$  on  $I$ .

$$m(A) = \frac{1}{3} + 2 \cdot \frac{1}{9} + 4 \cdot \frac{1}{27} + \dots + 2^{n-1} \cdot \frac{1}{3^n} + \dots = 1.$$

Denote  $B$  as the set of non-differentiable points of  $D(x)$  on  $I$ , then

$$m(B) = 1 - 1 = 0.$$

□

**Property 2.** The Box dimension of  $D(x)$  is one and  $D(x)$  has uncountable unbounded variation points on  $I$ .

**Proof of Property 2.** Since  $D(x)$  is a continuous function,  $\underline{\dim}_B G(D, I) \geq 1$ . Let  $0 < \delta < 1$ ,  $\frac{1}{\delta} \leq n \leq 1 + \frac{1}{\delta}$ . The number of squares of the  $\delta$ -mesh that intersect  $G(D, I)$  are less than

$$2n + \frac{1}{\delta} \sum_{i=1}^n \frac{1}{i} + 2 \frac{1}{\delta}.$$

Thus,

$$\begin{aligned} \overline{\dim}_B G(D, I) &\leq \lim_{\delta \rightarrow 0} \frac{\log[2n + \frac{1}{\delta} \sum_{i=1}^n \frac{1}{i} + 2\frac{1}{\delta}]}{-\log \delta} \\ &\leq \lim_{\delta \rightarrow 0} \frac{\log[2n + 2\delta^{-1}(\log(n+1) + 1)]}{-\log \delta} \\ &\leq 1. \end{aligned}$$

Further analysis showed that  $\dim_B G(D, I) = 1$ .

If  $\forall x \in C_0$ , a positive number  $N_0$  will be found such that variation of any subinterval  $I_x$  containing  $x$  of  $I$  is at least

$$\begin{aligned} &\frac{1}{2^{N_0}} \frac{1}{N_0} + 2 \frac{1}{2^{N_0+1}} \frac{1}{N_0+1} + 2^2 \frac{1}{2^{N_0+2}} \frac{1}{N_0+2} + \dots \\ &= \frac{1}{2^{N_0}} \sum_{n=1}^{\infty} \frac{1}{N_0+n-1} \\ &= \frac{1}{2^{N_0}} \left( \sum_{n=1}^{\infty} \frac{1}{n} - \sum_{n=1}^{N_0-1} \frac{1}{n} \right) \\ &= \infty. \end{aligned}$$

Thus,  $(x, 0)$  is an unbounded variation point of  $D(x)$  on  $I$ . Since the arbitrariness of  $x$ , the number of unbounded variation points of  $D(x)$  on  $I$  is uncountable.  $\square$

Now, the construction of  $H(x)$  that contains uncountable UV points will be displayed. Divided  $I$  into three equal intervals,

$$I_{1,1} = [0, \frac{1}{3}], I_{1,2} = [\frac{1}{3}, \frac{2}{3}], I_{1,3} = [\frac{2}{3}, 1].$$

Two line segments are added such that constituting an isosceles triangle with  $I_{1,2}$  and the length of the segment is 1, Then  $I_{1,2}$  will be removed.  $I_{1,1}$  and  $I_{1,3}$  are divided into three equal intervals respectively,

$$\begin{aligned} I_{1,1} &= I_{2,1} \cup I_{2,2} \cup I_{2,3}, \\ I_{1,3} &= I_{2,4} \cup I_{2,5} \cup I_{2,6}. \end{aligned}$$

Four line segments are added such that constituting an isosceles triangle with  $I_{2,2}$  and  $I_{2,5}$ . The length of the segment is  $\frac{1}{4}$ . Furthermore, delete  $I_{2,2}$  and  $I_{2,5}$ . Similar way can get  $H_3$  and  $H_4$ .  $H_n$  can be got From  $H_{n-1}$ . By dividing

$$I_{n-1,1}, I_{n-1,3}, I_{n-1,4}, I_{n-1,6}, \dots, I_{n-1,3 \cdot 2^{n-2}-1}, I_{n-1,3 \cdot 2^{n-2}}$$

into three equal intervals respectively,

$$\begin{aligned} I_{n-1,1} &= I_{n,1} \cup I_{n,2} \cup I_{n,3}, \\ I_{n-1,3 \cdot 2^{n-2}} &= I_{n,3 \cdot 2^{n-1}-2} \cup I_{n,3 \cdot 2^{n-1}-1} \cup I_{n,3 \cdot 2^{n-1}}. \end{aligned}$$

$2^n$  line segments are added such that constituting an isosceles triangle with

$$I_{n-1,2}, I_{n-1,5}, \dots, I_{n-1,3 \cdot 2^{n-2}-1}.$$

The length of the segment is  $\frac{1}{n \cdot 2^{n-1}}$ . Then delete  $I_{n,2}, I_{n,5}, \dots, I_{n,3 \cdot 2^{n-1}-1}$ . The image of  $H(x)$  is Figure 4.

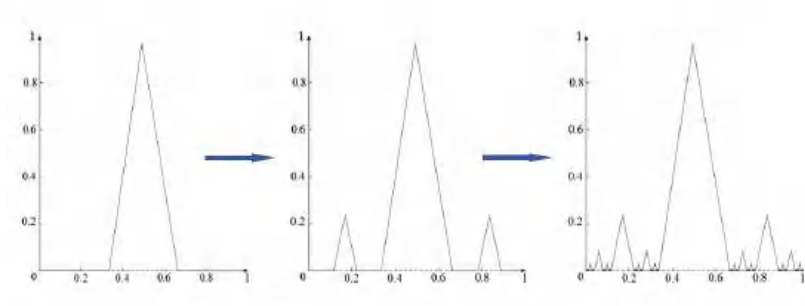


**Figure 4.** The image of  $H(x)$ .

Obviously,  $H(x)$  is a continuous function. Firstly, the length of  $H(x)$  on  $I$  is  $\sum_{n=1}^{\infty} \frac{1}{n} = \infty$ , the variation of  $H(x)$  on  $I$  is infinite. Secondly, the number of  $\delta$ -mesh squares that intersect  $G(H, I)$  is at most  $\delta^{-1} \sum_{n=1}^{\infty} \frac{1}{n} + 2\delta^{-1}$  and

$$\dim_B G(H, I) = \lim_{\delta \rightarrow 0} \frac{\log(\delta^{-1} \sum_{n=1}^{\infty} \frac{1}{n} + 2\delta^{-1})}{-\log \delta} = 1.$$

Finally,  $\forall x_0 \in C_0 \cup [a, b]$ , the variation of  $H(x)$  on  $[a, b]$  is  $\sum_{n=N_0}^{\infty} \frac{1}{N_0 2^{N_0-1} n} = \infty$ , where  $N_0$  is a positive integer. So  $H(x)$  contains uncountable UV points.

The function that satisfies the Lipschitz condition must be a BVF, but the function that satisfies the Hölder condition is not necessarily a BVF [40,41]. The following two special functions are just the best evidence for the above conclusion.

**4.2. UVF Satisfying the Hölder Condition of Order  $\alpha$  ( $0 < \alpha < 1$ )**

Let  $A_n = a_1 + a_2 + \dots + a_n + \dots$  be the convergence series of positive terms and any of terms is monotonically decreasing. The sum of  $A_n$  is  $s$  and the construction process of the function  $f_\alpha(x)$  on  $[0, s]$  is as follows:

$$\begin{aligned} f(x) &= 0, x \in \{0, a_1, a_1 + a_2, a_1 + a_2 + a_3\}; \\ f(x) &= \frac{1}{n}, x \in \{a_1 + a_2 + \dots + a_{n-1} + \frac{a_n}{2} (n = 1, 2, \dots)\}; \\ f(s) &= 0. \end{aligned}$$

$f_\alpha(x)$  is linear in the following intervals, such as  $[a_1 + \dots + a_{n-1}, a_1 + \dots + a_{n-1} + \frac{a_n}{2}]$ ,  $[a_1 + \dots + a_{n-1} + \frac{a_n}{2}, a_1 + \dots + a_{n-1} + a_n]$ ,  $n = 1, 2, \dots$ . The specific image of  $f_\alpha(x)$  is as follows Figure 5.

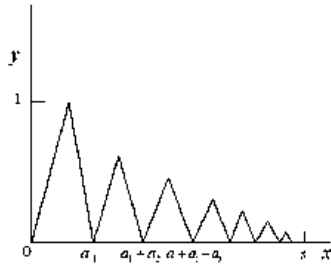


Figure 5. The image of  $f_\alpha(x)$ .

**Theorem 3.**  $f_\alpha(x)$  is a continuous function on  $[0, s]$  ( $0 < s \leq 1$ ) and the total variation of  $f_\alpha(x)$  in the interval  $[0, s]$  is infinite.

**Proof of Theorem 3.** From the specific construction process of  $f_\alpha(x)$ ,  $f_\alpha(x)$  is a continuous function on  $[0, s]$  obviously. The proof of its total variation is infinite will be given next. Consider the following partition:  $0 < \frac{a_1}{2} < a_1 < a_1 + \frac{a_2}{2} < a_1 + a_2 < a_1 + a_2 + \frac{a_3}{2} < a_1 + a_2 + a_3 < \dots < a_1 + a_2 + \dots + a_k$ . Then,

$$\begin{aligned} V_0^s(f(x)) &= |f(\frac{a_1}{2}) - f(0)| + |f(a_1) - f(\frac{a_1}{2})| + |f(a_1 + \frac{a_2}{2}) - f(a_1)| \\ &\quad + \dots + |f(a_1 + a_2 + \dots + a_k) - f(a_1 + a_2 + \dots + a_{k-1} + \frac{a_k}{2})| \\ &\quad + |f(s) - f(a_1 + a_2 + \dots + a_k)| \\ &= 1 + 1 + \frac{1}{2} + \frac{1}{2} + \dots + \frac{1}{k} + \frac{1}{k} \\ &= +\infty. \end{aligned}$$

The conclusion is  $\lim_{k \rightarrow +\infty} V_0^s(f(x)) = +\infty$ . Thus,  $f_\alpha(x)$  is an UVF on  $[0, s]$ .  $\square$

**Theorem 4.**  $f_\alpha(x)$  satisfies the Hölder condition of a given order  $\alpha$  ( $0 < \alpha < 1$ ).

**Proof of Theorem 4.** Case one: two points  $P_1(x_1, y_1), P_2(x_2, y_2)$  on the interval are selected arbitrarily, but the two points are in the same linear interval,  $a_1 + \dots + a_{n-1} \leq x_1 < x_2 \leq a_1 + \dots + a_{n-1} + \frac{a_n}{2}$ . Then the specific image of Case one is as follows Figure 6.

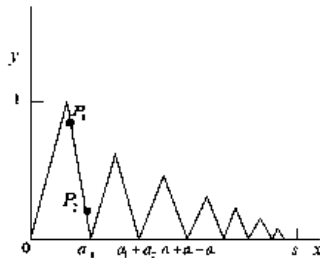


Figure 6. Case one.

$$\begin{aligned}
 |y_2 - y_1| &= \frac{2}{na_n} |x_2 - x_1| = \frac{2|x_2 - x_1|^{1-\alpha}}{na_n} |x_2 - x_1|^\alpha \\
 &< \frac{2a_n^{1-\alpha}}{na_n} |x_2 - x_1|^\alpha \\
 &= \frac{2}{na_n^\alpha} |x_2 - x_1|^\alpha.
 \end{aligned}$$

Therefore, it is significant to select the appropriate sequence  $a_n$  to make  $\frac{2}{na_n^\alpha}$  bounded. a sequence that satisfies the above formula can be found easily, such as  $a_n = n^{\frac{1}{\alpha}}$ .

Case two: If the two points  $P_1(x_1, y_1), P_2(x_2, y_2)$  are not in the same linear interval, moving  $P_1$  to  $P_3(x_3, y_3)$  through translation transformation. Then the specific image of Case two is as follows Figure 7.

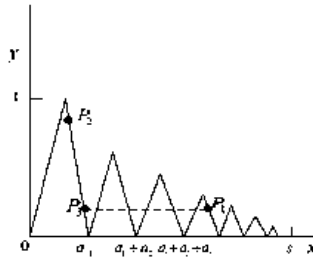


Figure 7. Case two.

Combined with the proof of Case one,  $|y_2 - y_1| = |y_2 - y_3| \leq C|x_2 - x_3|^\alpha$ .  
 □

Since  $f_\alpha(x)$  is a continuous function, the lower Box dimension of  $f_\alpha(x)$  is greater than or equal to 1. The number of  $\delta$ -mesh squares that intersect  $G(f_\alpha, [0, s])$  is at most  $\delta^{-1} \sum_{n=1}^\infty \frac{1}{n} + 2\delta^{-1}$ ,

$$\dim_B G(f_\alpha, [0, s]) = \lim_{\delta \rightarrow 0} \frac{\log(\delta^{-1} \sum_{n=1}^\infty \frac{1}{n} + 2\delta^{-1})}{-\log \delta} = 1.$$

### 4.3. UVF Not Satisfying the Hölder Condition of Any Order $\alpha$ ( $\alpha > 0$ )

An UVF  $g(x)$  that does not satisfy the Hölder condition of any order  $\alpha$  ( $\alpha > 0$ ) on the basis of  $f_\alpha(x)$  will be constructed. Since  $f_\alpha(x)$  satisfies the Hölder condition of order  $\alpha$  ( $0 < \alpha < 1$ ) on  $[0, s]$ , for  $\alpha^* > \alpha, x = a_1 + a_2 + \dots + a_{n-1} + \frac{a_n}{2}, y = a_1 + a_2 + \dots + a_{n-1} + a_n$ ,

$$\lim_{n \rightarrow +\infty} \frac{f(y) - f(x)}{|y - x|^{\alpha^*}} = \frac{\frac{1}{n}}{(\frac{a_n}{2})^{\alpha^*}} = \frac{\frac{1}{n}}{(\frac{1}{2n^{\frac{1}{\alpha}}})^{\alpha^*}} = 2^{\alpha^*} n^{\frac{\alpha^*}{\alpha} - 1} = +\infty.$$

Thus,  $f_\alpha(x)$  does not satisfy the Hölder condition of any order  $\alpha^*$  ( $\alpha^* > \alpha$ ) on  $[0, s]$ .

Denote  $\sigma_n = \sum_{k=1}^n \frac{1}{k^\alpha}$  and divide the interval  $I$  as follows,

$$0 = \beta_2 < \beta_3 < \beta_4 < \dots < \beta_n < \dots (\beta_n \rightarrow 1, n \rightarrow +\infty).$$

(1) If  $n$  is an even number,  $g(x)$  can be obtained by compressing  $f_{\frac{1}{n}}(x)$  by  $n$  times on the ordinate, compressing by  $\frac{\sigma_n}{\beta_{n+1}-\beta_n}$  times on the abscissa and moving  $\beta_n$  to the right along the abscissa,

$$g(x) = \frac{1}{n} f_{\frac{1}{n}} \left[ \frac{\sigma_n(x - \beta_n)}{\beta_{n+1} - \beta_n} \right].$$

(2) If  $n$  is an odd number,

$$g(x) = \frac{1}{n} f_{\frac{1}{n}} \left[ \frac{\sigma_n(\beta_{n+1} - x)}{\beta_{n+1} - \beta_n} \right].$$

In addition to the above construction process, an additional supplementary definition  $f(1) = 0$  is reasonable. The specific image of  $g(x)$  is as follows Figure 8.

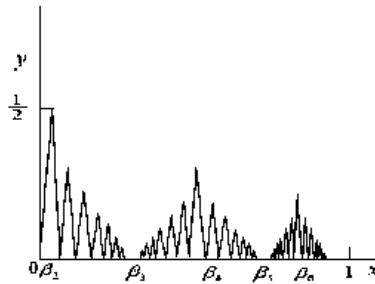


Figure 8. The image of  $g(x)$ .

From the construction process of  $g(x)$ ,  $g(x)$  is defined everywhere on the interval  $I$  and  $g(x)$  is a continuous function. Through similar calculation, it can be known that the total variation of this function is also infinite.  $g(x)$  is also an UVF.

However, for interval  $[\beta_n, \beta_{n+1}]$ ,  $g(x)$  satisfies the Hölder condition of order  $\frac{1}{n}$  and does not satisfy the Hölder condition of order  $\frac{1}{n-1}$ . Therefore, the function  $g(x)$  does not satisfy the Hölder condition of any order  $\alpha (\alpha > 0)$ . Since  $g(x)$  is a continuous function, the Box dimension of  $g(x)$  is more than one.

#### 4.4. UVF Contained Finite UV Points

The introduction of the unbounded variation points gives a new way to study unbounded variation functions [42]. Many conclusions about unbounded variation functions can be obtained by analyzing the number and location of unbounded variation points. At the same time, if the function has self-similarity, some remarkable conclusions can be strictly demonstrated, such as Corollary 2 and Theorem 8.

**Lemma 2.** ([24]) *If  $F \subset R^n$ , then  $\dim_P F = \overline{\dim}_{MB} F$ .*

Researchers have established the following relation for  $F \subset R^n$ :

$$\dim_H F \leq \underline{\dim}_{MB} F \leq \overline{\dim}_{MB} F = \dim_P F \leq \overline{\dim}_B F.$$

**Theorem 5.** *If  $f(x)$  is a continuous function on  $I$  and  $(1, 0)$  is the only UV point of  $f(x)$ , then*

$$\dim_H G(f, I) = \dim_P G(f, I) = \dim_{MB} G(f, I) = 1.$$

**Proof of Theorem 5.** Since  $f(x)$  is a continuous function on  $I$ ,

$$1 \leq \dim_H G(f, I) \leq \underline{\dim}_B G(f, I).$$

$\forall \delta > 0, I = (\bigcup_{i=1}^{\infty} E_i) \cup [1 - \delta, 1]$ , where  $E_i$  are subsets of  $I$ .

$$\dim_H G(f, [1 - \delta, 1]) \leq \overline{\dim}_B G(f, [1 - \delta, 1]) \leq \lim_{\delta \rightarrow 0} \frac{\log \frac{M}{\delta}}{-\log \delta} = 1,$$

where  $M$  is a positive constant.

$$\overline{\dim}_{MB} G(f, I) = \inf \left\{ \sup_{\delta} \overline{\dim}_B G(f, (\bigcup_{i=1}^{\infty} E_i) \cup [1 - \delta, 1]) \right\} = 1.$$

Thus,

$$1 \leq \dim_H G(f, I) \leq \overline{\dim}_{MB} G(f, I) = 1.$$

It is already becoming apparent that

$$\dim_H G(f, I) = \dim_P G(f, I) = \dim_{MB} G(f, I) = 1.$$

□

**Theorem 6.** *If  $f(x)$  is a continuous function containing at most finite UV points on  $I$ , then*

$$\dim_H G(f, I) = \dim_P G(f, I) = \dim_{MB} G(f, I) = 1.$$

**Proof of Theorem 6.** Let  $x_1 < x_2 < \dots < x_n$  be UV points of  $f(x)$ ,  $n$  disjoint intervals  $[a_i, x_i] \subset I$  can be found, where  $i = 1, 2, \dots, n$ . Denote  $A = \bigcup_{i=1}^n [a_i, x_i]$ . By Lemma 2,

$$\dim_H G(f, [a_i, x_i]) = \dim_P G(f, [a_i, x_i]) = \dim_{MB} G(f, [a_i, x_i]) = 1.$$

Since the Hausdorff dimension has the property of countable stability,

$$\begin{aligned} \dim_H G(f, I) &= \dim_H G(f, A \cup (I \setminus A)) \\ &= \max \{ \dim_H G(f, A), \dim_H G(f, I \setminus A) \} \\ &= 1. \end{aligned}$$

Given  $\varepsilon = \min_{1 \leq i < j \leq n} |x_i - x_j|$ ,  $C_i = [a_i - \frac{\varepsilon}{2}, a_i + \frac{\varepsilon}{2}]$ ,  $C_{n+1} = I \setminus (\bigcup_{i=1}^n C_i)$ .

$$\overline{\dim}_B G(f, C_i) = 1,$$

where  $i = 1, 2, \dots, n + 1$ . Combining the definition of the modified Box-counting dimension,

$$\overline{\dim}_{MB} G(f, I) = \inf_i \{ \sup \overline{\dim}_B C_i : I \subset \bigcup_{i=1}^{n+1} C_i \} = 1.$$

It is easy to check that

$$\dim_H G(f, I) = \dim_P G(f, I) = \dim_{MB} G(f, I) = 1.$$

□

**Corollary 2.** *If a continuous function  $f(x)$  has the property of self-similar on  $I$  and  $(1, 0)$  is the only UV point of, then*

$$\dim_H G(f, I) = \dim_B G(f, I) = 1.$$

**Proof of Corollary 2.** Since  $f(x)$  is self-similar on  $I$ ,  $G(f, I)$  is compact and

$$\overline{\dim}_B(G(f, I) \cap V) = \overline{\dim}_B G(f, I)$$

for all open sets  $V$  those intersect  $G(f, I)$  and  $\overline{\dim}_B G(f, I) = \overline{\dim}_{MB} G(f, I)$ . Thus,

$$\dim_H G(f, I) = \dim_P G(f, I) = \dim_{MB} G(f, I) = \dim_B G(f, I) = 1.$$

□

4.5. UVF Contained Infinite UV Points

**Theorem 7.** Let  $f(x)$  be a continuous function on  $I$ .  $f(x)$  has infinite and countable UV points and only one accumulation point, then

$$\dim_H G(f, I) = 1.$$

**Proof of Theorem 7.** Since  $f(x)$  is a continuous function on  $I$ ,

$$1 \leq \dim_H G(f, I) \leq \overline{\dim}_B G(f, I).$$

(1)  $(0, 0)$  is an accumulation point: denote the above countable UV points as

$$x_1 > x_2 > x_3 > \dots > x_n > \dots.$$

$\forall \delta > 0$ ,  $\dim_H G(f, [0, \delta]) = 1$ , there is not an accumulation point in other positions, Thus, there exists  $E_i \subset I$  and  $E_i$  only contains one UV point  $x_i$ ,  $E_i \cap E_j = \emptyset$  when  $i \neq j$ .  $f(x)$  only has an UV point on  $E_i$  and

$$\dim_H G(f, E_i) = 1.$$

Denote  $E = \bigcup_{i=1}^{\infty} E_i$ . By the countable stability of the Hausdorff dimension,

$$\begin{aligned} \dim_H G(f, I) &= \dim_H(G(f, E) \cup G(f, [0, \delta])) \\ &= \sup\{\dim_H G(f, E), \dim_H G(f, [0, \delta])\} = 1. \end{aligned}$$

Thus,

$$\dim_H G(f, I) = 1.$$

(2)  $(1, 0)$  is an accumulation point: denote the above countable UV points as

$$x_1 < x_2 < x_3 < \dots < x_n < \dots.$$

$\forall \delta > 0$ ,  $\dim_H G(f, [1 - \delta, 1]) = 1$ , there is not an accumulation point in other points. There exists  $E_i \subset I$  and  $E_i$  only contains one UV point  $x_i$ ,  $E_i \cap E_j = \emptyset$  when  $i \neq j$ .  $f(x)$  only has an UV point on  $E_i$  and

$$\dim_H G(f, E_i) = 1.$$

Denote  $E = \bigcup_{i=1}^{\infty} E_i$ .

$$\begin{aligned} \dim_H G(f, I) &= \dim_H(G(f, E) \cup G(f, [0, \delta])) \\ &= \sup\{\dim_H G(f, E), \dim_H G(f, [0, \delta])\} = 1. \end{aligned}$$

Thus

$$\dim_H G(f, I) = 1.$$

(3)  $x_n \in (0, 1)$ ,  $(x_n, 0)$  is an accumulation point:  $\forall \delta > 0, \dim_H G(f, [x_n - \delta, x_n + \delta]) = 1$ .  
 By the above discussions,

$$\dim_H G(f, I) = 1.$$

□

**Theorem 8.** Let  $f(x)$  be a continuous function containing countable UV points and  $f(x)$  only have an accumulation point on  $I$ . If  $f(x)$  is self-similar, then

$$\dim_H G(f, I) = \dim_B G(f, I) = 1.$$

**Proof.** Since  $f(x)$  is a continuous function on  $I$ ,

$$1 \leq \dim_H G(f, I) \leq \overline{\dim}_B G(f, I).$$

Denote the above uncountable UV points as  $x_1, x_2, x_3, \dots$ . There exists  $[a_i, x_i]$  and  $[a_i, x_i] \cap [a_j, x_j] = \emptyset$  when  $i \neq j$ . Thus,  $f(x)$  only have an UV point on  $[a_i, x_i]$  and

$$\dim_B G(f, [a_i, x_i]) = 1.$$

Thus,

$$\overline{\dim}_{MB} G(f, E) = \inf_i \{ \sup \overline{\dim}_B G(f, [a_i, x_i]) : E = \bigcup_{i=1}^{N-1} [a_i, x_i] \} = 1.$$

Denote  $E = \bigcup_{i=1}^{N-1} [a_i, x_i]$ ,  $F = [a_N, 1]$  and  $H = \bigcup_{i=1}^{N-1} [x_i, a_{i+1}]$  where  $a_1 = 0$ . Further inferences show that  $f(x)$  is a BVF on  $H$  and

$$\dim_H G(f, H) = \dim_B G(f, H) = 1.$$

It can be seen from the similar calculation process that

$$\begin{aligned} \overline{\dim}_{MB} G(f, I) &= \overline{\dim}_{MB} (G(f, E) \cup G(f, F) \cup G(f, H)) \\ &= \inf \{ \sup \{ \dim_H G(f, E), \dim_H G(f, F), \dim_H G(f, H) \} \} = 1. \end{aligned}$$

Since  $f(x)$  is self-similar on  $I$ ,  $G(f, I)$  is compact and

$$\overline{\dim}_B (G(f, I) \cap V) = \overline{\dim}_B G(f, I)$$

for all open sets  $V$  that intersect  $G(f, I)$ . Thus,

$$\overline{\dim}_B G(f, I) = \overline{\dim}_{MB} G(f, I).$$

Notice that the conclusion  $\overline{\dim}_B G(f, I) \geq 1$  remains true.

$$\dim_H G(f, I) = \dim_P G(f, I) = \dim_{MB} G(f, I) = \dim_B G(f, I) = 1.$$

□

### 5. Possible Applications in Reinforcement Learning

Since AlphaGo has shown amazing abilities in Go [43,44], reinforcement learning in machine learning has gradually been paid attention and researched by many scholars [45–48]. The core idea of reinforcement learning is to use the continuous interaction between the agent and the environment to maximize the long-term cumulative return expectation. The agent learns the optimal strategy through the mechanism of trial and error. Taking the expectation of maximizing returns as the goal makes reinforcement learning “foresight”, not

just focusing on the immediate situation, so the strategies obtained through reinforcement learning are scientific. Since the optimal strategy can be learned by reinforcement learning, Reinforcement learning has become an emerging method of researching decision theory. At the same time, the learning process of the agent in reinforcement learning is dynamic, and the required data is also generated through interaction with the environment, so a large amount of original label data is not required.

With the advent of deep neural networks, deep reinforcement learning can solve many complex problems. The seemingly complex fractal sets also have special regularity (self-similarity). Therefore, can fractals and fractal dimension be used in the learning process of the agent to speed up the learning speed of the agent or improve the search efficiency of algorithms? This section will introduce several possible applications of fractal and fractal dimension in reinforcement learning.

### 5.1. The Evaluation Model Based on Fractal Dimension

The main basis of the fractal evaluation model is the fractal dimension. Fractal dimension is an important indicator of system stability. The multi-dimensional vector can be formed by utilizing the parameters, such as actions and states of agents. Many multi-dimensional vectors may establish a special set. The fractal dimension of the set can determine the distance between the current state and the equilibrated state. The equilibrium state is that all agents are in a stable state and there is no motivation to change the current strategy. The main operational flows of the fractal evaluation model are as follows.

Step one: data standardization. The number of states and agents are  $K, N$  respectively. State  $\mathbb{S} = (s_1, s_2, \dots, s_N, a_1, a_2, \dots, a_N, r_1, r_2, \dots, r_N)$ . Standardization is to eliminate the differences caused by the species of each data. Standardized data is  $\mathbb{S} = (y_{ij})$ ,  $i = 1, 2, \dots, K \in \mathbb{Z}^+, j = 1, 2, \dots, 3N \in \mathbb{Z}^+$ .

Step two: weight.  $w_j = d_j / \sum_{i=1}^N d_j$ ,  
 where  $d_j = \max_{1 \leq i, k \leq K} |y_{ij} - y_{kj}|, j = 1, 2, \dots, N \in \mathbb{Z}^+$ .

Step three: calculate  $N(r)$ . The distance used in the algorithm is unified as Euclidean distance.  $3N$  data of each state can be regarded as points on each coordinate axis in the  $3n$ -dimensional space. These points constitute a subset of the  $3n$ -dimensional Euclidean space  $E^{3N}$ . The distance from each point to the origin is  $d_{ij}$  and let  $R = \max(d_{ij}), i = 1, 2, \dots, K \in \mathbb{Z}^+, j = 1, 2, \dots, 3N \in \mathbb{Z}^+$ . For a specific state,  $N(r)$  is the number of all points satisfying  $d_{ij} < r$  and  $r$  is the radius of the hypersphere. Keep adjusting the value of radius  $r$  until  $r = R$  and  $N(r) = N$ . When the radius is  $r$ , the number of points contained in the hypersphere is  $N(r) = \sum_{i=0}^{3N} \text{sgn}(r - d_{ij})$  and  $\text{sgn}(x)$  is a symbolic function,

$$\text{sgn}(x) = \begin{cases} 1, & x > 0 \\ 0, & x \leq 0 \end{cases}$$

Step four: calculate the fractal dimension.  $D = \log N(r) / \log r$ .

From the above calculation process, the number of sample points contained in the hypersphere with  $r$  will change continuously as the radius alters. At the same time, the graph of the function formed by the above standardized data points is usually non-linear. The fractal dimension  $D$  in this step can be fitted by the least square method,

$$D = \frac{3N \sum_{i=1}^{3N} \log N(r_i) \log r_i - \sum_{i=1}^{3N} \log N(r_i) \sum_{i=1}^{3N} \log r_i}{3N \sum_{i=1}^{3N} (\log r_i)^2 - \left( \sum_{i=1}^{3N} \log r_i \right)^2}$$

At present, most reinforcement learning algorithms are based on global information. However, due to the limitations of communication and observation, the agent cannot obtain all the information in practical. Therefore, the MDP(Markov decision process)

model used to solve basic reinforcement learning problems is not applicable. Researchers establish the POMDP (Partially observable markov decision process) model [49,50] to solve partially observable reinforcement learning problems. The main solutions include function approximation, opponent modeling, and graph theory.

Fractal dimension is another new idea to optimize POMDP. The theoretical foundation of using fractal dimension to evaluate stability is mainly based on the Lyapunov stability theory. The larger fractal dimension of the set, the more stable points in the set. Therefore, the set with larger fractal dimension is more stable than the set with small fractal dimension under the same disturbance. The advantage of this method is that the agent does not need to know global information. The strategy selection of agents can be guided by the fractal dimension, and the correct strategy direction can optimize the algorithm. At the same time, for a game where there is no pure strategy Nash equilibrium, it is still possible to compare the distance between any two situations and the equilibrium state by calculating the fractal dimension.

### 5.2. The Convergence Model Based on Fractal Attractor

At present, the convergence of most reinforcement learning algorithms lacks rigorous proofs. However, due to the powerful fitting ability of multiple neural networks [51–53], the algorithm can converge better in various experimental environments. The convergence obtained in the experiment cannot effectively understand the essence of the problem and optimize the existing algorithm. Obviously, the convergence of an algorithm is the fixed point of a particular function mathematically. Solving the fixed point problem can also be transformed into an attractor in fractal theory. Therefore, the convergence of the algorithm can be verified by calculating the existence of attractors. Surprisingly, the calculation of attractors has theoretical guarantees. Therefore, can the Bellman equation in reinforcement learning be regarded as an iterative function system, and then its solution is the attractor of the iterative function system? The idea of the model is shown in Figure 9.

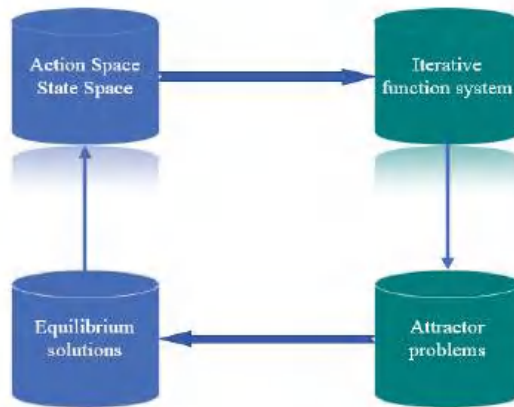


**Figure 9.** The frame of convergence model.

The advantage of this convergence model lies in its versatility, which can prove the convergence of a class of similar algorithms. The method of theoretical proof is conducive to finding the essence of the problem, so as to provide different ideas for the optimization algorithm.

### 5.3. The Random Search Algorithm Based on Fractal

Exploration and utilization is one of the important research directions in deep reinforcement learning. The goal of exploration is to find more information about the environment, and the purpose of utilization is to use the known environmental information to maximize

rewards. In short, exploration is to try behaviors that have not yet been tried, while utilization is to choose the next action from the knowledge that agents have already mastered. The balance between exploration and utilization is the basic issue of reinforcement learning. In deep reinforcement learning tasks, in order to obtain the best strategy, it is often necessary to collect more information. For solving the problem of exploration and utilization, researchers have proposed many classic methods. The  $\epsilon$ -greedy method is a commonly used strategy for greedy exploration.

However, the exploratory efficiency of this method is not good. Fractals generally have the following characteristics. One is that both the whole and the part have irregularities, and the other is that the internal structure has self-similarity and unevenness. The search method based on the fractal structure can reduce the search time as much as possible on the basis of ensuring that all spaces are explored. Due to the self-similar structure of the fractal, the algorithm does not always need to repeat the previous training during the training process. Thus the way can reduce a lot of unnecessary training time. Therefore, whether the above-mentioned characteristics of fractal can be used to achieve efficient search is looking forward to follow-up research and discussion. At present, there has been a lot of research on using fractals to improve search efficiency [54–56], but these algorithms can still continue to be optimized.

## 6. Conclusions

This manuscript systematically sorts out the conclusions about one-dimensional continuous functions. The Box dimension of bounded variation functions and the functions with the Weyl fractional integral are both one. The Box dimension of continuous functions that satisfy the Lipschitz condition is also one. These results also fully show that fractional calculus does not increase the dimensionality of functions. This conclusion seems simple, but no one seems to have carried out a rigorous proof. The structure of unbounded variation function is more complicated. The construction process of several special unbounded variation functions is displayed firstly, and a lot of general conclusions about unbounded variation functions are proved by using UV points. Combined with the self-similarity, the conclusions of the fractal dimension of some special functions are also strictly proved. These conclusions are very helpful for perfecting the theory of unbounded variation. At the same time, in order to increase the practical significance of the above conclusions, some applications of fractal and fractal dimension in reinforcement learning are also introduced. On the one hand, these works can sort out the current results, and on the other hand, some useful ideas and research directions can also be shown to other researchers. The evaluation model based on fractal dimension proposed in this manuscript can effectively accelerate the convergence speed of many reinforcement learning algorithms by using fractal dimension to judge the stability of any state. This model is an important result of the combination of the two theories, and it is believed that more fractal theories will be applied to reinforcement learning.

However, the research on one-dimensional continuous functions is far from over. In particular, what are the necessary and sufficient conditions for the conversion between unbounded variation and bounded variation? Are there other theories and tools that can be used to study one-dimensional continuous functions? Can existing relevant conclusions about one-dimensional continuous functions be extended to multi-dimensional continuous functions? Can the conclusion of the unbounded variation function be used in other fields?

**Author Contributions:** Conceptualization, W.J., and C.L.; methodology W.J.; Data curation, W.B.; formal analysis, G.H. writing original draft, W.J. and T.W. All authors have read and agreed to the published version of the manuscript.

**Funding:** Research was funded by National Natural Science Foundation of China (grant number 61806221387 and 12071218).

**Institutional Review Board Statement:** The study was conducted according to the guidelines of the Declaration of Helsinki, and approved by the Institutional Review Board.

**Informed Consent Statement:** Informed consent was obtained from all subjects involved in the study.

**Data Availability Statement:** Not applicable.

**Acknowledgments:** Research is supported by National Natural Science Foundation of China (61806221 and 12071218).

**Conflicts of Interest:** The authors declare no conflict of interest.

## References

1. Srivastava, H.M.; Kashuri, A.; Mohammed, P.O.; Nonlaopon, K. Certain inequalities pertaining to some new generalized fractional integral operators. *Fractal Fract.* **2021**, *5*, 160. [CrossRef]
2. Khan, M.B.; Noor, M.A.; Abdeljawad, T.; Mousa, A.A.A.; Abdalla, B.; Alghamdi, S.M. LR-preinvex interval-valued functions and Riemann–Liouville fractional integral inequalities. *Fractal Fract.* **2021**, *5*, 243. [CrossRef]
3. Machado, J.T.; Mainardi, F.; Kiryakova, V. Fractional calculus: Quo vadimus? (Where are we going?). *Fract. Calc. Appl. Anal.* **2015**, *18*, 495–526. [CrossRef]
4. Butera, S.; Paola, M.D. A physically based connection between fractional calculus and fractal geometry. *Ann. Phys.* **2014**, *350*, 146–158. [CrossRef]
5. Kolwankar, K.M.; Gangal, A.D. Fractional differentiability of nowhere differentiable functions and dimensions. *Chaos Solitons Fractals* **1996**, *6*, 505–513. [CrossRef]
6. Kolwankar, K.M.; Gangal, A.D. Hölder exponent of irregular signals and local fractional derivatives. *Pramana J. Phys.* **1997**, *48*, 49–68. [CrossRef]
7. Nigmatullin, R.R.; Baleanu, D. Relationships between 1D and space fractals and fractional integrals and their applications in physics. In *Applications in Physics, Part A*; De Gruyter: Berlin, Germany, 2019; Volume 4, pp. 183–220.
8. Tatom, F.B. The relationship between fractional calculus and fractals. *Fractals* **1995**, *3*, 217–229. [CrossRef]
9. Zähle, M.; Ziezold, H. Fractional derivatives of weierstrass-type functions. *J. Comput. Appl. Math.* **1996**, *76*, 265–275. [CrossRef]
10. Liang, Y.S. The relationship between the Box dimension of the Besicovitch functions and the orders of their fractional calculus. *Appl. Math. Comput.* **2008**, *200*, 197–207. [CrossRef]
11. Ruan, H.J.; Su, W.Y.; Yao, K. Box dimension and fractional integral of linear fractal interpolation functions. *J. Approx. Theory* **2009**, *161*, 187–197. [CrossRef]
12. Liang, Y.S. Box dimensions of Riemann–Liouville fractional integrals of continuous functions of bounded variation. *Nonlinear Anal.* **2010**, *72*, 4304–4306. [CrossRef]
13. Liang, Y.S. Fractal dimension of Riemann–Liouville fractional integral of 1-dimensional continuous functions. *Fract. Calc. Appl. Anal.* **2018**, *21*, 1651–1658. [CrossRef]
14. Wu, J.R. On a linearity between fractal dimensions and order of fractional calculus in Hölder space. *Appl. Math. Comput.* **2020**, *385*, 125433. [CrossRef]
15. Verma, S.; Viswanathan, P. A note on Katugampola fractional calculus and fractal dimensions. *Appl. Math. Comput.* **2018**, *339*, 220–230. [CrossRef]
16. Verma, S.; Viswanathan, P. Bivariate functions of bounded variation: Fractal dimension and fractional integral. *Indag. Math.* **2020**, *31*, 294–309. [CrossRef]
17. Bush, K.A. Continuous functions without derivatives. *Am. Math. Mon.* **1952**, *59*, 222–225. [CrossRef]
18. Shen, W.X. Hausdorff dimension of the graphs of the classical Weierstrass functions. *Math. Z.* **2018**, *289*, 223–266. [CrossRef]
19. Su, W.Y. Construction of fractal calculus. *Sci. China Math. Chin. Ser.* **2015**, *45*, 1587–1598. [CrossRef]
20. Xie, T.F.; Zhou, S.P. On a class of fractal functions with graph box dimension 2. *Chaos Solitons Fractals* **2004**, *22*, 135–139. [CrossRef]
21. Liang, Y.S.; Su, W.Y. Von Koch curves and their fractional calculus. *Acta Math. Sin. Chin. Ser.* **2011**, *54*, 227–240.
22. Wang, J.; Yao, K. Construction and analysis of a special one-dimensional continuous functions. *Fractals* **2017**, *25*, 1750020. [CrossRef]
23. Wang, J.; Yao, K.; Liang, Y.S. On the connection between the order of Riemann–Liouville fractional calculus and Hausdorff dimension of a fractal function. *Anal. Theory Appl.* **2016**, *32*, 283–290. [CrossRef]
24. Falconer, K.J. *Fractal Geometry: Mathematical Foundations and Applications*; John Wiley Sons Inc.: Chichester, PA, USA, **1990**.
25. Wen, Z.Y. *Mathematical Foundations of Fractal Geometry*; Science Technology Education Publication House: Shanghai, China, 2000. (In Chinese)
26. Hu, T.Y.; Lau, K.S. Fractal dimensions and singularities of the weierstrass type functions. *Trans. Am. Math. Soc.* **1993**, *335*, 649–665. [CrossRef]
27. Zheng, W.X.; Wang, S.W. *Real Function and Functional Analysis*; High Education Publication House: Beijing, China, 1980. (In Chinese)
28. Tian, L. The estimates of Hölder index and the Box dimension for the Hadamard fractional integral. *Fractals* **2021**, *29*, 2150072. [CrossRef]
29. Wang, C.Y. R-L Algorithm: An approximation algorithm for fractal signals based on fractional calculus. *Fractals* **2020**, *24*, 2150243. [CrossRef]

30. Oldham, K.B.; Spanier, J. *The Fractional Calculus*; Academic Press: New York, NY, USA, 1974.
31. Teodoro, G.S.; Machado, J.A.; Oliveira, E.C. A review of definitions of fractional derivatives and other operators. *J. Comput. Phys.* **2019**, *388*, 195–208. [CrossRef]
32. Kiryakova, V.S. *Generalized Fractional Calculus and Applications*; CRC Press: Boca Raton, FL, USA, 1993.
33. Miller, K.S.; Ross, B. *An Introduction to the Fractional Calculus and Fractional Differential Equations*; John Wiley Sons Inc.: New York, NY, USA, 1976.
34. Podlubny, I. Geometric and physical interpretation of fractional integration and fractional differentiation. *Fract. Calc. Appl. Anal.* **2002**, *5*, 367–386.
35. Mu, L.; Yao, K.; Wang, J. Box dimension of weyl fractional integral of continuous functions with bounded variation. *Anal. Theory Appl.* **2016**, *32*, 174–180. [CrossRef]
36. Kilbas, A.A.; Titioura, A.A. Nonlinear differential equations with marchaud-hadamard-type fractional derivative in the weighted sapce of summable functions. *Math. Model. Anal.* **2007**, *12*, 343–356. [CrossRef]
37. Tian, L. Hölder continuity and box dimension for the Weyl fractional integral. *Fractals* **2020**, *28*, 2050032. [CrossRef]
38. Yao, K.; Liang, Y.S.; Su, W.Y.; Yao, Z.Q. Fractal dimension of fractional derivative of self-affine functions. *Acta Math. Sin. Chin. Ser.* **2013**, *56*, 693–698.
39. Xu, Q. Fractional integrals and derivatives to a class of functions. *J. Xuzhou Norm. Univ.* **2006**, *24*, 19–23.
40. Stein, E.M. *Singular Integrals and Differentiability Properties of Functions*; Princeton University Press: Princeton, NJ, USA, 1970.
41. Liang, Y.S.; Su, W.Y. Fractal dimensions of fractional integral of continuous functions. *Acta Math. Sin.* **2016**, *32*, 1494–1508. [CrossRef]
42. Liang, Y.S.; Zhang, Q. 1-dimensional continuous functions with uncountable unbounded variation points. *Chin. J. Contemporary Math.* **2018**, *39*, 129–136.
43. Silver, D.; Schrittwieser, J.; Simonyan, K.; Antonoglou, I.; Huang, A.; Guez, A.; Hubert, T.; Baker, L.; Lai, M.; Bolton, A.; et al. Mastering the game of go without human knowledge. *Nature* **2017**, *550*, 354–359. [CrossRef]
44. Magnani, L. *AlphaGo, Locked Strategies, and Eco-Cognitive Openness*; Eco-Cognitive Computationalism Springer: Cham, Switzerland, 2021; pp. 45–71.
45. Liu, S.; Pan, Z.; Cheng, X. A novel fast fractal image compression method based on distance clustering in high dimensional sphere surface. *Fractals* **2017**, *25*, 1740004. [CrossRef]
46. Li, S.; Wu, Y.; Cui, X.; Dong, H.; Fang, F.; Russell, S. Robust multi-agent reinforcement learning via minimax deep deterministic policy gradient. *Proc. Aaai Conf. Artif. Intell.* **2019**, *33*, 4213–4220. [CrossRef]
47. Li, G.; Jiang, B.; Zhu, H.; Che, Z.; Liu, Y. Generative attention networks for multi-agent behavioral modeling. *Proc. Aaai Conf. Artif. Intell.* **2020**, *34*, 7195–7202. [CrossRef]
48. Liu, S.; Wang, S.; Liu, X.Y.; Gandomi, A.H.; Daneshmand, M.; Muhammad, K.; de Albuquerque, V.H.C. Human Memory Update Strategy: A multi-layer template update mechanism for remote visual monitoring. *IEEE Trans. Multimed.* **2021**, *23*, 2188–2198. [CrossRef]
49. Hoerger, M.; Kurniawati, H. An on-line POMDP solver for continuous observation spaces. In Proceedings of the 2021 IEEE International Conference on Robotics and Automation (ICRA), Xi'an, China, 30 May–5 June 2021; pp. 7643–7649.
50. Igl, M.; Zintgraf, L.; Le, T.A.; Wood, F.; Whiteson, S. Deep variational reinforcement learning for POMDPs. *Int. Conf. Mach. Learn.* **2018**, *16*, 2117–2126.
51. Zhou, Z.H. *Neural Networks*. In *Machine Learning*; Springer: Singapore, 2021.
52. Yang, L.; Zhang, R.Y.; Li, L.; Xie, X. Simam: A simple parameter-free attention module for convolutional neural networks. *Int. Conf. Mach. Learn.* **2021**, *26*, 11863–11874.
53. Almatroud, A.O. Extreme multistability of a fractional-order discrete-time neural network. *Fractal Fract.* **2021**, *5*, 202. [CrossRef]
54. Alomoush, M.I. Optimal combined heat and power economic dispatch using stochastic fractal search algorithm. *J. Mod. Power Syst. Clean Energy* **2020**, *8*, 276–286. [CrossRef]
55. Tran, T.T.; Truong, K.H. Stochastic fractal search algorithm for reconfiguration of distribution networks with distributed generations. *Ain Shams Eng. J.* **2020**, *11*, 389–407. [CrossRef]
56. Pham, L.H.; Duong, M.Q.; Phan, V.D.; Nguyen, T.T.; Nguyen, H.N. A high-performance stochastic fractal search algorithm for optimal generation dispatch problem. *Energies* **2019**, *12*, 1796. [CrossRef]



## Article

# On Transformation Involving Basic Analogue to the Aleph-Function of Two Variables

Dinesh Kumar <sup>1,\*</sup>, Dumitru Baleanu <sup>2,3</sup>, Frédéric Ayant <sup>4,5</sup> and Norbert Südland <sup>6</sup>

<sup>1</sup> Department of Applied Sciences, College of Agriculture-Jodhpur, Agriculture University Jodhpur, Jodhpur 342304, India

<sup>2</sup> Department of Mathematics, Cankaya University, Ankara 06530, Turkey; dumitru@cankaya.edu.tr

<sup>3</sup> Institute of Space Sciences, 077125 Magurele-Bucharest, Romania

<sup>4</sup> Collège Jean L'herminier, Allée des Nymphéas, 83500 La Seyne-sur-Mer, France; fredericayant@gmail.com

<sup>5</sup> Department VAR, Avenue Joseph Raynaud Le parc Fleuri, 83140 Six-Fours-les-Plages, France

<sup>6</sup> Aage GmbH, Röntgenstraße 24, 73431 Aalen, Baden-Württemberg, Germany;

norbert.suedland@aage-leichtbauteile.de

\* Correspondence: dinesh\_dino03@yahoo.com

**Abstract:** In our work, we derived the fractional order  $q$ -integrals and  $q$ -derivatives concerning a basic analogue to the Aleph-function of two variables (AFTV). We discussed a related application and the  $q$ -extension of the corresponding Leibniz rule. Finally, we presented two corollaries concerning the basic analogue to the  $I$ -function of two variables and the basic analogue to the Aleph-function of one variable.

**Keywords:** Fractional  $q$ -integral;  $q$ -derivative operators; basic analogue to the Aleph-function; basic analogue to the  $I$ -function;  $q$ -Leibniz rule

**Citation:** Kumar, D.; Baleanu, D.;

Ayant, F.; Südland, N. On

Transformation Involving Basic Analogue to the Aleph-Function of Two Variables. *Fractal Fract.* **2022**, *6*, 71. <https://doi.org/10.3390/fractalfract6020071>

Academic Editors: António M. Lopes, Alireza Alfi, Liping Chen and Sergio A. David

Received: 12 December 2021

Accepted: 19 January 2022

Published: 28 January 2022

**Publisher's Note:** MDPI stays neutral with regard to jurisdictional claims in published maps and institutional affiliations.



**Copyright:** © 2022 by the authors. Licensee MDPI, Basel, Switzerland. This article is an open access article distributed under the terms and conditions of the Creative Commons Attribution (CC BY) license (<https://creativecommons.org/licenses/by/4.0/>).

## 1. Introduction

Fractional calculus represents an important part of mathematical analysis. The concept of fractional calculus was born from a famous correspondence between L'Hopital and Leibniz in 1695. In the last four decades, it has gained significant recognition and found many applications in diverse research fields (see [1–6]). The fractional basic (or  $q$ -) calculus is the extension of the ordinary fractional calculus in the  $q$ -theory (see [7–10]). We recall that basic series and basic polynomials, particularly the basic (or  $q$ -) hypergeometric functions and basic (or  $q$ -) hypergeometric polynomials, are particularly applicable in several fields, e.g., Finite Vector Spaces, Lie Theory, Combinatorial Analysis, Particle Physics, Mechanical Engineering, Theory of Heat Conduction, Non-Linear Electric Circuit Theory, Cosmology, Quantum Mechanics, and Statistics. In 1952, Al-Salam introduced the  $q$ -analogue to Cauchy's formula [11] (see also [12]). Agarwal [13] studied certain fractional  $q$ -integral and  $q$ -derivative operators. In addition, various researchers reported image formulas of various  $q$ -special functions under fractional  $q$ -calculus operators, for example, Kumar et al. [14], Sahni et al. [15], Yadav and Purohit [16], Yadav et al. [17,18], and maybe more. The  $q$ -extensions of the Saigo's fractional integral operators were defined by Purohit and Yadav [19]. Several authors utilised such operators to evaluate a general class of  $q$ -polynomials, the basic analogue to Fox's  $H$ -function, basic analogue to the  $I$ -function, fractional  $q$ -calculus formulas for various special functions, etc. The readers can see more related new details in [16–18,20] on fractional  $q$ -calculus.

The purpose of the present manuscript is to discuss expansion formulas, involving the basic analogue to AFTV [21]. The  $q$ -Leibniz formula is also provided.

We recall that  $q$ -shifted factorial  $(a; q)_n$  has the following form [22,23]

$$(a; q)_n = \begin{cases} 1, & (n = 0) \\ \prod_{i=0}^{n-1} (1 - aq^i), & (n \in \mathbb{N} \cup \{\infty\}) \end{cases} \quad (1)$$

such that  $a, q \in \mathbb{C}$  and it is assumed that  $a \neq q^{-m}$  ( $m \in \mathbb{N}_0$ ).

The expression of the  $q$ -shifted factorial for negative subscript is written by

$$(a; q)_{-n} = \frac{1}{(1 - aq^{-1})(1 - aq^{-2}) \cdots (1 - aq^{-n})} \quad (n \in \mathbb{N}_0). \tag{2}$$

Additionally, we have

$$(a; q)_\infty = \prod_{i=0}^{\infty} (1 - aq^i) \quad (a, q \in \mathbb{C}; |q| < 1). \tag{3}$$

Using (1)–(3), we conclude that

$$(a; q)_n = \frac{(a; q)_\infty}{(aq^n; q)_\infty} \quad (n \in \mathbb{Z}), \tag{4}$$

its extension to  $n = \alpha \in \mathbb{C}$  as:

$$(a; q)_\alpha = \frac{(a; q)_\infty}{(aq^\alpha; q)_\infty} \quad (\alpha \in \mathbb{C}; |q| < 1), \tag{5}$$

such that the principal value of  $q^\alpha$  is considered.

We equivalently have a form of (1), given as

$$(a; q)_n = \frac{\Gamma_q(a+n)(1-q)^n}{\Gamma_q(a)} \quad (a \neq 0, -1, -2, \dots), \tag{6}$$

where the  $q$ -gamma function is expressed as [8]:

$$\Gamma_q(a) = \frac{(q; q)_\infty}{(q^a; q)_\infty(1-q)^{a-1}} = \frac{(q; q)_{a-1}}{(1-q)^{a-1}}, \quad (a \neq 0, -1, -2, \dots). \tag{7}$$

The expression of the  $q$ -analogue to the Riemann–Liouville fractional integral operator (RLI) of  $f(x)$  has the following expression [12]:

$$I_q^\mu \{f(x)\} = \frac{1}{\Gamma_q(\mu)} \int_0^x (x-t)_{\mu-1} f(t) d_q t, \tag{8}$$

here,  $\Re(\mu) > 0$ ,  $|q| < 1$  and

$$[x-y]_v = x^v \prod_{n=0}^{\infty} \left[ \frac{1 - (y/x)q^n}{1 - (y/x)q^{n+v}} \right] = x^v \left( \frac{y}{x}; q \right)_v \quad (x \neq 0). \tag{9}$$

The basic integral [8] is given by

$$\int_0^x f(t) d_q t = x(1-q) \sum_{k=0}^{\infty} q^k f(xq^k). \tag{10}$$

Equation (8), in conjunction with (10); then, we have the series representation of (RLI), as follows

$$I_q^\mu f(x) = \frac{x^\mu(1-q)}{\Gamma_q(\mu)} \sum_{k=0}^{\infty} q^k [1 - q^{k+1}]_{\mu-1} f(xq^k). \tag{11}$$

We mention that for  $f(x) = x^{\lambda-1}$ , the following can be written [16]

$$I_q^\mu (x^{\lambda-1}) = \frac{\Gamma_q(\lambda)}{\Gamma_q(\lambda + \mu)} x^{\lambda + \mu - 1} \quad (\Re(\lambda + \mu) > 0). \tag{12}$$

### 2. Basic Analogue to Aleph-Function of Two Variables

We recall that AFTV [21] is an extension of the  $I$ -function possessing two variables [24]. Here, in the present article, we define a basic analogue to AFTV.

We record

$$G(q^a) = \left[ \prod_{n=0}^{\infty} (1 - q^{a+n}) \right]^{-1} = \frac{1}{(q^a; q)_{\infty}}. \tag{13}$$

Next, we have

$$\begin{aligned} & \aleph(z_1, z_2; q) \\ &= \aleph_{P_i, Q_i, \tau_i, r; P_{i'}, Q_{i'}, \tau_{i'}, r'; P_{i''}, Q_{i''}, \tau_{i''}, r''}^{0, n_1; m_2, n_2; m_3, n_3} \left( \begin{matrix} z_1 \\ z_2 \end{matrix} ; q \left| \begin{matrix} (a_j; \alpha_j, A_j)_{1, n_1}, [\tau_i(a_{ji}; \alpha_{ji}, A_{ji})]_{n_1+1, P_i} \\ [\tau_i(b_{ji}; \beta_{ji}, B_{ji})]_{1, Q_i} \\ (c_j, \gamma_j)_{1, m_2}, [\tau_{i'}(c_{ji'}; \gamma_{ji'})]_{n_2+1, P_{i'}}; (e_j, E_j)_{1, m_3}, [\tau_{i''}(e_{ji''}; \gamma_{ji''})]_{n_3+1, P_{i''}} \\ (d_j, \delta_j)_{1, m_2}, [\tau_{i'}(d_{ji'}; \delta_{ji'})]_{m_2+1, Q_{i'}}; (f_j, F_j)_{1, m_3}, [\tau_{i''}(f_{ji''}; F_{ji''})]_{m_3+1, Q_{i''}} \end{matrix} \right) \\ &= \frac{1}{(2\pi\omega)^2} \int_{L_1} \int_{L_2} \pi^2 \phi(s_1, s_2; q) z_1^{s_1} z_2^{s_2} d_q s_1 d_q s_2, \end{aligned} \tag{14}$$

where  $\omega = \sqrt{-1}$ , and

$$\begin{aligned} \phi(s_1, s_2; q) &= \frac{\prod_{j=1}^{n_1} G(q^{1-a_j+a_j s_1+A_j s_2})}{\sum_{i=1}^r \tau_i \left\{ \prod_{j=1}^{Q_i} G(q^{1-b_{ji}+\beta_{ji} s_1+B_{ji} s_2}) \prod_{j=n_1+1}^{P_i} G(q^{a_{ji}-\alpha_{ji} s_1-A_{ji} s_2}) \right\}} \\ &\times \frac{\prod_{j=1}^{m_2} G(q^{d_j-\delta_j s_1}) \prod_{j=1}^{n_2} G(q^{1-c_j+\gamma_j s_1})}{\sum_{i'=1}^{r'} \tau_{i'} \left\{ \prod_{j=m_2+1}^{Q_{i'}} G(q^{1-d_{ji'}+\delta_{ji'} s_1}) \prod_{j=n_2+1}^{P_{i'}} G(q^{c_{ji'}-\gamma_{ji'} s_1}) \right\} G(q^{1-s_1}) \sin \pi s_1} \\ &\times \frac{\prod_{j=1}^{m_3} G(q^{f_j-F_j s_2}) \prod_{j=1}^{n_3} G(q^{1-e_j+E_j s_2})}{\sum_{i''=1}^{r''} \tau_{i''} \left\{ \prod_{j=m_3+1}^{Q_{i''}} G(q^{1-f_{ji''}+F_{ji''} s_2}) \prod_{j=n_3+1}^{P_{i''}} G(q^{e_{ji''}-E_{ji''} s_2}) \right\} G(q^{1-s_2}) \sin \pi s_2}, \end{aligned} \tag{15}$$

where  $z_1, z_2 \neq 0$  and are real or complex. An empty product is elucidated as unity, and  $P_i, P_{i'}, P_{i''}, Q_i, Q_{i'}, Q_{i''}, m_1, m_2, m_3, n_1, n_2, n_3$  are non-negative integers, such that  $Q_i, Q_{i'}, Q_{i''} > 0; \tau_i, \tau_{i'}, \tau_{i''} > 0 (i = 1, \dots, r; i' = 1, \dots, r'; i'' = 1, \dots, r'')$ . All the  $A_s, a_s, \gamma_s, \delta_s, E_s$ , and  $F_s$  are presumed to be positive quantities for standardization intention, the  $a_s, b_s, c_s, d_s, e_s$ , and  $f_s$  are complex numbers. The definition of a basic analogue to AFTV will, however, make sense, even if some of these quantities are equal to zero. The contour  $L_1$  is in the  $s_1$ -plane and goes from  $-\omega\infty$  to  $+\omega\infty$ , with loops where necessary, to make sure that the poles of  $G(q^{d_j-\delta_j s_1}) (j = 1, \dots, m_2)$  are to the right-hand side and all the poles of  $G(q^{1-a_j+\alpha_j s_1+A_j s_2}) (j = 1, \dots, n_1), G(q^{1-c_j+\gamma_j s_1}) (j = 1, \dots, n_2)$  lie to the left-hand side of  $L_1$ . The contour  $L_2$  is in the  $s_2$ -plane and goes from  $-\omega\infty$  to  $+\omega\infty$ , with loops where necessary, to ensure that the poles of  $G(q^{f_j-F_j s_2}) (j = 1, \dots, m_3)$  are to the right-hand side and all the poles of  $G(q^{1-a_j+\alpha_j s_1+A_j s_2}) (j = 1, \dots, n_1), G(q^{1-e_j+E_j s_2}) (j = 1, \dots, n_2)$  lie to the left-hand side of  $L_2$ . For values of  $|s_1|$  and  $|s_2|$ , the integrals converge, if  $\Re(s_1 \log(z_1) - \log \sin \pi s_1) < 0$  and  $\Re(s_2 \log(z_2) - \log \sin \pi s_2) < 0$ .

### 3. Main Formulas

Here, we obtain fractional  $q$ -integral and  $q$ -derivative formulas concerning the basic analogue to AFTV. Here, we have the following notations:

$$A_1 = (a_j; \alpha_j, A_j)_{1, n_1}, [\tau_i(a_{ji}; \alpha_{ji}, A_{ji})]_{n_1+1, P_i}; B_1 = [\tau_i(b_{ji}; \beta_{ji}, B_{ji})]_{1, Q_i}. \tag{16}$$

$$C_1 = (c_j, \gamma_j)_{1, n_2}, [\tau_{i'}(c_{j i'}; \gamma_{j i'})]_{n_2+1, P_{i'}}; (e_j, E_j)_{1, n_3}, [\tau_{i''}(e_{j i''}; \gamma_{j i''})]_{n_3+1, P_{i''}}. \tag{17}$$

$$D_1 = (d_j, \delta_j)_{1, m_2}, [\tau_{i'}(d_{j i'}; \delta_{j i'})]_{m_2+1, Q_{i'}}; (f_j, F_j)_{1, m_3}, [\tau_{i''}(f_{j i''}; F_{j i''})]_{m_3+1, Q_{i''}}. \tag{18}$$

**Theorem 1.** Let  $\Re(\mu) > 0$ ,  $\rho_i \in \mathbb{Z}^+$  ( $i = 1, 2$ ), and  $|q| < 1$ ; then, the Riemann–Liouville fractional  $q$ -integral of (14) exists and is given as

$$I_q^\mu \left\{ x^{\lambda-1} \aleph_{P_i, Q_i; \tau_i; r; P_{i'}, Q_{i'}, \tau_{i'}; r'}; P_{i''}, Q_{i''}, \tau_{i''}; r''} \left( \begin{matrix} z_1 x^{\rho_1} \\ z_2 x^{\rho_2} \end{matrix} ; q \left| \begin{matrix} A_1; C_1 \\ B_1; D_1 \end{matrix} \right. \right) \right\} = (1-q)^\mu x^{\lambda+\mu-1} \\ \times \aleph_{P_i+1, Q_i+1, \tau_i; r; P_{i'}, Q_{i'}, \tau_{i'}; r'}; P_{i''}, Q_{i''}, \tau_{i''}; r''} \left( \begin{matrix} z_1 x^{\rho_1} \\ z_2 x^{\rho_2} \end{matrix} ; q \left| \begin{matrix} (1-\lambda; \rho_1, \rho_2), A_1; C_1 \\ B_1, (1-\lambda-\mu; \rho_1, \rho_2); D_1 \end{matrix} \right. \right), \tag{19}$$

where  $\Re(s; \log(z_i) - \log \sin \pi s_i) < 0$  ( $i = 1, 2$ ).

**Proof.** We apply the definitions (8) and (14) in the left-hand side of (19), we have (say  $\mathcal{I}$ )

$$\mathcal{I} = \frac{1}{\Gamma_q(\alpha)} \int_0^x (x-yq)_{\alpha-1} \left\{ y^{\lambda-1} \frac{1}{(2\pi\omega)^2} \int_{L_1} \int_{L_2} \pi^2 \phi(s_1, s_2; q) \prod_{i=1}^2 (z_i y^{\rho_i})^{s_i} d_q s_1 d_q s_2 \right\} d_q y. \tag{20}$$

By using standard calculations, we arrive at

$$\mathcal{I} = \frac{y^{\lambda-1}}{\Gamma_q(\alpha)} \frac{1}{(2\pi\omega)^2} \\ \times \int_{L_1} \int_{L_2} \pi^2 \phi(s_1, s_2; q) \prod_{i=1}^2 z_i^{s_i} \left\{ \int_0^x (x-yq)_{\alpha-1} y^{\lambda+\sum_{i=1}^2 \rho_i s_i - 1} d_q y \right\} d_q s_1 d_q s_2 \\ = \frac{1}{(2\pi\omega)^2} \int_{L_1} \int_{L_2} \pi^2 \phi(s_1, s_2; q) \prod_{i=1}^2 z_i^{s_i} I_q^\mu \left\{ x^{\lambda+\sum_{i=1}^2 \rho_i s_i - 1} \right\} d_q s_1 d_q s_2. \tag{21}$$

Next, we apply formula (12) to the equation above; then, we get

$$\mathcal{I} = \frac{1}{(2\pi\omega)^2} \int_{L_1} \int_{L_2} \pi^2 \phi(s_1, s_2; q) \prod_{i=1}^2 z_i^{s_i} \frac{\Gamma_q(\lambda + \sum_{i=1}^2 \rho_i s_i)}{\Gamma_q(\lambda + \mu + \sum_{i=1}^2 \rho_i s_i)} x^{\lambda+\mu+\sum_{i=1}^2 \rho_i s_i - 1} d_q s_1 d_q s_2. \tag{22}$$

Considering the above  $q$ -Mellin–Barnes double contour integrals in terms of the basic analogue to AFTV, we obtain (19).  $\square$

If we use a fractional  $q$ -derivative operator without initial values, defined as

$$I_q^{-\mu} \{f(x)\} = D_{x,q}^\mu \{f(x)\} = \frac{1}{\Gamma_q(-\mu)} \int_0^x (x-tq)_{-\mu-1} f(t) d_q t, \tag{23}$$

where  $\Re(\mu) < 0$ ; then, we yield the following result:

**Theorem 2.** For  $\Re(\mu) > 0$ ,  $\rho_i \in \mathbb{Z}^+$  ( $i = 1, 2$ ), and  $|q| < 1$ , the Riemann–Liouville fractional  $q$ -derivative of (14) exists and is given by

$$D_{x,q}^\mu \left\{ x^{\lambda-1} \mathfrak{N}_{P_i, Q_i, \tau_i; r; P_i, Q_i, \tau_i; r'; P_i, Q_i, \tau_i; r''}^{0, n_1; m_2; n_2; m_3; n_3} \left( \begin{matrix} z_1 x^{\rho_1} \\ z_2 x^{\rho_2} \end{matrix} ; q \left| \begin{matrix} A_1; C_1 \\ B_1; D_1 \end{matrix} \right. \right) \right\} = (1-q)^{-\mu} x^{\lambda-\mu-1} \\ \times \mathfrak{N}_{P_i+1, Q_i+1, \tau_i+1; r; P_i, Q_i, \tau_i; r'; P_i, Q_i, \tau_i; r''}^{0, n_1+1; m_2; n_2; m_3; n_3} \left( \begin{matrix} z_1 x^{\rho_1} \\ z_2 x^{\rho_2} \end{matrix} ; q \left| \begin{matrix} (1-\lambda; \rho_1, \rho_2), A_1; C_1 \\ B_1, (1-\lambda+\mu; \rho_1, \rho_2); D_1 \end{matrix} \right. \right), \quad (24)$$

where  $\Re(s; \log(z_i) - \log \sin \pi s_i) < 0$  ( $i = 1, 2$ ).

**Proof.** If we replace  $\mu$  by  $-\mu$  in (19), and follow the proof of Theorem 1, then we can easily obtain (24).  $\square$

**4. Leibniz’s Formula**

The  $q$ -expression of the Leibniz rule for the fractional  $q$ -derivatives [13] is written below

**Lemma 1.** For regular functions  $U(x)$  and  $V(x)$ , we have

$$D_{x,q}^\alpha \{U(x)V(x)\} = \sum_{n=0}^\infty \frac{(-1)^n q^{\frac{n(n+1)}{2}} [q^{-\mu}; q]_n}{(q; q)_n} D_{x,q}^{\mu-n} \{U(xq^n)\} D_{x,q}^n \{V(x)\}. \quad (25)$$

Next, we have the following formula:

**Theorem 3.** For  $\Re(\mu) < 0$ ,  $\rho_i \in \mathbb{Z}^+$  ( $i = 1, 2$ ), then the Riemann–Liouville fractional  $q$ -derivative of a product of two basic function is written as

$$\mathfrak{N}_{P_i+1, Q_i+1, \tau_i+1; r; P_i, Q_i, \tau_i; r'; P_i, Q_i, \tau_i; r''}^{0, n_1+1; m_2; n_2; m_3; n_3} \left( \begin{matrix} z_1 x^{\rho_1} \\ z_2 x^{\rho_2} \end{matrix} ; q \left| \begin{matrix} (1-\lambda; \rho_1, \rho_2), A_1; C_1 \\ B_1, (1-\lambda+\mu; \rho_1, \rho_2); D_1 \end{matrix} \right. \right) \\ = \sum_{n=0}^\infty \frac{(-1)^n q^{n\lambda + \frac{n(n-1)}{2}} [q^{-\mu}; q]_n}{(q; q)_n (q^\lambda; q)_{n-\mu}} \\ \times \mathfrak{N}_{P_i+1, Q_i+1, \tau_i+1; r; P_i, Q_i, \tau_i; r'; P_i, Q_i, \tau_i; r''}^{0, n_1+1; m_2; n_2; m_3; n_3} \left( \begin{matrix} z_1 x^{\rho_1} \\ z_2 x^{\rho_2} \end{matrix} ; q \left| \begin{matrix} (0; \rho_1, \rho_2), A_1; C_1 \\ B_1, (n; \rho_1, \rho_2); D_1 \end{matrix} \right. \right), \quad (26)$$

where  $\Re(s; \log(z_i) - \log \sin \pi s_i) < 0$  ( $i = 1, 2$ ).

**Proof.** To apply the  $q$ -Leibniz rule, we take

$$U(x) = x^{\lambda-1} \text{ and } V(x) = \mathfrak{N}_{P_i, Q_i, \tau_i; r; P_i, Q_i, \tau_i; r'; P_i, Q_i, \tau_i; r''}^{0, n_1; m_2; n_2; m_3; n_3} \left( \begin{matrix} z_1 x^{\rho_1} \\ z_2 x^{\rho_2} \end{matrix} ; q \left| \begin{matrix} A_1; C_1 \\ B_1; D_1 \end{matrix} \right. \right).$$

By using Lemma 1, we obtain the following relation:

$$D_{x,q}^\mu \left\{ x^{\lambda-1} \mathfrak{N}_{P_i, Q_i, \tau_i; r; P_i, Q_i, \tau_i; r'; P_i, Q_i, \tau_i; r''}^{0, n_1; m_2; n_2; m_3; n_3} \left( \begin{matrix} z_1 x^{\rho_1} \\ z_2 x^{\rho_2} \end{matrix} ; q \left| \begin{matrix} A_1; C_1 \\ B_1; D_1 \end{matrix} \right. \right) \right\} \\ = \sum_{n=0}^\infty \frac{(-1)^n q^{\frac{n(n+1)}{2}} [q^{-\mu}; q]_n}{(q; q)_n} D_{x,q}^{\mu-n} (xq^n)^{\lambda-1} D_{x,q}^n \{ \mathfrak{N}(z_1 x^{\rho_1}, z_2 x^{\rho_2}; q) \}. \quad (27)$$

Next, by using Theorem 2 and setting  $\lambda = 1$ , we obtain

$$D_{x,q}^n \{ \aleph(z_1 x^{\rho_1}, z_2 x^{\rho_2}; q) \} = (1-q)^{-n} x^{-n} \aleph_{P_i+1, Q_i+1, r; P_i', Q_i', r'; P_i'', Q_i'', r''}^{0, n_1+1; m_2, n_2; m_3, n_3} \left( \begin{matrix} z_1 x^{\rho_1} \\ z_2 x^{\rho_2} \end{matrix} ; q \left| \begin{matrix} (0; \rho_1, \rho_2), A_1; C_1 \\ B_1, (n; \rho_1, \rho_2); D_1 \end{matrix} \right. \right). \tag{28}$$

By using the above equation and the following result:

$$D_{x,q}^\mu \{ x^{\lambda-1} \} = \frac{\Gamma_q(\lambda)}{\Gamma_q(\lambda-\mu)} x^{\lambda-\mu-1} \quad (\lambda \neq -1, -2, \dots), \tag{29}$$

We can easily obtain the desired result (26) after several algebraic manipulations.  $\square$

**5. Particular Cases**

By setting  $\tau_i, \tau_i', \tau_i'' \rightarrow 1$ , the basic analogue to AFTV reduces to the basic analogue to the  $I$ -function of two variables [24].

Let

$$A'_1 = (a_j; \alpha_j, A_j)_{1, n_1}, (a_{ji}; \alpha_{ji}, A_{ji})_{n_1+1, P_i}; B'_1 = (b_{ji}; \beta_{ji}, B_{ji})_{1, Q_i}. \tag{30}$$

$$C'_1 = (c_j, \gamma_j)_{1, n_2}, (c_{ji}', \gamma_{ji}')_{n_2+1, P_i'}; (e_j, E_j)_{1, n_3}, (e_{ji}'', \gamma_{ji}'')_{n_3+1, P_i''}. \tag{31}$$

$$D'_1 = (d_j, \delta_j)_{1, m_2}, (d_{ji}'', \delta_{ji}'')_{m_2+1, Q_i'}; (f_j, F_j)_{1, m_3}, (f_{ji}'', F_{ji}'')_{m_3+1, Q_i''}. \tag{32}$$

We have the following result:

**Corollary 1.**

$$\begin{aligned} & I_{P_i+1, Q_i+1, r; P_i', Q_i', r'; P_i'', Q_i'', r''}^{0, n_1+1; m_2, n_2; m_3, n_3} \left( \begin{matrix} z_1 x^{\rho_1} \\ z_2 x^{\rho_2} \end{matrix} ; q \left| \begin{matrix} (1-\lambda; \rho_1, \rho_2), A'_1; C'_1 \\ B'_1, (1-\lambda+\mu; \rho_1, \rho_2); D'_1 \end{matrix} \right. \right) \\ &= \sum_{n=0}^{\infty} \frac{(-1)^n q^{n\lambda + \frac{n(n-1)}{2}} [q^{-\mu}; q]_n}{(q; q)_n (q^\lambda; q)_{n-\mu}} \\ &\times I_{P_i+1, Q_i+1, r; P_i', Q_i', r'; P_i'', Q_i'', r''}^{0, n_1+1; m_2, n_2; m_3, n_3} \left( \begin{matrix} z_1 x^{\rho_1} \\ z_2 x^{\rho_2} \end{matrix} ; q \left| \begin{matrix} (0; \rho_1, \rho_2), A'_1; C'_1 \\ B'_1, (n; \rho_1, \rho_2); D'_1 \end{matrix} \right. \right), \end{aligned} \tag{33}$$

where  $\Re(s_i \log(z_i) - \log \sin \pi s_i) < 0 \ (i = 1, 2)$ .

**Proof.** By setting  $\tau_i, \tau_i', \tau_i'' \rightarrow 1$  and following the proof of Theorem 3, we can easily obtain the desired result (33).  $\square$

**Remark 1.** If the basic analogue to the  $I$ -function of two variables reduces to the basic analogue to the  $H$ -function of two variables [25], then we can obtain the result due to Yadav et al. [18].

The basic analogue to AFTV reduces to the basic analogue to AFTV, defined by Ahmad et al. [26].

Let

$$A = (a_j, A_j)_{1, m'}, \dots, [\tau_i(a_{ji}, A_{ji})]_{n+1, p_i}. \tag{34}$$

$$B = (b_j, B_j)_{1, m'}, \dots, [\tau_i(b_{ji}, B_{ji})]_{m+1, q_i}. \tag{35}$$

Then, we have following relation:

**Corollary 2.**

$$\begin{aligned} & \mathfrak{N}_{p_i+1, q_i+1, \tau_i, r}^{m, n+1} \left( zx^\rho; q \left| \begin{array}{l} (1-\lambda; \rho), A \\ B, (1-\lambda+\mu; \rho) \end{array} \right. \right) \\ &= \sum_{n=0}^{\infty} \frac{(-1)^n q^{n\lambda + \frac{n(n-1)}{2}} [q^{-\mu}; q]_n}{(q; q)_n (q^\lambda; q)_{n-\mu}} \mathfrak{N}_{p_i+1, q_i+1, \tau_i, r}^{m, n+1} \left( zx^\rho; q \left| \begin{array}{l} (0; \rho), A \\ B, (n; \rho) \end{array} \right. \right). \end{aligned} \quad (36)$$

If we set  $\tau_i \rightarrow 1$  in (36), then the basic analogue to AFTV reduces to the basic analogue to the  $I$ -function of one variable. We have

**Corollary 3.**

$$\begin{aligned} & I_{p_i+1, q_i+1, r}^{m, n+1} \left( zx^\rho; q \left| \begin{array}{l} (1-\lambda; \rho), (a_j, A_j)_{1, n'} \cdots, (a_{j_i}, A_{j_i})_{n+1, p_i} \\ (b_j, B_j)_{1, m'} \cdots, (b_{j_i}, B_{j_i})_{m+1, q_i'} \end{array} \right. (1-\lambda+\mu; \rho) \right) \\ &= \sum_{n=0}^{\infty} \frac{(-1)^n q^{n\lambda + \frac{n(n-1)}{2}} [q^{-\mu}; q]_n}{(q; q)_n} \\ & \times I_{p_i+1, q_i+1, r}^{m, n+1} \left( zx^\rho; q \left| \begin{array}{l} (0; \rho), (a_j, A_j)_{1, n'} \cdots, (a_{j_i}, A_{j_i})_{n+1, p_i} \\ (b_j, B_j)_{1, m'} \cdots, (b_{j_i}, B_{j_i})_{m+1, q_i'} \end{array} \right. (n; \rho) \right). \end{aligned} \quad (37)$$

**Remark 2.** If the basic analogue to AFTV reduces to the basic analogue to the  $H$ -function of one variable (see [27]), then we can report a similar expression.

**Remark 3.** We can generalize the  $q$ -extension of the Leibniz rule for the basic analogue to special multivariable functions; by this, we can obtain similar formulas by using similar methods.

**6. Conclusions**

After the famous letter between L'Hopital and Leibniz from 1695, using integral transformations, we obtained a new field in mathematics, called fractional calculus. Among other things, there are fractional derivative and fractional integrals, as well as fractional differential equations. It is also well-known that fractional calculus operators and their basic (or  $q$ -) analogues have many applications, such as signal processing, bio-medical engineering, control systems, radars, sonars, to solve dual integral and series equations in elasticity, etc. In this article, we have proposed the fractional-order  $q$ -integrals and  $q$ -derivatives involving a basic analogue to AFTV [11,12,26,28]. Some remarkable applications of these integrals and derivatives have also been discussed. By specializing the various parameters as well as the variables in the basic analogue to AFTV, we can obtain a large number of  $q$ -extensions of the Leibniz rule, involving a large set of basic functions, that is, the product of such basic functions, which are describable in terms of the basic analogue to the  $H$ -function [25,27], the basic analogue to Meijer's  $G$ -function [27], the basic analogue to MacRobert's  $E$ -function [29], and the basic analogue to the hypergeometric function [10,16–18].

**Author Contributions:** Conceptualization, D.K.; Data curation, D.B., F.A. and N.S.; Formal analysis, D.K., D.B., F.A. and N.S.; Funding acquisition, D.B.; Investigation, D.K. and F.A.; Methodology, D.K., D.B. and F.A.; Resources, F.A. and N.S.; Supervision, D.B. and N.S. All authors have read and agreed to the published version of the manuscript.

**Funding:** This research received no external funding.

**Institutional Review Board Statement:** Not applicable.

**Informed Consent Statement:** Not applicable.

**Data Availability Statement:** Not applicable.

**Acknowledgments:** The author (D.K.) would like to thank the Agriculture University Jodhpur for supporting and encouraging this work.

**Conflicts of Interest:** All authors declare that they have no conflict of interest.

## References

1. Kumar, D.; Choi, J. Generalized fractional kinetic equations associated with Aleph function. *Proc. Jangjeon Math. Soc.* **2016**, *19*, 145–155.
2. Kumar, D.; Gupta, R.K.; Shaktawat, B.S.; Choi, J. Generalized fractional calculus formulas involving the product of Aleph-function and Srivastava polynomials. *Proc. Jangjeon Math. Soc.* **2017**, *20*, 701–717.
3. Kumar, D.; Ram, J.; Choi, J. Certain generalized integral formulas involving Chebyshev Hermite polynomials, generalized  $M$ -series and Aleph-function, and their application in heat conduction. *Int. J. Math. Anal.* **2015**, *9*, 1795–1803. [CrossRef]
4. Ram, J.; Kumar, D. Generalized fractional integration of the  $\aleph$ -function. *J. Raj. Acad. Phy. Sci.* **2011**, *10*, 373–382.
5. Samko, G.; Kilbas, A.A.; Marichev, O.I. *Fractional Integrals and Derivatives: Theory and Applications*; Gordon and Breach Science Publishers: New York, NY, USA, 1993.
6. Südländ, N.; Volkmann, J.; Kumar, D. Applications to give an analytical solution to the Black Scholes equation. *Integral Transform. Spec. Funct.* **2019**, *30*, 205–230. [CrossRef]
7. Exton, H.  $q$ -hypergeometric functions and applications. *Ellis Horwood Series: Mathematics and its Applications*; Ellis Horwood Ltd.: Chichester, UK, 1983; 347p.
8. Gasper, G.; Rahman, M. *Basic Hypergeometric Series*; Cambridge University Press: Cambridge, UK, 1990.
9. Rajkovic, P.M.; Marinkovic, S.D.; Stankovic, M.S. Fractional integrals and derivatives in  $q$ -calculus. *Appl. Anal. Discrete Math.* **2007**, *1*, 311–323.
10. Slater, L.J. *Generalized Hypergeometric Functions*; Cambridge University Press: Cambridge, UK, 1966.
11. Al-Salam, W.A.  $q$ -analogues of Cauchy's formula. *Proc. Am. Math. Soc.* **1952–1953**, *17*, 182–184.
12. Al-Salam, W.A. Some fractional  $q$ -integrals and  $q$ -derivatives. *Proc. Edinburgh Math. Soc.* **1966**, *15*, 135–140. [CrossRef]
13. Agarwal, R.P. Certain fractional  $q$ -integrals and  $q$ -derivatives. *Proc. Camb. Phil. Soc.* **1969**, *66*, 365–370. [CrossRef]
14. Kumar, D.; Ayant, F.Y.; Tariboon, J. On transformation involving basic analogue of multivariable  $H$ -function. *J. Funct. Spaces* **2020**, *2020*, 2616043. [CrossRef]
15. Sahni, N.; Kumar, D.; Ayant, F.Y.; Singh, S. A transformation involving basic multivariable  $I$ -function of Prathima. *J. Ramanujan Soc. Math. Math. Sci.* **2021**, *8*, 95–108.
16. Yadav, R.K.; Purohit, S.D. On applications of Weyl fractional  $q$ -integral operator to generalized basic hypergeometric functions. *Kyungpook Math. J.* **2006**, *46*, 235–245.
17. Yadav, R.K.; Purohit, S.D.; Kalla, S.L.; Vyas, V.K. Certain fractional  $q$ -integral formulae for the generalized basic hypergeometric functions of two variables. *J. Inequal. Spec. Funct.* **2010**, *1*, 30–38.
18. Yadav, R.K.; Purohit, S.D.; Vyas, V.K. On transformations involving generalized basic hypergeometric function of two variables. *Rev. Téc. Ing. Univ. Zulia.* **2010**, *33*, 176–182.
19. Purohit, S.D.; Yadav, R.K. On generalized fractional  $q$ -integral operators involving the  $q$ -gauss hypergeometric function. *Bull. Math. Anal. Appl.* **2010**, *2*, 35–44.
20. Galué, L. Generalized Erdélyi-Kober fractional  $q$ -integral operator. *Kuwait J. Sci. Eng.* **2009**, *36*, 21–34.
21. Kumar, D. Generalized fractional differintegral operators of the Aleph-function of two variables. *J. Chem. Biol. Phys. Sci. Sec. C* **2016**, *6*, 1116–1131.
22. Jia, Z.; Khan, B.; Agarwal, P.; Hu, Q.; Wang, X. Two new Bailey Lattices and their applications. *Symmetry* **2021**, *13*, 958. [CrossRef]
23. Jia, Z.; Khan, B.; Hu, Q.; Niu, D. Applications of generalized  $q$ -difference equations for general  $q$ -polynomials. *Symmetry* **2021**, *13*, 1222. [CrossRef]
24. Sharma, C.K.; Mishra, P.L. On the  $I$ -function of two variables and its certain properties. *Acta Ciencia Indica* **1991**, *17*, 1–4.
25. Saxena, R.K.; Modi, G.C.; Kalla, S.L. A basic analogue of  $H$ -function of two variable. *Rev. Tec. Ing. Univ. Zulia* **1987**, *10*, 35–39.
26. Ahmad, A.; Jain, R.; Jain, D.K.  $q$ -analogue of Aleph-function and its transformation formulae with  $q$ -derivative. *J. Stat. Appl. Pro.* **2017**, *6*, 567–575. [CrossRef]
27. Saxena, R.K.; Modi, G.C.; Kalla, S.L. A basic analogue of Fox's  $H$ -function. *Rev. Tec. Ing. Univ. Zulia* **1983**, *6*, 139–143.
28. Ayant, F.Y.; Kumar, D. Certain finite double integrals involving the hypergeometric function and Aleph-function. *Int. J. Math. Trends Technol.* **2016**, *35*, 49–55. [CrossRef]
29. Agarwal, R. A basic analogue of MacRobert's  $E$ -function. *Glasg. Math. J.* **1961**, *5*, 4–7. [CrossRef]



Article

# Switched Fractional Order Multiagent Systems Containment Control with Event-Triggered Mechanism and Input Quantization

Jiaxin Yuan <sup>\*,†</sup> and Tao Chen <sup>†</sup>

School of Air Transportation, Shanghai University of Engineering Science, Shanghai 201620, China; chentao960520@163.com

\* Correspondence: yuanke2964@sjtu.edu.cn

† These authors contributed equally to this work.

**Abstract:** This paper studies the containment control problem for a class of fractional order nonlinear multiagent systems in the presence of arbitrary switchings, unmeasured states, and quantized input signals by a hysteresis quantizer. Under the framework of the Lyapunov function theory, this paper proposes an event-triggered adaptive neural network dynamic surface quantized controller, in which dynamic surface control technology can avoid “explosion of complexity” and obtain fractional derivatives for virtual control functions continuously. Radial basis function neural networks (RBFNNs) are used to approximate the unknown nonlinear functions, and an observer is designed to obtain the unmeasured states. The proposed distributed protocol can ensure all the signals remain semi-global uniformly ultimately bounded in the closed-loop system, and all followers can converge to the convex hull spanned by the leaders’ trajectory. Utilizing the combination of an event-triggered scheme and quantized control technology, the controller is updated aperiodically only at the event-sampled instants such that transmitting and computational costs are greatly reduced. Simulations compare the event-triggered scheme without quantization control technology with the control method proposed in this paper, and the results show that the event-triggered scheme combined with the quantization mechanism reduces the number of control inputs by 7% to 20%.

**Keywords:** fractional order multiagent systems; containment control; event-triggered mechanism; input quantization; switched systems; neural network; observer

**Citation:** Yuan, J.; Chen, T. Switched Fractional Order Multiagent Systems Containment Control with Event-Triggered Mechanism and Input Quantization. *Fractal Fract.* **2022**, *6*, 77. <https://doi.org/10.3390/fractalfract6020077>

Academic Editors: António M. Lopes, Alireza Alfi, Liping Chen and Sergio A. David

Received: 23 December 2021

Accepted: 28 January 2022

Published: 31 January 2022

**Publisher’s Note:** MDPI stays neutral with regard to jurisdictional claims in published maps and institutional affiliations.



**Copyright:** © 2022 by the authors. Licensee MDPI, Basel, Switzerland. This article is an open access article distributed under the terms and conditions of the Creative Commons Attribution (CC BY) license (<https://creativecommons.org/licenses/by/4.0/>).

## 1. Introduction

Multiagent systems (MASs) cooperative control technology has been widely used in many fields [1–4]. As the most basic research content of multiagent cooperative control, the consensus problem has made much progress [5–11]. Further study of the cooperative control problem of multiagent systems, extending the consensus control of a single leader, considers multiagent cooperative control in the case of multiple leaders, and designs a controller to make the followers converge to a convex hull composed of multiple leaders, which is called containment control. As a special case of cooperative control, many research results of MASs containment control have been reported in the field of integer order control, such as adaptive control [12,13], feedback control [14,15], linear matrix inequalities (LMIs) [16,17], sliding mode control [18], and so on.

Due to the unique memory properties of fractional calculus and the ability to accurately model the system, fractional calculus is suitable for describing real physical systems with genetics [19,20]. At present, the Caputo fractional differential definition is widely used in engineering, and there have been many achievements on the fractional derivative definition and control research of fractional order nonlinear systems. For example, Ref. [21] studied the numerical approximation for the spread of the SIQR model with a Caputo fractional derivative. Ref. [22] expanded the garden equation to the Caputo derivative and

Atangana-Baleanu fractional derivative in the sense of Caputo. Ref. [23] established the Caputo fractional derivatives for exponential  $s$ -convex functions. Some new  $k$ -Caputo fractional derivative inequalities were established in [24] by using Hermite-Hadamard-Mercer type inequalities for differentiable mapping. Ref. [25] proposed two fractional derivatives by taking the Caputo fractional derivative and replacing the simple derivative with a proportional type derivative, which can be expressed as a combination of existing fractional operators in several different ways. In order to perform reliable and effective numerical processing of nonlinear singular fractional Lane-Emden differential equations, based on fractional Meyer wavelet artificial neural network optimization, combined with the comprehensive strength of genetic algorithm-assisted active set method, Ref. [26] proposed a stochastic calculation solver fractional Meyer Wavelet Artificial Neural Network Genetic Algorithm and Active Sets. In reference [27], the authors studied variable order fractional order and constant order fractional order systems with uncertain and external disturbance terms and proposed a variable order fractional control method for tracking control.

At present, the research into the multiagent systems containment control problem has made some progress in the field of fractional order systems. In reference [28], the authors applied the matrices singular value decomposition and LMI techniques for obtaining sufficient conditions to solve the containment problem of fractional order multiagent systems (FOMASs). In reference [29], the authors considered the distributed containment control problem for FOMASs with a double-integrator and designed a distributed projection containment controller for each follower. Due to the general approximation theory of the neural network (NN) and fuzzy logic system, it is often used to deal with the uncertainty of nonlinear systems to obtain unknown nonlinear functions [30]. For example, based on the neural network algorithm, reference [31] designed a distributed control algorithm to ensure that the follower converged to the leader signal in FOMASs. For the FOMASs containment control, an adaptive NN containment controller was designed in reference [12], in which RBFNNs were applied for the unknown functions. In most practical applications, it is usually necessary to obtain the unmeasurable state of the system through a state observer. For example, reference [32] designed a state observer to provide an estimate for unmeasured consensus errors and disturbances of FOMASs. Reference [33] designed an observer to obtain the state of the agent for FOMASs containment control. It should be recognized that the abovementioned fractional order nonlinear system is a kind of non-switched system, and the switched system is another more complex system, which is composed of multiple subsystems and is formed by signal switching between the systems. For the switched system, when switching between subsystems, the system parameters will change greatly, and the nonlinear function of its system will become discontinuous, so the performance of the system may be affected or even unstable [34]. Therefore, it is well worth investigating how to obtain conditions that make the switching system stable for all switching signals. Reference [35] studied the stability and robust stabilization of switched fractional order systems and provided two stability theorems for switched fractional order systems under the arbitrary switching. Based on the fractional Lyapunov stability criterion, reference [36] designed an adaptive fuzzy controller for the uncertain fractional-order switched nonlinear systems and ensured that the tracking error converged to a small neighborhood of the origin regardless of arbitrary switching. The switching control method for strictly feedback switched nonlinear systems was studied by using the average dwell time method in references [37,38].

The traditional time sampling mechanism will cause unnecessary waste of communication resources. In modern technology, an event-triggered mechanism and quantized mechanism can reduce the action frequency of the controller, thus overcoming the problem of wasting communication resources [39]. For example, reference [40] solved the problem of event-triggered fuzzy adaptive tracking control for MASs with input quantization and reduced the communication burden by combining an asymmetric hysteresis quantizer and event triggering mechanism. Based on quantized feedback control, Reference [41] studied the problem of adaptive event-triggered tracking for nonlinear systems with ex-

ternal disturbances. In reference [42], the authors designed an adaptive neural control scheme for integer order uncertain nonlinear systems by combining an event-triggered scheme with input quantization technology. For the containment problem of MASs with unmeasured states, reference [43] developed a quantized control scheme based on the event-triggered backstepping control technique. To the best of our knowledge, the containment control problem of switched fractional order multiagent systems (SFOMAS) combining an event-triggered mechanism and input quantization techniques has not been studied, which motivates the research presented in this paper. Furthermore, the combination of the event-triggered mechanism and the input quantification can reduce the operating frequency of the actuation system and thus reduce energy consumption. Therefore, the research in this paper has great value in the practical engineering application of MASs and reducing the fatigue loss in the system.

Based on the previous discussion, this paper designs an observer-based event-triggered adaptive neural network dynamic surface quantized controller to address the containment control of SFOMASs. Compared with the previous research work, the main contributions of the control method discussed in this paper are summarized as follows.

(1) Comparison with [34,37,38], an adaptive neural network dynamic surface controller is proposed to address the containment control problem of SFOMASs, in which the controller combines the event-triggered mechanism and input quantization to reduce controller action frequency in this paper.

(2) Compared with references [38,40], the state observer is used to estimate system states, and the RBFNN is developed to estimate uncertain parts. In comparison with references [41,43], fractional order DSC technology is used to avoid the “explosion of complexity” that can occur during traditional backstepping design processes and to obtain fractional derivatives for virtual control continuously.

The rest of the paper is organized as follows. Section 2 introduces basic theory about fractional calculus and SFOMASs. In Section 3, first, we construct an observer to estimate the system state, then a controller is proposed based on the adaptive dynamic surface control method; finally, the stability is proved by the Lyapunov function theory. Section 4 provides the numerical simulations to show the viability and efficiency of the proposed controller. Section 5 offers conclusions.

## 2. Preliminaries

### 2.1. Fractional Calculus

The Caputo fractional derivative [44] is defined as

$${}_0^C D_t^\alpha f(t) = \frac{1}{\Gamma(n - \alpha)} \int_0^t \frac{f^{(n)}(\tau)}{(t - \tau)^{1+\alpha-n}} d\tau,$$

where  $n \in \mathbb{N}$  and  $n - 1 < \alpha \leq n$ ,  $\Gamma(z) = \int_0^\infty t^{z-1} e^{-t} dt$  is the Gamma function.

**Lemma 1** ([45]). *For a complex number  $\beta$  and two real numbers  $\alpha, v$  satisfying  $\alpha \in (0, 1)$  and*

$$\frac{\pi\alpha}{2} < v, v < \min\{\pi, \pi\alpha\}$$

*For all integers  $n \geq 1$ , we can obtain*

$$E_{\alpha,\beta}(\zeta) = - \sum_{j=1}^{\infty} \frac{1}{\Gamma(\beta - \alpha j)} + o\left(\frac{1}{|\zeta|^{n+1}}\right)$$

*when  $|\zeta| \rightarrow \infty, v \leq |\arg(\zeta)| \leq \pi$ .*

**Lemma 2** ([45]). *If  $v$  satisfies the condition of Lemma 1, then the following inequality relation holds*

$$|E_{\alpha,\beta}(\zeta)| \leq \frac{\mu}{1+|\zeta|}$$

where  $\alpha \in (0, 2)$  and  $\beta$  is an arbitrary real number,  $\mu > 0$ ,  $v \leq |\arg(\zeta)| \leq \pi$ , and  $|\zeta| \geq 0$ .

**Lemma 3** ([46]). *Let  $x(t) \in R^l$  be a vector of differentiable function. Then, the following inequality holds*

$$D^\alpha(x^T(t)Px) \leq 2x^T(t)PD^\alpha x(t)$$

where  $\alpha \in (0, 1)$  and  $P$  is a positive definite diagonal matrix.

**Lemma 4** ([47]). *(Young's inequality) For any  $x, y \in R^n$ , the following inequality relationship holds*

$$x^T y \leq \frac{c^a}{a} \|x\|^a + \frac{1}{bc^b} \|y\|^b$$

where  $a > 1$ ,  $b > 1$ ,  $c > 0$ , and  $(a-1)(b-1) = 1$ .

**Lemma 5** ([48]). *For  $m \in R$  and  $n > 0$ , the following inequality holds*

$$0 \leq |m| - \frac{m^2}{\sqrt{m^2 + n^2}} \leq n$$

**Lemma 6** ([44]). *Suppose that the Lyapunov function  $V(t, x)$  satisfies  $D^\alpha V(t, x) \leq -CV(t, x) + D$ . Let  $0 < \alpha < 1$ ,  $C > 0$  and  $D \geq 0$ , the following inequality holds*

$$V(t, x) \leq V(0)E_\alpha(-Ct^\alpha) + \frac{D\mu}{C}, \quad t \geq 0$$

Then,  $V(t, x)$  is bounded on  $[0, t]$  and fractional order systems are stable, where  $\mu$  is defined in Lemma 2.

## 2.2. Problem Formulation

In the paper, we consider the following fractional order multiagent system.

$$\begin{cases} D^\alpha x_{i,1}(t) = x_{i,2} + f_{i,1}^{\sigma(t)}(x_{i,1}) \\ D^\alpha x_{i,l}(t) = x_{i,l+1} + f_{i,l}^{\sigma(t)}(x_{i,1}, x_{i,2}, \dots, x_{i,l}) \\ D^\alpha x_{i,n}(t) = u_i(t) + f_{i,n}^{\sigma(t)}(x_{i,1}, x_{i,2}, \dots, x_{i,n}) \\ y_i = x_{i,1} \end{cases} \quad (1)$$

where  $l = 2, \dots, n-1$ ,  $\alpha \in (0, 1)$ ;  $X_{i,l} = (x_{i,1}, x_{i,2}, \dots, x_{i,l})^T \in R^l$  are the system state vectors, and  $u_i(t)$  is the control input of the system. It should be noted that the control input in this paper considers the quantization mechanism and the event-triggered technology.  $y_i$  is the system output, and  $f_{i,l}^{\sigma(t)}(x_{i,1}, x_{i,2}, \dots, x_{i,l})$  are unknown nonlinear functions.  $\sigma(t)$  is a piecewise continuous function that is used to describe the triggering conditions for switching between subsystems. It is called a switching signal, for example, if  $\sigma(t) = q$ , it means that  $q$ -th subsystem is activated.

Rewriting system (1):

$$D^\alpha X_i = A_i X_i + K_i y_i + \sum_{l=1}^n B_{i,l} \left[ f_{i,l}^q(X_{i,l}) \right] + B_i u_i(t) \quad (2)$$

where  $A_i = \begin{bmatrix} -k_{i,1} & & & \\ \vdots & & I_{n-1} & \\ -k_{i,n} & 0 & \cdots & 0 \end{bmatrix}$ ,  $K_i = \begin{bmatrix} k_{i,1} \\ \vdots \\ k_{i,n} \end{bmatrix}$ ,  $B_i = \begin{bmatrix} 0 \\ \vdots \\ 1 \end{bmatrix}$ ,  $B_{i,l} = [0 \dots 1 \dots 0]^T$ , and given a positive matrix  $Q_i^T = Q_i$ , there exists a positive matrix  $P_i^T = P_i$  satisfying

$$A_i^T P_i + P_i A_i = -2Q_i \tag{3}$$

*Control objectives:* This paper aims to design an observer-based adaptive neural network dynamic surface controller, so that all the signals remain bounded in the closed-loop system and enable all followers to converge to the leaders' convex hull. Meanwhile, we utilize the combination of an event-triggered scheme and quantized mechanism to reduce the transmission frequency of the control input.

### 2.3. Hysteresis Quantizer

In this paper, the hysteresis quantizer is used to reduce chattering. The quantizer  $q_i(\omega_i(t))$  is shown as the following form [49].

$$q_i(\omega_i(t)) = \begin{cases} \omega_{is} \text{sign}(\omega_i), & \frac{\omega_{is}}{1+d} < |\omega_i| \leq \frac{\omega_{is}}{1-d} \\ \omega_{is}(1+d)\text{sign}(\omega_i), & \omega_{is} < |\omega_i| \leq \frac{\omega_{is}(1+d)}{1-d} \\ 0, & 0 \leq |\omega_i| < \omega_{\min} \end{cases} \tag{4}$$

where  $\omega_{is} = n^{1-s}\omega_{\min}(s = 1, 2, \dots)$  with parameters  $\omega_{\min} > 0$  and  $0 < n < 1$ ,  $d = \frac{1-n}{1+n}$ . Meanwhile,  $q_i(\omega_i(t))$  is in the set  $U = [0, \pm\omega_{is}, \pm\omega_{is}(1+d)]$ , and  $s = 1, 2, \dots$ .  $\omega_{\min}$  determines the magnitude of the dead-zone for  $q_i(\omega_i(t))$ .

**Lemma 7** ([49]). *The system inputs  $q_i(\omega_i(t))$  can be described as*

$$q_i(\omega_i(t)) = H(\omega_i)\omega_i(t) + L_i(t) \tag{5}$$

where  $1 - d \leq H(\omega_i) \leq 1 + d, |L_i(t)| \leq \omega_{\min}$ .

### 2.4. Graph Theory

Suppose that there exist  $N$  followers, labeled as agents 1 to  $N$ , and  $M$  leaders, labeled as agents  $N + 1$  to  $N + M$ . The information exchange between followers is represented by a directed graph  $G = (w, \varepsilon, \bar{A})$ , in which  $w = \{n_1, \dots, n_{N+M}\}$ . The set of edge is exhibited as  $\varepsilon = \{(n_i, n_j)\} \in w \times w$ , which expresses that follower  $i$  and follower  $j$  can exchange information, and  $N_i = \{j | (n_i, n_j) \in \varepsilon\}$  means the neighbor set of followers  $i$ . Furthermore,  $\bar{A} = \{a_{ij}\} \in R^{(N+M) \times (N+M)}$  is the Adjacency matrix,  $a_{ij}$  of  $\bar{A}$  is represented as if  $(n_i, n_j) \notin \varepsilon, a_{ij} = 0$ ; if not,  $a_{ij} = 1$ . It is supposed that  $a_{ij} = 0$ . A directed graph  $G$  has a spanning tree if there exists at least one node called a root node, which has a directed path to all the other nodes. Define the Laplacian matrix  $L = D - \bar{A} \in R^{(N+M) \times (N+M)}$  and the diagonal matrix  $D = \text{diag}(d_1, \dots, d_{N+M})$ , in which  $d_i = \sum_{j=1}^{N+M} a_{ij}$ .

Suppose that leaders  $N + 1, \dots, N + M$  do not receive the information from followers and other leaders, and the followers  $1, \dots, N$  have at least one neighbor. Therefore, the Laplacian matrix  $L$  related to directed communication graph  $G$  is described as follows:

$$L = \begin{bmatrix} L_1 & L_2 \\ 0_{M \times N} & 0_{M \times M} \end{bmatrix}$$

where  $L_1 \in R^{N \times N}$  is the matrix related to the communication between the  $N$  followers, and  $L_2 \in R^{N \times M}$  is the communication from  $M$  leaders to  $N$  followers. Let  $r(t) = [r_{N+1}, r_{N+2}, \dots, r_{N+M}]^T$ , and  $\text{Co}(r(t)) = \{\sum_{j=N+1}^{N+M} \theta_j r_j | r_j \in r(t), \theta_j > 0, \sum_{j=N+1}^{N+M} \theta_j = 1\}$ . Define the convex hull as  $r_d(t) = [r_{d,1}(t), r_{d,2}(t), \dots, r_{d,M}(t)]^T = -L_1^{-1}L_2r(t)$ . The con-

tainment errors are defined as  $e_i = y_i - r_{d,i}$ . Let  $e = [e_1, e_2, \dots, e_N]^T$ ,  $y = [y_1, y_2, \dots, y_N]^T$ , then  $e = y - r_d(t)$ .

### 2.5. Neural Network Approximation

Due to its universal approximation characteristics, neural networks have been widely used in the identification and control of uncertain nonlinear systems [10]. In this paper, we employ an RBFNNs to identify the nonlinear functions. The unknown function  $f(Z)$  can be expressed as

$$f_m(Z) = \theta^T \varphi(Z)$$

where  $\theta$  is the weight vector and  $\varphi(Z)$  is the basis function vector. In this paper, due to applying radial basis function neural networks (RBFNNs), Gaussian basis functions are used. For any unknown function  $f(Z)$  defined over a compact set  $U$ , there exists the neural network  $\theta^{*T} \varphi(Z)$  and arbitrary accuracy  $\varepsilon(Z)$  such that

$$f(Z) = \theta^{*T} \varphi(Z) + \varepsilon(Z)$$

where  $\theta^*$  is the vectors of optimal parameters defined by  $\theta^* = \arg \min_{\theta \in \Omega} [\sup_{Z \in U} |f(Z) - \theta^T \varphi(Z)|]$ , and  $\varepsilon(Z)$  denotes the minimum approximation error.

**Assumption 1.** *The optimal approximation errors remain bounded, there exists a positive constant  $\varepsilon_0$ , satisfying  $|\varepsilon(Z)| \leq \varepsilon_0$ .*

## 3. Main Results

### 3.1. Observer Design

**Assumption 2.** *In this paper, we employ neural networks to identify the nonlinear functions. The unknown functions  $f_i(X)$ ,  $i = 1, \dots, n$  can be expressed as*

$$f_i(X_i | \theta_i) = \theta_i^T \varphi_i(X_i), 1 \leq i \leq n. \quad (6)$$

Furthermore, we assume that the state variables of system (1) are not available. The state observer is designed as follows:

$$\begin{aligned} D^\alpha \hat{X}_i &= A_i \hat{X}_i + K_i y_i + \sum_{l=1}^n B_{i,l} \hat{f}_{i,l}^q(\hat{X}_{i,l} | \theta_{i,l}) + B_i u_i(t) \\ \hat{y}_i &= C_i \hat{X}_i \end{aligned} \quad (7)$$

where  $C_i = [1 \dots 0 \dots 0]$ , and  $\hat{X}_{i,l} = (\hat{x}_{i,1}, \hat{x}_{i,2}, \dots, \hat{x}_{i,l})^T$  are the estimated values of  $X_{i,l} = (x_{i,1}, x_{i,2}, \dots, x_{i,l})^T$ .

We define  $e_i = X_i - \hat{X}_i$  as the observation error, and then, according to Equations (2) and (6), one has

$$D^\alpha e_i = A_i e_i + \sum_{l=1}^n B_{i,l} [f_{i,l}^q(\hat{X}_{i,l}) - \hat{f}_{i,l}^q(\hat{X}_{i,l} | \theta_{i,l}) + \Delta f_{i,l}^q] \quad (8)$$

where  $\Delta f_{i,l}^q = f_{i,l}^q(X_{i,l}) - f_{i,l}^q(\hat{X}_{i,l})$ .

By Assumption 2, we can obtain

$$\hat{f}_{i,l}^q(\hat{X}_{i,l} | \theta_{i,l}) = \theta_{i,l}^T \varphi_{i,l}(\hat{X}_{i,l}). \quad (9)$$

According to the definition of a neural network, the optimal parameter vector is defined as

$$\theta_{i,l}^* = \arg \min_{\theta_{i,l} \in \Omega_{i,l}} \left[ \sup_{\hat{X}_{i,l} \in U_{i,l}} \left| \hat{f}_{i,l}^q(\hat{X}_{i,l} | \theta_{i,l}) - f_{i,l}^q(\hat{X}_{i,l}) \right| \right]$$

where  $1 \leq l \leq n$ ,  $\Omega_{i,l}$  and  $U_{i,l}$  are compact regions for  $\theta_{i,l}$ ,  $X_{i,l}$  and  $\hat{X}_{i,l}$ . Furthermore, we define that the following equation holds

$$\begin{aligned} \varepsilon_{i,l}^q &= f_{i,l}^q(\hat{X}_{i,l}) - \hat{f}_{i,l}^q(\hat{X}_{i,l} | \theta_{i,l}^*) \\ \tilde{\theta}_{i,l} &= \theta_{i,l}^* - \theta_{i,l}, l = 1, 2, \dots, n \end{aligned}$$

where  $\varepsilon_{i,l}$  is the optimal approximation error, and  $\tilde{\theta}_{i,l}$  is the parameters estimation error.

**Assumption 3.** The optimal approximation errors remain bounded, there exist positive constants  $\varepsilon_{i0}$ , satisfying  $\left| \varepsilon_{i,l}^q \right| \leq \varepsilon_{i0}$ .

**Assumption 4.** The following relationship holds

$$\left| f_i(X) - f_i(\hat{X}) \right| \leq \gamma_i \|X - \hat{X}\|$$

where  $\gamma_i$  is a set of known constants.

By Equations (8) and (9), we have

$$\begin{aligned} D^\alpha e_i &= A_i e_i + \sum_{l=1}^n B_{i,l} \left[ f_{i,l}^q(\hat{X}_{i,l}) - \hat{f}_{i,l}^q(\hat{X}_{i,l} | \theta_{i,l}) + \Delta f_{i,l}^q \right] \\ &= A_i e_i + \sum_{l=1}^n B_{i,l} \left[ \varepsilon_{i,l}^q + \Delta f_{i,l}^q + \tilde{\theta}_{i,l}^T \varphi_{i,l}(\hat{X}_{i,l}) \right] \\ &= A_i e_i + \Delta f_i + \varepsilon_i + \sum_{l=1}^n B_{i,l} \left[ \tilde{\theta}_{i,l}^T \varphi_{i,l}(\hat{X}_{i,l}) \right] \end{aligned} \tag{10}$$

where  $\varepsilon_i = \left[ \varepsilon_{i,1}^q, \dots, \varepsilon_{i,n}^q \right]^T$ ,  $\Delta f_i = \left[ \Delta f_{i,1}^q, \dots, \Delta f_{i,n}^q \right]^T$ .

We construct the first Lyapunov function:

$$V_0 = \sum_{i=1}^N V_{i,0} = \sum_{i=1}^N \frac{1}{2} e_i^T P_i e_i. \tag{11}$$

According to Lemma 3, we obtain

$$D^\alpha V_{i,0} \leq -e_i^T Q_i e_i + e_i^T P_i (\varepsilon_i + \Delta f_i) + e_i^T P_i \sum_{l=1}^n B_{i,l} \tilde{\theta}_{i,l}^T \varphi_{i,l}(\hat{X}_{i,l}). \tag{12}$$

By Lemma 4 and Assumption 4, we obtain

$$\begin{aligned}
 & e_i^T P_i (\varepsilon_i + \Delta f_i) + e_i^T P_i \sum_{l=1}^n B_{i,l} \tilde{\theta}_{i,l}^T \varphi_{i,l} (\hat{X}_{i,l}) \\
 & \leq |e_i^T P_i \varepsilon_i| + |e_i^T P_i \Delta f_{i,l}^q| + \frac{1}{2} e_i^T P_i^T P_i e_i + \frac{1}{2} \sum_{l=1}^n \tilde{\theta}_{i,l}^T \varphi_{i,l} \varphi_{i,l}^T \tilde{\theta}_{i,l}^2 \\
 & \leq \|e_i\|^2 + \frac{1}{2} \|P_i \varepsilon_i\|^2 + \frac{1}{2} \|P_i\|^2 \sum_{l=1}^n |\Delta f_{i,l}^q|^2 + \frac{1}{2} \lambda_{i,\max}^2(P_i) \|e_i\|^2 + \frac{1}{2} \sum_{l=1}^n \tilde{\theta}_{i,l}^T \tilde{\theta}_{i,l} \\
 & \leq \|e_i\|^2 \left( 1 + \frac{1}{2} \|P_i\|^2 \sum_{l=1}^n \gamma_{i,l}^q + \frac{1}{2} \lambda_{i,\max}^2(P_i) \right) + \frac{1}{2} \|P_i \varepsilon_i\|^2 + \frac{1}{2} \sum_{l=1}^n \tilde{\theta}_{i,l}^T \tilde{\theta}_{i,l}.
 \end{aligned} \tag{13}$$

By Equations (12) and (13), one has

$$D^\alpha V_{i,0} \leq -q_{i,0} \|e_i\|^2 + \frac{1}{2} \|P_i \varepsilon_i^*\|^2 + \frac{1}{2} \sum_{l=1}^n \tilde{\theta}_{i,l}^T \tilde{\theta}_{i,l} \tag{14}$$

where  $q_{i,0} = -\left(1 + \frac{1}{2} \|P_i\|^2 \sum_{l=1}^n \gamma_{i,l}^q + \frac{1}{2} \lambda_{i,\max}^2(P_i)\right) + \lambda_{i,\min}(Q_i)$ .

Combining (11) and (14), we can obtain

$$\begin{aligned}
 D^\alpha V_0 & \leq \sum_{i=1}^N \left( -q_{i,0} \|e_i\|^2 + \frac{1}{2} \|P_i \varepsilon_i\|^2 + \frac{1}{2} \sum_{l=1}^n \tilde{\theta}_{i,l}^T \tilde{\theta}_{i,l} \right) \\
 & \leq -q_0 \|e\|^2 + \frac{1}{2} \|P \varepsilon\|^2 + \sum_{i=1}^N \sum_{l=1}^n \frac{1}{2} \tilde{\theta}_{i,l}^T \tilde{\theta}_{i,l}.
 \end{aligned} \tag{15}$$

### 3.2. Controller Design

**Theorem 1.** For the SFOMASs (1) where Assumptions 1-4 hold, we construct a state observer (7), by designing an event-triggered adaptive neural network dynamic surface quantized controller (86), virtual control laws (28), (46) and (62), together with the presented designs, which can ensure that all the signals remain bounded, and enables all followers to converge to the leader's convex hull.

**Proof.** In this section, under the framework of adaptive backstepping design, based on Lyapunov stability theory, combined with quantized control, event-triggered technology, and neural network technology, we design virtual control laws and control input.

We define the error surfaces as follows:

$$\begin{aligned}
 s_{i,1} & = \sum_{j=1}^N a_{ij} (y_i - y_j) + \sum_{j=N+1}^{N+M} a_{ij} (y_i - y_{d_j}(t)) \\
 s_{i,l} & = \hat{x}_{i,l} - v_{i,l} \\
 w_{i,l} & = v_{i,l} - \alpha_{i,l-1}, l = 2, \dots, n - 1
 \end{aligned} \tag{16}$$

where  $w_{i,l}$  is the error between  $v_{i,l}$  obtained by the fractional order filter, and the virtual control function  $\alpha_{i,l-1}$ ;  $s_{i,l}$  denotes error surfaces;  $\hat{x}_{i,l}$  is the estimation of  $x_{i,l}$ ;  $y_i$  is the system output; and  $y_{d_j}(t)$  represents the leader signal. □

**Step 1.** According to Equations (16) and (1), we have

$$\begin{aligned}
 D^\alpha s_{i,1} & = d_i \left( x_{i,2} + \theta_{i,1}^T \varphi(\hat{X}_{i,1}) + \tilde{\theta}_{i,1}^T \varphi(\hat{X}_{i,1}) + \varepsilon_{i,1}^q + \Delta f_{i,1}^q \right) - \sum_{j=N}^{N+M} a_{ij} D^\alpha y_d \\
 & \quad - \sum_{j=1}^N a_{ij} \left( x_{j,2} + \theta_{j,1}^T \varphi(\hat{X}_{j,1}) + \tilde{\theta}_{j,1}^T \varphi(\hat{X}_{j,1}) + \varepsilon_{j,1}^q + \Delta f_{j,1}^q \right).
 \end{aligned} \tag{17}$$

Substituting  $x_{*,2} = e_{*,2} + \hat{x}_{*,2}$  and (16) into (17), one has

$$D^\alpha s_{i,1} = d_i \left( s_{i,2} + w_{i,2} + \alpha_{i,1} + e_{i,2} + \theta_{i,1}^T \varphi(\hat{X}_{i,1}) + \tilde{\theta}_{i,1}^T \varphi(\hat{X}_{i,1}) + \varepsilon_{i,1}^q + \Delta f_{i,1}^q \right) - \sum_{j=N+1}^{N+M} a_{ij} D^\alpha y_{dj} - \sum_{j=1}^N a_{ij} (\hat{x}_{j,2} + e_{j,2} + \theta_{j,1}^T \varphi(\hat{X}_{j,1}) + \tilde{\theta}_{j,1}^T \varphi(\hat{X}_{j,1}) + \varepsilon_{j,1}^q + \Delta f_{j,1}^q) \tag{18}$$

where  $\tilde{\theta}_{*,1} = \theta_{*,1}^* - \theta_{*,1}$ ,  $d_i = \sum_{j=1}^{N+M} a_{ij}$ ,  $\theta_{*,1}$  denotes the estimation of  $\theta_{*,1}^*$ .

We construct the Lyapunov function:

$$V_1 = V_0 + \sum_{i=1}^N V_{i,1} = V_0 + \frac{1}{2} \sum_{i=1}^N \left( s_{i,1}^2 + \frac{1}{\sigma_{i,1}} \tilde{\theta}_{i,1}^T \tilde{\theta}_{i,1} + \frac{1}{r_{i,1}} \tilde{\delta}_{i,1}^2 + \sum_{j=1}^N a_{ij} \left( \frac{1}{\sigma_{j,1}} \tilde{\theta}_{j,1}^T \tilde{\theta}_{j,1} + \frac{1}{r_{j,1}} \tilde{\delta}_{j,1}^2 \right) \right) \tag{19}$$

where  $\tilde{\theta}_{*,l} = \theta_{*,l}^* - \theta_{*,l}$  are the parameter estimation errors,  $\tilde{\delta}_{*,l} = \delta_{*,l}^* - \delta_{*,l}$  are the upper bound estimation errors, and  $\sigma_{*,l}$  and  $r_{*,l}$  denote design constant parameters.

Then, we can obtain

$$D^\alpha V_1 = D^\alpha \left( V_0 + \sum_{i=1}^N V_{i,1} \right) = D^\alpha V_0 + \sum_{i=1}^N \left\{ s_{i,1} D^\alpha s_{i,1} + \frac{1}{\sigma_{i,1}} \tilde{\theta}_{i,1}^T D^\alpha \tilde{\theta}_{i,1} + \frac{1}{r_{i,1}} \tilde{\delta}_{i,1} D^\alpha \tilde{\delta}_{i,1} + \sum_{j=1}^N a_{ij} \left( \frac{1}{\sigma_{j,1}} \tilde{\theta}_{j,1}^T D^\alpha \tilde{\theta}_{j,1} + \frac{1}{r_{j,1}} \tilde{\delta}_{j,1} D^\alpha \tilde{\delta}_{j,1} \right) \right\}. \tag{20}$$

Substituting (18) into (20), we arrive at

$$D^\alpha V_1 \leq D^\alpha V_0 + \sum_{i=1}^N \left\{ s_{i,1} [d_i (s_{i,2} + w_{i,2} + \alpha_{i,1} + e_{i,2} + \theta_{i,1}^T \varphi(\hat{X}_{i,1}) + \tilde{\theta}_{i,1}^T \varphi(\hat{X}_{i,1}) + \varepsilon_{i,1}^q + \Delta f_{i,1}^q) - \sum_{j=N+1}^{N+M} a_{ij} D^\alpha y_{dj} - \sum_{j=1}^N a_{ij} (\hat{x}_{j,2} + e_{j,2} + \theta_{j,1}^T \varphi(\hat{X}_{j,1}) + \tilde{\theta}_{j,1}^T \varphi(\hat{X}_{j,1}) + \varepsilon_{j,1}^q + \Delta f_{j,1}^q)] + \frac{1}{\sigma_{i,1}} \tilde{\theta}_{i,1}^T D^\alpha \tilde{\theta}_{i,1} + \frac{1}{r_{i,1}} \tilde{\delta}_{i,1} D^\alpha \tilde{\delta}_{i,1} + \sum_{j=1}^N a_{ij} \left( \frac{1}{\sigma_{j,1}} \tilde{\theta}_{j,1}^T D^\alpha \tilde{\theta}_{j,1} + \frac{1}{r_{j,1}} \tilde{\delta}_{j,1} D^\alpha \tilde{\delta}_{j,1} \right) \right\}. \tag{21}$$

Following Lemma 4, one has

$$s_{i,1} d_i (s_{i,2} + w_{i,2}) \leq s_{i,1}^2 + \frac{d_i^2}{2} (s_{i,2}^2 + w_{i,2}^2) \tag{22}$$

$$s_{i,1} d_i e_{i,2} + s_{i,1} \sum_{j=1}^N a_{ij} e_{j,2} \leq s_{i,1}^2 + \frac{d_i^2}{2} (\|e_{i,2}\|^2 + \|e_{j,2}\|^2). \tag{23}$$

Denoting  $\varepsilon_{*,l}^q + \Delta f_{*,l}^q = \Delta_{*,l}$  and  $|\Delta_{i,l}| \leq \delta_{i,l}^*$ , the following inequalities hold

$$s_{*,1} \Delta_{*,1} \leq |s_{*,1} \Delta_{*,1}| \leq |s_{*,1}| |\Delta_{*,1}| \leq |s_{*,1}| \delta_{*,1}^* = |s_{*,1}| (\tilde{\delta}_{*,1} + \delta_{*,1}). \tag{24}$$

Considering (24), one has

$$\begin{aligned}
 D^\alpha V_1 \leq & D^\alpha V_0 + \sum_{i=1}^N \left\{ s_{i,1} \left[ d_i \left( \alpha_{i,1} + \theta_{i,1}^T \varphi(\hat{X}_{i,1}) + \tilde{\theta}_{i,1}^T \varphi(\hat{X}_{i,1}) + \varepsilon_{i,1}^q + \Delta f_{i,1}^q \right) \right. \right. \\
 & \left. \left. - \sum_{j=N+1}^{N+M} a_{ij} D^\alpha y_{dj} - \sum_{j=1}^N a_{ij} (\hat{x}_{j,2} + \theta_{j,1}^T \varphi(\hat{X}_{j,1}) + \tilde{\theta}_{j,1}^T \varphi(\hat{X}_{j,1}) + \varepsilon_{j,1}^q + \Delta f_{j,1}^q) \right] \right. \\
 & \left. + s_{i,1} d_i (s_{i,2} + w_{i,2}) + s_{i,1} d_i e_{i,2} + s_{i,1} \left( - \sum_{j=1}^N a_{ij} e_{j,2} \right) + \frac{1}{\sigma_{i,1}} \tilde{\theta}_{i,1}^T D^\alpha \tilde{\theta}_{i,1} \right. \\
 & \left. + \frac{1}{r_{i,1}} \tilde{\delta}_{i,1} D^\alpha \tilde{\delta}_{i,1} + \sum_{j=1}^N a_{ij} \left( \frac{1}{\sigma_{j,1}} \tilde{\theta}_{j,1}^T D^\alpha \tilde{\theta}_{j,1} + \frac{1}{r_{j,1}} \tilde{\delta}_{j,1} D^\alpha \tilde{\delta}_{j,1} \right) \right\}. \tag{25}
 \end{aligned}$$

Substituting (22) and (23) into (25) produces

$$\begin{aligned}
 D^\alpha V_1 \leq & D^\alpha V_0 + \sum_{i=1}^N \left\{ s_{i,1} \left[ d_i \left( \alpha_{i,1} + \theta_{i,1}^T \varphi(\hat{X}_{i,1}) + \tilde{\theta}_{i,1}^T \varphi(\hat{X}_{i,1}) + \varepsilon_{i,1}^q + \Delta f_{i,1}^q \right) \right. \right. \\
 & \left. \left. - \sum_{j=N+1}^{N+M} a_{ij} D^\alpha y_{dj} - \sum_{j=1}^N a_{ij} (\hat{x}_{j,2} + \theta_{j,1}^T \varphi(\hat{X}_{j,1}) + \tilde{\theta}_{j,1}^T \varphi(\hat{X}_{j,1}) + \varepsilon_{j,1}^q + \Delta f_{j,1}^q) \right] \right. \\
 & \left. + s_{i,1}^2 + \frac{d_i^2}{2} (s_{i,2}^2 + w_{i,2}^2) + s_{i,1}^2 + \frac{d_i^2}{2} (\|e_{i,2}\|^2 + \|e_{j,2}\|^2) \right. \\
 & \left. + \frac{1}{\sigma_{i,1}} \tilde{\theta}_{i,1}^T D^\alpha \tilde{\theta}_{i,1} + \frac{1}{r_{i,1}} \tilde{\delta}_{i,1} D^\alpha \tilde{\delta}_{i,1} + \sum_{j=1}^N a_{ij} \left( \frac{1}{\sigma_{j,1}} \tilde{\theta}_{j,1}^T D^\alpha \tilde{\theta}_{j,1} + \frac{1}{r_{j,1}} \tilde{\delta}_{j,1} D^\alpha \tilde{\delta}_{j,1} \right) \right\}. \tag{26}
 \end{aligned}$$

Substituting (15) into (26), one has

$$\begin{aligned}
 D^\alpha V_1 \leq & -q_1 \|e\|^2 + \frac{1}{2} \|P\varepsilon\|^2 + \sum_{i=1}^N \sum_{l=1}^n \frac{1}{2} \tilde{\theta}_{i,l}^T \tilde{\theta}_{i,l} + \sum_{i=1}^N \left\{ s_{i,1} \left[ d_i \left( \alpha_{i,1} + \theta_{i,1}^T \varphi(\hat{X}_{i,1}) \right. \right. \right. \\
 & \left. \left. + \varepsilon_{i,1}^q + \Delta f_{i,1}^q \right) - \sum_{j=N+1}^{N+M} a_{ij} D^\alpha y_{dj} - \sum_{j=1}^N a_{ij} (\hat{x}_{j,2} + \theta_{j,1}^T \varphi(\hat{X}_{j,1}) + \tilde{\theta}_{j,1}^T \varphi(\hat{X}_{j,1}) \right. \right. \\
 & \left. \left. + \varepsilon_{j,1}^q + \Delta f_{j,1}^q \right) \right] + 2s_{i,1}^2 + \frac{d_i^2}{2} (s_{i,2}^2 + w_{i,2}^2) - \frac{1}{\sigma_{i,1}} \tilde{\theta}_{i,1}^T D^\alpha \theta_{i,1} - \frac{1}{r_{i,1}} \tilde{\delta}_{i,1} D^\alpha \delta_{i,1} \\
 & \left. + \sum_{j=1}^N a_{ij} \left( - \frac{1}{\sigma_{j,1}} \tilde{\theta}_{j,1}^T D^\alpha \theta_{j,1} - \frac{1}{r_{j,1}} \tilde{\delta}_{j,1} D^\alpha \delta_{j,1} \right) \right\} \tag{27}
 \end{aligned}$$

where  $q_1 = q_0 - \sum_{i=1}^N d_i^2$ .

We design the virtual control function  $\alpha_{i,1}$  and parameters adaptive laws

$$\begin{aligned}
 \alpha_{i,1} = & \frac{1}{d_i} \left( -c_{i1} s_{i,1} - 2s_{i,1} + \sum_{j=1}^N a_{ij} (\hat{x}_{j,2} + \theta_{j,1}^T \varphi_{j,1}) + \sum_{j=N+1}^{N+M} a_{ij} D^\alpha y_{dj} \right) \\
 & - \tilde{\theta}_{i,1}^T \varphi_{i,1} - \text{sign}(s_{i,1}) \left( \delta_{i,1} - \sum_{j=1}^N \frac{a_{ij}}{d_i} \delta_{j,1} \right). \tag{28}
 \end{aligned}$$

$$D^\alpha \theta_{i,1} = \sigma_{i,1} d_i \varphi_{i,1}(\hat{X}_{i,1}) s_{i,1} - \rho_{i,1} \theta_{i,1} \tag{29}$$

$$D^\alpha \theta_{j,1} = -\sigma_{j,1} \varphi_{j,1}(\hat{X}_{j,1}) s_{i,1} - \rho_{j,1} \theta_{j,1} \tag{30}$$

$$D^\alpha \delta_{i,1} = r_{i,1} d_i |s_{i,1}| - \eta_{i,1} \delta_{i,1} \tag{31}$$

$$D^\alpha \delta_{j,1} = -r_{j,1} |s_{i,1}| - \eta_{j,1} \delta_{j,1} \tag{32}$$

Substituting (29)–(32) into (27) produces

$$\begin{aligned}
 & D^\alpha V_1 \\
 & \leq -q_1 \|e\|^2 + \frac{1}{2} \|P\varepsilon\|^2 + \sum_{i=1}^N \sum_{l=1}^n \frac{1}{2} \tilde{\theta}_{i,l}^T \tilde{\theta}_{i,l} + \sum_{i=1}^N \left\{ s_{i,1} \left[ d_i \left( \alpha_{i,1} + \theta_{i,1}^T \varphi(\hat{X}_{i,1}) + \varepsilon_{i,1}^q + \Delta f_{i,1}^q \right) \right. \right. \\
 & - \sum_{j=N+1}^{N+M} a_{ij} D^\alpha y_{dj} - \sum_{j=1}^N a_{ij} \left( \hat{x}_{j,2} + \theta_{j,1}^T \varphi(\hat{X}_{j,1}) + \varepsilon_{j,1}^q + \Delta f_{j,1}^q \right) \left. \right] + \frac{\rho_{i,1}}{\sigma_{i,1}} \tilde{\theta}_{i,1}^T \theta_{i,1} - \tilde{\delta}_{i,1} d_i |s_{i,1}| \\
 & + \frac{\eta_{i,1}}{r_{i,1}} \tilde{\delta}_{j,1} \delta_{i,1} + \sum_{j=1}^N a_{ij} \left( \frac{\rho_{j,1}}{\sigma_{j,1}} \tilde{\theta}_{j,1}^T \theta_{j,1} + \tilde{\delta}_{j,1} |s_{i,1}| + \frac{\eta_{j,1}}{r_{j,1}} \tilde{\delta}_{j,1} \delta_{j,1} \right) + 2s_{i,1}^2 + \frac{d_i^2}{2} (s_{i,2}^2 + w_{i,2}^2) \left. \right\}. \tag{33}
 \end{aligned}$$

Substituting (28) into (33), we have

$$\begin{aligned}
 D^\alpha V_1 & \leq -q_1 \|e\|^2 + \frac{1}{2} \|P\varepsilon\|^2 + \sum_{i=1}^N \sum_{l=1}^n \frac{1}{2} \tilde{\theta}_{i,l}^T \tilde{\theta}_{i,l} \\
 & + \sum_{i=1}^N \left\{ s_{i,1} \left[ -c_{i1} s_{i,1} - \text{sign}(s_{i,1}) \left( d_i \delta_{i,1} - \sum_{j=1}^N a_{ij} \delta_{j,1} \right) + d_i \left( \varepsilon_{i,1}^q + \Delta f_{i,1}^q \right) \right] \right. \\
 & - \sum_{j=1}^N a_{ij} \left( \varepsilon_{j,1}^q + \Delta f_{j,1}^q \right) \left. \right] + \frac{\rho_{i,1}}{\sigma_{i,1}} \tilde{\theta}_{i,1}^T \theta_{i,1} - \tilde{\delta}_{i,1} d_i |s_{i,1}| + \frac{\eta_{i,1}}{r_{i,1}} \tilde{\delta}_{i,1} \delta_{i,1} \\
 & + \sum_{j=1}^N a_{ij} \left( \frac{\rho_{j,1}}{\sigma_{j,1}} \tilde{\theta}_{j,1}^T \theta_{j,1} + \tilde{\delta}_{j,1} |s_{i,1}| + \frac{\eta_{j,1}}{r_{j,1}} \tilde{\delta}_{j,1} \delta_{j,1} \right) + \frac{d_i^2}{2} (s_{i,2}^2 + w_{i,2}^2) \left. \right\}. \tag{34}
 \end{aligned}$$

Substituting (24) into (34), we have

$$\begin{aligned}
 D^\alpha V_1 & \leq -q_1 \|e\|^2 + \frac{1}{2} \|P\varepsilon\|^2 + \sum_{i=1}^N \sum_{l=1}^n \frac{1}{2} \tilde{\theta}_{i,l}^T \tilde{\theta}_{i,l} + \sum_{i=1}^N \left\{ -c_{i1} s_{i,1}^2 + \frac{\rho_{i,1}}{\sigma_{i,1}} \tilde{\theta}_{i,1}^T \theta_{i,1} + \frac{\eta_{i,1}}{r_{i,1}} \tilde{\delta}_{i,1} \delta_{i,1} \right. \\
 & \left. + \sum_{j=1}^N a_{ij} \left( \frac{\rho_{j,1}}{\sigma_{j,1}} \tilde{\theta}_{j,1}^T \theta_{j,1} + \frac{\eta_{j,1}}{r_{j,1}} \tilde{\delta}_{j,1} \delta_{j,1} \right) + \frac{d_i^2}{2} (s_{i,2}^2 + w_{i,2}^2) \right\}. \tag{35}
 \end{aligned}$$

By using the DSC technique, the state variable  $v_{i,2}$  can be obtained by the following equation:

$$\lambda_{i,2} D^\alpha v_{i,2} + v_{i,2} = \alpha_{i,1}, \quad v_{i,2}(0) = \alpha_{i,1}(0). \tag{36}$$

According to Equations (16) and (36), we have

$$D^\alpha w_{i,2} = D^\alpha v_{i,2} - D^\alpha \alpha_{i,1} = -\frac{v_{i,2} - \alpha_{i,1}}{\lambda_{i,2}} - D^\alpha \alpha_{i,1} = -\frac{w_{i,2}}{\lambda_{i,2}} + B_{i,2} \tag{37}$$

where  $B_{i,2}$  is a continuous function of variables  $s_{i,1}, s_{i,2}, w_{i,2}, \theta_{i,1}, \theta_{j,1}, \delta_{i,1}, \delta_{j,1}, s_{j,3}, w_{j,3}, y_{dj}, D^\alpha y_{dj}, D^\alpha (D^\alpha y_{dj})$ , and there may exist an unknown constant  $M_{i,2}$  such that  $|B_{i,2}| \leq M_{i,2}$  holds.

**Step 2.** Defining the second surface error  $s_{i,2} = \hat{x}_{i,2} - v_{i,2}$ , we have

$$D^\alpha s_{i,2} = D^\alpha \hat{x}_{i,2} - D^\alpha v_{i,2} = \hat{x}_{i,3} + k_{i,2} e_{i,1} + \tilde{\theta}_{i,2}^T \varphi_{i,2} + \theta_{i,2}^T \varphi_{i,2} + \varepsilon_{i,2}^q + \Delta f_{i,2}^q - D^\alpha v_{i,2}. \tag{38}$$

According to Equation (16), we can obtain

$$D^\alpha s_{i,2} = s_{i,3} + w_{i,3} + \alpha_{i,2} + k_{i,2} e_{i,1} + \tilde{\theta}_{i,2}^T \varphi_{i,2} + \theta_{i,2}^T \varphi_{i,2} + \varepsilon_{i,2}^q + \Delta f_{i,2}^q - D^\alpha v_{i,2}. \tag{39}$$

Select the Lyapunov function as follows:

$$V_2 = V_1 + \sum_{i=1}^N V_{i,2} = V_1 + \frac{1}{2} \sum_{i=1}^N \left( s_{i,2}^2 + \frac{1}{\sigma_{i,2}} \tilde{\theta}_{i,2}^T \tilde{\theta}_{i,2} + \frac{1}{r_{i,2}} \tilde{\delta}_{i,2}^2 + w_{i,2}^2 \right). \tag{40}$$

Further, we can obtain

$$D^\alpha V_2 \leq D^\alpha V_1 + \sum_{i=1}^N (s_{i,2}(s_{i,3} + w_{i,3} + \alpha_{i,2} + k_{i,2}e_{i,1} + \tilde{\theta}_{i,2}^T \varphi_{i,2} + \theta_{i,2}^T \varphi_{i,2} + \Delta_{i,2} - D^\alpha v_{i,2}) + \frac{1}{\sigma_{i,2}} \tilde{\theta}_{i,2}^T D^\alpha \tilde{\theta}_{i,2} + \frac{1}{r_{i,2}} \tilde{\delta}_{i,2} D^\alpha \tilde{\delta}_{i,2} + w_{i,2} D^\alpha w_{i,2}). \quad (41)$$

Similar to the previous calculation, the following inequalities hold

$$s_{i,2}(s_{i,3} + w_{i,3}) \leq s_{i,2}^2 + \frac{1}{2}(s_{i,3}^2 + w_{i,3}^2) \quad (42)$$

$$s_{i,2}k_{i,2}e_{i,1} \leq \frac{1}{2}s_{i,2}^2 + \frac{k_{i,2}^2}{2}\|e_{i,1}\|^2 \quad (43)$$

$$s_{i,2}\Delta_{i,2} \leq |s_{i,2}\Delta_{i,2}| \leq |s_{i,2}|\|\Delta_{i,2}\| \leq |s_{i,2}|\delta_{i,2}^* = |s_{i,2}|(\tilde{\delta}_{i,2} + \delta_{i,2}). \quad (44)$$

Substituting (42)–(44) into (41), we obtain

$$D^\alpha V_2 \leq D^\alpha V_1 + \sum_{i=1}^N (s_{i,2}(\alpha_{i,2} + \tilde{\theta}_{i,2}^T \varphi_{i,2} + \theta_{i,2}^T \varphi_{i,2} - D^\alpha v_{i,2}) + |s_{i,2}|(\tilde{\delta}_{i,2} + \delta_{i,2}) + \frac{3}{2}s_{i,2}^2 + \frac{1}{2}(s_{i,3}^2 + w_{i,3}^2) + \frac{k_{i,2}^2}{2}\|e_{i,1}\|^2 - \frac{1}{\sigma_{i,2}} \tilde{\theta}_{i,2}^T D^\alpha \tilde{\theta}_{i,2} - \frac{1}{r_{i,2}} \tilde{\delta}_{i,2} D^\alpha \tilde{\delta}_{i,2} + w_{i,2} D^\alpha w_{i,2}). \quad (45)$$

We select the virtual controller  $\alpha_{i,2}$  and the parameters adaptive laws as follows:

$$\alpha_{i,2} = -c_{i,2}s_{i,2} - \frac{3}{2}s_{i,2} - \frac{d_i^2}{2}s_{i,2} - \theta_{i,2}^T \varphi_{i,2} + \frac{\alpha_{i,1} - v_{i,2}}{\lambda_{i,2}} - \text{sign}(s_{i,2})\delta_{i,2} \quad (46)$$

$$D^\alpha \theta_{i,2} = \sigma_{i,2} \varphi_{i,2} (\hat{X}_{i,2}) s_{i,2} - \rho_{i,2} \theta_{i,2} \quad (47)$$

$$D^\alpha \delta_{i,2} = r_{i,2}|s_{i,2}| - \eta_{i,2}\delta_{i,2}. \quad (48)$$

Substituting (35), (38) and (47)–(48) into (45), we have

$$D^\alpha V_2 \leq -q_1 \|e\|^2 + \frac{1}{2} \|P\varepsilon\|^2 + \sum_{i=1}^N \sum_{l=1}^n \frac{1}{2} \tilde{\theta}_{i,l}^T \tilde{\theta}_{i,l} + \sum_{i=1}^N \left\{ -c_{i,1}s_{i,1}^2 + \frac{\rho_{i,1}}{\sigma_{i,1}} \tilde{\theta}_{i,1}^T \theta_{i,1} + \frac{\eta_{i,1}}{r_{i,1}} \tilde{\delta}_{i,1} \delta_{i,1} + \sum_{j=1}^N a_{ij} \left( \frac{\rho_{j,1}}{\sigma_{j,1}} \tilde{\theta}_{j,1}^T \theta_{j,1} + \frac{\eta_{j,1}}{r_{j,1}} \tilde{\delta}_{j,1} \delta_{j,1} \right) + \frac{d_i^2}{2} (s_{i,2}^2 + w_{i,2}^2) \right\} + \sum_{i=1}^N \left\{ s_{i,2} \left[ -c_{i,2}s_{i,2} - \frac{3}{2}s_{i,2} - \frac{d_i^2}{2}s_{i,2} - \theta_{i,2}^T \varphi_{i,2} + \frac{\alpha_{i,1} - v_{i,2}}{\lambda_{i,2}} - \text{sign}(s_{i,2})\delta_{i,2} + \tilde{\theta}_{i,2}^T \varphi_{i,2} + \theta_{i,2}^T \varphi_{i,2} - D^\alpha v_{i,2} \right] + |s_{i,2}|(\tilde{\delta}_{i,2} + \delta_{i,2}) + \frac{3}{2}s_{i,2}^2 + \frac{1}{2}(s_{i,3}^2 + w_{i,3}^2) + \frac{k_{i,2}^2}{2}\|e_{i,1}\|^2 - \frac{1}{\sigma_{i,2}} \tilde{\theta}_{i,2}^T (\sigma_{i,2} \varphi_{i,2} (\hat{X}_{i,2}) s_{i,2} - \rho_{i,2} \theta_{i,2}) - \frac{1}{r_{i,2}} \tilde{\delta}_{i,2} (r_{i,2}|s_{i,2}| - \eta_{i,2}\delta_{i,2}) + w_{i,2} \left( -\frac{w_{i,2}}{\lambda_{i,2}} + B_{i,2} \right) \right\}. \quad (49)$$

By Lemma 4, we have

$$w_{i,2}B_{i,2} \leq \frac{1}{2}w_{i,2}^2 + \frac{1}{2}M_{i,2}^2. \quad (50)$$

Then, we have

$$\begin{aligned}
 D^\alpha V_2 \leq & -q_2 \|e\|^2 + \frac{1}{2} \|P\varepsilon\|^2 + \sum_{i=1}^N \sum_{l=1}^n \frac{1}{2} \tilde{\theta}_{i,l}^T \tilde{\theta}_{i,l} + \sum_{i=1}^N \left\{ -c_{i1} s_{i,1}^2 - c_{i2} s_{i,2}^2 + \frac{\rho_{i,1}}{\sigma_{i,1}} \tilde{\theta}_{i,1}^T \theta_{i,1} \right. \\
 & + \frac{\eta_{i,1}}{r_{i,1}} \tilde{\delta}_{i,1} \delta_{i,1} + \frac{\rho_{i,2}}{\sigma_{i,2}} \tilde{\theta}_{i,2}^T \theta_{i,2} + \frac{\eta_{i,2}}{r_{i,2}} \tilde{\delta}_{i,2} \delta_{i,2} + \sum_{j=1}^N a_{ij} \left( \frac{\rho_{j,1}}{\sigma_{j,1}} \tilde{\theta}_{j,1}^T \theta_{j,1} + \frac{\eta_{j,1}}{r_{j,1}} \tilde{\delta}_{j,1} \delta_{j,1} \right) \\
 & \left. - \left( \frac{1}{\lambda_{i,2}} - \frac{1}{2} - \frac{d_i^2}{2} \right) w_{i,2}^2 + \frac{1}{2} (s_{i,3}^2 + w_{i,3}^2) + \frac{1}{2} M_{i,2}^2 \right\}
 \end{aligned} \tag{51}$$

where  $q_2 = q_1 - \sum_{i=1}^N k_{i,2}^2$ .

Similar to (36), we have

$$\lambda_{i,3} D^\alpha v_{i,3} + v_{i,3} = \alpha_{i,2}, \quad v_{i,3}(0) = \alpha_{i,2}(0). \tag{52}$$

By Equation (52), we can obtain

$$D^\alpha w_{i,3} = D^\alpha v_{i,3} - D^\alpha \alpha_{i,2} = -\frac{v_{i,3} - \alpha_{i,2}}{\lambda_{i,3}} - D^\alpha \alpha_{i,2} = -\frac{w_{i,3}}{\lambda_{i,3}} + B_{i,3} \tag{53}$$

where  $B_{i,3} = -D^\alpha \alpha_{i,2}$ . Furthermore, there exists an unknown constant  $M_{i,3}$  such that  $|B_{i,3}| \leq M_{i,3}$  holds.

**Step m.** The Caputo fractional derivatives of  $s_{i,m}$  are as follows:

$$D^\alpha s_{i,m} = D^\alpha \hat{x}_{i,m} - D^\alpha v_{i,m} = \hat{x}_{i,m+1} + k_{i,m} e_{i,1} + \tilde{\theta}_{i,m}^T \varphi_{i,m} + \theta_{i,m}^T \varphi_{i,m} + \varepsilon_{i,m}^q + \Delta f_{i,m}^q - D^\alpha v_{i,m}. \tag{54}$$

Substituting (16) into (54) produces

$$D^\alpha s_{i,m} = s_{i,m+1} + w_{i,m+1} + \alpha_{i,m} + k_{i,m} e_{i,1} + \tilde{\theta}_{i,m}^T \varphi_{i,m} + \theta_{i,m}^T \varphi_{i,m} + \varepsilon_{i,m}^q + \Delta_i^q - D^\alpha v_{i,m}. \tag{55}$$

We construct a Lyapunov function candidate as

$$V_m = V_{m-1} + \sum_{i=1}^N V_{i,m} = V_{m-1} + \frac{1}{2} \sum_{i=1}^N \left\{ s_{i,m}^2 + \frac{1}{\sigma_{i,m}} \tilde{\theta}_{i,m}^T \tilde{\theta}_{i,m} + \frac{1}{r_{i,m}} \tilde{\delta}_{i,m}^2 + w_{i,m}^2 \right\}. \tag{56}$$

According to Lemma 3 and (55), we can obtain

$$\begin{aligned}
 D^\alpha V_m \leq & D^\alpha V_{m-1} + \sum_{i=1}^N \left( s_{i,m} D^\alpha s_{i,m} + \frac{1}{\sigma_{i,m}} \tilde{\theta}_{i,m}^T D^\alpha \tilde{\theta}_{i,m} + \frac{1}{r_{i,m}} \tilde{\delta}_{i,m} D^\alpha \tilde{\delta}_{i,m} + w_{i,m} D^\alpha w_{i,m} \right) \\
 \leq & D^\alpha V_{m-1} + \sum_{i=1}^N \left\{ s_{i,m} [s_{i,m+1} + w_{i,m+1} + \alpha_{i,m} + k_{i,m} e_{i,1} + \tilde{\theta}_{i,m}^T \varphi_{i,m} + \theta_{i,m}^T \varphi_{i,m} \right. \\
 & \left. + \varepsilon_{i,m}^q + \Delta f_{i,m}^q - D^\alpha v_{i,m}] + \frac{1}{\sigma_{i,m}} \tilde{\theta}_{i,m}^T D^\alpha \tilde{\theta}_{i,m} + \frac{1}{r_{i,m}} \tilde{\delta}_{i,m} D^\alpha \tilde{\delta}_{i,m} + w_{i,m} D^\alpha w_{i,m} \right\}.
 \end{aligned} \tag{57}$$

Similar to (22) and (23), the following inequalities hold

$$s_{i,m} k_{i,m} e_{i,1} \leq \frac{1}{2} s_{i,m}^2 + \frac{1}{2} k_{i,m}^2 \|e_{i,1}\|^2 \tag{58}$$

$$s_{i,m} (s_{i,m+1} + w_{i,m+1}) \leq s_{i,m}^2 + \frac{1}{2} s_{i,m+1}^2 + \frac{1}{2} w_{i,m+1}^2 \tag{59}$$

$$s_{i,m} \Delta_{i,m} \leq |s_{i,m} \Delta_{i,m}| \leq |s_{i,m}| |\Delta_{i,m}| \leq |s_{i,m}| \Delta_{i,m}^* = |s_{i,m}| (\tilde{\delta}_{i,m} + \delta_{i,m}). \tag{60}$$

Substituting (58)–(60) into (57) produces

$$\begin{aligned} D^\alpha V_m \leq & D^\alpha V_{m-1} + \sum_{i=1}^N \left\{ s_{i,m} \left( \alpha_{i,m} + \tilde{\theta}_{i,m}^T \varphi_{i,m} + \theta_{i,m}^T \varphi_{i,m} - D^\alpha v_{i,m} \right) \right. \\ & + \frac{3}{2} s_{i,m}^2 + \frac{1}{2} k_{i,m}^2 \|e_{i,1}\|^2 + |s_{i,m}| (\tilde{\delta}_{i,m} + \delta_{i,m}) + \frac{1}{2} s_{i,m+1}^2 + \frac{1}{2} w_{i,m+1}^2 \\ & \left. - \frac{1}{\sigma_{i,m}} \tilde{\theta}_{i,m}^T D^\alpha \theta_{i,m} - \frac{1}{r_{i,m}} \tilde{\delta}_{i,m} D^\alpha \delta_{i,m} + w_{i,m} D^\alpha w_{i,m} \right\}. \end{aligned} \quad (61)$$

We design the  $m$ -th virtual control function  $\alpha_{i,m}$  and parameters adaptive laws

$$\alpha_{i,m} = -c_{i,m} s_{i,m} - 2s_{i,m} - \theta_{i,m}^T \varphi_{i,m} + \frac{\alpha_{i,m-1} - v_{i,m}}{\lambda_{i,m}} - \text{sign}(s_{i,m}) \delta_{i,m} \quad (62)$$

$$D^\alpha \theta_{i,m} = \sigma_{i,m} \varphi_{i,m} (\hat{X}_{i,m}) s_{i,m} - \rho_{i,m} \theta_{i,m} \quad (63)$$

$$D^\alpha \delta_{i,m} = r_{i,m} |s_{i,m}| - \eta_{i,m} \delta_{i,m}. \quad (64)$$

Substituting Equations (62)–(64) into (61), we can obtain

$$\begin{aligned} D^\alpha V_m \leq & D^\alpha V_{m-1} + \sum_{i=1}^N \left\{ s_{i,m} \left[ -c_{i,m} s_{i,m} - 2s_{i,m} - \theta_{i,m}^T \varphi_{i,m} + \frac{\alpha_{i,m-1} - v_{i,m}}{\lambda_{i,m}} \right. \right. \\ & \left. \left. - \text{sign}(s_{i,m}) \delta_{i,m} + \tilde{\theta}_{i,m}^T \varphi_{i,m} + \theta_{i,m}^T \varphi_{i,m} - D^\alpha v_{i,m} \right] + |s_{i,m}| (\tilde{\delta}_{i,m} + \delta_{i,m}) + \frac{3}{2} s_{i,m}^2 \right. \\ & + \frac{1}{2} k_{i,m}^2 \|e_{i,1}\|^2 + \frac{1}{2} s_{i,m+1}^2 + \frac{1}{2} w_{i,m+1}^2 - \frac{1}{\sigma_{i,m}} \tilde{\theta}_{i,m}^T (\sigma_{i,m} \varphi_{i,m} (\hat{X}_{i,m}) s_{i,m} - \rho_{i,m} \theta_{i,m}) \\ & \left. - \frac{1}{r_{i,m}} \tilde{\delta}_{i,m} (r_{i,m} |s_{i,m}| - \eta_{i,m} \delta_{i,m}) + w_{i,m} D^\alpha w_{i,m} \right\}. \end{aligned} \quad (65)$$

Similar to (52),  $v_{i,m}$  can be obtained as

$$\lambda_{i,m} D^\alpha v_{i,m} + v_{i,m} = \alpha_{i,m-1}, \quad v_{i,m}(0) = \alpha_{i,m-1}(0). \quad (66)$$

By Equation (66), we have

$$D^\alpha w_{i,m} = -\frac{w_{i,m}}{\lambda_{i,m}} + B_{i,m} \quad (67)$$

where  $|B_{i,m}| \leq M_{i,m}$ , and  $M_{i,m}$  is an unknown constant.

By employing Young's inequality, we have

$$w_{i,m} B_{i,m} \leq \frac{1}{2} w_{i,m}^2 + \frac{1}{2} M_{i,m}^2. \quad (68)$$

From (65)–(68), we have

$$\begin{aligned} D^\alpha V_m \leq & D^\alpha V_{m-1} + \sum_{i=1}^N \left\{ -c_{i,m} s_{i,m}^2 + \frac{\rho_{i,m}}{\sigma_{i,m}} \tilde{\theta}_{i,m}^T \theta_{i,m} + \frac{\eta_{i,m}}{r_{i,m}} \tilde{\delta}_{i,m} \delta_{i,m} + \frac{1}{2} s_{i,m+1}^2 \right. \\ & \left. + \frac{1}{2} w_{i,m+1}^2 - \left( \frac{1}{\lambda_{i,m}} - \frac{1}{2} \right) w_{i,m}^2 + \frac{1}{2} M_{i,m}^2 - \frac{1}{2} s_{i,m}^2 + \frac{1}{2} k_{i,m}^2 \|e_{i,1}\|^2 \right\}. \end{aligned} \quad (69)$$

Combining (15), (35) and (51) together leads to

$$\begin{aligned}
 D^\alpha V_{m-1} &\leq -q_{m-1}\|e\|^2 + \frac{1}{2}\|P\varepsilon\|^2 + \sum_{i=1}^N \sum_{l=1}^n \frac{1}{2} \tilde{\theta}_{i,l}^T \tilde{\theta}_{i,l} \\
 &+ \sum_{i=1}^N \left\{ \sum_{l=1}^{m-1} \left( -c_{i,l} s_{i,l}^2 + \frac{\rho_{i,l}}{\sigma_{i,l}} \tilde{\theta}_{i,l}^T \theta_{i,l} + \frac{\eta_{i,l}}{r_{i,l}} \tilde{\delta}_{i,l} \delta_{i,l} \right) + \sum_{j \in N_i} a_{ij} \left( \frac{\rho_{j,1}}{\sigma_{j,1}} \tilde{\theta}_{j,1}^T \theta_{j,1} + \frac{\eta_{j,1}}{r_{j,1}} \tilde{\delta}_{j,1} \delta_{j,1} \right) \right. \\
 &\left. - \left( \frac{1}{\lambda_{i,2}} - \frac{1}{2} - \frac{d_i^2}{2} \right) w_{i,2}^2 - \sum_{l=3}^{m-1} \left( \frac{1}{\lambda_{i,l}} - 1 \right) w_{i,l}^2 + \frac{1}{2} (s_{i,m}^2 + w_{i,m}^2) + \sum_{l=2}^{m-1} \frac{1}{2} M_{i,l}^2 \right\}.
 \end{aligned} \tag{70}$$

Substituting (70) into (69), we can obtain

$$\begin{aligned}
 D^\alpha V_m &\leq -q_m\|e\|^2 + \frac{1}{2}\|P\varepsilon\|^2 + \sum_{i=1}^N \sum_{l=1}^n \frac{1}{2} \tilde{\theta}_{i,l}^T \tilde{\theta}_{i,l} \\
 &+ \sum_{i=1}^N \left\{ \sum_{l=1}^m \left( -c_{i,l} s_{i,l}^2 + \frac{\rho_{i,l}}{\sigma_{i,l}} \tilde{\theta}_{i,l}^T \theta_{i,l} + \frac{\eta_{i,l}}{r_{i,l}} \tilde{\delta}_{i,l} \delta_{i,l} \right) + \sum_{j=1}^N a_{ij} \left( \frac{\rho_{j,1}}{\sigma_{j,1}} \tilde{\theta}_{j,1}^T \theta_{j,1} + \frac{\eta_{j,1}}{r_{j,1}} \tilde{\delta}_{j,1} \delta_{j,1} \right) \right. \\
 &\left. - \left( \frac{1}{\lambda_{i,2}} - \frac{1}{2} - \frac{d_i^2}{2} \right) w_{i,2}^2 - \sum_{l=3}^m \left( \frac{1}{\lambda_{i,l}} - 1 \right) w_{i,l}^2 + \frac{1}{2} (s_{i,m+1}^2 + w_{i,m+1}^2) + \sum_{l=2}^m \frac{1}{2} M_{i,l}^2 \right\}
 \end{aligned} \tag{71}$$

where  $q_m = q_{m-1} - \sum_{i=1}^N k_{i,m}^2$ .

**Step n.** As in the previous design steps, we define the following equations:

$$s_{i,n} = \hat{x}_{i,n} - v_{i,n} \tag{72}$$

$$w_{i,n} = v_{i,n} - \alpha_{i,n-1}. \tag{73}$$

Similar to (66), we can obtain  $v_{i,n}$  as

$$\lambda_{i,n} D^\alpha v_{i,n} + v_{i,n} = \alpha_{i,n-1}, \quad v_{i,n}(0) = \alpha_{i,n-1}(0). \tag{74}$$

By Equations (73) and (74), we have

$$D^\alpha w_{i,n} = -\frac{w_{i,n}}{\lambda_{i,n}} + B_{i,n}. \tag{75}$$

Further, the fractional derivative  $D^\alpha s_{i,n}$  is given by

$$\begin{aligned}
 D^\alpha s_{i,n} &= D^\alpha \hat{x}_{i,n} - D^\alpha v_{i,n} = u_i(t) + k_{i,n} e_{i,1} + \tilde{\theta}_{i,n}^T \varphi_{i,n} + \theta_{i,n}^T \varphi_{i,n} + \varepsilon_{i,n}^q + \Delta f_{i,n}^q - D^\alpha v_{i,n} \\
 &= q_i(\omega_i(t)) + k_{i,n} e_{i,1} + \tilde{\theta}_{i,n}^T \varphi_{i,n} + \theta_{i,n}^T \varphi_{i,n} + \varepsilon_{i,n}^q + \Delta f_{i,n}^q - D^\alpha v_{i,n}.
 \end{aligned} \tag{76}$$

We construct the Lyapunov function as follows:

$$V_n = V_{n-1} + \sum_{i=1}^N V_{i,n} = V_{n-1} + \frac{1}{2} \sum_{i=1}^N \left\{ s_{i,n}^2 + \frac{1}{\sigma_{i,n}} \tilde{\theta}_{i,n}^T \tilde{\theta}_{i,n} + \frac{1}{r_{i,n}} \tilde{\delta}_{i,n}^2 + w_{i,n}^2 \right\}. \tag{77}$$

Then, one has

$$\begin{aligned}
 D^\alpha V_n &= D^\alpha V_{n-1} + D^\alpha \left( \sum_{i=1}^N V_{i,n} \right) \\
 &\leq D^\alpha V_{n-1} + \sum_{i=1}^N \left\{ s_{i,n} D^\alpha s_{i,n} - \frac{1}{\sigma_{i,n}} \tilde{\theta}_{i,n}^T D^\alpha \theta_{i,n} - \frac{1}{r_{i,n}} \tilde{\delta}_{i,n} D^\alpha \delta_{i,n} + w_{i,n} D^\alpha w_{i,n} \right\}.
 \end{aligned} \tag{78}$$

Substituting Equation (76) into (78), we have

$$D^\alpha V_n \leq D^\alpha V_{n-1} + \sum_{i=1}^N \left\{ s_{i,n} [q_i(\omega_i(t)) + k_{i,n} e_{i,1} + \tilde{\theta}_{i,n}^T \varphi_{i,n} + \theta_{i,n}^T \varphi_{i,n} + \varepsilon_{i,n}^q + \Delta f_{i,n}^q - D^\alpha v_{i,n}] - \frac{1}{\sigma_{i,n}} \tilde{\theta}_{i,n}^T D^\alpha \theta_{i,n} - \frac{1}{r_{i,n}} \tilde{\delta}_{i,n} D^\alpha \delta_{i,n} + w_{i,n} D^\alpha w_{i,n} \right\}. \tag{79}$$

According to (5), we have

$$D^\alpha V_n \leq D^\alpha V_{n-1} + \sum_{i=1}^N \left\{ s_{i,n} [H(\omega_i)\omega_i(t) + L_i(t) + k_{i,n} e_{i,1} + \tilde{\theta}_{i,n}^T \varphi_{i,n} - D^\alpha v_{i,n}] + \theta_{i,n}^T \varphi_{i,n} + \varepsilon_{i,n}^q + \Delta f_{i,n}^q - \frac{1}{\sigma_{i,n}} \tilde{\theta}_{i,n}^T D^\alpha \theta_{i,n} - \frac{1}{r_{i,n}} \tilde{\delta}_{i,n} D^\alpha \delta_{i,n} + w_{i,n} D^\alpha w_{i,n} \right\}. \tag{80}$$

The actual controller  $\omega_i(t)$  is designed as

$$D^\alpha \theta_{i,n} = \sigma_{i,n} \varphi_{i,n} (\hat{X}_{i,n}) s_{i,n} - \rho_{i,n} \theta_{i,n} \tag{81}$$

$$D^\alpha \delta_{i,n} = r_{i,n} |s_{i,n}| - \eta_{i,n} \delta_{i,n} \tag{82}$$

$$\bar{\alpha}_{in} = c_{i,n} s_{i,n} + \frac{3}{2} s_{i,n} + \theta_{i,n}^T \varphi_{i,n} + \text{sign}(s_{i,n}) \delta_{i,n} - \frac{\alpha_{i,n-1} - v_{i,n}}{\lambda_{i,n}} \tag{83}$$

$$\omega_i(t) = \frac{1}{1-d} \left( -\bar{\alpha}_{in} - \frac{s_{i,n} (\kappa_{i1} \bar{\alpha}_{in})^2}{\sqrt{(s_{i,n} \kappa_{i1} \bar{\alpha}_{in})^2 + \kappa_{i2}^2}} - \frac{s_{i,n} M_{i,1}^2}{\sqrt{(s_{i,n} M_{i,1})^2 + \kappa_{i,2}^2}} \right). \tag{84}$$

Notice that, from (5) and (84), we can obtain

$$H(\omega_i)\omega_i(t) \leq -\bar{\alpha}_{in} - \frac{s_{i,n} (\kappa_{i1} \bar{\alpha}_{in})^2}{\sqrt{(s_{i,n} \kappa_{i1} \bar{\alpha}_{in})^2 + \kappa_{i2}^2}} - \frac{s_{i,n} M_{i,1}^2}{\sqrt{(s_{i,n} M_{i,1})^2 + \kappa_{i,2}^2}}. \tag{85}$$

We define the event-triggered controller  $u_i(t)$  as follows

$$u_i(t) = q_i(\omega_i(t_k)) \forall t \in [t_k, t_{k+1}). \tag{86}$$

The triggering condition for the sampling instants are as follows:

$$t_{k+1} = \inf \{ t \in R \mid |\Delta_i(t)| \geq \kappa_{i1} |u_i(t)| + H_{i1} \} \tag{87}$$

where  $\Delta_i(t) = q_i(\omega_i(t)) - u_i(t)$  is the event sampling error,  $0 < \kappa_{i1} < 1$ ,  $H_{i1}$  is a positive constant, and  $t_k, k \in \mathbb{Z}^+$  is the controller update time.

### 3.3. Stability Analysis

From Equation (87), we have

$$\Delta_i(t) = q_i(\omega_i(t)) - u_i(t) = \beta_{i1}(t) \kappa_{i1} u_i(t) + \beta_{i2}(t) H_{i1} \tag{88}$$

where  $\beta_{i1}(t), \beta_{i2}(t)$  are time-varying parameters satisfying  $|\beta_{i1}(t)| \leq 1, |\beta_{i2}(t)| \leq 1$ . Accordingly, one can obtain

$$u_i(t) = \frac{q_i(\omega_i(t)) - \beta_{i2}(t) H_{i1}}{1 + \beta_{i1}(t) \kappa_{i1}}. \tag{89}$$

Thus, it follows that

$$D^\alpha V_n \leq D^\alpha V_{n-1} + \sum_{i=1}^N \left\{ s_{i,n} \left[ \frac{q_i(\omega_i(t)) - \beta_{i2}(t)H_{i1}}{1 + \beta_{i1}(t)\kappa_{i1}} + k_{i,n}e_{i,1} + \tilde{\theta}_{i,n}^T \varphi_{i,n} + \theta_{i,n}^T \varphi_{i,n} \right. \right. \\ \left. \left. + \varepsilon_{i,n}^q + \Delta f_{i,n}^q - D^\alpha v_{i,n} \right] - \frac{1}{\sigma_{i,n}} \tilde{\theta}_{i,n}^T D^\alpha \theta_{i,n} - \frac{1}{r_{i,n}} \tilde{\delta}_{i,n} D^\alpha \delta_{i,n} + w_{i,n} D^\alpha w_{i,n} \right\}. \quad (90)$$

Substituting Equations (81) and (82) into (90), we can obtain

$$D^\alpha V_n \leq D^\alpha V_{n-1} + \sum_{i=1}^N \left\{ s_{i,n} \left[ \frac{q_i(\omega_i(t)) - \beta_{i2}(t)H_{i1}}{1 + \beta_{i1}(t)\kappa_{i1}} + \theta_{i,n}^T \varphi_{i,n} - D^\alpha v_{i,n} \right] + s_{i,n} (k_{i,n}e_{i,1} + \tilde{\theta}_{i,n}^T \varphi_{i,n} \right. \\ \left. + \varepsilon_{i,n}^q + \Delta f_{i,n}^q) - \frac{1}{\sigma_{i,n}} \tilde{\theta}_{i,n}^T (\sigma_{i,n} \varphi_{i,n} s_{i,n} - \rho_{i,n} \theta_{i,n}) - \frac{1}{r_{i,n}} \tilde{\delta}_{i,n} (r_{i,n} |s_{i,n}| - \eta_{i,n} \delta_{i,n}) + w_{i,n} D^\alpha w_{i,n} \right\}. \quad (91)$$

Then, we can obtain

$$D^\alpha V_n \leq D^\alpha V_{n-1} + \sum_{i=1}^N \left\{ s_{i,n} \left[ \frac{q_i(\omega_i(t)) - \beta_{i2}(t)H_{i1}}{1 + \beta_{i1}(t)\kappa_{i1}} + \bar{a}_{in} \right] - c_{in} s_{i,n}^2 - \frac{3}{2} s_{i,n}^2 \right. \\ \left. - |s_{i,n}| \delta_{i,n} + s_{i,n} (\varepsilon_{i,n}^q + \Delta f_{i,n}^q) + \frac{\rho_{i,n}}{\sigma_{i,n}} \tilde{\theta}_{i,n}^T \theta_{i,n} + s_{i,n} k_{i,n} e_{i,1} \right. \\ \left. - \frac{1}{r_{i,n}} \tilde{\delta}_{i,n} (r_{i,n} |s_{i,n}| - \eta_{i,n} \delta_{i,n}) + w_{i,n} D^\alpha w_{i,n} \right\}. \quad (92)$$

Similar to the previous calculation, we have

$$s_{i,n} k_{i,n} e_{i,1} \leq \frac{1}{2} s_{i,n}^2 + \frac{1}{2} k_{i,n}^2 \|e_{i,1}\|^2 \quad (93)$$

$$s_{i,n} (\varepsilon_{i,n}^q + \Delta f_{i,n}^q) \leq |s_{i,n}| (\delta_{i,n} + \delta_{i,n}). \quad (94)$$

From Equations (92)–(94), we can obtain

$$D^\alpha V_n \leq D^\alpha V_{n-1} + \sum_{i=1}^N \left\{ s_{i,n} \left[ \frac{q_i(\omega_i(t)) - \beta_{i2}(t)H_{i1}}{1 + \beta_{i1}(t)\kappa_{i1}} + \bar{a}_{in} \right] - c_{in} s_{i,n}^2 - s_{i,n}^2 \right. \\ \left. + \frac{\rho_{i,n}}{\sigma_{i,n}} \tilde{\theta}_{i,n}^T \theta_{i,n} + \frac{\eta_{i,n}}{r_{i,n}} \tilde{\delta}_{i,n} \delta_{i,n} + \frac{1}{2} k_{i,n}^2 \|e_{i,1}\|^2 + w_{i,n} \left( -\frac{w_{i,n}}{\lambda_{i,n}} + B_{i,n} \right) \right\}. \quad (95)$$

By employing Young's inequality, we have

$$w_{i,n} B_{i,n} \leq \frac{1}{2} w_{i,n}^2 + \frac{1}{2} M_{i,n}^2. \quad (96)$$

Then we have

$$D^\alpha V_n \leq D^\alpha V_{n-1} + \sum_{i=1}^N \left\{ s_{i,n} \left[ \frac{q_i(\omega_i(t)) - \beta_{i2}(t)H_{i1}}{1 + \beta_{i1}(t)\kappa_{i1}} + \bar{a}_{in} \right] - c_{in} s_{i,n}^2 - s_{i,n}^2 \right. \\ \left. + \frac{\rho_{i,n}}{\sigma_{i,n}} \tilde{\theta}_{i,n}^T \theta_{i,n} + \frac{\eta_{i,n}}{r_{i,n}} \tilde{\delta}_{i,n} \delta_{i,n} + \frac{1}{2} k_{i,n}^2 \|e_{i,1}\|^2 - \frac{w_{i,n}^2}{\lambda_{i,n}} + \frac{1}{2} w_{i,n}^2 + \frac{1}{2} M_{i,n}^2 \right\}. \quad (97)$$

Substituting Equations (5), (84) and (85) into (97), we have

$$\begin{aligned}
 D^\alpha V_n \leq D^\alpha V_{n-1} &+ \sum_{i=1}^N \left\{ -c_{in} s_{i,n}^2 - s_{i,n}^2 + \frac{\rho_{i,n}}{\sigma_{i,n}} \tilde{\theta}_{i,n}^T \theta_{i,n} + \frac{\eta_{i,n}}{r_{i,n}} \tilde{\delta}_{i,n} \delta_{i,n} + \frac{1}{2} k_{i,n}^2 \|e_{i,1}\|^2 - \frac{w_{i,n}^2}{\lambda_{i,n}} \right. \\
 &\left. + \frac{1}{2} w_{i,n}^2 + \frac{1}{2} s_{i,n}^2 + \frac{\omega_{\min}^2}{2(1-\kappa_{i1})^2} + \frac{1}{2} M_{i,n}^2 + \frac{2\kappa_{i2}}{1-\kappa_{i1}} \right\}.
 \end{aligned} \tag{98}$$

From Equation (71), we can obtain

$$\begin{aligned}
 D^\alpha V_{n-1} &\leq -q_{n-1} \|e\|^2 + \frac{1}{2} \|P\varepsilon\|^2 + \sum_{i=1}^N \sum_{l=1}^n \frac{1}{2} \tilde{\theta}_{i,l}^T \tilde{\theta}_{i,l} \\
 &+ \sum_{i=1}^N \left\{ \sum_{l=1}^{n-1} \left( -c_{i,l} s_{i,l}^2 + \frac{\rho_{i,l}}{\sigma_{i,l}} \tilde{\theta}_{i,l}^T \theta_{i,l} + \frac{\eta_{i,l}}{r_{i,l}} \tilde{\delta}_{i,l} \delta_{i,l} \right) \right. \\
 &+ \sum_{j=1}^N a_{ij} \left( \frac{\rho_{j,1}}{\sigma_{j,1}} \tilde{\theta}_{j,1}^T \theta_{j,1} + \frac{\eta_{j,1}}{r_{j,1}} \tilde{\delta}_{j,1} \delta_{j,1} \right) - \left( \frac{1}{\lambda_{i,2}} - \frac{1}{2} - \frac{d_i^2}{2} \right) w_{i,2}^2 \\
 &\left. - \sum_{l=3}^{n-1} \left( \frac{1}{\lambda_{i,l}} - 1 \right) w_{i,l}^2 + \frac{1}{2} (s_{i,n}^2 + w_{i,n}^2) + \sum_{l=2}^{n-1} \frac{1}{2} M_{i,l}^2 \right\}.
 \end{aligned} \tag{99}$$

Substituting (99) into (98) yields

$$\begin{aligned}
 D^\alpha V_n &\leq -q_n \|e\|^2 + \frac{1}{2} \|P\varepsilon\|^2 + \sum_{i=1}^N \sum_{l=1}^n \frac{1}{2} \tilde{\theta}_{i,l}^T \tilde{\theta}_{i,l} + \sum_{i=1}^N \left\{ \sum_{l=1}^n \left( -c_{i,l} s_{i,l}^2 + \frac{\rho_{i,l}}{\sigma_{i,l}} \tilde{\theta}_{i,l}^T \theta_{i,l} + \frac{\eta_{i,l}}{r_{i,l}} \tilde{\delta}_{i,l} \delta_{i,l} \right) \right. \\
 &+ \sum_{j=1}^N a_{ij} \left( \frac{\rho_{j,1}}{\sigma_{j,1}} \tilde{\theta}_{j,1}^T \theta_{j,1} + \frac{\eta_{j,1}}{r_{j,1}} \tilde{\delta}_{j,1} \delta_{j,1} \right) - \left( \frac{1}{\lambda_{i,2}} - \frac{1}{2} - \frac{d_i^2}{2} \right) w_{i,2}^2 \\
 &\left. - \sum_{l=3}^n \left( \frac{1}{\lambda_{i,l}} - 1 \right) w_{i,l}^2 + \frac{\omega_{\min}^2}{2(1-\kappa_{i1})^2} + \sum_{l=2}^n \frac{1}{2} M_{i,l}^2 + \frac{2\kappa_{i2}}{1-\kappa_{i1}} \right\}
 \end{aligned} \tag{100}$$

where  $q_n = q_{n-1} - \sum_{i=1}^N k_{i,n}^2$ . According to Lemma 4, we have

$$\tilde{\theta}_{*,l}^T \theta_{*,l} \leq -\frac{1}{2} \tilde{\theta}_{*,l}^T \tilde{\theta}_{*,l} + \frac{1}{2} \theta_{*,l}^{*T} \theta_{*,l}^* \tag{101}$$

$$\tilde{\delta}_{*,l} \delta_{*,l} \leq -\frac{1}{2} \tilde{\delta}_{*,l}^2 + \frac{1}{2} \delta_{*,l}^{*2}. \tag{102}$$

From Equations (100)–(102), we can obtain

$$\begin{aligned}
 D^\alpha V_n &\leq -q_n \|e\|^2 + \frac{1}{2} \|P\varepsilon\|^2 + \sum_{i=1}^N \sum_{l=1}^n \frac{1}{2} \tilde{\theta}_{i,l}^T \tilde{\theta}_{i,l} \\
 &+ \sum_{i=1}^N \left\{ \sum_{l=1}^n \left( -c_{i,l} s_{i,l}^2 - \frac{\rho_{i,l}}{2\sigma_{i,l}} \tilde{\theta}_{i,l}^T \tilde{\theta}_{i,l} - \frac{\eta_{i,l}}{2r_{i,l}} \tilde{\delta}_{i,l}^2 \right) + \sum_{j=1}^N a_{ij} \left( -\frac{\rho_{j,1}}{2\sigma_{j,1}} \tilde{\theta}_{j,1}^T \tilde{\theta}_{j,1} - \frac{\eta_{j,1}}{2r_{j,1}} \tilde{\delta}_{j,1}^2 \right) \right. \\
 &- \left( \frac{1}{\lambda_{i,2}} - \frac{1}{2} - \frac{d_i^2}{2} \right) w_{i,2}^2 - \sum_{l=3}^n \left( \frac{1}{\lambda_{i,l}} - 1 \right) w_{i,l}^2 \\
 &+ \sum_{l=1}^n \left( \frac{\rho_{i,l}}{2\sigma_{i,l}} \theta_{i,l}^{*T} \theta_{i,l}^* + \frac{\eta_{i,l}}{2r_{i,l}} \delta_{i,l}^{*2} \right) + \sum_{j \in N_i} a_{ij} \left( \frac{\rho_{j,1}}{2\sigma_{j,1}} \theta_{j,1}^{*T} \theta_{j,1}^* + \frac{\eta_{j,1}}{2r_{j,1}} \delta_{j,1}^{*2} \right) \\
 &\left. + \frac{\omega_{\min}^2}{2(1-\kappa_{i1})^2} + \sum_{l=2}^n \frac{1}{2} M_{i,l}^2 + \frac{2\kappa_{i2}}{1-\kappa_{i1}} \right\}.
 \end{aligned} \tag{103}$$

Denote

$$\begin{aligned} \zeta = & \frac{1}{2} \|P\varepsilon\|^2 + \sum_{i=1}^N \left\{ \sum_{l=1}^n \left( \frac{\rho_{i,l}}{2\sigma_{i,l}} \theta_{i,l}^{*T} \theta_{i,l}^* + \frac{\eta_{i,l}}{2r_{i,l}} \delta_{i,l}^{*2} \right) + \sum_{j=1}^N a_{ij} \left( \frac{\rho_{j,1}}{2\sigma_{j,1}} \theta_{j,1}^{*T} \theta_{j,1}^* + \frac{\eta_{j,1}}{2r_{j,1}} \delta_{j,1}^{*2} \right) \right. \\ & \left. + \frac{\omega_{\min}^2}{2(1-\kappa_{i1})^2} + \sum_{l=2}^n \frac{1}{2} M_{i,l}^2 + \frac{2\kappa_{i2}}{1-\kappa_{i1}} \right\}. \end{aligned} \tag{104}$$

Then Equation (103) can be written as

$$\begin{aligned} D^\alpha V_n \leq & -q_n \|e\|^2 + \sum_{i=1}^N \left\{ \sum_{l=1}^n \left( -c_{i,l} s_{i,l}^2 - \left( \frac{\rho_{i,l}}{2\sigma_{i,l}} - \frac{1}{2} \right) \tilde{\theta}_{i,l}^T \tilde{\theta}_{i,l} \right. \right. \\ & \left. \left. - \frac{\eta_{i,l}}{2r_{i,l}} \delta_{i,l}^2 \right) + \sum_{j=1}^N a_{ij} \left( -\frac{\rho_{j,1}}{2\sigma_{j,1}} \tilde{\theta}_{j,1}^T \tilde{\theta}_{j,1} - \frac{\eta_{j,1}}{2r_{j,1}} \delta_{j,1}^2 \right) \right. \\ & \left. - \left( \frac{1}{\lambda_{i,2}} - \frac{1}{2} - \frac{d_i^2}{2} \right) w_{i,2}^2 - \sum_{l=3}^n \left( \frac{1}{\lambda_{i,l}} - 1 \right) w_{i,l}^2 \right\} + \zeta \end{aligned} \tag{105}$$

where  $c_{i,l} > 0, (l = 1, \dots, n), \left( \frac{1}{\lambda_{i,2}} - \frac{1}{2} - \frac{d_i^2}{2} \right) > 0, \left( \frac{1}{\lambda_{i,l}} - 1 \right) > 0, l = 3, \dots, n, \left( \frac{\rho_{i,l}}{2\sigma_{i,l}} - \frac{1}{2} \right) > 0, \frac{\eta_{i,l}}{2r_{i,l}} > 0, \frac{\rho_{i,l}}{2\sigma_{i,l}} > 0$ .

Define

$$C = \min \left\{ 2q_n / \lambda_{\min}(P), 2c_{i,l}, 2 \left( \frac{\rho_{i,l}}{2\sigma_{i,l}} - \frac{1}{2} \right), \frac{\eta_{i,l}}{r_{i,l}}, \frac{\rho_{i,l}}{\sigma_{i,l}}, 2 \left( \frac{1}{\lambda_{i,2}} - \frac{1}{2} - \frac{d_i^2}{2} \right), 2 \left( \frac{1}{\lambda_{i,l}} - 1 \right) \right\}. \tag{106}$$

Then Equation (105) becomes

$$D^\alpha V_n \leq -CV_n + \zeta. \tag{107}$$

According to Equation (107), we can obtain

$$D^\alpha V_n + Q(t) = -CV_n + \zeta \tag{108}$$

where  $Q(t) \geq 0$ .

According to Lemma 6, we can obtain

$$V_n \leq V(0)E_\alpha(-Ct^\alpha) + \frac{\zeta\mu}{C}. \tag{109}$$

Then, we have

$$\lim_{t \rightarrow \infty} |V_n(t)| \leq \frac{\zeta\mu}{C}. \tag{110}$$

Since  $\frac{1}{2} |s_{i,1}|^2 \leq V_n(t)$ , and we can obtain  $|s_{i,1}| \leq \sqrt{\frac{2\zeta\mu}{C}}$ , invoking  $s_{i,1} = \sum_{j=1}^N a_{ij} (y_i - y_j) + \sum_{j=N+1}^{N+M} a_{ij} (y_i - y_{d_j}(t))$ , note the fact that  $s_1 = L_1 y + L_2 r(t)$ , where  $s_1 = [s_{1,1}, \dots, s_{N,1}]^T$ . Because the convex hull spanned by leaders is defined as  $r_d(t) = -L_1^{-1} L_2 r(t)$ , then, the containment errors satisfy  $\|e\| = \|y - r_d(t)\| \leq \frac{\sqrt{2\zeta\mu/C}}{\|L_1\|_F}$ .

The proof process that the proposed control method can avoid Zeno phenomenon is as follows:

By  $\Delta_i(t) = q_i(\omega_i(t)) - u_i(t)$ , we have  $D^\alpha |\Delta_i| = D^\alpha (\sqrt{|\Delta_i \cdot \Delta_i|}) = \text{sign}(\Delta_i) D^\alpha (\Delta_i) \leq |D^\alpha (q_i(\omega_i(t)))| = |D^\alpha (H(\omega_i)\omega_i(t))| \leq (1+d)|D^\alpha(\omega_i(t))|$ . According to Equation (84),  $D^\alpha(\omega_i(t))$  is bounded in a closed interval  $[0, t]$ . Therefore, there exists a constant  $\zeta > 0$  such that  $|D^\alpha(\omega_i(t))| \leq \zeta$ . From  $\Delta(t_k) = 0$  and  $\lim_{t \rightarrow t_{k+1}} \Delta(t) = H_{i1}$ , thus, there exists  $t^*$  such that  $t^* \geq H_{i1}/\zeta$ . Therefore, there exists  $t^* \geq 0$  such that  $\forall k \in \mathbb{Z}^+, \{t_{k+1} - t_k\} \geq t^*$ , the Zeno phenomenon will not occur.

**Remark 1.** It should be noted that the classical local theories used in this paper do not have the ability to describe the material heterogeneities and the fluctuations of different scales. In future research, we will use a more appropriate definition of a fractional differential, such as the Atangana-Baleanu [50] or Caputo-Fabrizio [51] fractional derivative definition.

#### 4. Simulation

In this section, to verify the effectiveness of the proposed method, the following fractional Duffing-Holmes chaotic system [52] is considered.

$$\begin{cases} D^\alpha x_{i,1} = x_{i,2} + f_{i,1}^q(X_{i,1}) \\ D^\alpha x_{i,2} = u_i(t) + f_{i,2}^q(X_{i,2}) \\ y_i = x_{i,1} \end{cases} \quad (111)$$

where the system order is  $\alpha = 0.98, i = 1, 2, 3, 4$ .  $y_{d1} = 0.2 \sin t$  and  $y_{d2} = \sin 0.3t$  are defined as the leaders. The unknown functions are  $f_{1,1}^q = f_{2,1}^q = f_{3,1}^q = f_{4,1}^q = 0, f_{1,2}^q = x_{1,1} - 0.25x_{1,2} - x_{1,1}^3 + 0.3 \cos(t), f_{1,2}^q = 2x_{1,1} - 0.25x_{1,2} - x_{1,1}^3, f_{2,2}^q = x_{2,1} - 0.25x_{2,2} - x_{2,1}^3 + 0.1(x_{2,1}^2 + x_{2,2}^2)^{1/2}, f_{2,2}^q = x_{2,1}^2, f_{3,2}^q = x_{3,1} - 0.25x_{3,2} - x_{3,1}^3 + 0.2 \sin(t)(x_{3,1}^2 + 2x_{3,2}^2)^{1/2}, f_{3,2}^q = x_{3,1}^2 - x_{3,1}^3, f_{4,2}^q = x_{4,1}^2, and f_{4,2}^q = x_{4,1} - 0.25x_{4,2} - x_{4,1}^3 + 0.2 \sin(t)(2x_{4,1}^2 + 2x_{4,2}^2)^{1/2}$ . We chose the design parameters as  $c_{i,1} = 20, c_{i,2} = 30, \sigma_{i,2} = r_{i,2} = 1, \rho_{i,2} = 40, \eta_{i,2} = 20, \lambda_{i,2} = 0.05, \kappa_{i1} = 0.5, \kappa_{i2} = 2, M_{i,1} = 1, \omega_{min} = 1$ , and  $d = 0.4$ . We chose the initial conditions of the system as  $x_1(0) = [0.1, 0.1]^T, x_2(0) = [0.2, 0.2]^T, x_3(0) = [0.3, 0.3]^T$ , and  $x_4(0) = [0.4, 0.4]^T$ . The observer initial conditions were chosen as  $\hat{x}_1(0) = [0.2, 0.2]^T, \hat{x}_2(0) = [0.3, 0.3]^T, \hat{x}_3(0) = [0.4, 0.4]^T$ , and  $\hat{x}_4(0) = [0.5, 0.5]^T$ .

The communication graph of the multiagent system is shown in Figure 1. Figures 2–13 show the simulation results. Figure 2 displays the trajectories of  $y_{d1}, y_{d2}$  and  $x_{i,1} (i = 1, \dots, 4)$ . Figure 3 shows the trajectories of the containment tracking errors. Figure 3a shows the trajectories of the containment tracking errors based on the event-triggered quantized controller, and Figure 3b shows the trajectories of containment tracking errors based on the event-triggered controller without input quantization. Figure 4 shows the trajectories of the  $x_{i,1} (i = 1, \dots, 4)$  estimation values. Figure 5 gives the error surfaces  $s_{i,1}$  of the two controllers. Figure 6 gives the trajectories of  $x_{i,2}$  and  $\hat{x}_{i,2}$ . We use  $x_{1,1}$  and  $x_{1,2}$  as examples in Figure 7 to show the results of the neural network observer designed in this paper. Figures 8–11 show the trajectories of  $\omega_i, q(\omega_i)$ , and  $u_i$ . Meanwhile, we compared the event-triggered control input without quantitative control technology with the control input mentioned in this article. From Figures 8–11, the triggered number of control input via the quantized mechanism was reduced by 7% to 20%, among which  $u_1$  was reduced by 20% (see Figure 8), and  $u_4$  was reduced by 7% (see Figure 11). In order to better highlight the advantages of the method proposed in this paper, we have compared the triggered number under different sampling mechanisms. It can be seen from Figure 13 that the proposed method can significantly reduce the number of control input samples. This means that the combination of event-triggered control and quantized control mechanisms can effectively reduce the number of transmissions of control input signals, so it has more practical significance and potential engineering value. Figure 12 shows the trajectories of the switching signal  $\sigma_i(t)$ . From the simulation results, the proposed method can ensure all followers converge to the leaders' convex hull, and the control performance is satisfactory.

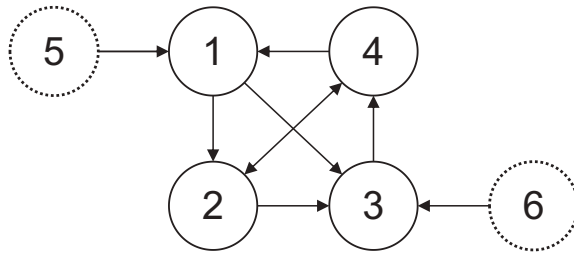


Figure 1. Communication graph.

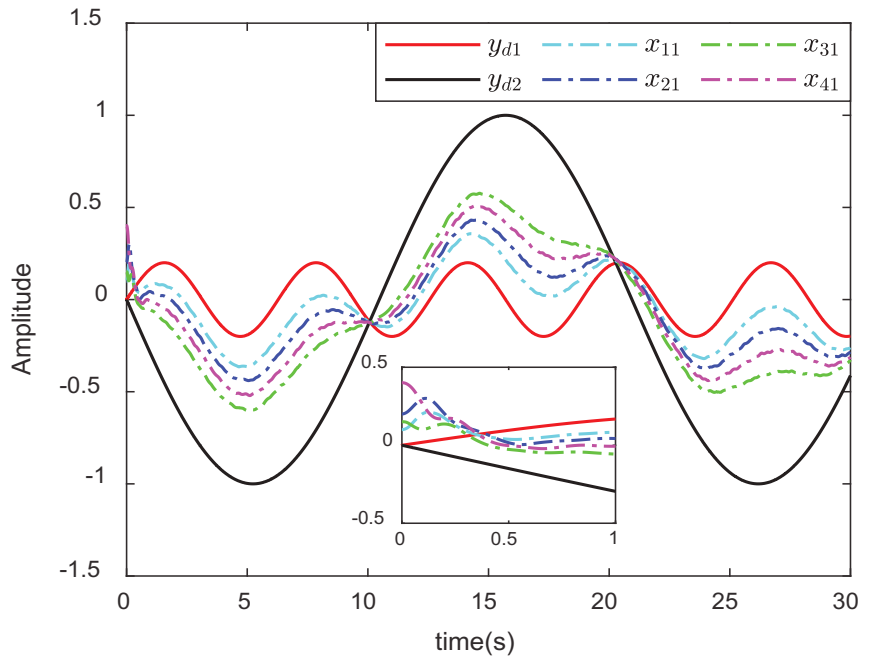
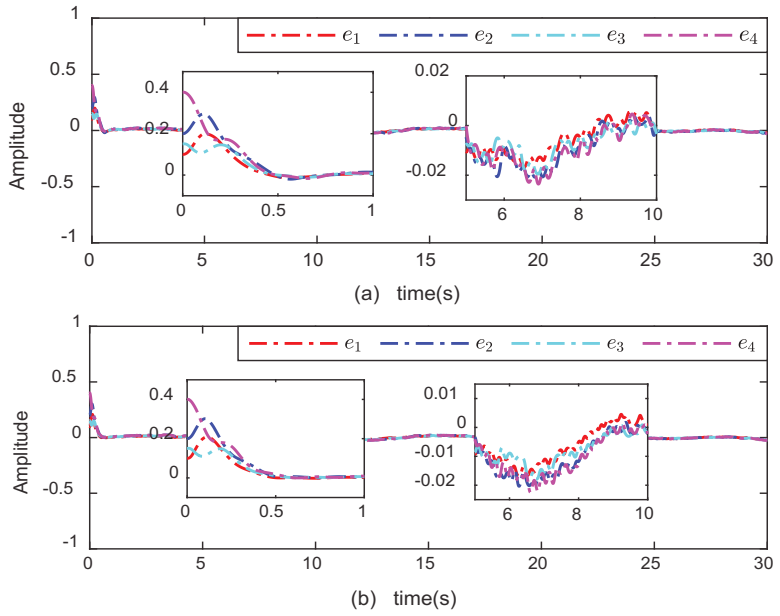
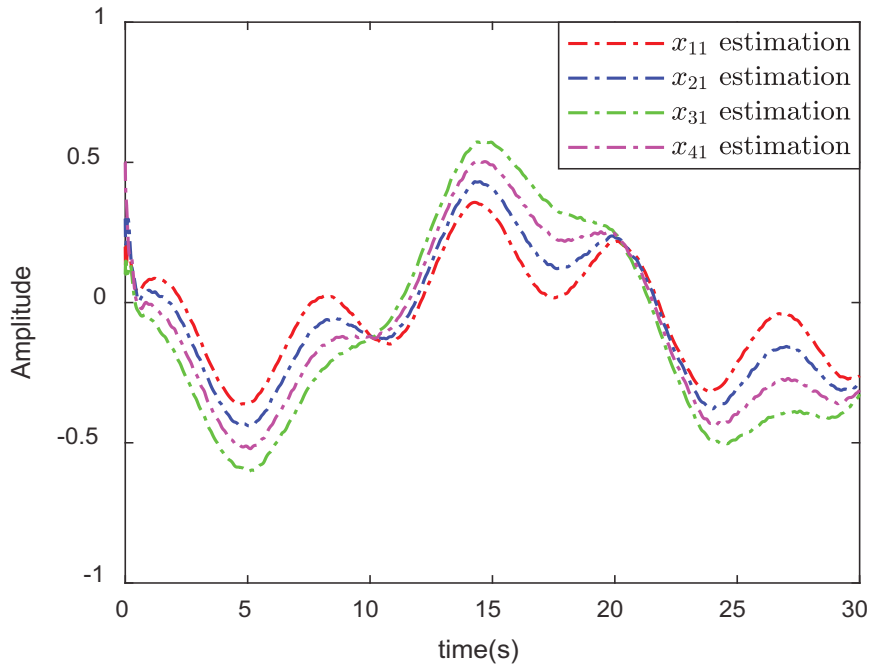


Figure 2. The trajectories of  $y_{d1}, y_{d2}$  and  $x_{i,1}(i = 1, \dots, 4)$ .



**Figure 3.** The trajectories of the containment tracking errors. (a) with quantized control. (b) without quantized control.



**Figure 4.** The trajectories of the  $x_{i,1}$  ( $i = 1, \dots, 4$ ) estimation values.

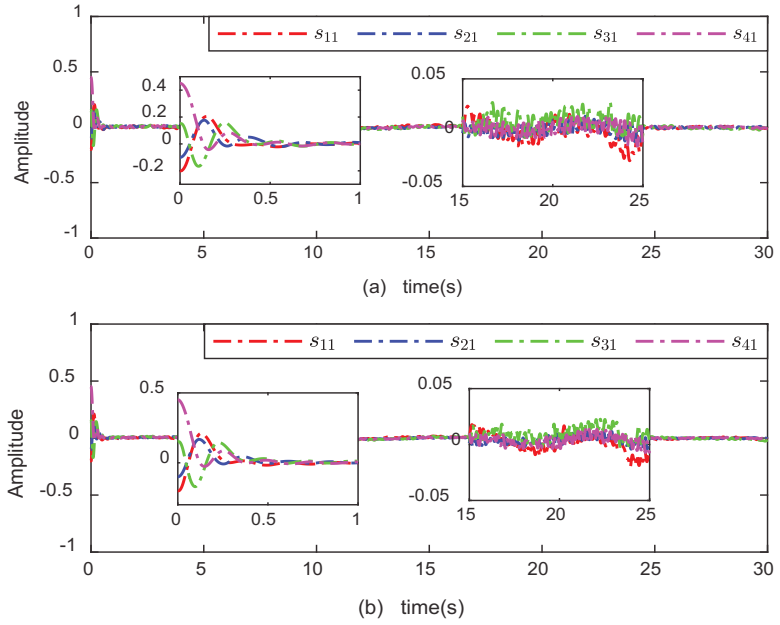


**Figure 5.** The trajectories of the error surfaces  $s_{i,1}(i = 1, \dots, 4)$ . (a) with quantized control. (b) without quantized control.

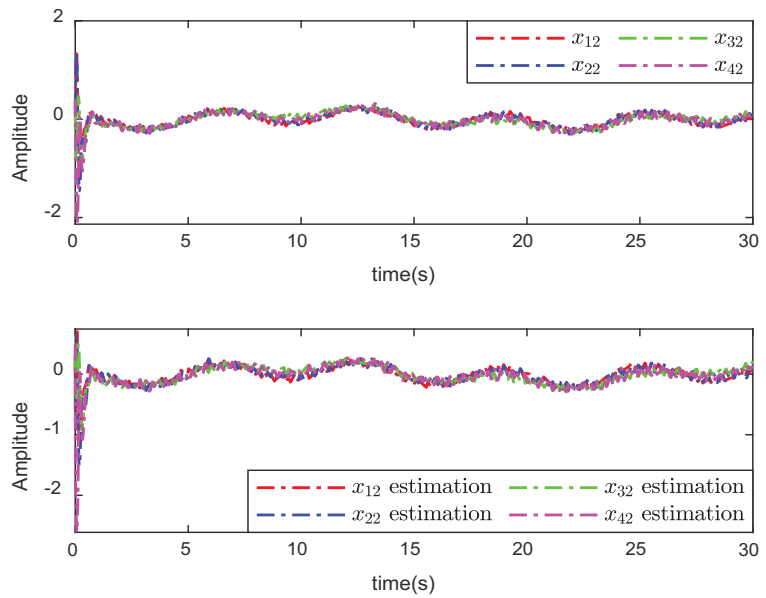


**Figure 6.** The trajectories of the  $x_{i,2}(i = 1, \dots, 4)$  and  $x_{i,2}(i = 1, \dots, 4)$  estimation values.